University College London

The Circadian Clock and The Cell Cycle

Catherine Ann Cox

Thesis for PhD.
Cell and Developmental Biology
Division of Biosciences
University College London

I, Catherine Ann Cox, confirm that this work presented in this thesis is my own. Where information has been derived from other sources, I confirm that this has been indicated in the thesis.

For Barry John Cox

Acknowledgments

I would like to thank my primary supervisor David for making this project possible and being a constant source of support and my second supervisor Claudio for his perspective and insight. I would like to thank all the members of the Whitmore Lab. In particular I'm very grateful to Kathy, who has been a wealth of knowledge and experience, Pete for his help and technical support, Elodie for her time, answering my constant questions and reassuring cups of tea and finally Helen for her enthusiasm and encouragement. I would also like to thank former lab member Lucy Young for her inspiration and advice. I am very grateful to the Medical Research Council and the British Biological Research Council for funding my project. The support of all my friends has been invaluable. Laura, Harriet, Anna and Becky, thank you for all your encouragement and offers of proof-reading. Lizzie, Joe and Emily, Gillian, Katherine, Esmé and Rob thank you for keeping everything in perspective. Finally, to my mum, Ann, thank you for everything.

Abstract

The circadian clock is an endogenous time-keeping mechanism that allows an organism to coordinate its biology with the 24 hour variations in its external environment. Epidemiological studies have linked clock disruption to an increase incidence of cancer, in particular breast malignancy. On a molecular level, clock components have been shown to regulate cell cycle gene expression and its progression in a number of models. This thesis set out to further dissect the link between these two important systems.

Within the zebrafish cell-line, PAC2, mitosis was demonstrated to be under circadian control via clock regulation of the cell cycle mediator, *Cyclin B1*. Techniques used were then translated into a human cell-line model to study species specific clock function, with particular reference to breast epithelial tissue. Glucocorticoids, putative clock synchronisation agents *in vivo*, were observed to induce cellular clock synchronisation in HEK 293 cells and the benign breast epithelial cell-line MCF10A. Clock disruption inhibited cell growth. Study of the breast epithelial cell cycle mutant, MDA-MB-231, demonstrated a functional clock, revealing no reciprocal regulation. In contrast, decreased expression levels of clock gene and putative tumour suppressor, *Per1,* were observed within the malignant breast epithelial cell-line, MCF7, leading to greatly disrupted clock function and circadian independent cell growth.

Unlike the zebrafish model, no intracellular clock regulation of cell cycle genes expression or function was observed, expression being preferentially modified by homeral circadian regulators such as glucocorticoids and melatonin. This also

contradicts mammalian *in vivo* studies, leading to the hypothesis that the clock and cell cycle maybe uncoupled in immortalised cell cultures.

In conclusion this study has demonstrated that clock regulation of the cell cycle in mammalian system is a multifactorial process and that disruption of this system leads to changes in the character of the cell cycle within the host tissue. Further work must explore this relationship in an *in vivo* setting.

Abbreviations

ACTH, *adrenocorticotrophic hormone.*
ANOVA, *analysis of variance*.
Bp, *base pair.*
BrdU, *bromodeoxyuridine*
cAMP, *cyclic adenosine monophosphate.*
CCG, *clock controlled gene.*
CDK, *cyclin dependent kinase.*
Chk1, *checkpoint 1.*
Chk2, *checkpoint 2.*
CK1ε, *Casein Kinase ε*.
CK1δ, *Casein Kinase δ.*
CPS, *counts per second.*
Cry, *Cryptochrome.*
CT, *circadian time*.
DAPI, *4',6-diamidino-2-phenylindole*.
DD, *constant darkness.*
DL, *dark-light cycle*.
DMEM, *Dulbecco's Modified Eagle's Medium.*
DMSO, *dimethyl sulfoxide.*
DN, *dominant negative*.
DNA, *deoxyribonucleic acid.*
cDNA, *complementary DNA.*
dsDNA, *double stranded DNA*.
dNTP, *deoxyribonucleotide triphosphate.*
DTT, *dithiothreitol.*
E-Box, *enhancer box.*
EGF, *epidermal growth factor.*
ER, *oestrogen receptor.*
EDTA, *ethylenediaminetetraacetic acid.*
FACS, *fluorescence-activated cell sorting.*
FAPS, *familial advanced sleep phase disorder.*
GR, *glucocorticoid receptor.*
HAT, *histone acetyltransferase.*
HEK, *human embryonic kidney.*
HLH, *helix-loop-helix.*
HPA, *hypothalamic–pituitary-adrenal*.
HRP, *horseradish peroxidase*.
IR, *ionising radiation.*
LD, *light-dark cycle.*
LL, *constant light.*
LNvs, *lateral neurons.*
MT, *melatonin receptor.*
NAD, *nicotinamide adenine dinucleotide.*
NS, *not significant.*
Oligo DT, *deoxy-thymine nucleotides.*
PACAP, *pituitary adenylate cyclase–activating protein.*
PAS, *Period-Arntl-Single minded.*
PBS, *phosphate buffered saline.*
PBT, *phosphate buffered saline with tween.*
PCR, *polymerase chain reaction.*
Per, *Period.*
PI, *propidium iodide*
Q-PCR, *Quantitative PCR.*
rd/rd cl, *rodless coneless mice.*
RHT, retinohypothalamic tract.
RL13, *ribosomal protein L13*.
RNA, *riboxynucleic Acid.*
mRNA, *messenger RNA.*
RNase, *ribonuclease.*
RORE, *related orphan receptor response elements.*
RT-PCR, *real-time PCR.*
SCN, *suprachiasmatic nucleus.*
SEM, *standard error of the mean.*
SD, *standard deviation.*
SNP, *single nucleotide polymorphism.*
STET, *saline/tris/EDTA/triton.*
τ, *period*.
TBP, *TATA-Box binding protein,*
TIM, *Timeless.*
UV, *ultraviolet.*
WT, Wild-type.
ZT, *zeitgeber* t

Table of Contents

Index of Figures

Index of tables

CHAPTER 1

GENERAL INTRODUCTION

This general introduction is designed to give an overview of the field, more specific introductions can be found at the beginning of each results chapter (Chapters 3-6).

1.1 INTRODUCTION TO THE CIRCADIAN CLOCK

1.1.1 Background

The external environment is in constant change. Although some of these changes are unique, many events repeat over time: The daily transition from daytime to night-time, the monthly tidal shifts and seasonal environmental changes. In order to survive it is imperative that an organism be able to adapt to these changes. As a result most organisms have evolved endogenous time-keeping mechanisms that allow them not only to adapt to but also anticipate these cyclic events.

One of the most fundamental cyclic events we experience is the 24-hour variation in light intensity during the day. Almost all organisms, from complex eukaryotes to prokaryotes especially cyanobacteria (Kondo & Ishiura, 2000), have as a result developed an endogenous clock with a periodicity close to 24 hours. The first documented study of this endogenous mechanism was in 1727. Geophysicist Jean Jacques d'Ortus de Marian observed that the perennial herb *Mimosa pudica* opened its leave during the day and closed them with the onset of dusk. These events continued when the plant was placed into constant darkness (de Mairan, 1729. Sweeney, 1987).

It would not be until the 1960's that chronobiologist Franz Halberg would name the driving force behind this phenomenon the circadian clock (from the Latin *circa* meaning "about" and *dies* meaning "day"). However, even the simple observations made by De Marian 250 years before demonstrate the three key components understood to be integral to the clock today. At the centre is a self-sustaining oscillator, which maintains rhythmic outputs even when isolated from external

cues. These endogenous rhythms often have a period (τ) of 23-25 hours. When a clock is disconnected from the external environment the system runs at its own pace, as such is it regarded as "free-running". The second component is the *zeitgeber* (from the German meaning *time-giver*). This is the external input, predominately light, that synchronises the clock mechanism to the external environment, a process known as entrainment. The final component, or components, to the clock are the 24-hour output rhythms it generates. As will be discussed later, such rhythms are now known to permeate throughout an organism's behaviour, physiology and even cell biology (Foster & Lucas, 1999).

A fundamental characteristic of these rhythmic outputs is that they display temperature compensation. The majority of biochemical processes are influenced by temperature; increasing temperature fuelling an increase in reaction rate, subject to the Q10 temperature co-efficient (Pittendrigh, 1954). However, circadian rhythms are able to compensate for temperature fluctuation, showing little variation in reaction rate in response to temperature change. This is found ubiquitously across ectothermic, poikilothermic and even homoeothermic organisms (Kaushnik *et al*, 2007. Takeuchi, 2007). Within the latter some evidence of over-compensation has even been noted in a response to lower temperatures (Dibner, 2009).

1.1.2 The "Master" Clock

Initially, these 24-hour processes were seen as part of a diffuse time-measuring capacity of the organism as a whole. However, Colin Pittendrigh, regarded as a co-founder of modern chronobiology, questioned this idea in 1960's. He proposed that there was a distinct light-sensitive oscillator that acted as an internal clock for

the organism (Pittendrigh, 1960). From this point on chronobiologists sought a central master clock; within the mammal, studies centred on the eye and brain. Within other models such as the zebrafish, the eye, brain and pineal were considered. Similarly in *Drosophila*, the lateral neurons (LNvs) were the main focus (Helfrich-Förster *et al*, 2007). From now on I will concentrate on describing the mammalian mechanism only, as it is most applicable to this thesis. (The zebrafish model is discussed in more detail during Chapter 3).

Lesioning experiments within rodent brains led investigators to a paired structure within the hypothalamus, just above the optic chiasm, known as the Suprachiasmatic Nucleus (SCN). Circadian behaviour and rhythmic corticosteroid secretion observed in test animals was lost when this area was ablated (Moore *et al*, 1972. Stephan & Zucker, 1972). This loss of behavioural character could be restored when foetal SCN tissue was transplanted into the third ventricle of the test subjects (Lehman *et al*, 1987). Transplant experiments using naturally occurring circadian mutants, such as the *Tau* hamster, which has a shortened periodicity, further confirmed this result; subjects receiving SCN tissues from *Tau* mutants took on *Tau* characteristics, and vice versa (Ralph *et al*, 1990. Sujino *et al*, 2003).

Upon further investigation it was found that this SCN tissue could be kept in culture, during which time it generated autonomous, circadian, electrical activity (Green *et al*, 1982. Groos *et al*, 1982), for up to 3 weeks (Bos *et al*, 1990). In addition, neuronal cultures from the tissue and, in fact, single neurons in isolation displayed autonomous, rhythmic, electrical firing (Welsh *et al*, 1995). Metabolic activity, such as glucose uptake, was also rhythmic within the SCN *in vitro*, as was

the expression of proteins known to be essential to clock function at the time (Schwartz *et al*, 1977. Sun *et al*, 1997. Hastings *et al*, 1999). This evidence suggested that this hypothalamic "island" was unique in its ability to produce independent and sustained circadian activity *in* and *ex vivo*, and it was vital for the production of rhythmic activity throughout the body. In short it was the site of the circadian clock.

1.1.2.1 Inputs into the SCN

Light is the main *zeitgeber* for the mammalian system. Studies on mice lacking visual photoreceptors (the *rodless/coneless, rd/rd cl*, mutant) revealed that these animals were able to maintain their circadian behaviour, even if to an attenuated extent (Semo *et al*, 2003). However, mice completely lacking retinal tissue, via degeneration or experimental design, displayed a total lack of circadian rhythmicity. Previous experiments demonstrated the presence of non-image forming photoreceptors within the retinal ganglion cells of the retina (Berson *et al*, 2002). These cells expressed a photo-pigment named melanopsin, a homolog to the non-visual photo-pigments found within amphibians (Provencio *et al*, 1998. Provencio *et al*, 2000. Gooley *et al*, 2001. Hatter *et al*, 2002). It was shown that these cells were independent circadian photoreceptors. Photic information is transduced directly from them, along the Retinohypothalamic Tract (RHT) to the ventrolateral region of the SCN (Moore *et al*, 1972). Excitatory glutamenergic (Castel *et al*, 1993) and neuropeptide pituitary adenylate cyclase–activating protein (PACAP) pathways (Hannibal *et al*, 1997) are thought to transmit this photic signal leading to the activation of certain signalling pathways (in particular

Ca^{2+} release), evocation of chromatin remodelling and the induction of core clock components within the SCN (Reviewed in Hirota, 2004).

1.1.3 Peripheral Clocks

However, as work centred on how this master clock exerted influence on peripheral tissues evidence built to suggest these tissues contained self-sustaining oscillators themselves. It was later discovered that the core clock components (genes whose protein products are fundamental for the generation and co-ordination of individual cell rhythms) expressed by the SCN were also expressed by some peripheral tissues (Balsolobre *et al*, 1998. Yamazaki *et al*, 2000. Yagita *et al*, 2001). Cultured cells from a variety of peripheral tissues, including liver, kidney, spleen, heart, skeletal muscle and thyroid all displayed the ability to express core clock components in a rhythmic fashion (Yamamoto *et al*, 2004. Yamzaki *et al*, 2009. Yoo *et al*, 2004). Tissues thought to gain their circadian rhythm from external homeral input, such as liver tissue, were also found to maintain rhythmic oxygen consumption in culture. However, initial observation suggested these oscillations dampened over time (Langner *et al*, 1972). It was thought, although peripheral tissues had the machinery and capability to produce individual oscillations, they were merely slave oscillators requiring governance from the master clock within the SCN.

It was the emergence of bioluminescent assaying to monitor gene expression (as will be described in detail later) as well as single cell imaging that revealed these rhythms were in fact self-sustained and cell-autonomous. Some tissues, liver and lung explants, displayed much more robust outputs than expected from a dampening system; when monitoring *Per*2 output by luciferase over 20 cycles

were observed in culture before rhythms dampened (Yoo *et al*, 2004). In 1998 Balsolobre *et al* showed that cultured Rat-1 fibroblasts (cells that had been in culture for a number of years) displayed intact circadian oscillations when stimulated (Balsolobre *et al*, 1998). Similar circadian oscillations have now been studied in a number of cell lines: the mouse embryonic fibroblast line NIH-3T3, primary fibroblasts from rodents and humans, and even some cancer cell lines such as the osteosarcoma cell line U2OS (Akashi *et al*, 2000. Brown *et al*, 2005. Hughes *et al,* 2009). Using the same techniques employed to gather the explant data, it was shown that these rhythms did not dampen without central control, but rather each cell contained a robust, independent clock. Upon withdrawal of extracellular inputs, these clocks merely desynchronised from their neighbouring oscillators (Nagoshi *et al*, 2004. Welsh *et al*, 2004). Similarly lesioning of the SCN *in vivo* did not affect peripheral clock function, but led to desynchronsation of phase between tissues (Yoo *et al*, 2004. Guo *et al*, 2006).

From such data the SCN is now understood to be more a relay centre; processing inputs from the external environment and then coordinating the peripheral clocks accordingly.

1.1.3.1 Coordination of peripheral clock in vivo

The central pacemaker, SCN, uses a number of pathways to maintain coherence of phase between peripheral clocks. A number of behavioural cues such as feeding rhythms driven by the SCN are thought to act as predominant *zeitgebers* for peripheral clocks (Yamazaki *et al*, 2000). The expression patterns of core clock genes within the liver, kidney and spleen of rodents, are greatly affected by changes in circadian driven feeding. When feeding (an activity which is normally

coupled to circadian activity) is forcibly uncoupled from the clock, a dramatic phase shift is observed in the circadian gene expression (Damiola *et al*, 2000). Hormonal changes in accordance to feeding/fasting states are thought to be the primary method of control. In addition molecular markers of metabolism SIRTI and NAD+ have been shown to play a significant role in controlling the DNA binding activity of CLOCK-BMAL (core clock components) (Asher *et al*, 2008, Nakahata *et al* 2008). This indicates a multi-faceted system. Numerous factors are thought to act as control points at different stages of signal transduction to coordinate peripheral outputs.

As circadian driven activity levels cycle during the day so does body temperature. Temperature fluctuations are strong *zeitgebers* within the circadian systems of *Neurospora* and *Drosophila* (Liu *et al*, 2003. Sehadova *et al*, 2009). They are also thought to play a role as a peripheral *zeitgeber* within the mammalian system (Brown *et al*, 2002).

Furthermore, the SCN is also known to govern the secretion of a number of hormones involved in the hypothalamic–pituitary-adrenal axis; another possible source of regulatory stimuli (Oster *et al*, 2006). Glucocortoid expression in particular is profoundly circadian. Glucocorticoid receptors are found in all tissues of the body, with the interesting exception of the SCN itself (Balsolobre *et al*, 2000).

Finally, the autonomic nervous system has been shown to play a role in coordination. Surgical denervation of hepatic tissues leads to a desynchronsation of peripheral clocks. Correspondingly the autonomic pathway is required for the resetting of peripheral clock phase, after a phase-shifting light impulse (Vujovic *et al*, 2008).

There is also a marked amount of communication between these pathways *in vivo* (Konturek *et al*, 2004). It is likely that a culmination of these factors is necessary to produce complete coherence within the peripheral clock population.

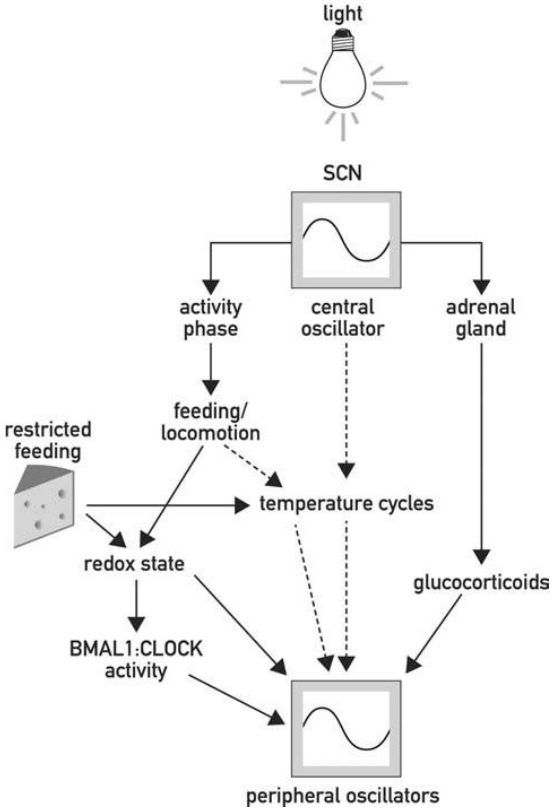

Figure 1.1. Schematic diagram taken from Stratmann & Schibler, 2006, demonstrating the pathways responsible for synchronising the peripheral clocks within mammals.

1.1.4 The Molecular Clock

The basic structural mechanism of the circadian clock is ubiquitous across the kingdoms: A select number of "clock genes" and their protein products arranged to form an auto-regulatory feedback loop based on transcription and translation (Schibler & Naef, 2005). In fact, it is this universality that is strong evidence for the systems standing as an evolved, adaptive advantage. This is certainly true for the clock in *Drosophila*, *Danio Rerio*, and rodents (Young & Kay, 2001).

Within mammals the primary loop consists of four components: Firstly, two basic helix-loop-helix (HLH), Period-Arntl-Single minded (PAS) transcription factors, CLOCK and BMAL. CLOCK (or its homolog NPAS2) and BMAL heterodimerise and interact with E-box *cis* regulatory enhancer sequences within the promoters of the second pair of genes Period *(Per1, 2 and 3)* and Cryptochrome *(Cry 1 and 2)*. This initiates transcription. PER and CRY proteins themselves then heterodimerise and translocate back into the nucleus, where they act in a negative manner upon the CLOCK: BMAL dimers, repressing CLOCK:BMAL function and thus their own transcription (Gekakis *et al,* 1998. Kune *et al*, 1999. Shermann *et al*, 2000. Sato *et al*, 2006).

CLOCK: BMAL also acts within a secondary loop, promoting the transcription of members of the retinoic acid-related orphan nuclear receptor families, Rev-erb and Ror. REV-ERB (α, β and γ) and ROR (α and β) subsequently bind to retinoic acid-related orphan receptor response elements (ROREs) with the *Bmal* promoter, repressing and promoting *Bmal* transcription respectively (Guillaumond *et al*, 2005).

These loops take approximately ~24 hours to complete one cycle. The timing of these loops is controlled by post-translational modification, such as ubiquitination and phosphorylation. Both processes governing the degradation of core clock components and the timing of translocation back into the nucleus. These post-translational modifications are thought to be driven by protein kinases, Casein Kinase epsilon (CK1ε) and Casein Kinase delta (CK1δ) (Lowry *et al*, 2000. Akashi *et al*, 2002): mutation of these enzymes is of particular interest within the humans, where they have been linked to the circadian disorder FASPS - Familial advanced sleep phase disorder (Toh *et al*, 2001). However the regulation of protein turnover is not completely understood, previous study has implied small ubiquitin-related modifier protein modification of BMAL1 also contributed to the temporal organization of this system (Cardone *et al*, 2005).

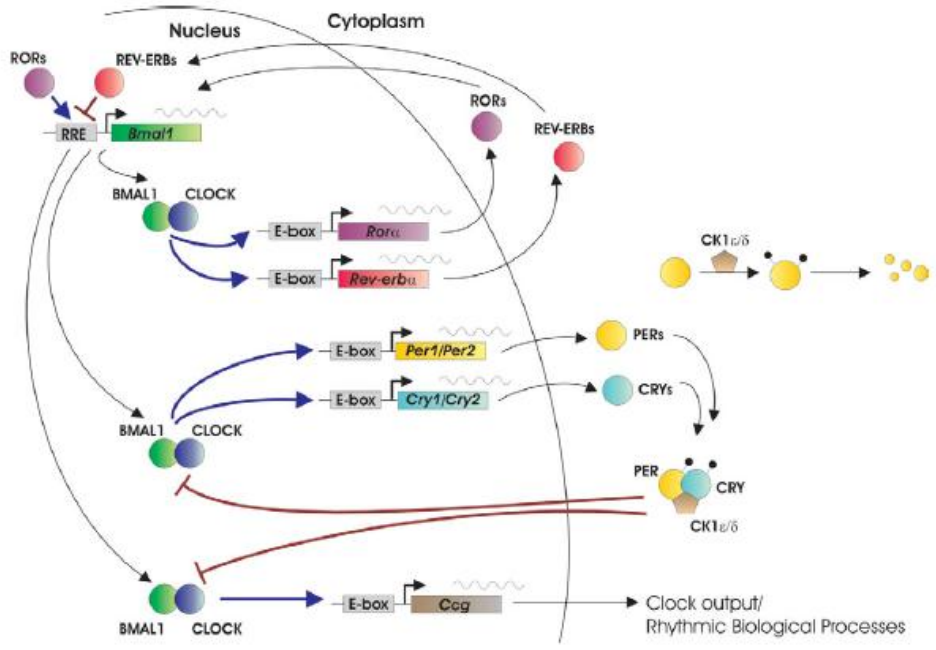

Figure 1.2.Diagram showing the molecular mechanism of the mammalian circadian clock taken from Ko & Takahashi, 2006.

1.1.5 The clock in different mammalian tissues

As mentioned above, it is now believed that almost every cell within the mammal contains a molecular clock, which functions in a self-sustaining, autonomous manner. The two known exceptions to this rule are the cells within the thymus and testis. Clock component gene expression within these tissues is not circadian in character, but either does not oscillate or oscillates with an ultradian 12-hour period (Alvarez *et al*, 2005). Similar lack of rhythmicity was observed with mouse embryonic stems cells. Peripheral clocks are subsequently thought to not function fully within immature or non-differentiated tissues, which predominately make up these organs (Stratmann & Schibler, 2006).

However, as more work is carried out on peripheral clock function it is becoming clear that the specific contribution of each molecular component of the clock is highly tissue-specific. This is demonstrated by differential expression patterns of *Clock* mRNA between tissues. *Clock* mRNA has been shown to oscillate within peripheral systems, but is constitutively expression within the SCN (Lowry *et al,* 2004). Expression pattern of *Reverb* and *Ror* family members also show tissue-dependency. *Reverb* (α, β and γ) present markedly differing expression patterns across tissues (Sato *et al*, 2003. Akashi e*t al*, 2005). While *Ror*-α displays robust oscillations within the SCN, little rhythmic expression is observed in the periphery. *Ror -γ* has been shown to contribute within certain peripheral clocks; however is not expressed or functional within the SCN (Guillamound *et al*, 2005).

It is therefore thought that circadian genes may play different regulatory roles depending upon the tissue. This hypothesis would explain the variety of different phenotypes that arise from clock mutations, such as the *Bmal1 (-/-)* knockout

mouse, which displays loss of circadian rhythms, decreased body weight, infertility, progressive arthropathy and shortened life span (Rudic *et al*, 2004. Bunger *et al*, 2005. Shimba *et al*, 2005).

Contribution of clock components to the regulation of each other is also tissue specific. For example *Per1* mRNA rhythms remain robust with the CLOCK-deficient liver, and are found at increased expression levels. However *Per1* mRNA rhythmicity is lost within the SCN of these animals (DeBruyne *et al*, 2006).

In conclusion, it is crucial to observe peripheral clock behaviour on a tissue specific level to fully comprehend their function. This is becoming particularly important as an increasing number of diseases are associated with circadian clock disruption.

1.1.6 Clock regulated outputs.

Through the complex and wide-reaching structure described above, the Circadian System is now known to influence a plethora of biological processes, from behavioural (sleep-wake, activity cycles), physiological (body temperature, blood pressure), hormonal and neuronal outputs, to biochemical reactions. Remarkably 10-15% of all mammalian transcripts undergo circadian fluctuations in their expression. (Akhtar *et al*, 2002. Duffield *et al,* 2002. Panda *et al*, 2002).

1.2 THE CELL CYCLE

1.2.1 Introduction to the cell cycle

The cell cycle is another prominent, oscillatory system, which allows the cell to safely and effectively "reproduce"

Within *Eukaryotes* the cycle is split into four main phases of major activity. Each daughter cell emerges into a stage known as G1. During G1 the cell may become larger; however there is no distinct morphological change, any activity that occurs is on a molecular and biochemical level preparing the cell to replicate its DNA. Thus having prepared, the cells will enter Synthesis or S-phase upon which is it duplicate its DNA. The cell will proceed into a subsequent rest phase G2 where the cell will continue to grow and prepare biochemically for mitosis. The former three stages together are known as interphase. Upon completion of this pathway the cell will undergo mitosis (Schibler, 2003).

Mitosis, also known as M or Mitotic phase, consists of four sub-phases: prophase - during which the cell condenses its chromatin into chromosome, the nuclear envelope disperses and microtubules are produced, metaphase – the chromosome align and the microtubules length to attach to the chromosome centromere, anaphase – the pulling and separation of the chromosomes by the microtubules and lastly telophase – where cytokinesis occurs (the separation of the cytoplasm, membrane and formation of new nucleus) (Bolsover, 2004)

Upon completion of the cycle, cells may enter quiescence or senescence/G0 phase (enter stasis on a temporary or permanent basis respectively). The cell will cease dividing and remain in situ for a prolonged period of time, or in the case of neurons

indefinitely. These cells may have become fully differentiated and have no further stimulus to divide, or may enter quiescence as the result of damage or DNA assault (Bolsover, 2004).

Figure 1.3 The cell cycle. Diagram adapted from Cell Biology, Bolsover, 2004.

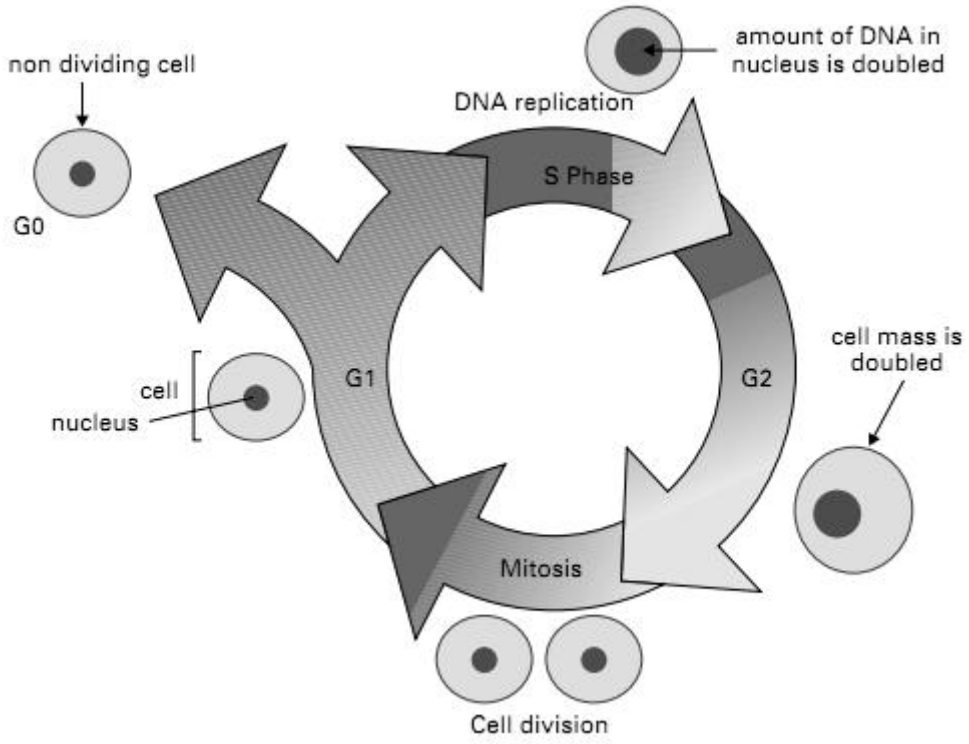

1.2.2 Cell Cycle regulation

1.2.2.1 Cell Cycle Checkpoints

The cell cycle is highly regulated to ensure cell viability, to detect any DNA damage within the cell and prevent this being passed onto the daughter cells.

Molecular checkpoints occur to gate the progression of a cell through the cycle and ensure fidelity of cell division within eukaryotic cells. Through multiple studies these checkpoints have been characterized as protein complexes, each containing a cyclin and cyclin dependent kinase (CDK) (Nigg, 2005). The cyclin acts as the regulator, the CDK as the catalytic subunit, in this way heterodimerisation allows for CDK activation and subsequent phosphorylation of cell cycle components. This Cyclin/CDK regulation is a highly conserved process found across species, although more complex organisms have evolved a higher number of specific functional complexes (Nigg, 2005).

Checkpoints are found throughout the cell cycle however the two major sites of regulation are the G1/S transition checkpoint and the G2/M transition checkpoint. At the G1/S transition check-point Cyclin E binds to CDK2, this initiates the G1/S transition. Cyclin E1 (along with Cyclin A, DNA polymerase and thymidine kinase) is transcribed in response to activation of the transcription factor E2F (Gréchez-Cassiau *et al*, 2008). The cyclin dependant kinase inhibitor p21, regulates the transition by repressing the function Cyclin E1/CDK2 and Cyclin A/CDK2 complexes.

Progression of the cell cycle is initiated in response to certain growth factors. Initially Cyclin D1 is transcribed in response to these growth factors and in

dimerisation with CDC2 hyper-phosphorylates a protein known as retinoblastoma protein. This is often found in an inhibitory complex with E2F – dissociation therefore releases E2F and promotes progression through G1/S (Blais & Dynlacht, 2007).

At the G2/M transition checkpoint Cyclin B1 binds to CDK2. This complex is activated in two ways; its activity is governed by the nuclear concentration of Cyclin B1, which is found in the cytoplasm until migration through the nuclear envelope at the G2/M border (Takizawa, 2005). Once in complex its activity is controlled by excitatory phosphorylation of threonine sites by CAK, or inhibitory phosphorylation such as that of tyrosine-15 by Wee1 (Shackleford *et el*, 1999).

Figure 1.4 Schematic illustrating the molecules active at each progression stage of the cell cycle as described in section 1.2.2.1

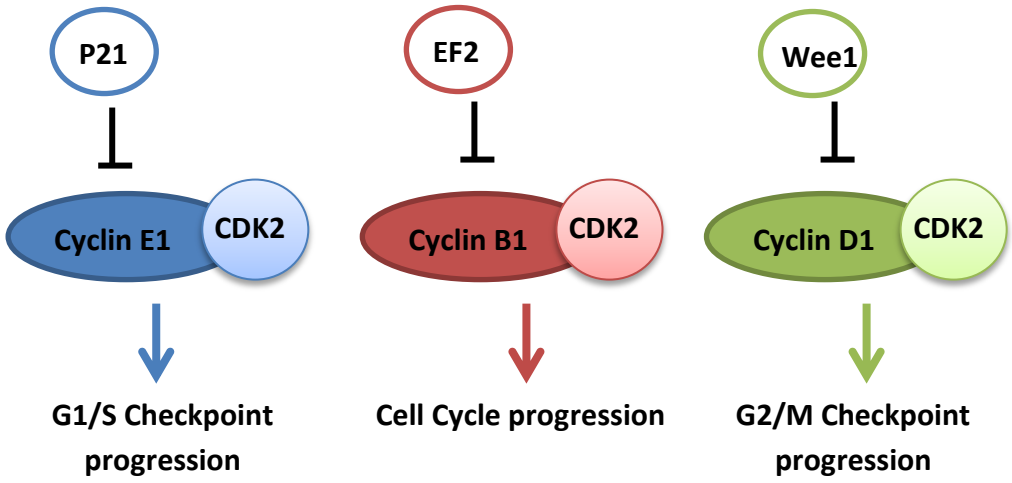

1.2.2.2 DNA Repair pathways

There is also a secondary system of check-points, which are interlinked with cell cycle progression, which must be mentioned to gain a comprehensive view of the system. This is the DNA repair pathway. This system is designed to eliminate any DNA damage, which can be defined as any covalent change in DNA structure (Sancar *et al*, 2004). The system contains multiple pathways, which are activated via one of two DNA repair checkpoints. Checkpoint 1 (Chk1) is activated by UV, UV-mimetic agents, and chemical agents that inhibit replication fork progression, and Checkpoint 2 (Chk2) is activated by double-strand breaks that are induced by ionizing radiation (IR) and radiomimetic agents (Sancar *et al,* 2010). Damage is detected by ATR and ATM kinases at their respective checkpoints. These signals are then transduced through mediator kinases to phosphorylate p53, Cdc25, and Cdc45 proteins; proteins that govern the progression through the G1/S and G2/M gateways mentioned above (Sancar *et al*, 2010).

The DNA repair itself takes place via a number of mechanisms: Direct repair via photolyases and alkyl transferases, base excision repair via glycosylases and AP endonucleases, nucleotide excision repair, and double-strand break/crosslink repair (Sancar *et al*, 2004).

Finally the proliferative regulators p53 and c-Myc are known to play a crucial role in cell cycle regulation: the c-Myc oncogene, which plays a key role in cellular proliferation as a bHLH transcription factor positively regulating a number of genes critical for G1/S transition (Fu *et al,* 2002). p53 inhabiting a contrary role, regarded as tumour suppressor, and negatively regulating progression through the cycle at numerous stages (Fu *et al*, 2002).

1.3 THE CIRCADIAN CLOCK AND THE CELL CYCLE

The concept that the circadian clock may be able to influence the timing of the cell cycle was first proposed by Franz Halberg (Halberg *et al*, 1954). However, it was not until the molecular mechanism of the clock had been elucidated that any direct mechanistic links could be drawn. Recent studies, precipitated by these advances, have shown that in many organisms cell proliferation is restricted to a specific time of day by the circadian clock, a process known as "gating". Early experiments using microscopic observation of the algae flagellate *Euglena gracillis* revealed that not only did population growth appear rhythmic; occurring only in subjective night, but also was under circadian control (Bolgie *et al*, 2005). Similar "gating" phenomena have also been described in Cyanobacteria (Goto & Johnson, 1995), where the gating of cell division, so as not to occur in the early subjective night, continues in constant light. This rhythm is still seen in species whose doubling time is shorter than an hour, suggesting that although the circadian clock can regulate the cell cycle, no reciprocal control occurs (Mori *et al*, 1996). Studies by the same author then reported that the mechanism of such gating lay in the circadian control of the cell division gene, *FtsZ* (Mori & Johnson, 2001).

Within zebrafish it has been shown that the progression of the cell cycle is regulated by light through the circadian clock. Using BrdU incorporation techniques it was shown that S-phase within zebrafish larvae was under circadian control (Dekens *et al,* 2003).

1.3.1 Current Molecular interactions

In mammals the suggestion of circadian regulation of cell division genes was supported by a study by Matsuo *et al* in mice (Matsuo *et al*, 2003). Cell division in mice during liver regeneration was seen to be under circadian regulation, with the hypothesis that this regulation was occurring at the G2/M transition (Matsuo *et al*, 2003). To test this theory, the expression patterns of 68 genes related to such transition points were analysed. The expression level of one gene in particular was of interest. *Wee1* expression showed a robust circadian rhythm, which correlated with the CLOCK-BMAL1 activated gene *Per1*. The expression also had a perfect, inverse correlation to the activity of the Cyclin B1/CDC2 complex (Schibler, 2003), leading to the conclusion that CLOCK: BMAL have transcriptional control over *Wee1*. Wee1 then inhibits progression through the G2/M checkpoint to specific times of day. Mutations in *Cry* also lead to changes in *Wee1* expression and function. *Cry* mutant mice have elevated levels of *Wee1* expressed in the liver. Upon hepatectomy, also the regenerating cells proceed though S-phase at a rate similar to wild-type mice (WT), entry into mitosis is delayed and regeneration is subsequently slowed (Matsuo *et al*, 2003). However within $Cry^{-/-}/Cry^{-/-}$ mouse fibroblasts elevated levels of *Wee*1 expression does not seem to affect the timing to mitotic progression, suggesting a context-dependent modulation of the cell cycle (Gauger *et al,* 2005).

In addition, the Delaunay Group (Gréchez-Cassiau *et al*, 2008), recently showed that in mouse liver cells and fibroblasts, the protein kinase p21, a regulator of the S-phase checkpoint complex, is directly regulated by Reverb-α. In $Bmal^{-/-}$ knockout mice, the circadian expression profile previously observed in wild-type mice was

replaced by a non-rhythmic, decreased level of cell proliferation (Gréchez-Cassiau *et al*, 2008). This decrease in proliferation is thought to be due to the decrease in CLOCK: BMAL mediated activation of *Reverbα* transcription. A decrease in *Reverbα,* leads to a decrease in *Reverbα*'s negative regulation of *p21*, and an increase in transcription. As mentioned above p21 plays an inhibitory role in regulating the G1/S checkpoint. In addition p21 can interact with pCNA, inhibits DNA replication and participates in intra-S phase regulation. These combined functioned lead to the decrease in proliferation observed.

Furthermore the *Clock* mutation strongly affects the expression of cell cycle related genes and leads to a reduction in proliferation rates of mouse fibroblasts (Miller *et al*, 2010).

In association DNA repair process and in particular Nucleotide Excision Repair appears to be under circadian control resulting in generation of single-stranded DNA in the form of excision gaps in a rhythmic manner (Kang *et al*, 2009. Kang *et al*, 2010)

Other key genes regulating the cell proliferation and differentiation pathways such as c-Myc, have been implicated as being under circadian control. *Per2* mutations, which are associated with an increase in spontaneous and radiation-induced neoplasm, display increase levels of c-Myc (Lee, 2010). *C-Myc's* promoter region displays canonical E-boxes, the regions used by CLOCK: BMAL complexes to bind and regulate transcription, suggesting direct clock interaction.

The evidence suggests that clock control of the cell cycle may have become a ubiquitous and fundamental mechanism, allowing cells to coordinate important

events such as DNA repair and cell division with the most advantageous times in the external environment. However, whether this phenomenon can be studied in culture is currently rather a contentious issue. In 2004, it was published that mouse 3T3 fibroblasts displayed robust cell autonomous rhythms and that the circadian clock appeared to gate cytokinesis to defined time windows, the subsequent mitosis eliciting a phase shift response in the circadian clock (Nagoshi, 2004). However a recent paper describing work on Rat-1 fibroblasts observed no influence on the cell cycle timing by the clock, through similar techniques (Yoem, 2010). This issue will be discussed in depth later in this thesis.

1.4 THE CIRCADIAN CLOCK AND CANCER

Although the question of circadian/cell cycle interaction is fascinating from a biological standpoint, it is also relevant in a clinical setting. The first suggestion that the circadian clock, or disruption of it, had a role in cancer development was made within Halberg's work of the 1950's (Halberg, 1954). Throughout the 80's, within complementary medicine, the circadian hormone, melatonin, was described as a potent adjuvant therapy for breast cancer treatment, displaying extensive anti-proliferative affects (Miles & Philbrick, 1987). This suggested some influence of the clock upon chemotherapeutic activity through various pathways; however study was limited due to technological requirements. Over the past decade a large body of evidence has grown from different disciplines to confirm the two systems may be linked.

1.4.1 Epidemiological evidence

Intriguingly, there has been a surge in epidemiological evidence linking disruption in clock function to increased susceptibility to cancer in humans over the past 10 years. Current endemic levels of breast cancer were once a "western" phenomenon, but incidence is now rising to "western" levels within increasingly industrialised, developing countries (Stevens, 2005). One explanation for this, and the increase in a number of other cancer types, is the use of artificial lighting regimes, and artificial working patterns linked to industrialisation (Stevens, 2006). The "light at night" theory claims that exposure to artificial lighting conditions through shift work, disrupts the body's ability to entrain effectively to a 24hr time-frame. Subsequently clock outputs, which have potent downstream effects, become similarly deregulated.

The first large scale study to be carried out was The Nurses' Health study involving 121,000 nurses aged less than 55 years old. It showed a 36% increased risk of breast cancer following prolonged periods of rotating night shift-work (colorectal cancer risk increased by 35%, endometrial cancer risk by 43%) (Schernhammer *et al*, 2001. Schernhammer *et al*, 2003. Viswanathan *et al*, 2007). These results were followed by a second Nurses' Health Study, containing a cohort less than 42 years of age at entry. It confirmed a similar increased risk of 36%, and more importantly a relative risk increase of 78% (These cohort studies were independent of other known risk factors) (Megdal *et al*, 2005). Studies involving male shift-workers from two separate cohorts from Canada and Japan independently found an increased risk in prostate cancer in association with prolonged, irregular shift-work (Kubo *et al*, 2006. Conlon *et al*, 2007). One cannot discount the plethora of

variables that must be accounted for when considering industrialised work patterns as a risk factor for carcinogenesis. However, laboratory studies have also produced evidence to confirm a link between circadian function and cancer risk.

1.4.2 Clock polymorphism and Cancer risk

A relatively high degree of polymorphism has been observed within human clock genes (Ciarleglio *et al*, 2008. Von Schantz *et al*, 2008. Hawkins *et al*, 2008. Allebrandt *et al,* 2008) and several of the germ-line clock genes variants have been shown to affect the phenotype of the subject (Takahashi *et al*, 2008). A number of polymorphisms have been shown to influence the risk of developing breast, prostate and non-Hodgkin's lymphoma (Zhu *et al*, 2009. Chu *et al,* 2008. Zhu *et al,* 2007. Hoffman *et al*, 2009. Zhu *et al* 2005. Zhu *et al*, 2008). For example those carrying the rs2305160 variant of clock component *Npas2*, have a lower risk of developing these cancers (Zhu et al, 2005). The mechanism that links SNPs and carcinogenesis remains unclear, it cannot be overlooked that the molecular clock has been documented to interact with the oestrogen, androgen and haemopoietic pathways which play a central role in the development of breast, prostatic and haematological malignancies (Gery *et al*, 2009. Gery *et al*, 2007. Hoffman *et al*, 2008).

1.4.3 Circadian disruption and cancer risk

There is also a distinct association between circadian disruption and prognosis in clinical studies (Filipski *et al*, 2004. Filipski *et al*, 2002. Filipski *et al*, 2005). A number of techniques can be used to measure circadian function within patients. One study looking at a cohort of patients with metastatic breast cancer, measuring

cortisol slopes throughout the day. Cortisol levels normally surge in the early morning and follow a diurnal slope. Patients with a disrupted cortisol slope had a 50% reduced median survival compared to those with normal circadian function (Sephton *et al*, 2000). A number of studies have also looked for signs of circadian disruption within patients with metastatic colorectal disease; A process in which diurnal activity patterns are monitored by actigraphs worn on the patients wrists. Out of a total of 339 patients, 25% showed circadian disruption, which was associated with a 50% reduction in median survival (Innominato *et al,* 2009. Mormount *et al*, 2000).

1.4.4 Circadian control of tumour suppressor pathways

The cellular clock has also for a long time been implicated in the regulation of the cell cycle within the cancerous state. A primary characteristic of cancer is the deregulation of the cell cycle (Goodspeed *et al*, 2007) and apoptosis, and an abnormal high prevalence of neoplastic growth has been seen in subjects with clock mutations, for example, mice carrying the *mPer2*$^{-/-}$ mutation (Fu *et al*, 2002). This study showed that a number of genes, including cyclins, demonstrated circadian regulation, and the hypothesis proposed for the regulation of the G1 checkpoint shares a number of similarities with Matsuo's proposal for G2/M transition (Matsuo *et al*, 2003).

The cyclin/cyclin-dependent kinase complex at the G1 transition has been shown to be under the control of the protein p53, which gates progress and promotes apoptosis. *Per2* loss has been seen to reduce the function of the p53 protein and is associated with a 10 fold increase in tumorgenosis following IR treatment when compared to wild-type (Fu *et al*, 2002). In addition, the oncogene *cMyc* has been

shown to be inhibited by *Bmal*. In humans, *Per1* has also been seen to confer cell cycle regulatory properties and a similar suppressor function (Goodspeed *et al,* 2007. Gery, 2007); Matuso also highlighted the lack of cell proliferation in *Cry* deficient mice. Therefore the clock has a role in cell cycle regulation and tumour suppression (Matsuo *et al*, 2003).

However, additional experiments using other clock mutants paint a much more complicated picture. *Cry* deficient mice lack a functional circadian clock; however display an identical response to IR treatment when compared to wild-type. Combining this cry deficiency with *p53* mutation would be thought to accentuate the pro-oncogenic phenotype of *p53* mutants, however the converse occurs, and the cry mutant appears protective against tumorgenosis. This has also been shown in fibroblast cell lines (Ozturk *et al*, 2009).

Clock and *Bmal* mutant animals, although displaying signs of clock disruption, display no increased incidence of malignancy (Antoch *et al*, 2008. Kondratov *et al*, 2006).

1.4.5 Chronotherpeutics

The effect of genotoxic chemotherapeutic drugs such as cisplatin on cancer cells is dictated, in addition to pharmacokinetic and pharmacodynamics factors, by the cellular response to DNA damage, including DNA repair, DNA damage checkpoints, and apoptosis. Taking into consideration the above literature on the circadian regulation of these cellular mechanisms, it would be logical to consider that timed administration of such agents may increase efficacy. Such time-dependent drug administration is known as chronochemotherapeutics. Small scale trials have

shown dramatic increases in efficacy and reduction in side effects observed (Kobayshi *et al*, 2002). These trials studied the implication of timed chemotherapeutics on gynaecological and genitourinary malignancies. Larger scale trials, although giving positive results have had much more moderate effects (as reviewed Levi & Schibler, 2007). Such chronotherapy is not current implemented on a wide scale within oncology. However as more is understood about the underlying mechanism of these results, it is thought that the practice will become more widely disseminated and accepted. This in turn will allow for greater clinical investigation.

1.4.6 The Role of melatonin

As mentioned earlier, the circadian hormone melatonin has been suggested to have anti-proliferative effects. This indolamine hormone is produced by a number of tissues within the body (gut and retina) (Hill *et al*, 2009), however the major centre of synthesis is within the pineal. Under direct control from the SCN, the pineal synthesises and releases melatonin into the circulation in response to darkness, its secretion being suppressed by light (Reiter, 1980). Melatonin receptors are found within nearly all tissues and systems, wherein it plays a plethora of regulatory roles (Hill *et al*, 2009). In breast tissue, however, it has a much more critical role in the regulation of cell proliferation: thus appearing an ideal candidate to explain much of the epidemiological data (Hill *et al,* 2011)

Under replicated physiological conditions *in vitro*, melatonin has been shown to be a potent suppressor of cell proliferation in oestrogen receptor positive (ER+) cell lines and some oestrogen receptor negative (ER-) cell-lines, (Gonzales *et al*, 2007) with similar results being seen within other cancers types including prostate, ovarian, endometrial, liver and osteosarcomas (Hill *et al*, 2009). This proliferative

inhibition within the breast is thought to be due to melatonin directly suppressing the transcription activity of the oestrogen receptor – alpha (ERα) which in turn is responsible for the regulation of cell proliferation through regulating cyclin activity. (Dauchy *et al*, 2004) But could oestrogen be playing an additive role in this interaction between the clock and the cell cycle? A recent study by the Block group has shown that oestrogen pulsing increases *Per1*, *Per2* and *Bmal* expression within MCF7 cells, a breast adenocarcinoma cell-line (Nakumura *et al*, 2010). This modulation of clock gene expression has also been shown in uterine and ovarian tissues (Nakumura *et al*, 2008). However *Per2* has also been shown to regulate oestrogen receptor activity (Gery *et al*, 2007). *Per*1 has also been shown to play a critical role in the regulation of proliferation within prostatic cancer cells, by modulation of hormonally regulated growth (Cao *et al*, 2009).

1.4.7 Summary of Evidence

Epidemiological evidence suggests there is a gross link between industrialisation and the current increased incidence of cancer. Despite the plethora of variables contained within this hypothesis, specific studies have determined artificial lighting to be a significant risk factor for carcinogenesis. Approaching the hypothesis from a genetic angle, it has been shown that polymorphisms within circadian genes have a significant impact (both positive and negative) upon cancer incidence. Similarly patients with circadian disruption display worse prognoses. However is it not known how this disruption is contributing to disease progression. The wide-reaching influence of the clock means there are many possible confounding. The study of clock mutations and their impact on cell cycle regulators has produced more supportive evidence, and timing of

chemotherapeutic regimes has shown some positive results. However, just as the peripheral clock is believed to be controlled by a multitude of synchronizing factors, it would be possible that the cell cycle is also controlled by multiple output of the clock. Melatonin has been shown to have particular effect on cell growth, suggesting multi-level regulation.

1.5 AIMS

Evidence suggests that the circadian clock is able to influence the timing of the cell cycle, and that this mechanism might be conserved throughout species. Owing to the complexity of the mammalian circadian system, the zebrafish lends itself as a more suitable model for primary studies. This is greatly aided by the direct light responsiveness of cells. The next hurdle in studying circadian phenomena in humans is to develop a reliable synchronisation technique to allow circadian function to be studied in vitro. This will also allow down-stream pathways, such as the cell cycle, to be studied; especially the relationship between the two in the pathological setting.

Therefore, the aims of this thesis are:

1. **To investigate the circadian clocks role in governing the cell cycle with zebrafish, and elucidate key mechanism behind this link.**

   The circadian regulation of mitosis has not been studied in the zebrafish. In this thesis an immunocytochemical approach is used to study the timing of mitosis within zebrafish cell lines. Molecular biology techniques are used to elucidate the mechanism of this regulation.

2. **To develop mechanisms to characterize circadian clock function within human immortalized cell lines.**

   The circadian clock in human immortalized cell-lines has yet to be effectively characterized. This thesis addresses the topic of synchronisation of peripheral clocks in culture, and the use of immortalized cell-lines to

study circadian regulated outputs. Time-course RNA, protein and behavioural studies have been carried out to characterize circadian clock function within HEK 293 cells.

3. **To characterize circadian clock function in benign and malignant breast epithelial cell lines.**

   Clock disruption has been linked to increased risk of carcinogenesis and poor prognosis within cancer patients. Clock influence seems to be greater within hormonally regulated tissues such as the breast. This thesis compares clock function in benign and different forms of malignant breast tissue in culture. This is a novel approach to dissecting the link between these two systems. Cell cycle regulation and progression is also analysed in these cell-lines to investigate further the use of immortalised cell-lines for mammalian circadian research

4. **To investigate the effect melatonin has on circadian clock function within benign and malignant breast epithelium.**

   Melatonin is a key output of the circadian clock and is known to affect growth of breast epithelium. The effect of melatonin on circadian function in peripheral clocks has yet to tested. The hypothesis being that melatonin may play a role in peripheral clock synchronisation due to its strong circadian expression pattern. Here mRNA expression analysis is carried out to investigate the effect acute melatonin pulses have on peripheral clocks and cell cycle regulators.

CHAPTER 2

GENERAL METHODS

2.1 CELL CULTURE

For details of specific cell-lines and individual culture conditions please see the chapter specific methods.

2.1.1. Cell Culture and Counting

All cell-lines were maintained 25cm^3 or 75cm^3 culture flasks (Nunclon Easyfilter, Thermo Fisher Scientific Inc., U.S.A) containing a total of 7ml and 21ml of culture medium respectively. Cultures were maintained until confluent and split at a ratio of 1:3 or 1:5 as required. Passage number was noted for each mammalian cell-line. Frozen stocks of all cell-lines were maintained. Zebrafish cell-lines were kept in freezing media containing Lebowitz 15 medium (Invitrogen at Life Technologies Ltd., U.S.A), 30% foetal calf serum (FCS, Biochrom AG, Germany) and 10% dimethyl sulfoxide (DMSO, Sigma-Aldrich Company Ltd., U.S.A) at -80°C. Mammalian lines were maintained in Dulbecco's Modified Eagle Medium (Invitrogen at Life Technologies Ltd.) containing 10% FCS and 10% DMSO in liquid nitrogen.

2.1.2. Growth Assay

For each cell-type and for each day to be counted, cells were seeded using 2.5ml (100,000cells/ml) onto three wells of a 6 well plates. Each day of the experiment the culture medium was removed and the cells washed with 1ml Trypsin, 0.05% solution with 0.5mM EDTA (Invitrogen at Life Technologies Ltd.). 0.5ml of Trypsin was then added to each well, and the plate incubated at room temperature for zebrafish cell-lines or 37°C for mammalian lines until thoroughly trypsinised. Cells were detached from the plate by tapping. The total volume for each well was then

brought up to 1.5ml with the appropriate growth medium, mixed well and then transferred into a 1.5ml eppendorf tube. Before counting a 50µl aliquot of cell suspension was mixed with 50µl of Trypan Blue (Sigma-Aldrich Company Ltd.). Trypan Blue is a vital dye that selectively colours dead cells blue. 10µl of this mix was then loaded into the two chambers of the haemocytometer (Bright Line Haemocytometer – Cell counting chamber, Sigma-Aldrich Company Ltd.). The number of cells loaded was counted using the haemocytometer following manufacturer's instructions. The average number of cells was then calculated, as was the concentration of cells within the original 2.5ml of medium. The data was then processed using Microsoft Excel® (Microsoft, U.S.A)

2.1.3 Cell Cycle Synchronisation

2.1.2.1 Double Thymidine Block (Early S-phase block)

Thymidine is a pyrimidine deoxynucleoside, which binds to the deoxyadenosine with double stranded DNA. Upon doing so it prevents DNA replication from taking place and the cell arrests in early S-phase (Bostock *et al*, 1970)

Cells were plated onto 6 wells dishes at concentrations appropriate to reach ~70% confluency within 2 days (See cell-line specific growth charts for details). On the third day of culture the culture media was removed and the cells were washed twice with 1ml Phosphate Buffer Solution (PBS, Please see section 2.8.2). 2.5ml of standard culture medium for the cell-type was added to each well with the addition of 2mM Thymidine (Sigma-Aldrich Company Ltd.). Cells were incubated at 37°C for 18 hours. After this the medium was removed, cells washed with 1ml PBS, 2.5ml of the standard culture medium was replaced. Cells were left to 9 hours to release the block. The second block was then performed, the cells were washed

with 1ml PBS and 2.5ml of standard culture medium containing 2mM Thymidine was added to each well. The samples were then left to incubate for 17 hours. The second block was removed in by washing the cells with 1ml PBS and medium was replaced with standard growth medium.

The cells would then synchronously progress through G2/M allowing characterisation of cell cycle progression. Cells were harvested as described for the cell cycle analysis.

2.1.2.2 Serum Starvation (G1 cell cycle block)

Serum starvation of cell cultures results in nutrient deprivation. In response to this cells halt their cell cycle during G1 (Shin *et al*, 2008).

Cells were plated onto a 6 well plate at a concentration appropriate for them to reach ~70% confluency within 2 days (See cell-line specific growth charts for details section 8.1). Following two days of culture, the culture medium was then removed and the cells washed with 1ml PBS. 2.5ml standard cell culture medium without serum or antibiotics was placed into the wells. They were cultured at 37°C for 48 hours. After this time the media was removed, cells were washed with 1ml PBS and standard culture medium with serum and antibiotics was added into the wells. Cells would then be released from the G1 block and progress through the cell cycle. Samples were harvested as appropriate for the experiment.

2.1.4 Cell Cycle Analysis

Cells were plated in 2.5ml media in 6 well dishes and treated as appropriate for the experiment. Upon harvest, culture medium was aspirated and cells were washed with 1ml Trypsin (0.05% solution with 0.5mM EDTA). 500µl of Trypsin was then

pipetted into each well and the plate was placed into the 37°C incubator until the cells were thoroughly trypsinised and would detach from the plate upon tapping. 1ml of culture media was then added to each well and mixed thoroughly with the cells before being transferred into a 10ml glass Falcon® tubes (Scientific Laboratory Supplies, UK). Samples were then centrifuged for 5 minutes at 4°C 2000rpm. The trypsin/culture media supernatant was aspirated from the pellet of cells. Ice cold 70% ethanol was then added drop-wise to the sample will vortexing, to fix the sample and prevent cell clumping. These samples were then stored at -20°C until ready for processing.

Propidium Iodide is a fluorescent molecule, which intercalates stoichiometrically into nucleic acid sequences. When excited with 488nm wavelength light with fluoresces red, and upon binding with nucleic acid this fluorescent signal increases 20 to 30 fold. It can therefore be used to quantitatively assess the amount of DNA within a cell (Krishan, 1975). Owing to its ability to bind to RNA, use of an RNase is necessary. Propidium Iodide is also impermeable to the cell membrane so samples must be fixed prior to staining.

To stain with Propidium Iodide (Sigma-Aldrich Company Ltd.) the samples were first centrifuged for 5 minutes at 12000g 4°C. The ethanol was then aspirated and the cells washed with 1ml PBS, vortexed gently and the spun again for 5 minutes 16000g at 4°C. This PBS wash was repeated another two times. Following this, to ensure that only DNA was stained by the Propidium Iodide, 50µl of 100µg/ml of the ribonucleas RNase (Sigma-Aldrich Company Ltd, Dorset UK) was added to the cells. 200µl of 50µg/ml Propidium Iodide in distilled water was then added to each sample, and left to incubate in the dark from at least 30 minutes.

The levels of fluorescence emitted by these samples were then measured using flow cytometery on a FACS LSR Fortessa cell analyser (BD Biosciences Ltd, UK). The flow cytometery software, FloJo® (Treestar Inc., USA) was used to analyse the fluorescence data. Firstly parameters were set so that only the fluorescent output of singlet cells was processed. This was done by manual exclusion, defining the singlet population by size on a bivariate graph of the cell population. DNA histograms like that shown in Figure 2.1, were then produced for each sample. The exact percentage of cell within each phase can be calculated by applying the Watson Pragmatic Model. This model is a mathematical curve fitting algorithm, which deconvolutes the DNA histogram into three mathematics distributions each representing a population of cells in each phase (Watson *et al*, 1987). The Watson Pragmatic Model was applied through the FloJo® software.

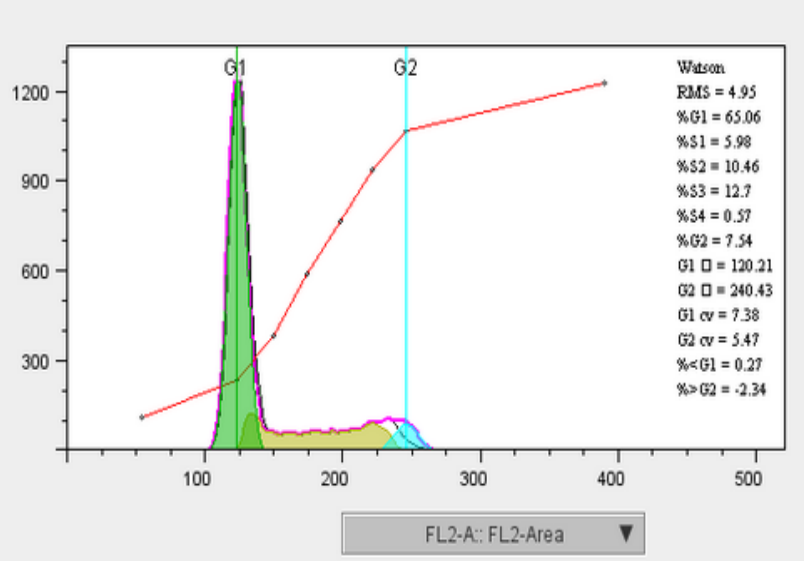

Figure 2.1. Screen shot of Watson pragmatic analysis software. The DNA histogram determined by FACS analysis can be seen outlined in pink. The Watson Pragmatic Model has then determined cell in G1 (green), S (yellow) and G2 (turquoise) (FloJo®)

2.2 MOLECULAR BIOLOGY TECHNIQUES

2.2.1 Total RNA extraction

RNA was extracted from cell culture samples. Cells were cultured on 25cm^3 flasks until the confluency required. Upon harvesting cell culture medium was aspirated and the cells washed with 1ml PBS. This was then aspirated and 1ml of TRIzol® Reagent (Invitrogen by Life Technologies) added to the flask. A cell scrapper was then used to aid removal of adherent cells. After 1 minute of scrapping the TRIzol® Reagent mixture was removed from the flask and added to a pre-labeled 1.5ml eppendorf tube. To homogenise the sample, it was passed five times through a 21 gauge needle and syringe. Once homogenised it was stored at -20°C or placed on ice for immediate processing.

While on ice, 300µl of chloroform was added, and the sample vortexed for 15 seconds and left to stand for 2 minutes. Samples were then centrifuged for 30 minutes at 10000g 4°C. Once centrifuged the sample forms two distinct layers. The top layers was then pipetted away from the second and placed in a new pre-labeled 1.5ml eppendorf tube. 500µl isopropanol was then added to this new tube, and the samples placed at -20°C overnight. The following day the samples were centrifuged for 20 minutes at 10000g 4°C. Following this a clear pellet of RNA could be seen within the tube. The supernatant was removed and the pellet washed with 500µl 75% ethanol. A second spin was carried out for 10 minutes 10000g 4°C. The supernatant was then removed and a final quick spin was performed at room temperature. The remaining wash was removed and the pellet left for 20 minutes to air-dry. Once the pellet was dry it was re-suspended in 20-40µl of purified water. Re-suspended samples were then stored at -20°C.

2.2.2 cDNA Synthesis

cDNA synthesis was carried out using reagents from Invitrogen by Life Technologies. PCR tubes were placed on ice. For each reaction 2µg of RNA was added to each tube and the volume brought up to 7µl with PCR grade water. A master mix containing 1µl of Random Primers, dNTPs, and Oligo DT for each reaction prepared, vortexed and centrifuged. 3µl of this mix was then added to each tube.

The first stage of the reaction was then carried out; samples were heated to 65°C for 5 minutes, and then cooled to 4°C. A reverse transcriptase master mix was then prepared containing 1X Buffer, PCR grade H_20, DTT, RNaseOut™ and SuperScript™ II. 10µl of this mix was added to each reaction. Reverse transcription was carried out via the following program: 25°C for 10 minutes, 42°C for 60 minutes, 70°C for 15 minutes, then cooled to 4°C. cDNA samples were then stored at 4°C until further use.

2.2.3 Polymerase Chain Reaction

Polymerase chain reaction was carried out to amplify fragments of DNA. In this thesis it has been used to isolate DNA fragments that were them cloned and used in bioluminescent and expression vectors. See chapter specific methods for details of primers used and plasmids produced

The Clontech Advantage® 2 PCR system was used (Clontech, Takara Bio Company). Primers were designed using Primer3 (v4.0) Software. Primers were designed to be optimally 20bp in length, have a 50% GC content, and a melting temperature of ~70°C.

PCRs were carried out in a total reaction volume of 50µl containing 100nM dNTP, 100nM of each forward and reverse primer, 1X Advantage® 2 buffer solution, 1X Advantage®2 Taq polymerase, and the DNA template. A "no template control" was run in parallel, containing molecular grade water instead of DNA sample, to check reagents for contamination. The PCR was carried out on an Eppendorf Mastercycle Pro S (Eppendorf Ltd) using the following cycling conditions. For DNA fragments between 1-5kb in length: 95°C for 1 minutes, followed by 25-30 cycles of 95°C for 30 seconds, 68°C for 3 minutes, and finally a 68°C step for 3 minutes. Samples were then cooled to 4°C. Combines annealing/extension temperatures varied depending upon melting temperature of the primers.

2.2.4 Gel Electrophoresis of DNA samples

PCR products were separated and visualised by Agarose Gel electrophoresis. Gels were prepared from 1-1.5% Agarose in 1xTAE (See Section 2.8.1). The Agarose was dissolved in the TAE by heating. After was cooled to approximately 50°C, ethidium bromide (0.5µg/ml) was added. The gel was poured into a sealed tray, and the appropriate sized combed inserted to make loading wells. The gel was allowed to cool on the bench top. 1% gels were used to separate and visualise larger DNA products (250kb - 5kb), 1.5 % gels were used to resolved smaller fragments (<250kb). Prior to loading Blue Loading Buffer (See section 2.8.1) (1X final concentration) was mixed with the samples. 10µl of sample, including loading buffer, was loaded into the well. A 100bp or 1kb Ladder (Fermentas at Thermo Fisher Scientific Ltd.) was loaded onto the gel as a reference. The gel was submerged in 1X TAE in a gel tank and electrophoresed to the desired separation at 120V. The gel was then removed and the DNA visualised on a UVP Bio-Doc™ gel

documentation system (Ultra-violet products Ltd, UK). An image of the gel was then taken and printed.

2.2.5 Gel electrophoresis of RNA samples.

To visual RNA samples and test the quality of the RNA extracted samples were run on a 1% Agarose gel (as described above). 1µl of RNA sample was placed in a 1.5ml eppendorf tube and then 9ul of 11.1% glycerol was then added and mixed with the RNA. This 10µl of glycerol/RNA mix was then loaded onto the gel. The gel was run at a voltage of 120 for 30 minutes. After this the bands of RNA were visualised using A UVP Bio-Doc™ gel documentation system (Ultra-Violet Products Ltd., UK), an image of the gel was then taken and printed.

2.2.6 Band Purification

If PCR products were visualised on the Agarose gel then the band was purified for further cloning. The Gel was viewed on a UV transluminator (Ultra-Violet Products Ltd.); bands of interest were then excised using a scalpel blade. The band was then purified using the Qiagen Gel Extraction Kit (Qiagen Ltd., Crawley, UK) following the manufacturers guidelines for extraction. The DNA was finally eluted in buffer EB supplied by the kit.

2.2.7 Cloning PCR products

2.2.7.1 Ligation

The purified PCR product was ligated into the pGEM®-TEasy vector (Promega UK Ltd, Southampton UK). The ligation reaction was carried out in a total of 10µl containing: 50µl 2X DNA ligase buffer, 1µl pGEM®-TEasy vector (50ng), 1µl T4 DNA ligase buffer (3µ/µl) and 3µl of purified PCR product. The ligation was carried out at 4°C overnight.

2.2.7.2 Transformation

The vector was transformed into XL Gold® competent cells (Invitrogen at Life Technologies Ltd.). The ligation reaction was placed on ice, while the competent cells were thawed on ice. 50µl of competent cells were pipetted into a 1.5ml eppendorf tube, the ligation reaction was then aliquoted into the eppendorf tube, and tapped to mix, and then incubated for 30 minutes on ice. The competent cells were then heat-shocked by placing them in a water bath at 42°C for 45 seconds, after which they were quenched with ice. 500µl of LB broth (See section 2.8.1) was added to the cells and they were incubated in a shaker incubator for 1 hour at 37°C. Prior to transformation LB agar plates (See section 2.8.1) containing the antibiotic ampicillin (final concentration 50µg/ml, Invitrogen at Life Technologies Ltd UK), were warmed in a 37°C incubator and treated with IPTG/XGal (20µl 0.1M IPTG and 20µl 20µg/ml XGal, Invitrogen at Life Technologies Ltd.) for blue/white colony screening. The transformed cells were then spread onto the plates (50µl and 450µl respectively), which were inverted and incubated overnight at 37°C.

2.2.7.3 Mini-plasmid prep

3mls of Luria Bertini Broth (LB) Ampicillin (50µg/ml, See section 2.8.1) was pipetted into sterile 15ml Falcon® culture tubes (Scientific Laboratory Supplies, UK). Single colonies from the bacterial plates described above were then picked using a pipette tip, which was then placed into a culture tube. 10-20 colonies were selected for each plasmid tested. These cultures were grown overnight in a shaker-incubator at 37°C.

The following day approximately 1ml of the culture media was aliquoted into a 1.5ml eppendorf tube. This was then centrifuged for 2 minutes at 13,200rpm room temperature. The supernatant was aspirated from the bacterial pellet and 300ul STET (See section 2.8.1) was added to the tubed and the pellet re-suspended. 10ul Lysozyme (20mg/ml, Invitrogen at Life Technologies Ltd.) was then added to each tube, vortexed and left to incubate at room temperature for 2 minutes. Following this samples were boiled at 100°C on a heat block from 2 minutes. Once removed from the heat block the tubes were then centrifuged for 5 minutes at 10000g at room temperature. The chromosomal debris was then removed from the tube. To precipitate the DNA 150µl 7.5M NH_4Ac and 900µl 100% ethanol was added to each tube and mixed well, before being spun for 5 minutes at 10000g, room temperature. The supernatant was then removed and the DNA pellet washed with 500ul 70% ethanol. The ethanol was then removed and the DNA pellet allowed to air dry. Once the pellet was dry it was re-suspended in 100ul water contain RNase (10mg/ml, Invitrogen at Life Technologies Ltd.). The DNA was then quantified and subject to restriction digest and sequencing as described below.

2.2.7.4 Qiagen Mini-plasmid prep

DNA samples required for sequencing and further cloning were subject to a Qiagen mini-prep to ensure the highest quality DNA was used. For each samples a sterile 15ml culture tube was prepared and 3ml Luria Broth was added. This culture was then inoculated with the bacteria to be tested. It was placed in a shaker-incubator overnight at 37°C. 1ml of the mixture was then poured into a 2ml eppendorf tube and centrifuged at 13,200rpm for 2 minutes at room temperature. Plasmid preparation was then carried out using a Qiagen Mini-Plasmid Prep Kit (Qiagen Ltd.) as instructed by the manufacturers guidelines. Plasmid DNA was eluted into Qiagen elution buffer.

2.2.7.5 Maxi DNA Prep

The inoculated broth (200ml) was placed in a shaker-incubator and left at 37°C overnight. A cloudy culture suggested that the bacteria has replicated. First of all a glycerol stock was made of the culture, 500ul of bacterial culture was added to 500ul sterile glycerol (50%) in a cryovial, vortexed to mixed and then placed directly into a -80°C freezer. The Maxi Plasmid Prep was then carried out using the Qiagen Maxi Plasmid Prep Kit (Qiagen Ltd.) as described below, following the manufacturers guidelines.

The remaining culture was spun at 10000g for 20 minutes at 4°C. Following this the bacterial pellet was re-suspended in 20ml of Qiagen Maxi-prep buffer P1. 20ml of lysis Buffer P2 was the added and gently mixed by inversion. 20ml of neutralisation buffer P3 was the added and again mixed gently by inversion. This mixture was then placed on ice for 30 minutes. Following this incubation the mixture was centrifuged at 10000g for 30 minutes at 4°C. To ensure that all

chromosomal DNA was centrifuged out of solution, a second spin was performed for 10000g for 10 minutes.

During this process a Qiagen-tip 500 was equilibrated using 10ml of equilibration buffer QBT. The column was allowed to empty by gravity. The supernatant from the previous step was then applied to the column and allowed to enter by gravity. Once flow through had occurred the column was washed twice with 30ml wash buffer QC. DNA was then eluted from the column by placing the column into a 50ml falcon tube and pipetting 15ml of elution buffer QF onto the membrane of the column. DNA was then precipitated from the elution buffer by adding 10.5ml of isopropanol, mixing well and then centrifuging immediately at 16000g for 30mins at 4°C. The supernatant was carefully decanted and an additional 2 minute spin carried out to aid removal of residual liquid. The pellet was then left to air dry. The DNA was re-suspended in 100-200µl of distilled water. (If particles did not dissolve a phenol extraction and ethanol precipitation was carried out and the pellet re-suspended).

DNA quantity and quality was then assessed using a Nanodrop™ 2000 (Thermo Fisher Scientific Ltd.) as described below.

2.2.8 Sample Sequencing

For each sample sequenced the following reaction was set up within a PCR tube: 400ng template DNA, 1µl 3.2nM sequencing primer (T7 or SP6, Promega Ltd.), H_20 to 6µl, 4ul Big Dye Mix (Applied Biosystems). The sample was then processed using the following PCR reaction: 96°C for 3 minutes, followed by 25 cycles of 96°C for 30 seconds, 50°C for 15 seconds, 60°C for 4 minutes, finished by cooling to 4°C. DNA was then precipitated by transferring the 10µl PCR reaction into a 1.5ml

eppendorf tube, an addition 10µl PCR grade H_20 was then added to the tube. 2µl of 3M Sodium Acetate, pH 5.2, and 50µl 100% ethanol was then added to precipitate DNA. The reaction was placed on ice for 10 minutes the centrifuged at 4°C for 15 minutes at 10000g. The resulting pellet was washed with 70% ethanol and spun for a further 5 minutes at 4°C 10000g. The pellet was then air dried. Sequencing samples were processed by the UCL Sequencing and Genotyping Center. Resulting sequences were viewed and analyzed using Finch TV Sequence Software (Perkin Elmer Inc, USA)

2.2.9 Restriction Digests

Restriction digests were used for diagnostic purposes or to linearize plasmids for subsequent transcription, both plasmids and PCR products were cut with restriction endonucleases. A typical digest might include 1-10µg of DNA with 1X specific buffer with 1-20 units of enzyme; approximately 1 unit of restriction enzyme digests 1ug of DNA. (Promega Ltd). Most restriction digests were incubated at 37°C for 3-12 hours. The digested fragments were electrophoresed on an Agarose gel (as described earlier) and visualised using A UVP Bio-Doc™ gel documentation system (Ultra-violet products Ltd.), an image of the gel was then taken and printed.

2.2.10 Estimating concentration and purity of DNA and RNA

Nucleic acids absorb UV light with a peak absorbance at 260nm; spectrophotometry can be used to estimate the concentration of RNA or DNA in a solution. Conversion factors for absorbance to concentration for ssRNA, and double stranded DNA at 260nm are: pure RNA at 40µg/ml has an optical Density

(OD) of 1, and pure dsDNA at 50µg/ml has an OD of 1. The following equation can therefore be used to calculate the concentration:

$$\frac{\text{OD of samples at 260nm X total volume(µl) X conversion factor}}{\text{Sample volume (µl)}} = \text{RNA/DNA µg/ml}$$

The absorbance spectra for nucleic acids have a specific shape and they absorb little at 280nm. The purity of the RNA and DNA can therefore be assessed by comparing the absorbances of the sample at OD260nm and OD280nm. Pure DNA shows a ratio of ~1.8-1.9, and pure RNA a ratio of ~1.9-2.0.

The concentration of RNA/DNA was measured using a NanoDrop™ 1000 Spectrophotometer (Thermo Fisher Scientific Ltd.). The machine was first calibrated using 1µl pure molecular grade water. 1µl of each sample was then loaded onto the spectrophotometer and the absorbance spectra measured. The concentration and purity of the RNA/DNA was calculated by the machine.

Only RNA/DNA with an OD260nm/OD280nm ratio >1.7 was used for further investigation.

2.3 REAL-TIME QUANTITATIVE RT-PCR

2.3.1 Description of assay

Quantitative real-time PCR (QRT-PCR) using fluorescent DNA binding dyes allow visualization of PCR product accumulation throughout the PCR. A sample containing higher concentration of target sequence will accumulate PCR products at earlier cycles than a sample with a low concentration. The resulting amplification plots can be used to calculate either the absolute copy number of the target gene relative to a control condition. In the studies presented here real-time quantitative PCR was used to assess relative changes in gene expression.

Real time PCR was conducted using SYBR®green dye (Sigma-Aldrich Company Ltd.). This dye specifically binds to double stranded DNA, following each cycle of PCR as DNA content increases, the fluorescence intensity increases proportionately. The QRT-PCRs were carried out on a Mastercycler® ep. *Realplex*® thermocycler. This system comprises of a built-in thermocycler with 96 well

2.3.2 Primer Design

Since the SYBR®green dye used in these assays binds to any double stranded DNA the PCR must be highly specific. Since no probes are used the specificity of the assay relies on the specific and reliable primers. All the primers used were designed using Primer3 (v4.0) software (developed by the Whitehead Institute and the Howard Hughes Medical Institute) with the following specifications:

1) Optimal length 20bp

2) G/C content at approx. 50%

3) Melting temperatures of between 50-60°C

4) The difference between primer pair melting temperatures to be only 1-2°C

5) Produce a 100-150bp product with Tm below 92°C

6) If possible to have only 1-2 G/Cs in the 3'end (reducing non-specific priming)

7) If possible the product should span an intron to prevent amplification of genomic DNA.

The primer pairs were checked using Primer3 (v4.0) software. This was to ensure that they did not form primer dimers, that they didn't show any complementarity, and to check that no other amplification products were produced from the target transcript. A BLAST search was carried out on the primers to check they were specific only to the target sequence. All primers were synthesis by Eurofins MWG operon, Germany.

2.3.3 Primer testing and product confirmation

Primers were tested in a PCR using the SYBR®green dye, the same reagent that would be used in the final qPCR. A sequence of tests were carried out to ensure that the product of the PCR was in fact the desired target. Firstly the size of the product was confirmed by gel electrophoresis using 10-15µl of PCR product (See section 2.2.5). Secondly the band was purified and sub- cloned into pGEM® - TEasy (Promega Ltd) for sequencing (See sections 2.2.7 to 2.2.8). Thirdly for each reaction a melting curve was performed after the PCR. The shape of a melting curve is a function of the DNA length, GC/AT ratio and sequence. Melting curve can

therefore be used to confirm the correct product and indicate the presence of multiple products, primer-dimers and possible contamination.

The efficiency of each primer set was established by running a standard curve. Primer efficiency can be affected by the length of the amplicon, the GC content, secondary structures such as primer dimers and concentration of reagents.

For the standard curve 5 (2-fold) serial dilutions were made of the sample DNA. The qPCR reaction was then carried out, with each dilution in triplicate with the test primers. These points are then plotted on a standard curve.

The slope of the standard curve can be used to calculate the reaction efficiency using the following equations:

Exponential amplification = 10 (1/slope)

Efficiency = 10(1/slope) -1

If the slope of the standard curve is -3.32 then the PCR is 100% efficient. With a reaction efficiency of 100%, a 2-fold dilution gives a Δct of 1 between dilutions.

2.3.4 Quantitative real-time PCR assay setup

Each QRT-PCR reaction was carried out in a reaction volume of 20µl loaded into a 96-well Twin Tec™ (Eppendorf) plate. cDNA produced by the above mentioned cDNA synthesis was diluted to a ratio of 1:10 with molecular grade water. 2µl of diluted cDNA was added to each well. To help reduce intra-assay variability master mixes were made that contained both primers and SYBR®green PCR Master Mix diluted in water. For each assay 100nM of primers were used. These mixes were made in excess to allow for residual losses during pipetting and on plastic ware.

The quantification for each cDNA sample was carried out in triplicate, enabling a measurement of intra-assay variance. 18µl of master mix was added to each well, mixed thoroughly. The plate was covered with a transparent PCR plate seal and centrifuged for 5 minutes at 4°C. A triplicate of no template control was also set up on each plate to check for contamination.

2.3.5 Thermocycling

The reaction was carried out under the following thermocycling program. . An initial activation step of 95°C for 2 minutes was followed by 40 cycles of 95°C denaturation for 15 seconds, a 58°C annealing step for 15 seconds and a 68°C extension step for 20 minutes. The cycle was finished by a 95°C denaturing step. As an addition measure to ensure efficiency of the reaction a melting curve was then carried out. The cycler temperature was dropped to 60°C for 15 seconds and the raised steadily over the next 20 minutes to 95°C. At this point the assay ended. Fluorescence was measured at the end of every cycle.

2.3.6 Data Analysis

Initial analysis of the data was carried out on the Mastercycler® ep. *Realplex*® thermocycler software. Ct values were given for each test sample. The Ct value (Cycle Threshold) is the cycle number required during the PCR to reach a standardised level of fluorescence; the more abundant the target the lower the Ct. The Ct values for each triplicate repeat were studied. If the standard deviation of these repeats was greater than 0.33, any incongruous replicate was deactivated within the software program.

The relative expression can be calculated within the Mastercycler® ep. *Realplex*® thermocycler software. However, in the thesis, relative expression was calculated manually by transferring the data files into Microsoft *Excel*™ (Microsoft). The following equations were used. In this case relative expression is determined in comparison to a specific sample (X), where the relative expression of X will equal 1.

Ct (Target gene) – Ct (reference gene) = ΔCt

ΔC t(Y) – ΔCt (X) = ΔΔCt

Relative expression = $2^{-\Delta\Delta Ct}$

2.3.7 Normalisation of data

There are multiple steps within the qPCR protocol that must be normalised to ensure data from one reaction set can be comparable to another. A critical parameter to control is the amount of cDNA within each reaction. Although pipetting errors and the quality of RNA are important factors to consider, it is the reverse transcription step that is thought to be source of most variability in q-PCR. (Freeman *et al*, 1999). The variability is due to the react being so sensitive to salts, alcohols and phenol contamination from the RNA extraction.

As an apparent change in expression of a gene in a treatment could be due to differing amounts of cDNA within the PCR, it is important that at least one internal reference gene is assays for each of the samples studied as a control. Reference

genes were chosen as that with most stable expression across all time-points and treatment compared.

Table 2.1 Zebrafish qPCR primers

Primer	Sequence	Efficiency	Accession No.
Reference gene			
RPL13a 5'	TCTGGAGGACTGTAAGAGGTATGC	93	NM_212784
RPL13a 3'	AGACGACAATCTTGAGAGCAG		
Clock genes			
Per1 5'	ATCCAGACCCCAATACAAC	101.81	NM_001030183
Per1 3'	GGGAGACTCTGCTCCTTCT		
Cell cycle genes			
Wee1 5'	GAGCAAAATGCACTTCGTGA	92.01	NM_001005770
Wee1 3'	TGCCCAGGCAGAATAATACC		
Cyclin B1 5'	GTACCCACCAGAGATTGCAG	104.7	NM_131513
Cyclin B1 3'	GGTAGAGGCCTTCCAAAACC		
CDC2 5'	TGTACGCCTGCTAGATGTGC	86.41	NM_212439
CDC2 3'	TGATGGGATGGAGTCCAAAT		

Table 2.1 Human qPCR primers

Primer	Sequence	Efficiency	Accession No.
Reference Gene			
TBP 5'	CGGCTGTTTAACTTCGCTTC (20bp)	97.62	NM_001172085.1
TBP 3'	CCAGCACACTCTTCTCAGCA (20bp)		
Clock Genes			
Per1 5'	ACTTCAGAACCAGGATACCTTCTCA (23bp)	118.12	NM_002616.2
Per1 3'	CTGCTCCGAAATGTAGACGATTC (20bp)		
Per2 5'	TCATGGCATTCATGCTACCC (20bp)	118.35	NM_022817.2
Per2 3'	CATCTCGGATGTGAGTGTG (20bp)		
Per3 5'	GACCTCACCCGGAAGGAGAAT (20bp)	102.36	NM_016831.1
Per3 3'	AAGCTGGGTAAGGCTGCAA (19bp)		
Clock 5'	CCAGAAGGGGAACATTCAGA (20bp)	98.56	NM_004898.2
Clock 3'	TGGCTCCTTTGGGTCTATTG (20bp)		
NPas2 5'	TGGGAACCTCAGGCTATGAC (20bp)	92.45	NM_002518.3
NPas2 3'	AGTCTGCAGCCAGATCCACT(20bp)		
Bmal 5'	GAGCAGCTCTCCTCCTCTGA (20bp)	98.45	NM_001030272.1
Bmal 3'	CGTCGTGCTCCAGAACATAA (20bp)		
Reverb-a 5'	CTTCCGTGACCTTTCTCAGC (20bp)	89.98	NM_021724.3
Reverb a 3'	TCACTGTCTGGTCCTTCACG (20bp)		
Cell Cycle			
p21 5'	ATGAAATTCACCCCCTTTCC (20bp)	101.12	NM_000389.4
p21 3'	AGGTGAGGGGACTCCAAAGT (20bp)		
pCNA 5'	GAACACCAAACCAGGAGAA (20bp)	96.83	NM_002592.2
pCNA 3'	TCTGGCATATATACGTGCA (20bp)		
Cyclin E1 5'	ATCCTCCAAAGTTGCACCAG (20bp)	94.62	NM_001238.2
Cyclin E1 3'	AGGGGACTTAAACGCCACTT (20bp)		
Cyclin D1 5'	TGGCCTCTAAGATGAAGGAG (20bp)	92.45	NM_053056.2
Cyclin D1 3'	GGTTCCACTTGAGCTTGTTC (20bp)		
Cyclin B1 5'	CAAGCCCAATGGAAACATCT (20bp)	91.23	NM_031966.2
Cyclin B1 3'	GGATCAGCTCCATCTTCTGC (20bp)		
p53 5'	AGGCCTTGGAACTCAAGGAT (20bp)	98.7	NM_000546.4
p53 3'	TGAGTCAGGCCCTTCTGTCT (20bp)		
Wee1 5'	ACCTCGGATACCACAAGTGC (20bp)	99.11	NM_001143976.1
Wee1 3'	TACCAGTGCCATTGCTGAAG (20bp)		
cMYC 5'	TCAAGAGGCGAACACACAAC (20bp)	99.3	NM_002467.4
cMYC 3'	TAACTACCTTGGGGGCCTT (19bp)		

Primer	Sequence	Efficiency	Accession No.
Receptors			
ER1 5'	TAAATGCTGCCATGTTCCAA (20bp)	87.7	NM_000125.3
ER1 3'	AATGCAAAGGGGTCTGTGTC (20bp)		
ER2 5'	ACCACAAGCCCAAATGTGTT (20bp)	86.1	NM_001040275.1
ER2 3'	CTTGCTTCACACCAGGGACT (20bp)		
MT1 5'	AGTCAGTGGGTTCCTGATGG (20bp)	96.1	NM_005958.3
MT1 3'	GCACGTAGCAGAGGGAGTTC (20bp)		
MT2 5'	TAATCCTCGTGGCCATCTTC (20bp)	n/a	NM_005959.3
MT2 3'	TAATGGCGATGGCAGTGATA (20bp)		
GR1 5'	GGCAATACCAGGTTTCAGGA (20bp)	97.65	NM_000176.2
GR1 3'	TATGATCTCCACCCCAGAGC (20bp)		
Oncogenes			
BRCA1 5'	AACCACAGTCGGGAAACAAG (20bp)	89.23	NM_007294.3
BRCA1 3'	GGATTTGAAAACGGAGCAAA (20bp)		
BRCA2 5'	TAGGAAGGCCATGGAATCTG (20bp)	88.3	NM_000059.3
BRCA2 3'	TGATGGACGCCAAATACTCA(20bp)		

2.4 WESTERN BLOTTING

2.4.1 Cell preparation and harvest

Cells were plated in 25cm^3 dishes and grown to the confluency required of the experiment. Upon harvest flasks were placed on ice and the culture media was removed. The cells were then washed with 1ml PBS. Into each flask 100µl of lysis buffer (See Section 2.8.3) was pipetted. The samples were then scrapped thoroughly with a cell scrapper. The extract was then transferred into a pre-labeled 1.5ml eppendorf tube. Extracts were homogenised by placing them in a sonication bath and sonicating them for 1 minute. A small aliquot of each sample was removed and placed in a separate tube for protein quantification.

2.4.2 Protein quantification

Protein quantification for 2D assays was carried out using 2D Quant Kit (Amersham Biosciences Ltd, UK) as follows:

Firstly a standard curve control samples were prepared using the assay kit Bovine Serum Albumin Standard solutions. Six 2ml tubes were prepared and into each was put amounts of BSA ranging from 0 – 50µg. The 20µl of the samples to be tested were aliquoted into 2ml tubes also. 500µl precipitant solution was added to each tube, vortexed and left to incubate at room temperature for 2-3 minutes. 500µl Co-precipitant solution was then added, again vortexed and left to incubate for 2-3minutes. The samples were then centrifuged at a speed of 10000g for 5 minutes to sediment the proteins. The resulting supernatant was decanted quickly to avoid the dispersion of the protein pellet. The samples were subject to an additional quick spin at 10000g and any remaining liquid was removed with a micropipette. 100µl copper solution and 400µl distilled water was then added to

the protein pellet and vortexed briefly. 1ml of Colour solution (previously mixed solution) was then added to the samples and mixed by inversion. This was left to incubate at room temperature for 15-20 minutes. The absorbance of the each sample and those of the standard curve was then measured on a spectrophotometer. Absorbance was read at 480nm with distilled H_2O as a control. A standard curve was generated by plotting the absorbance of the standards against the quantity of protein contained. This was then used to quantify the amount of protein present within the test samples.

2.4.3 SDS polyacrylamide gel electrophoresis

The 10% SDS separating gel was made as described in section 2.8.3. The components were gently mixed by inversion and pipetted carefully between the prepared gel plates. A 1cm gap was left between the gel and the top of the plates. This was then overlaid with butanol saturated in H_20 and left to polymerise for 30 minutes.

Once this was set stacking gel (See section 2.8.3) was pipetted into the plates, the 1.5mm gel combs was inserted into the gel and it was allowed to polymerise for 30 minutes.

Once the gels were set they were placed within the running buffer (See section 2.8.3). Each well was rinsed with 1x running buffer before loading the protein samples. Protein Samples were prepared by mixing 1:1 with 2x Limeli running buffer (See section 2.8.3). 10µg of protein was loaded into each well. 2µl pre-stained protein marker (Pre-stained SDS-PAGE Ladder, BioRad Laboratories, UK) was added to the well at either end of the gel. 15µl-20µl of sample in loading buffer

was added to each well. The gel was run at 150 volts constant voltage until samples had entered the separating gel. The voltage was then increased to 200 volts and the gels left to run for 1 hour.

While the gel was running nitrocellulose membranes (one per gel, Whatman® Schleicher & Schuell, Germany) were soaked first in water and then transfer buffer (See section 2.8.3). In the same way filter paper (6 sheets per gel, Whatman® Schleicher & Schuell, Germany) and the transfer sponges were also soaked in transfer buffer.

The protein gel was removed from the running system when the protein samples had reached 1cm from the end of the gel. The stacking gel was removed and the separating gel placed onto the nitrocellulose membrane. The membrane was then sandwiched between the filter papers and transfer sponges. The transfer system was run at 100 volts constant voltage for 1 hour.

2.4.4 Immunostaining

Once the transfer was complete the nitrocellulose membrane was removed and stained with Ponceau stain (Sigma-Aldrich Company Ltd.) to check the quality of protein transfer. If transfer was efficient the membrane was then washed well with H_20 and then placed in 5% milk solution for 1 hour and room temperature to block.

Once the block had taken place, the 1° antibody was diluted in 5% fat free milk powder solution and placed onto the membrane and incubated overnight at 4°C. (See table 2.1 for antibody details).

The following day the membrane was placed at room temperature and washed with 3 x 10 minutes washes with PBT (See section 2.8.2). The secondary antibody was the diluted in 5% milk and placed on the membrane to incubate for 1 hour at room temperature. It was then washed with three 10 minutes washing in PBT.

The rest of the protocol was then carried out within a dark room. The membrane was then placed on saran wrap. 1ml of each reagent from the Amersham™ ECL™ western blotting detection reagents kit (Amersham Biosciences at GE Healthcare Ltd.) was mixed together and then placed onto the membrane to incubate for 5 minutes. Any excess fluid was blotted from the membrane before it was placed inside the exposure cartridge. Amersham™ Hyperfilm™ ECL™ exposure film was then placed onto the membrane and exposed for varying amounts of time dependent upon the experiment, antibody and abundance of protein. The film was then developed within a XoGraph Compact X2 Automatic Processor (Xograph Healthcare Ltd, UK).

The film was then scanned and processed using Adobe ® Photoshop® (Adobe Systems Incorporate)

2.4.5 Quantification of western blot.

Gels were then scanned on a flatbed scanner, with no enhancement (Canon Pixma MP560, Canon, UK). Images were then processed using the Image J®. Gel Analysis program. A control blot was run for each gel and used as a reference in this analysis.

2.5 IMMUNOCYTOCHEMISTRY

Cells were split onto coverslips placed in 4 well dishes (Nunc Greiner through Thermo Fisher Scientific Inc.) at a concentration appropriate for the experiment. To harvest, the culture media was removed from the cells and two PBS washes were carried out. After this 500ul of 4%PFA/4% Sucrose in PBS was added to each well. Cells were left to fix at room temperature for 20 minutes. After this the cells were washed twice with PBS. The samples were then permeabilised using 0.2% Triton-X-100/PBS for 5 minutes, before being rinsed twice with PBS again. A 5% Albumin/PBS block was then applied for an hour. The primary antibody was diluted accordingly in 1% Albumin/PBS and added to each well after blocking. This was left to incubate overnight at 4°C. (See table 2.1 for details of antibodies)

On the second day the cells were given three 5 minutes washes with PBS, before the secondary antibody, diluted in 1% Albumin/PBS was applied and left to incubate for 1 hour wrapped in foil. From now on the samples were kept wrapped at all times, to avoid bleaching the stain. Following this another set of three 5 minutes washes was performed. A 5 minute incubation with DAPI (1:50,000in PBS, Sigma-Aldrich Company Ltd.) followed that was then removed by three further 5 minutes washes with PBS.

The coverslips were mounted onto slides using 10ul of Citifluor™ (Citifluor Ltd) glycerol/PBS. The coverslips were placed facing cells downwards, and then secured to the slide using nail varnish.

Slides were then visualised on a Leica® DM LB fluorescence microscope and imaged using a Leica® DL330f Camera, with IMSO image software (all supplied by

Leica Microsystems, Germany).

Table 2.3 Antibody table.

	Antibody	Company	Application	Concentration
Primary				
	Anti - Phophoshistone H3 (rabbit)	Upstate Biotechnology	Immunocytochemistry	1:1000
			FACS	1:100
	Anti-Bmal H170 (rabbit)	Santa Cruz Biotechnology	Western Blot	1:2000
	Anti-Flag Tag (mouse)	Sigma Aldrich	Western Blot	1:500
			Immunocytochemistry	1:1000
	Anti-α-tubulin	Chemicon	Western Blot	1:2000
Secondary				
	Alexa Fluor 488 goat anti-rabbit	Molecular Probes	Immunocytochemistry	1:1000
			FACS	1:100
	Cy5 goat anti-rabbit	GE Healthcare	FACS	1:100
	Alexa 568 goat anti-mouse	Sigma Aldrich	Immunocytochemistry	1:1000
	goat anti-rat HRP	Santa Cruz Biotechnology	Western Blot	1:1000
	goat anti-rabbit HRP	Cell Signalling Technologies	Western Blot	1:1000
	goat anti-mouse HRP	Sigma Aldrich	Western Blot	1:1000

Table 2.4 Primers for constructs

Construct	5'	3'
zCyclin B1_Luciferase	TGATTCCAGAATAAGTGCTTT	CCATTATTTCTCGAGGTTTATTGC
pcDNA3.1+ His/Myc - Bmal DN	TGGATCTGGGATATCAGAACTGTG	GTGAGCCCTCGAAAGGTTGGG
hPer1_Luciferase	GGCCTCTCTGCGATATCTGTTCTGTTCT	GGACATAGGAGAAGAAGATCTCTCATGGAC

2.6 TRANSFECTION PROTOCOLS

2.6.1 Retroviral Transfection

Day 1: For each transfection a 10cm culture dish was coated with 5mls of 0.1% gelatin and incubated for 10 minutes at room temperature. The gelatin was then removed and the plate washed with 5ml PBS. A confluent 25cm^3 flask of GP2-293 Cells (Clontech, Takara Bio Company), a packaging cells line was the split in DMEM complete media (1:5) onto the gelatin coated plates.

Day2: For each transfection a 15ml culture tube containing 7.5µl 100X PO4 and 375µl 2X Hepes Buffer Solution (HBS, See section 2.8.1, Ph7.1 and a 1.5ml eppendorf tube containing 10µg retroviral plasmid (pCLNCX), 5µg envelope plasmid (pMD.G), 20µg carrier DNA (p BS-SK-), H20 to 367.5µl and 45µl 2M CaCl2 was prepared. All vector supplied by Promega Ltd.

The DNA solution was added drop-wise to 15ml culture tube, whilst it was bubbled using a Pasteur pipette. The solution was then added drop-wise to the GP2-293 cells. They were then incubated at 37°C, 5% CO2 for 4-6 hours before the medium was replaced with fresh DMEM complete medium and left to incubate overnight at 37°C, 5% CO2.

Day3: The medium of the GP2-293 cells was again refreshed with DMEM complete medium.

Day 4: Cells to be transfected were split into 25cm^3 flasks at a concentration of 3.5 x 105 cells/flask.

Day 5: For each transfection 1µl Polybrene (40mg/ml) and 1ml foetal calf serum was added to a 15ml culture tube. Viral media was removed from the GP2-293 cells and added to the polybrene and serum mixture. This was then filtered through a 0.45 um filter into a fresh Falcon® tube (~10ml), and diluted 1:1 with the appropriate culture media forming a total of 20ml.

The medium was removed from the target cells and replaced with 5ml viral medium. The remainder was stored at 4°C. The cultures were re-infected later that day by replacing the 5ml of viral medium.

Day 6: Replace viral media twice during the day.

Day 7: Remove viral medium. Replace with 7ml of standard culture medium, and incubate under standard conditions.

Day 8/9: Check for expression of transfected plasmid.

2.6.2 Lipofectamine transfection

Cells were plated so that they reached ~90% confluency on the day on transfection onto a 6-well plate. The day before transfection the culture media was removed and the cells washed with 1ml culture media without serum or antibiotics. 2.5ml of the plain culture media was then added to each well.

On the day of transfection two 1.5ml eppendorf tubes were prepared per transfection. Into the first tube was placed 100µl OptiMEM™ low serum media (Invitrogen at Life Technologies Ltd.) and 10µl of Lipofectamine® 2000 (Invitrogen at Life Technologies Ltd.). Into the second tube was placed 100µl OptiMEM™ low serum media and 4µg total of plasmid DNA. These two mixtures

were left to incubate at room temperature for 10 minutes. The contents of tube 2 was then carefully pipetted into tube 1 and mixed thoroughly. This was then left to incubate at room temperature for 20 minutes.

After 20 minutes the 200µl of solution was added to the appropriate well of cells. The cells were then left to incubate under standard conditions. After 8 hours the media with Lipofectamine® 2000 solution was removed and standard culture media with serum and antibodies. Expression of the transfected plasmid was tested for after 24-48 hours.

2.7 DATA ANALYSIS AND STATISTICS

Data was analysed using Microsoft *Excel*™ 2010 (Microsoft). Statistical tests were carried out using GraphPad Prism® (GraphPad Software, UK.).

2.8 RECIPES FOR GENERAL BUFFERS AND SOLUTIONS

2.8.1 Molecular Biology

TAE (50X stock): 242g Tris-acetate base, 37.5g di-sodium EDTA, 57.1ml G. acetic acid. Di sodium EDTA and Tris acetate were dissolved in 800ml distilled water then acetic acid and distilled water up to 1 litre were added. This was diluted with distilled water for 1X working concentration (0.4M Tris-acetate, 10mM EDTA).

1% Agarose/TAE (Electrophoresis gel): 5grams of Agarose was added to 500mls distilled water. This was then microwaved for 5 minutes, mixed and microwaved on low power for a further 10 minutes until all Agarose had dissolved. Once cool enough to handle 20µL ethodium bromide was added. This solution was then kept at 55°C to prevent it solidifying.

LB broth: 2.5% (w/v) LB Broth was mixed with distilled water and then autoclaved and allowed to cool.

LB Agar: 3.7% (w/v) LB Agar powder was mixed with distilled water and then autoclaved and allowed to cool.

Ampicillin Stocks: Ampicillin was diluted to 50mg/ml in molecular grade water and stored at -20°C.

2.8.2 Cell Culture and histology

PBS (1L): 10 tablets of Dulbecco A Phosphate Buffer Saline (Oxide Ltd, Basingstoke UK) was added for 800mls distilled water and allowed to dissolves. Volume was then brought up to 1000ml with distilled water. Final formula (g/l) = Sodium chloride 8.0, potassium chloride 0.2, Di-sodium hydrogen phosphate 1.15, potassium dihydrogen phosphate 0.2.

2.8.3 Western blotting

Lysis Buffer (1ml): 20mM Tris-HCL, pH 6.8, 1% SDS, 20% glycerol, H20 up to volume, 2ul 0.5M EDTA, 10ul 100mM Orthovanadate, 10ul Sigma Protease Inhibitor Cocktail.

10% Separating Gel: 4.05ml H20, 2.50ml 1.5M Tris-HCL Ph 8.8, 100ul 10% SDS, 3.30ml Acrylamide/Bis (30%.0.8%), 100ul 10% Ammonium persulfate, 10ul TEMED.

Stacking Gel: 3.70ml H20, 625ul 1.0M Tris-HCL, pH 6.8, 50ul 10% SDS, 670ul Acrylamide/Bis (30%/0.8%), 3% bromophenol blue, 50ul 10% Ammonium persulfate, 5ul TEMED.

10x Running Buffer (2L): Trizma base 60.2g, Glycine 288g, SDS 10g in sterile water.

10x Transfer Buffer (2L): Trizma base 60.54g, Glycine 289.46g in sterile water. To make 2L of buffer add 100ml 10 X stock to 1.4L H20. Mix well, then add 400ml Methanol to the solution and mix again. Store at 4°C.

Laemmli Buffer (20ml): 60mM Tris-Cl pH 6.8, 2% SDS, 10% Glycerol, 5% β-mercaptoethanol, 0.01% bromophenol blue.

PBT: PBS, plus 1% tween 20.

CHAPTER 3

THE CLOCK AND THE CELL CYCLE IN ZEBRAFISH

3.1 INTRODUCTION

3.1.1 Introduction to Danio Rerio

Danio rerio, known more colloquially, as the zebrafish, is a tropical, freshwater fish. It is a member of the minnow family (Cyprinidae), and native to the streams of the Himalayan region. Over the past 10 years the zebrafish has become a favoured model for developmental research due to its rapid, *ex vivo*, in chorion development. It can easily be subjected to a wide range of genetic manipulations. However, it also has a number of unique features that lend themselves to the study of chronobiology, as described below as described below (Carr *et al*, 2005).

3.1.2 Light entrainment and bioluminescence

Zebrafish bodies are highly transparent; however this originally was not seen as an advantage to the circadian biologist under the classical view of a centralised clock. According to this dogma, it was thought that the circadian system in the zebrafish was controlled by master clocks within the eyes and pineal (Menaker et al, 2007). However, in 1998, numerous organs of the zebrafish body – including the heart and kidney – were shown to express core clock genes, the basis of peripheral oscillators (Whitmore *et al*, 1998). In 2000, it was shown that the cellular clocks in these organs were directly sensitive to light and therefore could function autonomously. This, in combination with work by Schibler and his colleagues, brought about the new concept of the decentralised circadian clock (Whitmore *et al*, 2000). These peripheral oscillators remain operational and entrainable even *in vitro* within a cell-line culture.

Studies have shown that the circadian clock is functional very early on in zebrafish development (Kazimi & Cahill, 1999. Ziv *et al*, 2005). In a recent paper it was shown that *Per1* transcription begins autonomously during the first day of development (Dekens & Whitmore, 2008), although rhythms in *Bmal* and *Clock* are not detected until day 3 post fertilisation (Dekens & Whitmore, 2008). Zebrafish cell-lines can easily be produced from embryos or embryonic tissue explants (The Zebrafish Book, M, Westerfield). Owing to their intrinsic light sensitivity, and fully functional embryonic clock, these cell-lines can be placed under differing light dark (LD) cycles, and entrained to these conditions; thus creating a new model for the study of the clock. This system still represents the only directly light-responsive, vertebrate, circadian cell-line model.

This model also lends itself to the use of bioluminescent technologies. Bioluminescence takes advantage of the naturally occurring enzyme luciferase. The luciferase group are a family of oxidative enzymes, the first of which was isolated from the firefly, *Photinus pyralis*. Luciferase's substrate is the light-emitting, biological, photo-pigment luciferin. Luciferase oxidises the luciferin complex and a by-product of this reaction is light (Gould *et al*, 1998).

There are a number of luciferase reporter plasmids now available (Promega Ltd, UK). The promoter region of a gene of interest can be cloned into these vectors so that when the target gene's promoter is activated, luciferase is expressed. In the presence of luciferin it will then react to produce light, allowing bioluminescence to be a measure of target gene expression (Tamai *et al*, 2005). The amount of light emitted by each culture can then be monitored over a sustained time course using an automated luminometer, such as a Packard TopCount™ (Perkin Elmer Inc, USA).

Figure 3.1 shows the results from such an assay. The figure shows data from the P8 cell-line, which is a zebrafish embryonic cells line (of PAC-2 origin, Lin *et al*, 2004) that has been transfected with a *Per1* luciferase construct. This *Per1* luciferase construct was made by cloning a 428bp fragment of the *Per1* promoter into *XhoI* and *HindIII* sites of the pGL3 Basic (Promega Ltd.) luciferase vector. The P8 cell-line was constructed by Dr K Tamai in the Whitmore Lab.

These cells have been placed on forward and reverse Light-Dark (LD) cycles for four days respectivey. After this both cel-lines were placed in constant darkness (DD). Time is indicated in hours but as also *zeitgeber time* (ZT). ZT indicates the time after each *zeitgeber* was given. ZT0, therefore, indicates the time at which the lights were turned on. *Per1* expression levels, reflected through bioluminescent counts per second (CPS) ± SEM, can be seen to oscillate throughout the day on both forward and reverse LD cycles. A peak in expression is observed at ~ ZT3 in respect to each condition. The two traces are in perfect anti-phase with one another, demonstrating that the clock has been able to entrain onto each light cycle. Rhythmic *Per1* expression is seen to continue under DD, demonstrating this variation is circadian in origin. The validity of the bioluminescent reporter can be assessed by measuring endogenous *Per1* expression by Reverse Transcriptase Quantitative PCR (as described later). Critically, endogenous *Per1* expression patterns match those indicated by the reporter (data shown in section 3.3.8).

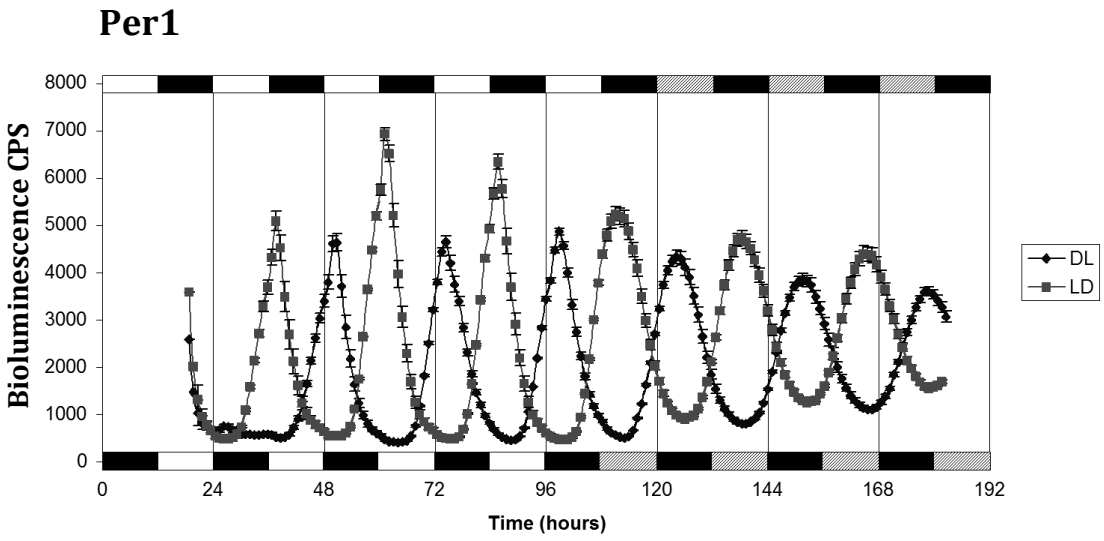

Figure 3.1. PAC-2 cells were transfected with a *Per1* luciferase reporter construct, a clonal population was selected known as P8. P8 cells were places of 12hr/12hr forward and reverse Light-Dark cycles for 4 days and then transferred into constant darkness (DD). This figure shows the bioluminescent trace measured in counts per second (CPS) ± SEM emitted from these cell-lines over the 7 days. Lighting conditions indicated by the white and black bars along the x-axis (LD cycle, lower axis and DL cycle, upper axis. DD is represented by the grey-scale bars) Data produced in collaboration with Dr. K Tamai.

3.1.3 The zebrafish molecular clock

The zebrafish clock appears to be almost a "hybrid" of the *Drosophila* and mammalian mechanisms. Gene duplication has also complicated the system by providing four *Per,* six *Cry* and three *Clock* genes (Hirayama, 2005). One of the main differences is the role played by the clock components *Per* and *Cry.*

Little is yet known about the cellular pathways that allow each peripheral clock to respond directly to light in the zebrafish. Within the *Drosophila* clock, a *Cry* homolog functions as the photoreceptive element. Upon sensing light dCRY interacts and degrades the core *Drosophila* clock protein dTIM. (TIM is the binding partner of PER within the *Drosophila* system) via this mechanism *Cry* coordinates clock oscillations with the external environment (Young & Kay, 2001).

In zebrafish the six *Crys* may have been "divided up" into certain roles, with *Cry3* being a core clock component. *Cry1a* however, although maintaining its mechanistic position, has been shown to be directly light responsive. Intensity and phase response curves reveal a strong correlation with induction of *Cry1a*. Overexpression of this protein causes the clock to apparently stop functioning, in a similar manner to that seen when the clock is placed under constant light conditions (LL) (Tamai *et al*, 2007).

Per2 has also been shown to be directly light responsive (Pando *et al*, 2001). Although this mechanism is not completely understood, this evidence suggests *Cry* and *Per* genes are important contributors to the light response pathway (Tamai et al, 2007).

The expression patterns of core clock genes also differ in the zebrafish compared to *Drosophilia* and mammalian systems. Within zebrafish, all *Clock* and *Bmal* genes are seen to oscillate. This differs from *Drosophila*, in which only *Clock* is rhythmic (Dunlap, 1999), and mouse, in which only *Bmal1* oscillates ubiquitously, while *Clock* expression is tissue specific (Pando & Sassone-corsi, 2002).

3.1.4 The circadian clock and the cell cycle in zebrafish.

Previous studies have indicated that the cell cycle may be coupled to the circadian clock in zebrafish. In a study by Dekens (Dekens *et al*, 2003), S-phase was shown to be rhythmic within zebrafish larvae. In this study, larvae, whose circadian clock is known to be already functioning (Cahill *et al*, 1998), were placed on forward and reverse 12/12 (12 hours of light followed by 12 hours of dark) LD/DL cycles as well as in constant darkness (DD) for a period of 6 days to entrain. Following this larvae were treated at 6 hourly intervals, starting at ZT3, with bromodeoxyuridine (BrdU). BrdU is a thymidine analog and is incorporated into DNA during replication. It is therefore used as an unambiguous S-phase marker (Nunez *et al,* 2001).

Over the four time points studied throughout the 24 hours, a clear rhythm in the level of BrdU incorporation and therefore the number of cells undergoing S-phase could be seen. The peak of S-phase activity was at ZT9, the trough in activity occurring 12 hours after at ZT21. Shifting the phase of the LD cycle 12 hours onto a DL cycle resulted in a coordinated shift in S-phase rhythm. This excluded the chance of developmental activity coordinating the rhythms seen. No rhythm was observed in the S-phase activity in larvae that had been kept in DD and therefore were not entrained.

Dekens went on to show that these rhythms are found throughout the body of the larvae, by presenting work on the larval heart, which showed matching results. This rhythm in S-phase could also be reproduced within the zebrafish embryonic cell-line PAC-2 (Dekens *et al*, 2003).

Within the lab unpublished RNA protection analysis of cell cycle regulators revealed that *Cyclin B1*, the G2/M checkpoint control protein, oscillates throughout the day in entrained the PAC-2 cell-line. Expression peaks at ZT21-ZT3 and troughs at ZT9. This suggests that mitosis is occurring during the last night/early morning. The phase difference seen between this G2/M checkpoint gene and those genes regulating S-phase suggests that most cell cycle activity is gated to periods of lower light intensity. As expected mitosis would happen after, out of phase with DNA replication as seen.

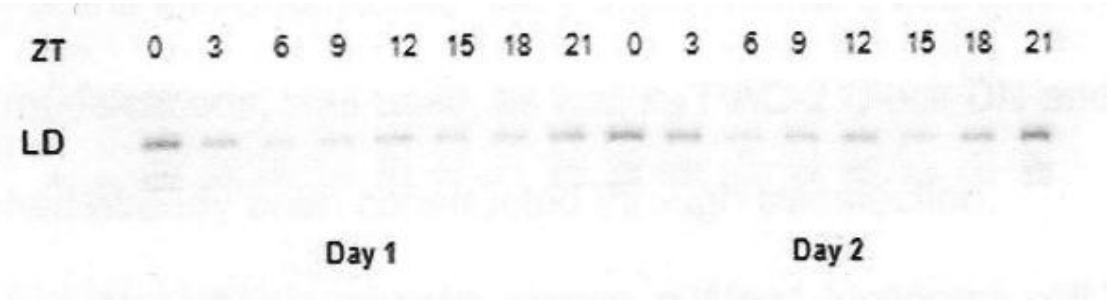

Figure 3.2. PAC-2 cells were entrained on a 12/12 Light-Dark cycle for 6 days and harvested on the 7th day at ZT0, ZT3, ZT6, ZT9, ZT12, T15, ZT18, ZT21. An RNA protections assay was carried out to look at the expression pattern of *Cyclin B1* over all time points. Work produced by Prof. D. Whitmore.

3.2 MATERIALS AND METHODS

3.2.1 Cell lines

For the immunocytochemistry and gene expression experiments the PAC-2 cell-line was used, which contained no genetic modifications, as well as PAC-2 *CLOCK1a DN* and PAC-2 *pCLNCX* cell-lines (PAC2 cell-lines transfection with a clock dominant negative construct and empty vector, used later in Chapter 3). The PAC-2 cell-line is a zebrafish embryonic cell-line originating from 24 hour old embryos (Culp *et al*, 1994). Although the specific cell-types contained within the culture are unknown, it is regarded as a fibroblastic cell-line (Senghaas *et al*, 2009).

For the bioluminescence assays *Cyclin B1* luciferase cell-lines were produced from PAC-2 cells. As a control for these experiments, a *Per1* Luciferase line was used. This cell-line contains a *Per1* luciferase construct, so upon *Per1* promoter activity, the luciferase enzyme is activated and, in the presence of luciferin, luminescence is seen. This construct had been described in conjunction with the P8 cell-line above. Clonal populations were produced via FACS sorted post transfection to ensure a homozygous culture.

Cell-lines were maintained in Lebowitz 15 (L15) medium (Invitrogen at Life Technologies Ltd UK), supplemented with 15% foetal calf serum (FCS, Biochrom AG), penicillin (100U/ml), streptomycin (100µg/ml) and gentamicin (50µg/ml) (Invitrogen at Life Technologies Ltd UK). They were incubated at 28°C in normal air.

3.2.2 Phospho-Histone H3 Flow Cytometry.

PAC-2 cells were plated in triplicate in 25 cm^2 flasks (Greiner) or 6-well dishes (Greiner) at a density of 100,000 cell/ml and maintained on a 12/12 LD cycle for 6-7 days at 28˚C. At the indicated *zeitgeber time* (ZT), cells were trypsinised, washed with PBS, fixed in cold 70% ethanol on day 6 or 7, and stored at -20˚C. To stain for phospho-Histone H3 (PH3), samples were spun at 10000g into a pellet and then blocked in 0.1% albumin in PBS, and incubated in rabbit anti-Phospho-Histone H3 (Ser10) (Upstate Biotechnology) diluted 1:100 in 0.1% albumin for 1 hour at room temperature. Samples were then washed three times with PBS, and incubated in Alexa Fluor 488 goat anti-rabbit (Molecular Probes) or Cy5 goat anti-rabbit (GE Healthcare) diluted 1:100 in 0.1% albumin for 30 min at room temperature. Cells were washed with PBS, treated with RNase A and stained with propidium iodide. 30,000 cells from each sample ($n \geq 3$ for each time point) were then analysed on a LSRII flow cytometer, or BD FACS Array Bioanalyzer in the FACS facility at Cancer Research UK (Lincoln's Inn Fields, London, UK). Using FlowJo software (Tree Star Inc.) and Excel (Microsoft), the mean percentage of cells labelled with phospho-Histone H3 ± SEM was calculated and plotted.

3.2.3 Phospho-Histone H3 immunocytochemistry.

Samples were plated as described in section 2.5 onto four well dishes and processed following the general immunocytochemistry protocol. To stain with Phospho-Histone H3, cells were incubated in rabbit anti-Phospho-Histone H3 (Ser10) (Upstate Biotechnology) diluted 1:1000 in 1% albumin overnight, following washing there were then incubate with Alexa Fluor 488 goat anti-rabbit

(Molecular Probes) diluted 1:1000 in 1% albumin for 1 hour. Slides were then then visualised on a Leica® DM LB fluorescence microscope and imaged using a Leica® DL330f Camera, with IMSO image software (all supplied by Leica Microsystems, Germany). For each experimental replicate, 2-4 coverslips were plated for each lighting condition and cell type. 10 images were taken at 10X from each coverslip for both Phospho-Histone H3 and DAPI staining. These images were then loaded into the Image J® software program in which the number of mitotic cells and total cells per image could be calculated. This data was then processed in Microsoft *Excel*™ (Microsoft), the mean percentage of cells labelled with Phospho-Histone H3 (±SEM) was calculated and plotted.

3.2.4 Packard Assay

Cells were plated in white bottomed, 96-well plates (Greiner Bio-one) at a concentration of 50,000-100,000 cells/well. Cells were incubated overnight at 28°C to allow them to adhere to the plate. The following day the culture medium was removed and replaced with standard culture media supplemented with 0.5mM luciferin and the plate sealed with a plastic TopSeal™ (Perkin Elmer Inc.).

Bioluminescence was measured on a Packard TopCount® luminometer (Perkin Elmer Inc.). The test plate was placed into the TopCount® stacker along with translucent stacker plates. These translucent plates allow light from the two fibre-optic lamps inside the stacker to reach the test plate. Each well was counted approximately every hour. The bioluminescence recorded as counts per second (CPS) was determined by the TopCount® luminometer and recorded using TopCount® software.

Packard data was then transferred into Microsoft *Excel*™ (Microsoft) and processed using the Import and Analysis macro of Kay *et al*.

3.2.5 Bioluminescent plasmid construction

Bioluminescent constructs were produced following the standard techniques described in Chapter 2. They were made in collaboration with Dr K. Tamai.

Cyclin B1 **Luciferase Construct**: A 4kb fragment of the *Cyclin B1* promoter was isolated by PCR from a BAC clone DKEY-267K7 (alternative reference HUKGB735K07267Q from RZPD) using the primers:

5' RI TGATTCCAGAATAAGTGCTTT

3' Xho CCATTATTTCTCGAGGTTTATTGC

Conditions were optimised by Dr Tamai. First this fragment was subcloned into pGEMTeasy™ for sequencing. It was then ligated and subcloned into the *EcoR1* and *Xho1* sites of the pGL3 Basic vector (Promega Ltd.). The construct was named pGL3 Cyclin B1 (4.0)

An additional plasmid was then constructed by ligating pGL3 *Cyclin B1* (4.0) with *HincII* and *HindIII*, and subcloning this 885bp fragment into the *SmaI* and *HindIII* sites of the pGL3 Basic vector. This created pGL3 *Cyclin B1* (0.8).

Cyclin B1_Luciferase Construct with E-box mutation:

Two fragments 5' and 3' were amplified by PCR separately from the p GL3 *Cyclin B1* (0.8). These resulted in the *PmlI* site within the E-box of the promoter being mutated into an *XhoI* site. The 5' fragment was first cloned into the *Acc651* and *XhoI* sites of p GL3, followed by the 3' fragment, which was cloned into the correct orientation into the *XhoI* site.

***Cyclin B1* Luciferase Construct with ΔE-box mutation**:

A ~700bp fragment was of the *Cyclin B1* promoter was amplified by PCR from the pGL3 *Cyclin B1* (4.0) plasmid and cloned into the *KpnI* and *SmaI* sites of the pGL3 Basic vector. This resulted in mutations in the E-box and E –box like elements found within the *Cyclin B1* promoter.

3.2.6 Electroporation

Electroporation of PAC-2 cell-lines were performed using the Nucleofection™ system (Lonza, Germany). 1.5µg of DNA was prepared for each transfection sample. For each transfection cells were trypsinised and then centrifuged for 10 minutes at 10000g, to remove them from suspension. The cell pellets were resuspended in Nucleofector™ solution at a concentration of $1x10^6$ to $5x10^6$ cells/100µl. The 100µl of cell suspension was added to the sample DNA, and then transferred into a cuvette. The cuvette was then placed into the Nucleofector™ for electroporation. The transfected cells were then transferred into a $25cm^3$ flask with standard cell culture medium and incubated at 28°C.

3.2.7 Disrupting clock function within zebrafish cell cultures.

A simple way to clarify whether a rhythmic output is truly circadian driven is to disrupt the clock mechanism within the cell. If the rhythmic output is similarly disrupted one can conclude the clock is responsible for coordination. Within *Drosophila* and mouse a number of clock mutants and "knock outs" are used to study both the clock mechanism and its outputs *in vivo*. These mutations can then be mimicked within the zebrafish. However, owing to the plasticity of the circadian clock and redundancy of some of its components, single-gene mutations do not always have an impact on circadian phenotype (DeBrunye *et al*, 2006)

There is, however, one well-documented, mutation found mouse and *Drosophila*, than results in complete arrhythmicity. The *Clk* mutant in both species harbours a mutation that results in the clock protein acting in a dominant negative manner (Takahashi *et al*, 1998. Takahashi *et al*, 1998. Allada *et al*, 1998). Studies have shown that this mutation leads to a deletion of the Q-rich trans-activation domain of the CLOCK protein, while the bHLH and PAS domains remain intact. The protein product therefore can bind to the *Per1* promoter, but lacks transcriptional activation capacity. The clock mechanism is therefore halted at this point.

A DNA construct comprising of an expression vector containing a truncated version of the zebrafish clock coding sequence was used to mimic this mutation and disrupt clock function within the zebrafish cell-line model. Dr K Tamai in the Whitmore lab generated the *CLOCK1a DN* plasmid used in this thesis.

To make the construct a ~1200bp fragment of the *Clock* coding region was ligated into the *HindIII* and *BamHI* sites of the pGAD vector. At the same time hybridised

oligos, coding for a Flag-Tag (protein sequence DYKDDDK, 1012 Da), with *HindIII-ClaI* compatible ends were subcloned into the expression pCLNCX. The clock fragment was subsequently cloned into the *HindIII* and *XhoI* sites of this new pCLNC – Flag vector.

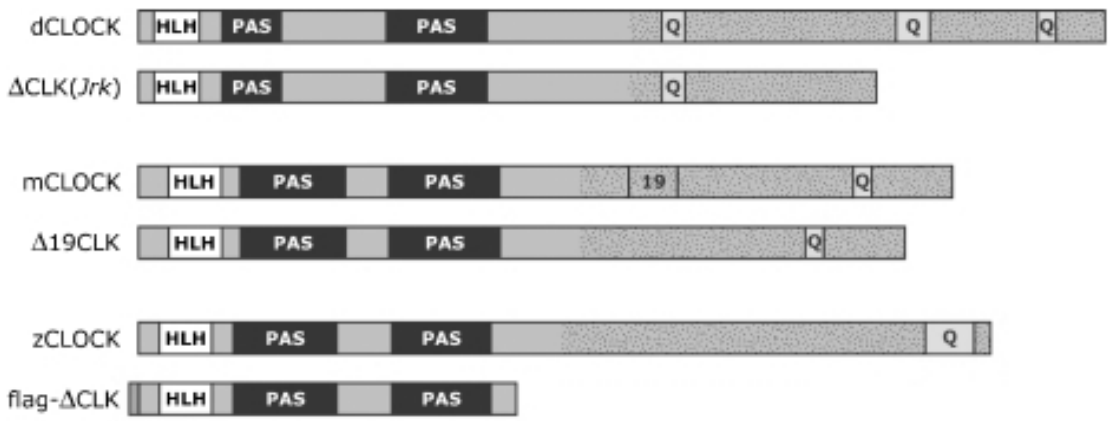

Figure 3.3. Representative diagram describing the structure of the CLOCK protein within *Drosophilia,* mouse and zebrafish. Along with the two naturally occurring CLOCK mutations in mouse and Drosophilia and the constructed equilivant mutation with zebrafish. (B-HLH, Basic Helix-Loop-Helix. PAS (Per-Arnt-Specific sites). Figure adapted from schematic in Dekens and Whitmore, 2008.

3.3 RESULTS

3.3.1 Mitosis is rhythmic within PAC-2 Cells on a LD cycle.

During mitosis, the condensation of chromatin in the nucleus is governed by the phosphorylation of the protein, Histone H3. An antibody to Phospho-Histone H3 was developed in order to study this phenomenon (Hendzel *et al,* 1997). Consequently, expression of Phospho-Histone H3 can be used as a "mitotic marker". Figure 3.4 shows images of PAC-2 cells taken at different stages of the mitosis stained with both Phospho-Histone H3, and the nuclear stain DAPI, which acts as a general DNA marker. It can be seen that Phospho-Histone H3 is expressed in all stages of mitosis with the exception of late telophase.

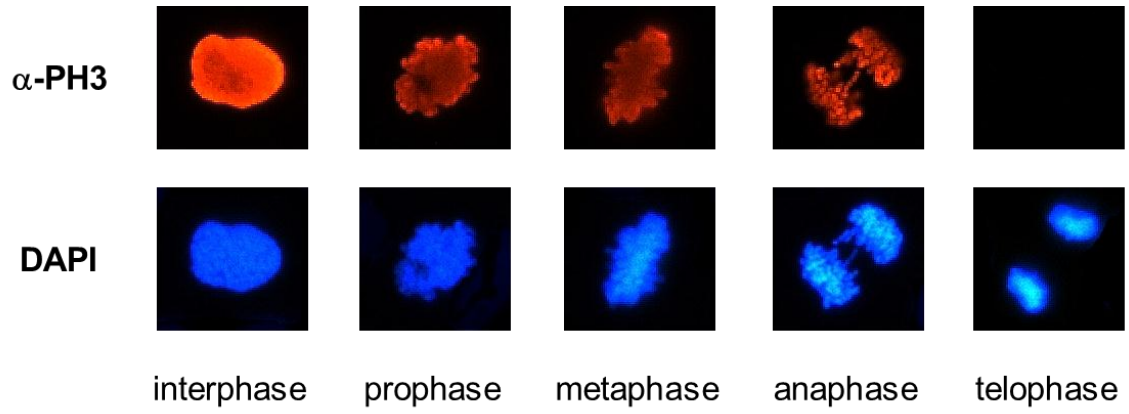

Figure 3.4. A selection of images taken at 60X, showing the florescence pattern of anti-Phospho-Histone H3 (α-PH3) in PAC-2 cells through the different stages of mitosis, accompanied by matching images of DAPI staining.

PAC-2 cells were entrained on 12/12 forward and reverse LD/DL cycles for 6 days and then harvested at ZT0, ZT6, ZT12 AND ZT18 on the 7th day. Figure 3.5 shows a selection of representative images from across all four time-points. It can be seen that there is an increased number of mitotic events, demonstrated by Phospho-Histone H3 staining, at time-points ZT0 and ZT18, with few mitotic events occurring at ZT 6 and ZT12.

The data from these images were quantified using Image J® Software (as described in section 3.2.3), to determine the percentage of mitotic cells within the population at each time-point. Figure 3.5B shows this analysis. Percentage of cells for each time-point is shown ± SEM, n = 3, variation over time was confirmed by one-way ANOVA (* = p-value < 0.05, ** = p-value < 0.01, *** = p-value < 0.001). It confirms that there are more mitotic events occurring during the subjective night/ early morning (ZT0 and ZT18) than the subjective day (ZT 6 and ZT12). On average, across the population 1.5% of cells are estimated to be undergoing mitosis at any given time. At the peak of mitotic activity (ZT18) 3% of cells are undergoing mitosis compared to the trough at activity (ZT12) where less than 1% of cells are dividing.

This experiment was repeated in collaboration with Dr K Tamai and L Young. In order to remove subjective error from hand quantification using Image J®, these phosphohistone H3 stained samples were processed via FACs array (as described in section 3.2.2). FACS analysis allowed a larger population of cells to be tested.

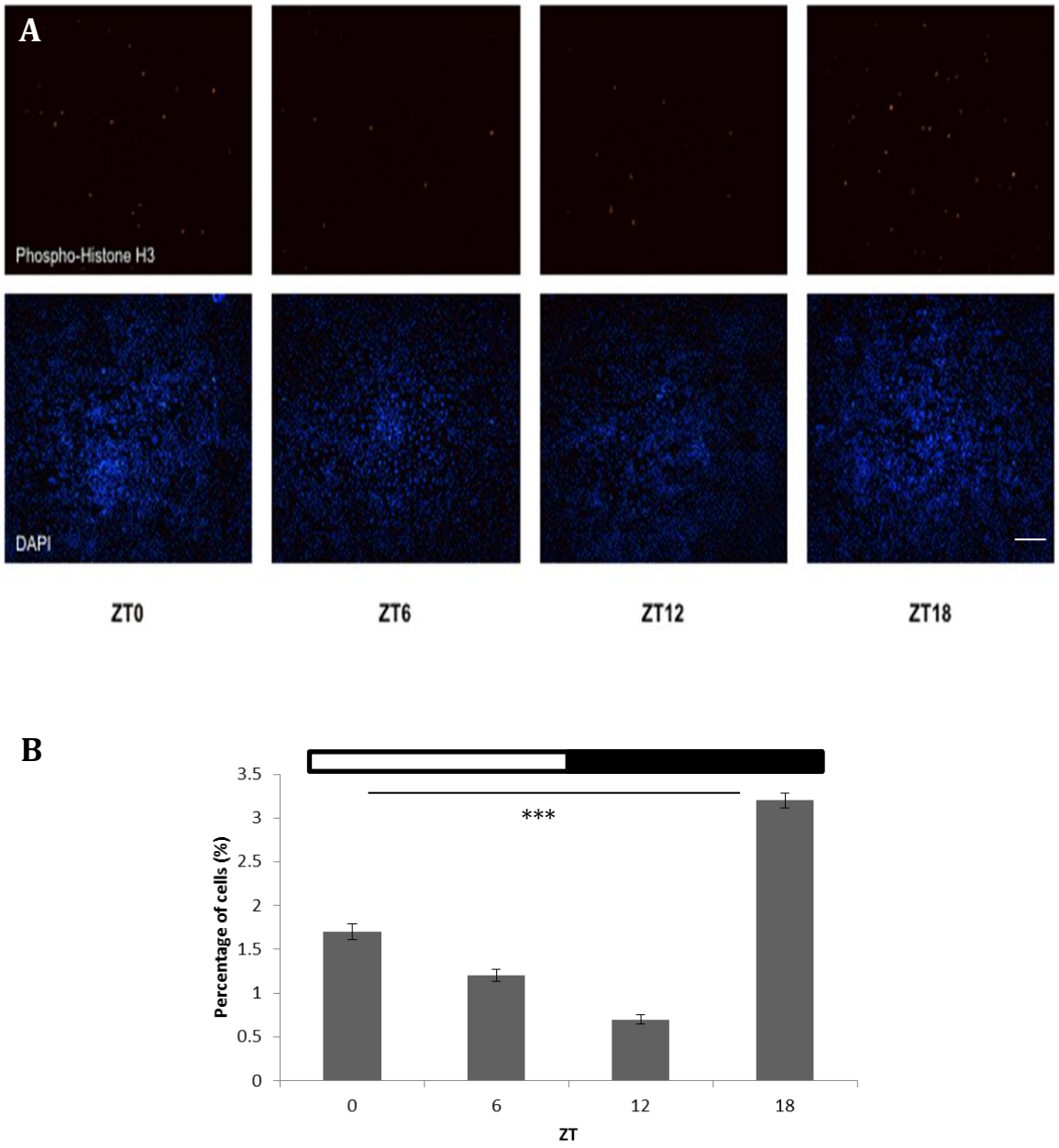

Figure 3.5 PAC-2 cells entrained onto a 12/12 LD cycles and harvested as time points ZT0, ZT6, ZT12 and ZT18. They were subsequently stained with mitotic "marker" phosphohistone H3 and DNA "marker" DAPI. Figure A shows representative 10X images taken of the cells at each time point. Figure B shows the quantification of data produced from these images using the Image J® analysis software. The graph shows percentage of mitotic cells within the population measured +/- SEM, n=3. Variance as analysed using a one-way ANOVA (*** = p-value < 0.001). Scale bar = 100µm.

3.3.2 Rhythmic mitosis in zebrafish cell persists in constant darkness.

As mentioned in Chapter 1, a key feature of a circadian output is that it continues to oscillate even when the zeitgeber is removed. To test whether the variable, mitotic activity described above was circadian, PAC-2 cells were cultured on forward and reverse LD/DL cycles for 6 days and transferred into constant darkness (DD) on the 7th day. Samples were harvested every six hours over day 6 and 7 and stained with anti-Phospho-Histone H3. The percentage of mitotic cells within the population was measured via FACS cytometery.

Figure 3.6 shows the quantified results of this experiment. Percentage of cells in mitosis is shown ± SEM for each time-point, n = 3 (ANOVA analysis confirmed variation across the timecourse *** = p-value < 0.001). It can be seen that the mitotic rhythm described above continues when external lighting cues are removed. This indicated that the rhythm is not the result of a direct light response (in which case no rhythm would have been observed in DD) suggesting that it is circadian in origin.

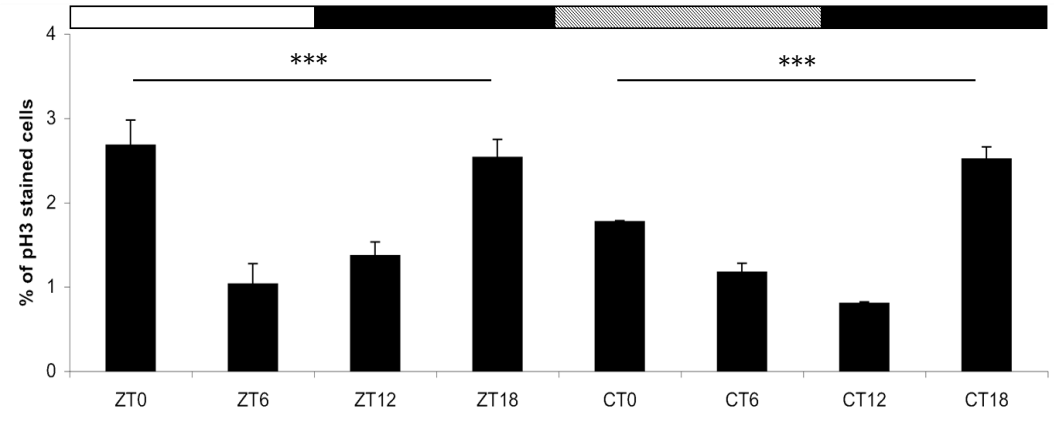

Figure 3.6 PAC-2 cells were entrained on a 12/12 LD/DL cycles for 6 days and transferred onto DD on the 7th day. Cells were harvested at time-points ZT0, ZT6, ZT12 and ZT18 over days 6 and 7. The graph shows the percentage of mitotic cell +/- SEM, n=3. Variance was analysed using a one-way ANOVA (*** = p-value < 0.001) for each time point. Lighting conditions are indicated by the light and dark bars along the x-axis. Percentages of cells were assessed by FACS analysis. Work was carried out in collaboration with Dr K Tamai and L Young.

3.3.3 Rhythmic mitosis is lost in clock mutant cell-lines

PAC-2 cells were transfected using retroviral transfection with a zebrafish *CLOCK1a DN* construct as described in section 2.6.1. This construct codes for a truncated form of the CLOCK protein, which is able to bind to the E-box activation sites within the target promoter, but lacks the Q-rich domain required to activate transcription.

Figure 3.7 shows the effect that this *CLOCK1a DN* construct has on clock function. This mutation has been studied at length previously within the lab (Tamai & Whitmore, unpublished). Figure 3.7A shows a bioluminescent trace of the P8 cell-line (a *Per1_luciferase* expressing cell-line described previously in section 3.1.2) transfected with the *CLOCK1a DN* construct and a *pCLNCX* control. *Per1* expression within the *CLOCK1a DN* cell-line can be seen to be highly attenuated. Figures B and C shows results from PAC-2 cells transfected with the *CLOCK1a DN* and *pCLNCX* constructs. Figure B shows an example image of PAC-2 *CLOCK1a DN* and *pCLNCX* cell-lines stained with mouse anti-Flag-Tag (1:1000, secondary antibody Alexa 568 goat anti-mouse 1:1000) and a matching image stained with DAPI. Expression of the Flag-Tag can be seen in the *CLOCK1a DN* cells. Expression of this protein is confirmed by western using the same antibodies. A protein matching the size of the Flag-Tag, 51kDa, is expressed in the *CLOCK1a DN* cells and is lacking in the control.

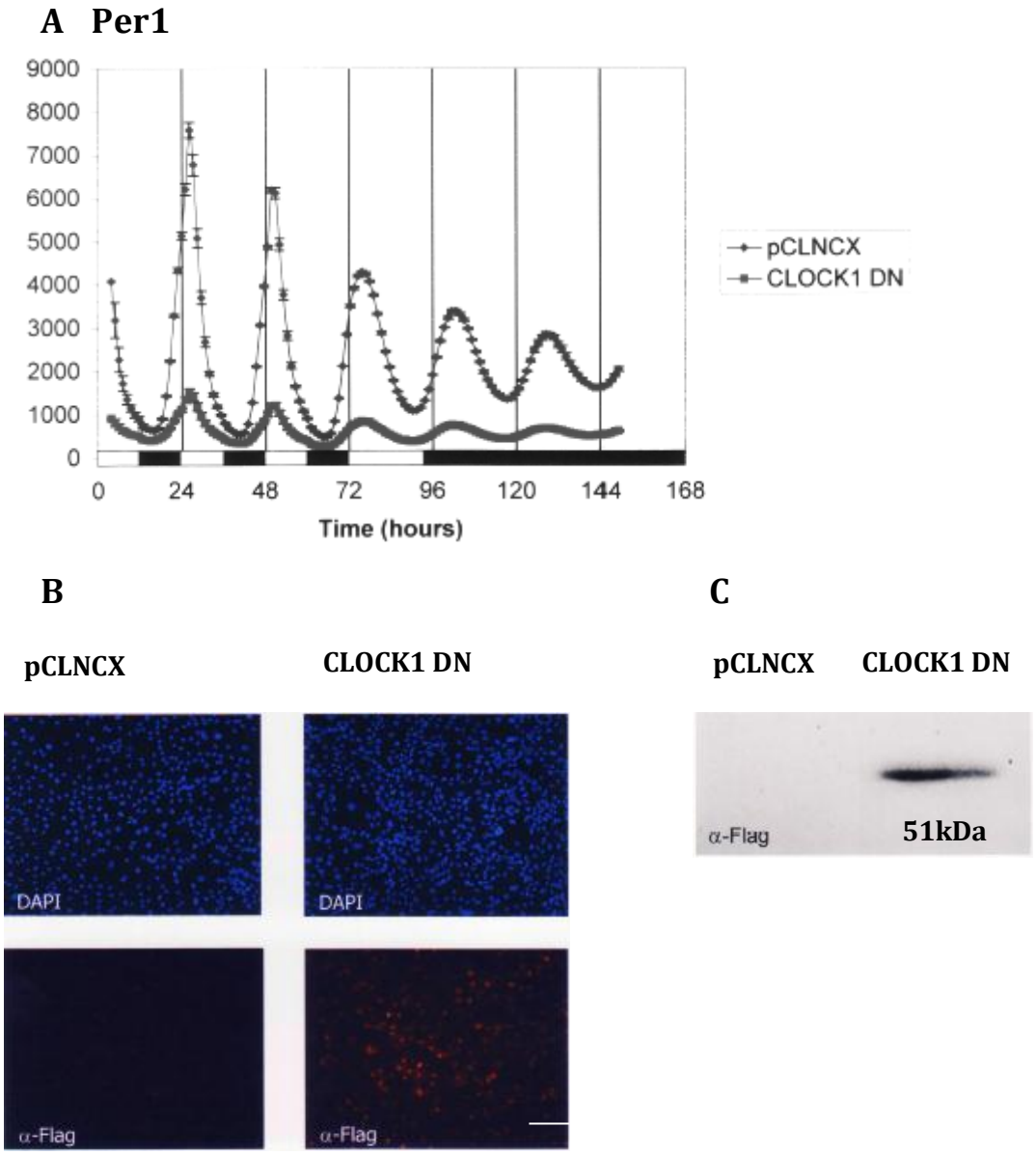

Figure 3.7. Expression of the *CLOCK1a DN* constructs within zebrafish cell-lines. Figure A. P8 cells were transfected with the *CLOCK1a DN* construct and *pCLNCX* as a control vector. Figure shows a bioluminescent trace reporting *Per1* expression shown as counts per second (CPS) ± SEM over 7 days. Figure B shows a representative 10x images of an immunocytochemistry on PAC-2 *pCLNCX* and PAC-2 *CLOCK1a DN* cell-lines stained with an anti-Flag-Tag anti-body and DAPI, Scale bar = 100μm. Figure C shows the results of a western blot on PAC-2 *pCLNCX* and PAC-2 *CLOCK1a DN* cell-lines staining with an anti-Flag-Tag antibody.

The previous experiments were then repeated within the PAC-2 *pCLNCX* and *CLOCK1a DN* cell lines. Both cell-lines were placed on forward and reverse LD cycles for 6 days and on the 7th placed into DD. Samples were harvested every 6 hours during days 6 and 7 and processed accordingly.

Figure 3.8 shows a selection of images showing Phospho-Histone H3 antibody staining for both cell lines and conditions tested. A clear rhythm in mitotic activity with a matching phase to those described in untransfected PAC-2 cells can be seen within the PAC-2 pCLNCX population. This rhythm is seen to continue into DD. No such rhythm is observed within the PAC-2 *CLOCK1a DN* cell-line, either under LD or DD conditions.

These results are quantified in figure 3.8. The PAC-2 *pCLNCX* cell-line displays a clear rhythm with an amplitude of 2%, equal to that seen in untransfected cells. This rhythm is abolished in the clock mutant cell-line. It displays a random pattern of mitotic activity across LD and DD, with the average number of mitotic events across all time-points being lower than in the control population.

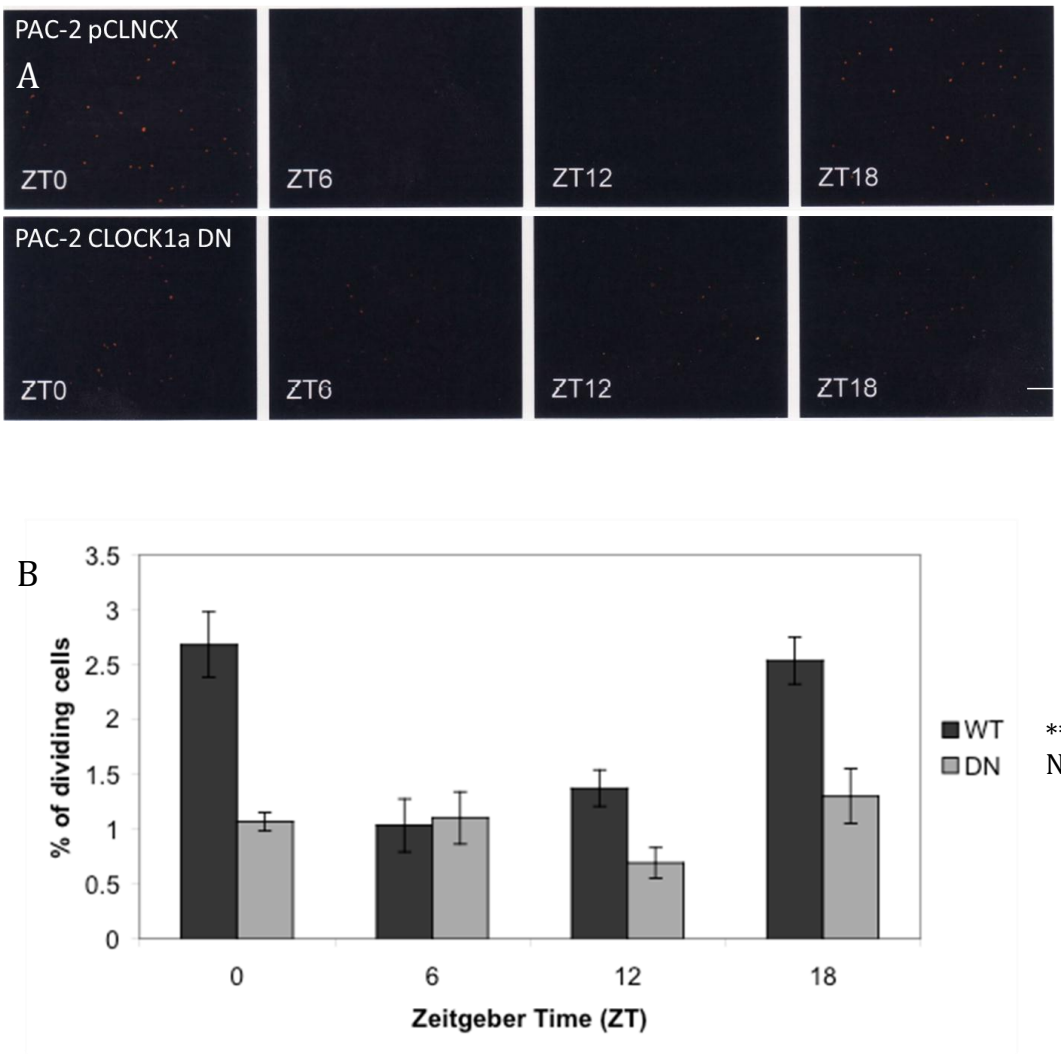

Figure 3.8. PAC-2 *pCLNCX* and PAC-2 *CLOCK1a DN* cell-lines were entrained on a 12/12 LD/DL cycles for 6 days and transferred into DD on the 7th day Cells were then harvested at ZT0, ZT6, ZT12, ZT18 and CT0, CT6, CT12 and CT18 over day 6 and day 7. They were stained with anti-Phospho-Histone H3 and the number of mitotic events assessed using Image J® Software. Figure A shows representative 10X images of PAC-2 *pCLNCX* cells stained with anti-Phospho-Histone H3 across all time point. Figure B shows representative 10X images of PAC-2 *CLOCK1a DN* cells stained with anti-Phospho-Histone H3 across all time points. Scale bar = 100µm. Figure C shows the quantified results of this experiment. Percentage of dividing cells is shown ± SEM, for each time point and cell type. Variance was analysed using a one way ANOVA (NS = p-value >0.05, ** = p-value < 0.01).

3.3.4 Growth of zebrafish PAC-2 is affected by loss of circadian function.

Previous experiments indicated a lower level of mitotic activity within clock disrupted cell-lines. Figure 3.9 shows a growth assay carried out on PAC-2 *pCLNCX* and PAC-2 *CLOCK1a DN* cell-lines concurrently. The graph shows the concentration of cells (cells/ml) ± SEM on each day of culture, n = 3. (* = p-value < 0.05, ** = p-value < 0.01). It can be clearly seen that the PAC-2 *pCLNCX* displays a steady rate of proliferation over the four days with a doubling time of approximately 48 hours. PAC-2 *CLOCK1a DN* cells show a significantly reduced level of proliferation across all four days. This reduction is similar to the limited proliferation seen when PAC-2 cells are placed under constant light (LL, an additional mechanism for disrupting clock function – data not shown). From this assay we can conclude that a fully functioning clock is required for optimal cell growth.

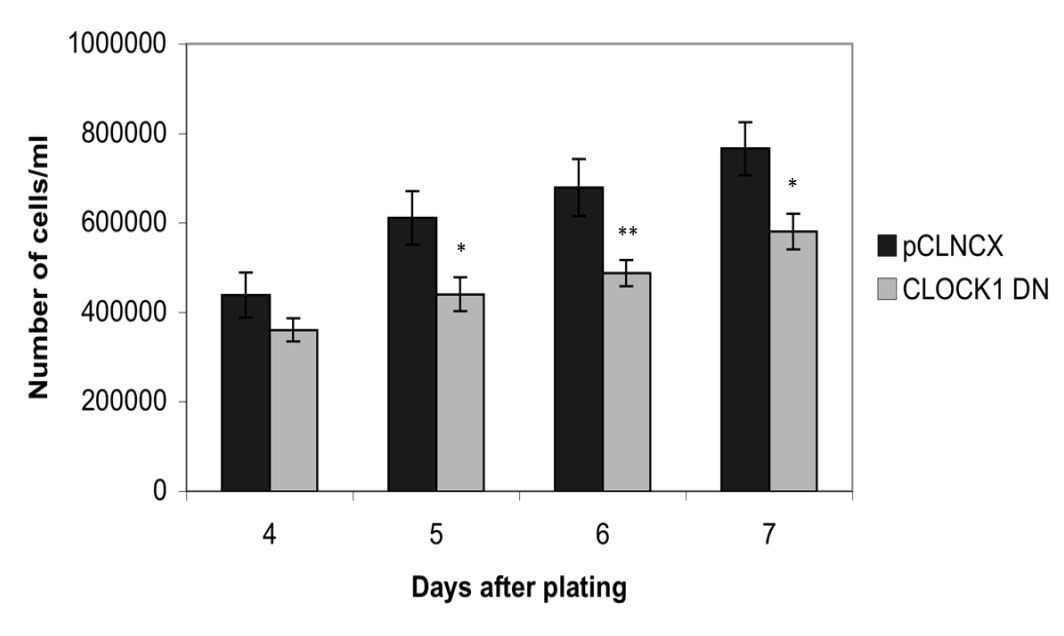

Figure 3.9. Growth rates of PAC-2 *pCLNCX* and PAC-2 *CLOCK1a DN* cells were assessed by growth assay. Cells were plated a 100,000 cells per well and grown for 5 days, assessing concentration each day. Concentration of cells (cells/ml ± SEM, n=3) is shown for each day assayed. Variance was measured by one way ANOVA followed by post-hoc T-test (* = p-value < 0.05, ** = p-value < 0.01)

3.3.5 Expression of mitotic regulators display circadian rhythmicity

Having established evidence for the circadian control of mitosis within this cell-line, it was necessary to elucidate a possible mechanism for this control. From the literature it had been shown that WEE1 was a possible target of circadian regulation within mice. As discussed in Chapter 1 this protein governs phosphorylation and therefore functions of the G2/M checkpoint complex Cyclin B1/Cdc2.

To look for circadian regulation the following work was carried out in collaboration with Dr K Tamai and L Young within the lab. The expression patterns of *Cyclin B1, Cdc2 and Wee1*, along with *Per1* as a marker of circadian function, were monitored over a day within PAC-2 *pCLNCX* and *CLOCK1a DN* cell-lines. Cell-lines were placed on forward and reverse 12/12 LD/DL cycles and harvested at four time-points throughout the 24 hours of day 6. Gene expression was measured using Reverse Transcriptase quantitative PCR (RT-PCR).

Figure 3.10 shows the results of this analysis. Relative expression compared to the reference gene RPL13a is shown ± SEM, n = 3. Results of one way ANOVA analysis id shown (* = p-value < 0.05, *** = p-value < 0.001). The shows the expression pattern of *Per1*. A clear rhythm can be seen within the control cell line, peaking at ZT0 and troughing at ZT 12, in accordance with what has been observed in bioluminescent assays, and showing a 55 fold difference between these two points. It can be seen in the clock mutant cell-line that this rhythm has been completely abolished, with levels of *Per1* expression throughout the day equal to that of the lowest expression level in the control. The circadian clock mechanism is therefore not functioning properly within this cell-line.

The upper panel shows the expression profile of *Cyclin B1*. Within the control cell-line a clear oscillation can be seen throughout the day. Levels of expression vary 3 fold between the trough of expression at ZT6 and the peak at ZT 18. This variation is abolished in the *CLOCK1a DN* cells were the expression pattern is constant and at trough levels in comparison to the control. The expression pattern of *Cyclin B1's* homolog, *Cyclin B2* and their complex partner *Cdc2* shows an identical expression pattern similarly lost within the clock mutant cell-line.

Figure 3.11 shows the expression pattern for the regulator of this complex, *Wee1*. It can be seen that there is no significant variation in the expression levels of *Wee1* over time. Expression analysis of the *Wee1* homolog, *Wee1-like* is also arrhythmic (data not shown).

These results show that the expression of *Cyclin B1* and *cdc2* are under circadian control. The lower fold induction difference seen between the expression of these genes and that of *Per1*, can be easily explained. *Per1* is core clock components and therefore would be expected to display the most robust rhythm. Downstream targets will be regulated by more than one system, therefore the circadian control will be diluted and the rhythm attenuated.

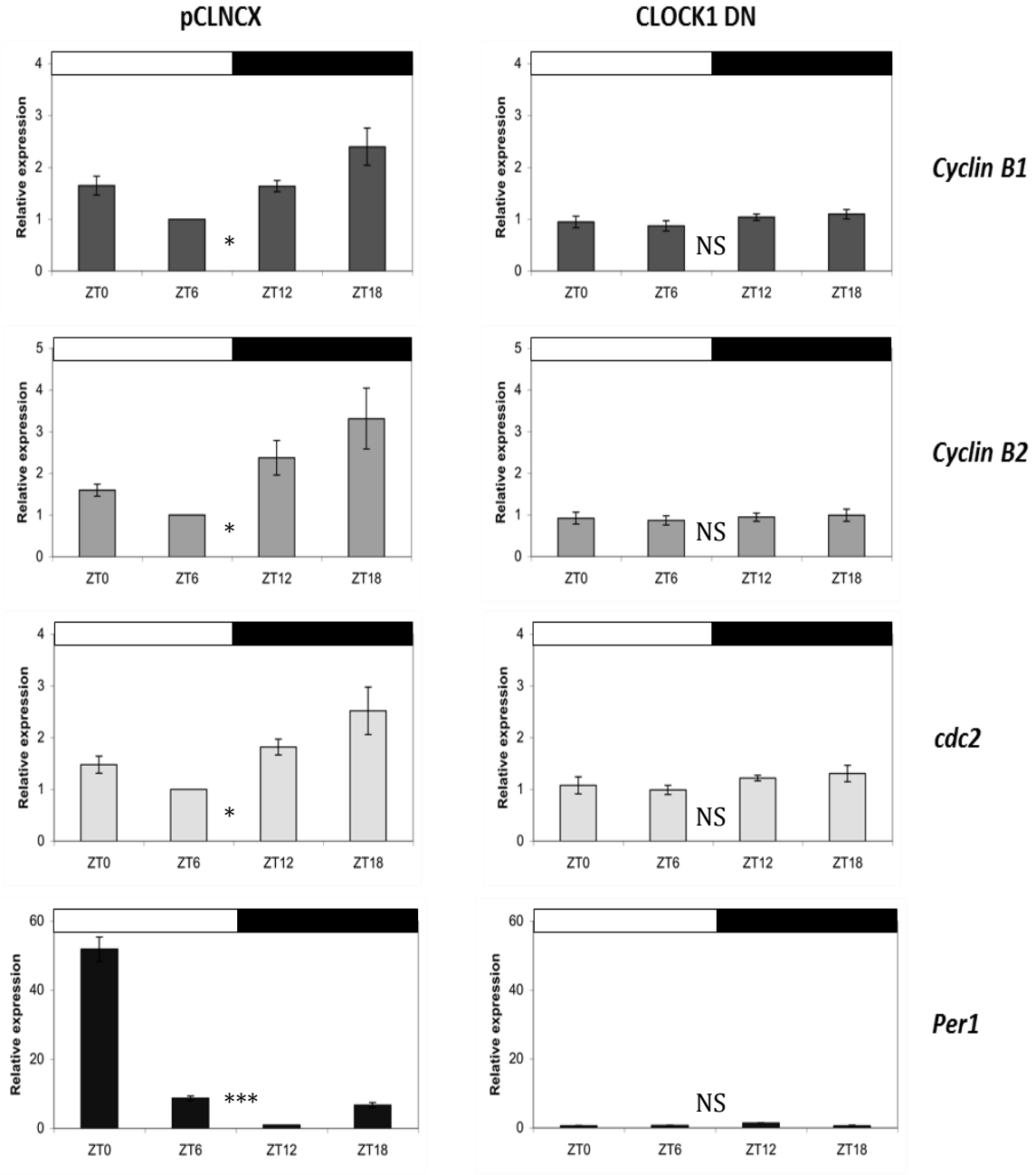

Figure 3.10. Expression patterns of cell cycle regulators was assessed by quantitative PCR reaction. PAC-2 pCLNCX and PAC-2 *CLOCK1a DN* cells were entrained on a 12/12 LD cycle for 6 days and harvested on the 7TH Day at time points ZT0 ZT6, ZT12 and ZT18. Figure 3.10 shows the relative expression of *Per1, Cyclin B1, Cyclin B2* and *cdc2* ± SEM for each time point. All relative expressions calibrated to the reference gene RPL131a and calibrated to the lowest trough value. n = 3. Variance was measured using one way ANOVA (Not significant, NS = P-value > 0.05, * = p-value < 0.05, *** = p-value < 0.001). Figure produced in collaboration with Dr K Tamai and L Young.

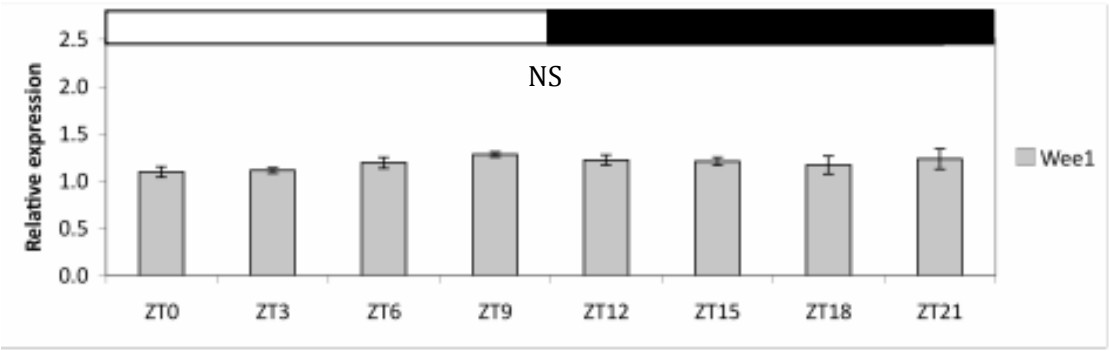

Figure 3.11. Expression patterns of cell cycle regulators was assessed by quantitative PCR reaction. PAC-2 pCLNCX cells were entrained on a 12/12 LD cycle for 6 days and harvested on the 7TH Day at time points ZT0, ZT3, ZT6, ZT9, ZT12, ZT15, ZT18 and ZT21. Figure 3.11 shows the relative expression of *Wee1* ± SEM for each time point. All relative expressions calibrated to the reference gene RPL131a and calibrated to the lowest trough value. n = 3. Variance was measured using one way ANOVA (Not significant, NS = P-value > 0.05). Figure produced in collaboration with Dr K Tamai and L Young.

3.3.6 Bioluminescent reporter cells show circadian regulation of Cyclin B1 expression.

In order to learn more about the possible circadian regulation of *Cyclin B1* expression, a *Cyclin B1* luciferase reporter was generated as described in section 3.2. This was transfected into PAC-2 cells by electroporation as described in section 3.2.6. Figure 3.12 show a bioluminescent trace from this cell-line. Counts per second (CPS) ± SEM are registered per time point, n = 3. Light cycles are indicated by the white and black bars along the x-axis.

Cyclin B1 Luciferase PAC-2 cells were placed onto the Pakard TopCount® for 3 days on a 12/12 LD cycle, on the fourth day the cells were exposed to constant light (LL) for 3 days and then transferred into constant darkness (DD) for the remainder of the experiment. As a control for clock function the P8 cell-line (section 3.1.2) was studied concurrently.

The P8 cell-line shows robust rhythms in luminescence on a LD cycle, peaking at ~ ZT3 as expected, in accordance with previous data. This rhythm is greatly attenuated on the first day after transfer into LL, and completely lost on the subsequent days under LL. This decreased degree of bioluminescence indicates that *Per1* transcription continues but at trough levels. This traces observed within LL are consistent with the theory that constant light disrupts clock function. Upon transfer into DD, bioluminescent rhythms recur with the period of the free-running cellular clock. They can be seen to dampen as DD continues due to lack of entrainment and coordination.

The *Cyclin B1* luminescent trace shows a robust rhythm through the LD cycles with expression peaking during the mid to late subjective night (ZT21-ZT0). This

correlates with the endogenous expression patterns observed above. Upon transfer into LL, bioluminescence becomes arrhythmic and expression of *Cyclin B1* is decreases to baseline. When cells are transferred into DD, a rhythm is restored with the a similar phase difference to the P8 traces as observed in LD. From this it can be concluded that LL a condition known to disrupt clock function also disrupts *Cyclin B1* rhythms and that *Cyclin B1* expression appears to free-run in constant darkness. Expression patterns *Cyclin B1* fulfils the required criteria for a circadian controlled output.

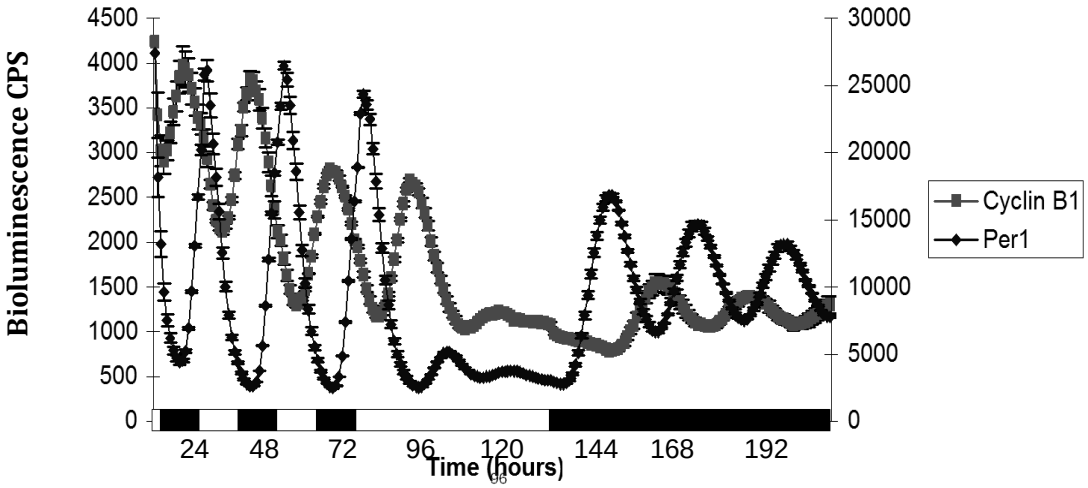

Figure 3.12. PAC-2 cells were transfected with a *Cyclin B1 luciferase* reporter construct. *Cyclin B1 luciferase* and P8 cells were then placed on 12/12 LD/DL cycles for 3 days, transferred into LL for 3 days and then placed into DD for the remainder of the experiments. The figure shows the bioluminescent trace resulting from this experiment. Reporter expression of *Cyclin B1* and *Per1* transcription was measured in counts per second (CPS) ± SEM, n=3, for both cell-lines. Lighting conditions indicated by white and black bars along the x-axis.

3.3.7 The role of E-Boxes in the circadian regulation of Cyclin B1.

The next question to be answered was how the circadian clock influences expression of *Cyclin B1*? As mentioned in section 1.1.4 CLOCK:BMAL heterodimers are known to drive rhythmic transcription of genes by binding to E-box transcriptional activation sites within the promoter regions of target genes. Could *Cyclin B1* be under direct control from these CLOCK:BMAL heterodimers? Sequence analysis of the *Cyclin B1* Promoter region was carried out and it was seen to contain one perfect E-box and two E-box-like sequences. (Dr K Tamai). E-box regions are made up of the canonical, palindromic sequence CACGTG. (E-box like regions, to which CLOCK:BMAL have been found to interact, contain the sequence CANNTG) (Hardin, 2004).

A *Cyclin B1* luciferase cell-lines containing a mutant E-box region (1Emut) and mutant E-box and E-box-like regions (2Emut) was then produced as described in section 3.2.5. Figure 3.13 show the bioluminescent trace taken of this reporter over 6 days of LD cycles, shown with the wild type (WT) *Cyclin B1* luciferase construct as a control. The graph shows bioluminescence measured as counts per second (CPS) ± SEM, n = 3. It can be seen that little difference between the bioluminescent traces of the E-box mutants and the control. The traces remain rhythmic and maintain the same phase. The amplitude of the rhythm is affected, but comparing cell-lines which may have different uptake in copy number of the vector is difficult. This suggests that this E-box region is important for the level of *Cyclin B1* expression but not required for rhythmic expression.

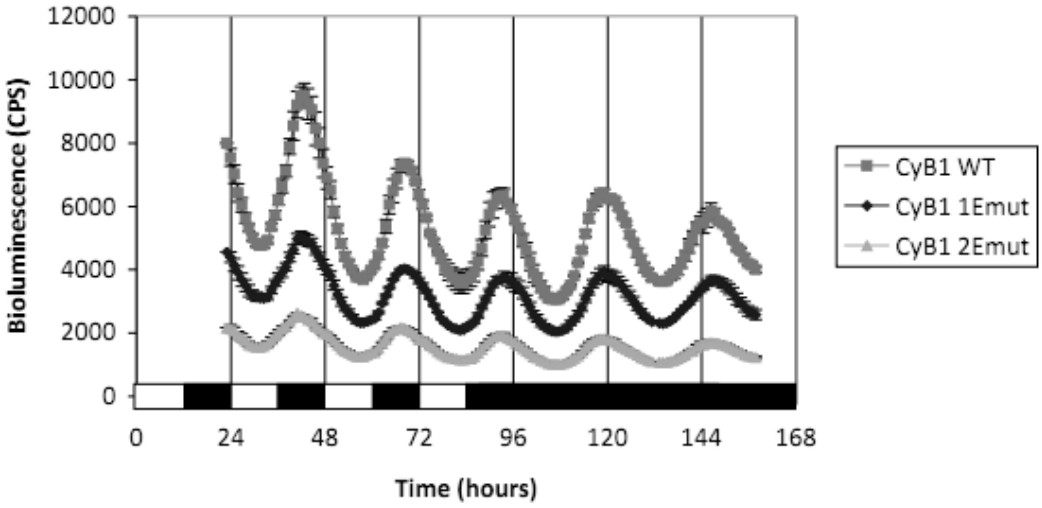

Figure 3.13 PAC-2 cell-lines were transfected with a *Cyclin B1* luciferase constructs in which the E-box (1Emut) and E-box-like (2Emut) activation sites of the promoter had been mutated. Figure shows the bioluminescent trance of this reporter over 4 days on an 12/12 LD cycle before transfer into DD. Bioluminescence is shown in counts per second (CPS) ± SEM, n=3.

3.4 DISCUSSION

Many elements of sunlight, UVb in particular, are known to be harmful to DNA (Ikehata *et al*, 2011). Through the production of genotoxic photoproducts, UV light can cause a number of detrimental mutations that lead to cell malfunction and even death. The cell has therefore evolved numerous strategies to prevent such damage occurring. One such mechanism is to harness light in order to induce and drive repair molecules such as DNA photolyases mentioned earlier in section 1.2.2 (Essen & Klar, 2006). Another method would be to prevent UV exposure of vulnerable DNA, synchronising the cell cycle so that events such as DNA synthesis and mitosis, occur during the night. Such a motive is particularly strong in a model such as the zebrafish, where every cell is open to UV damage.

The timing of DNA synthesis has already been shown in zebrafish larvae to be gated to the late day/early night, where light intensity is decreasing (Dekens *et al*, 2003). Here it can be seen that mitosis occurs in a similar oscillatory manner during the late-night/early dawn. Timing both S-phase and mitosis to the subjective night would greatly decrease the chance of UV DNA damage causing death or mutations being passed onto daughter cells. One can conclude from the initial data that this mitotic rhythm is clearly light sensitive.

However, further conclusions can be drawn from this data, as a complete loss of mitotic rhythm is seen in a clock mutant setting. This is the first time that it has been shown that mitotic rhythms rely on the circadian clock for coordination. Furthermore, light variation is unable to drive or "mask" any clock gene rhythms in *CLOCK1a DN* cells exposed to an LD cycle. This demonstrates that mitosis is

primarily clock-controlled; light itself appears to have little or no influence on rhythmic control of the cell cycle except via the circadian pacemaker.

The rhythmic mitotic activity previously studied in mouse regenerating liver was thought to be produced through direct clock interaction with the mitotic inhibitor, WEE1. Previous studies concluded that *Wee1* was directly light inducible through the *AP-1* pathways in zebrafish (Hirayama, 2005). However the expression levels of *Wee1* in these cell-lines do not show any light induced changes, and in fact, maintain a constant level of expression over time regardless of environmental change. This could be due to differential regulation of genes between different tissues and/or situations. One possible answer for this lack of rhythmicity within zebrafish may come from dissecting of the *Wee1* Promoter sequence.

The *Wee1* rhythms observed in mouse are driven through CLOCK:BMAL heterodimers binding to E-box transcription sites within the *mWee1* promoter (Matsuo *et al,* 2003). No such E-box is found within the zebrafish *Wee1* promoter (Dr K Tamai, unpublished). CLOCK:BMAL heterodimers, therefore, cannot directly influence this genes transcription. Interestingly there is a D-box (Dr K Tamai unpublished) within the promoter, another type of regulatory element utilised by other clock components to coordinate rhythmic outputs (Yan *et al,* 2008). However, this in itself is likely to be redundant due to the lack of rhythmicity seen.

The fact that *Wee1* does not oscillate does not in itself exclude the possibility that it is under some form of clock control. As more research is carried out on clock gene targets, it is being seen that some clock genes have non-circadian functions. Targets of such genes do not display rhythmic oscillation but become deregulated when the clock gene itself is modified (such as those reflected in Beaver *et al*,

2003). For instance, *p53* expression within the PAC2 cell-line is not rhythmic, but expression levels are altered by clock disruption (K. Tamai, unpublished). However, this again does not appear to be the case here, as no a change in basal expression level of *Wee1* is seen in the presence of the *CLOCK1a DN* construct.

In order to further understand whether *Wee1* was truly redundant within the zebrafish, a *Wee1* luciferase reporter construct was generated. A 2.2KB fragment of the *Wee1* promoter was isolated by PCR and subcloned into the *BgII* and *Nco1* sites of the pGL3 Basic vector. However, data from this bioluminescent reporter did not replicate the endogenous expression patterns of *Wee1*, as seen above. The reporter produced a rhythmic expression, which was out of phase for that expect, and was subsequently deemed unreliable and not used for further investigation. Focus was therefore turned to *Cyclin B1.*

Evidence put forward in this chapter suggests *Cyclin B1* may have taken on *Wee1's* role. It is clear that *Cyclin B1* has not developed any direct light responsiveness. If this were the case it would be expected for the expression patterns of *Cyclin B1* to follow a similar phase relationship to that of circadian light induced genes *Per2*, or *Cry1a*. These genes show rhythmic expression rising to a peak just after lights on (ZT3) and falling during the dark phase (Tamai *et al*, 2007). Instead, we see *Cyclin B1* being antiphasic to these genes. The rhythm, however, fulfils the criteria of a circadian output; it is persistent in constant darkness and is entrainable. *Cyclin B1*'s partner *cdc2* displays an identical expression pattern and it can therefore be concluded it is not light inducible either and appears to be a circadian output.

An interesting point of note of note is that the rhythm in zebrafish *Cyclin B1* expression is similar to that reported in regenerating mouse liver (Matsuo *et al*, 2003). This leads us to the question of how is the clock exerting its influence over Cyclin *B1*? It can be in seen that there is a clear phase difference in the expression of *Per1* and *Cyclin B1* genes. This suggests a these genes have differing control pathways. *Per1* transcription is promoted by CLOCK: BMAL heterodimers binding to a combination of up to four E-Boxes found within the *Per1* promoter (Vallone *et al*, 2004). It has been shown that *Cyclin B1's* promoter only contains one pure E-box (CACGTG) and that mutation of the region has no effect on the rhythmic expression pattern observed. In addition the promoter contains to E-box like sequences (CANNTG), mutation of these regulatory site again has little impact of the circadian expression pattern. This result suggests that *Cyclin B1* might not be a direct target of the circadian clock, again, in contrast to the mammalian situation. However, recent studies have shown that downstream circadian regulation is delivered through a number of other transcription factor binding sites, not just E-Boxes. This is described in more detail in Chapter 4.

In this way the system of regulation by the clock may be a lot more complicated than first predicted. It appears that the mechanistic link between the clock and the cell cycle might not be universally conserved, and that different tissues, cell types or even different organisms may use their own unique points of regulation. *Wee1* is important in regenerating mouse liver, but may not be the critical point of regulation in other tissues, or in this case species.

S-phase has been shown to be rhythmic within zebrafish larvae; dissecting the regulatory pathway by which the clock produces this rhythm would in turn shed

more light on mitotic regulation. S-phase has been shown to be rhythmic within the PAC-2 cell-line consist with the previous larval data. It has been found that within the G1/S checkpoint system it is the kinase inhibitor *p21*, is the link between the clock and the cell cycle. Work has shown that the promoter region of *p21* contains a number of E-Boxes, D-Boxes and ROREs, which work together to coordinate the timing *p21* expression.

The use of cell-lines to look at cell biology and behaviour is a complicated situation especially in higher vertebrates here immortalisation is required to create being cell-lines which are not growth limited. The results of cell culture is the artificial selection of cells adapted to the culture conditions, which after several passages may no longer reflect the true behaviour of the original cell population. Work has been transferred into zebrafish embryos in order to validate this cell-line based research, and to investigate the phenomenon of rhythmic cell division during development.

Another major finding within this study is that clock disruption slows growth within the PAC2 cell-line. This contradicts what would have been predicted as loss of clock-control is thought to play a role in accelerated or unregulated cell division in certain mammalian cancers (Filipski *et al*, 2002; Filipski *et al*, 2004). Our results, however, are consistent with observations in embryonic fibroblasts isolated from *clock* mutant mice, and in cells virally transfected with small interfering RNA constructs against mouse *Clock*, which show a significant decrease in growth rate compared to controls (Miller *et al*, 2007. Antoch *et al*, 2008). In the case of zebrafish, it is clear that possessing a functional cellular clock is not only essential for cell cycle timing, but also for achieving optimal growth rates.

In conclusion, this study has shown

- That mitosis within the zebrafish cell-line PAC2 is under circadian control; peaks in mitotic activity occur during the late subjective night and early morning.
- Within this cell line, circadian regulation is directed through clock targeting of G2/M checkpoint protein, Cyclin B1. However, the exact mechanism of interaction requires further exploration. E-box binding activity by clock components does not affect the circadian expression of *Cyclin B1*, suggesting clock regulation of this gene is through a number of pathways.
- Clock control of the cell cycle is a conserved phenomenon between species, the mechanism of this control is not. *Wee1* is the putative circadian target within the mammal. Here we show *Wee1* displays no characteristics of being under circadian control, the role being past to *Cyclin B1* instead.
- The circadian clock is crucial for optimal cell growth. This leads us to question the underlying mechanism by which clock disruption leads to increased incidence of neoplasm. This work has major implications for clinical understanding and study. However, the species specific modification of cell-cycle control seen within this chapter, leads to the conclusion that this work must be translated into a human model.

CHAPTER 4

Characterisation of the circadian clock in human cell lines.

4.1 INTRODUCTION

4.1.1 The Human Clock

The human circadian clock has been a subject of study for decades, far preluding the recent advances in understanding the mammalian molecular clock and its extensive influence. Physiologists and medical practitioners have noted, studied and utilised the 24 hour variations in physiology, circulating hormone levels and behaviour patterns for decades preceding these developments (Manchester, 1933). As a consequence the majority of human circadian research, until recently, has revolved around easy to monitor, gross circadian outputs such as sleep and behaviour patterns.

However, although knowledge of the clock is expanding rapidly, translation of this into human studies is slow (Takahashi *et al*, 2008). The recent discovery that clock function can be species specific (Kay & Young, 2005) and even further tissue specific, (Ko & Takaahashi, 2006) dictates a need to study the human circadian clock itself in much greater detail.

There are, however, major impediments to translating these advances into human studies. These are mainly the difficulty and expense incurred when assessing circadian function within people. Circadian experiments require strict regulation and temporal isolation (Aschoff, 1965. Czeisler *et al*, 1999). The demand on resources and facilities means there are only a hand full of suitable institutions, test subjects and means available (Takahashi *et al*, 2008).

Surrogate measures are therefore used to study the circadian clock within humans (Takahashi *et al,* 2008). From a functional or behavioural perspective, estimating a person's "chronotype" can be used to study how clock function affects downstream targets. For example a person's sleep/wake patterns and physiological markers can be used to assess the phase of entrainment of that person when living in the real world. This lends itself to association studies; looking at the relationship between a certain chronotype and a pre-established outcome, such as incidence of a disease (Ancoli-Israel *et al*, 2003. Horne *et al*, 1976. Sack *et al*, 2007). However, it does not allow assessment of the circadian clock mechanism itself.

Therefore, a second approach has been developed. The circadian clock can be studied *in vitro* using cell cultures, grown from people following biopsy or harvested as primary samples using phlebotomy. In 2005 members of the Brown Group (Brown *et al*, 2005) developed a technique to take skin biopsies from patients and culture the fibroblasts from the tissue. Using *Per1* luminescent constructs they were then able to monitor circadian function within these fibroblasts.

Due to the similar availability and ease of sampling, as mentioned above, blood samples have been frequently used to study human circadian function. Human peripheral leukocytes display robust circadian outputs. Peripheral blood mononuclear cells and polymorphonuclear neutrophils show strong 24 hour oscillations in *Per1, Per2* and *Per3* expression, in phase with the donor subject's environment (Kusangi *et al*, 2004. Fukuya *et al,* 2007. Teboul *et al*, 2005). Interestingly these cells do not display an antiphase rhythm in *Bmal1* expression. (Kusangi *et al,* 2004, Fukuya *et al*, 2007). In a recent study, expression levels in 10

core clock genes were measured within a cohort of patients to assess phase entrainment to the external environment. All 10, with the exception of *Clock,* were found to be strongly rhythmic, and in particular variations in *Per1, Per2* and *Per3* expression were noted to be characteristic of certain chronotypes (Kusanagi *et al*, 2008). Blood samples can also be studied in culture, and maintain robust circadian rhythms (Ebisawa *et al*, 2010).

Interestingly, circadian rhythms have also been monitored in erythrocytes. These cells contain no nucleus, and therefore DNA, and as a result would not be expected therefore to be able capable of circadian functions – transcription being the basis of the clock. However, highly conserved anti-oxidant proteins undergo ~ 24h hour redox cycles, which are able to persist for days in constant conditions (O'Neil & Reddy, 2011). This study points to the circadian system in mammals being more sophisticated than originally assumed.

However, considering that clock function is so tissue specific (Ko & Takahashi, 2006) it was necessary to expand this cell-culture model into other cell-types. Over time, the theory of clock regulated cell division has become more prominent, and clock disruption has become similarly associated with deregulated cell-growth and an increased incidence of neoplasm. This has precipitated studies of clock function within a number of human cancer cell-lines including pancreatic, hepatic, colorectal carcinomas and myeloid leukaemia (Oda *et al,* 2009. Sato *et al*, 2009. Oshima *et al*, 2011. Yang *et al*, 2011). Benign tissues such as the retinal and intestinal epithelium have also been studied (Yoshikawa *et al*, 2008. Pardini *et al* 2005).

However, these studies have not looked at circadian function over a time course; rather the effect modulating clock function has on downstream pathways. The lack of such *in vitro* study is due to the nature of peripheral clock entrainment.

4.1.2 Synchronisation of peripheral clock in vitro

As mentioned in section 1.1.3 peripheral clocks *in vivo* are synchronised into phase with the master clock and external environment by a culmination of neuronal, hormonal and metabolic factors (as reviewed in Dibner *et al*, 2010). This web of 24 hour cycles is impossible to replicate in an *in vitro* setting. However, synchronisation of mammalian peripheral clocks in culture has been achieved by modifying these signals.

It was first shown that serum shocking Rat-1 fibroblasts and H35 hepatoma cells in culture could synchronise their cellular clocks and produce rhythmic clock gene outputs. Circadian outputs were characterised by monitoring mRNA levels of clock genes using RNA protection assays. Robust oscillations of up for 3 days were elicited in clock genes *Per1, Per2* and *Rev-erb-α.* These rhythms corresponded with those observed in the animal *in vivo* (Balsolobre *et al*, 1998). Serum shocking is not an unlikely method of coordinating peripheral clocks as serum contains a lot of the humoural components known to influence peripheral clock function *in vivo*. Another notable result from this study was that *rPer* genes behaved in a similar way *to c-fos* after stimulation, displaying characteristics of immediate response genes. However, this response could hold the key to understanding the subsequent rhythm generation (Balsolobre *et al*, 1998).

This technique was later refined. It was shown that by pulsing the cells with dexamethasone alone, it was possible to produce coordinated clock outputs

(Balsolobre *et al*, 2000A). Dexamethasone is a synthetic glucocorticoid. Glucocorticoid signalling is one of the most prominent coordinating factors *in vivo* as described in section 1.1.3. Using a 100nM pulse of dexamethasone, rhythmic gene expression was produced in Rat-1 fibroblasts as well as transiently changing the phase of clock gene expression within the liver, kidney and heart upon injection *in vivo* (Balsolobre *et al*, 2000A). Interestingly, the rhythms of the SCN remained unaffected.

The same group then went on to test a variety of difference putative synchronisers. They found that cAMP, protein kinase C and Ca2+ can all transiently produce rhythms in *Per1* within Rat-1 fibroblasts (Balsolobre *et al,* 2000B). This once more suggests that the SCN utilises a number of different chemical pathways in peripheral clock co-ordination.

Additional studies have added even more agents to the list of possible synchronisers. Other stimulating agents have been used in order to produce bioluminescent traces that can be used in modelling the human clock . Forskolin, ethanol and DMSO pulsing was shown to produce rhythms in bioluminescence of a *Per1* reporter construct in these cells (Izumo *et al,* 2005). Furthermore, a study investigating the link between the clock and the cell cycle within fibroblasts, described the act of plating and changing the growth medium as producing coordinated circadian gene expression in their cell cultures (Gréchez-Cassiau *et al*, 2008).

Employing other methods, found *in vivo,* has also been successful. Temperature entrainment has been observed in fibroblasts *in vitro* on specific temperature cycles (Brown *et al*, 2002). Rat-1 fibroblasts were placed under a square wave

temperature rhythm with a (Delta) T of 4°C (12 hour 37°C/12 hour 33°C). Although these cycles were not able to elicit rhythmic gene expression *de novo*, they preserved such genes expression in synchronised populations, while rhythms in cultures maintained at constant temperatures damped over time (Brown *et al,* 2002).

In conclusion, there appears to be a number of suitable synchronisation methods to coordinate peripheral clocks in fibroblast culture, however little synchronisation work has been carried out within other cell-types, and must be further explored if tissue specific cellular models are to be defined.

4.1.3 Glucocorticoids and the Clock

4.1.3.1 Introduction to the glucocorticoid system

As mentioned above, glucocorticoid signalling plays a central role in the multifactorial synchronisation of peripheral clocks. Due to its far-reaching affect they have been used as the most robust agent for eliciting circadian rhythms in peripheral cell culture. Glucocorticoids are secreted by the adrenal gland in response to "stress" and physiological demands, primary control coming from the hypothalamic-pituitary axis (HPA) via adrenocorticotrophic hormone (ACTH) (Norris, 1997). Glucocorticoids act on target tissues through cytoplasmic based glucocorticoid receptors. Upon ligand binding these receptors translocate into the nucleus where than can act as both activators and repressors. They exert their influence by either binding to specific glucocorticoid response elements (GREs) within the DNA, or interacting with transcription factors (Reviewed by Kassel & Herrlich, 2007). In addition, glucocorticoids can also interact within

mineralocorticoid receptors, resulting is aldosterone axis modulation (Joels *et al*, 2008).

As mentioned above glucocorticoids are released by the adrenal gland with a diurnal pattern (reviews in Chrousos, 1998) synthesis peaking in the early morning. Release is controlled by the circadian clock on two levels. Firstly release is governed by the SCN. The master clock controls the function of the hypothalamus and pituitary, and ultimately the release of adrenocorticotrophic hormone (ATCH) (Dickmeis *et al*, 2009). However, ACTH is not crucial for rhythmic glucocorticoid release (Bortstein *et al*, 2008). Neuronal stimulation, especially in correlation with nocturnal light pulsing, has been shown to modulate rhythmic glucocorticoids in adrenoectomised rodents and it thought to represent an addition level of control (Meier, 1976. Buijs *et al*, 1999. Engeland & Arnhold, 2005). Secondly, the adrenal gland itself contains a functional clock, which has been shown to partly regulate the synthesis and release of glucocorticoids independent of inputs from the SCN (Oste *et al,* 2006. Son *et al*, 2008).

4.1.3.2 Glucocorticoids and cell proliferation.

Glucocorticoids have long been noted as both stimulators and repressors of cell proliferation (Mattern *et al*, 2007). These effects appear particularly tissue specific; adrenectomy causing increased proliferation within the brain, yet decreased proliferation within the small intestine in mice (Alonso *et al*, 2000. Foligne *et al,* 2001). Also of interest is the differential reaction to changing concentrations of glucocorticoids: lower concentration pulses have been generally associated with increased proliferation while higher concentrations having inhibitory affects (Mattern *et al*, 2007). Numerous mechanisms have been suggested for this

regulation, primarily interaction between GREs and cell cycle regulators such as *Cyclin D, cMyc, p53* and *p21.* Interestingly, as mentioned in Section 1 (Mattern *et al*, 2007. Chebotaev *et al*, 2007), these factors are putative targets for circadian regulation of the cell cycle. These pathways would provide interesting opportunities for cross talk between the clock and the cell cycle.

Glucocorticoids have been shown not only to affect the rate of cell proliferation but also to produce rhythms within cell proliferation. This has been documented in blood, bone marrow, intestine and skin studies in rodents (Smaaland *et al*, 2002. Bjarnason & Jordan, 2002. Brown *at al*, 1989). However, the results of these studies have limited interpretation as glucocorticoid signalling was not considered in conjunction with circadian function. Such experiments have however taken place in zebrafish. Glucocorticoids regulate circadian rhymes in cell proliferation rates in larvae and are severely attenuated in pituitary lacking animals (Dickmeis *et al*, 2009). This evidence suggests that glucocorticoids although not playing a dominant role, work symbiotically with the local and master clock signals to produce coordinated cell cycle progression.

4.2.3.3 Interactions between glucocorticoids and the clock.

In conjunction with the synchronization of peripheral clocks explored above, glucocorticoids demonstrate the ability to feedback, regulating clock function itself, although this is constrained to local influence on peripheral clocks (Balsolobre, 1998, 2000A). Glucocorticoids also appear to function on the clock in other areas. *Per2* rhythms in the brain, are lost in rodents following adrenectomy, and restored by delivering drinking water supplemented with glucocorticoids (Amir *et al*, 2004.

Segall *et al*, 2006). *Per1* is affected in a similar say within liver tissues (Son *et al*, 2008).

As well as acting as a direct synchronising agent (Balsolobre *et al*, 2000), glucocorticoids affect the synchronisation of peripheral clocks indirectly through modulation of the feeding entrainment. Peripheral clocks become uncoupled from the SCN under restricted day-time feeding schedules in rodents; the peripheral clock choosing the food entrainment as the primary *zeitgeber* (Damiola *et al*, 2000, Hara *et al,* 2001). Glucocorticoid administration inhibits the food induced phase shift in these peripheral rhythms (Le Minh *et al,* 2001). Multiple levels of regulation are also employed; affecting the clock on at the DNA level (binding and interacting with the circadian transcriptome) (Reddy *et al,* 2007) as well as inducing post-translational protein modifications (Nader *et al,* 2000).

4.14 The Clock within the Kidney

Within this chapter all experiments were carried out on the cell-line, Human Embryonic Kidney (HEK) 293. Although for the purpose of these experiments HEK 293 cells were used as a generic human cell-line (not a tissue specific model) it is important to take into consideration the characteristics of the cell-line. This is a cell-line, although of unspecific cell-type, derived from embryonic kidney explants. It is therefore presumed to contain cells of endothelial, epithelial and fibroblastic nature, as would be found within the developing kidney.

The kidney has been shown to be a highly rhythmic organ. Physiologist Vogel first reported daily fluctuations in urine volume over a century ago (Pons *et al*, 1996). There are clear diurnal variations in urine volume, urinary sodium, and potassium

and chloride excretion throughout the day (Manchester, 1933). However, although these are clearly circadian in nature, the underlying mechanism remains unknown.

There is a growing body of evidence supporting the role of the circadian clock within kidney tissues. These include chronotherapeutic trials (Stow & Gumz, 2011) and molecular studies which have shown a number of clock-controlled genes within the kidney (Nishoro *et al*, 2005. Yomata *et al*, 2010. Zuber *et al*, 2009); the most comprehensive of which involved a microarray analysis concluding a substantial presence of clock controlled kidney specific genes, including a number of transporters and channels (Zuber *et al,* 2009). Furthermore, *Per1* has been identified as a novel aldosterone target within murine inner medullary collecting duct. It is thought that *Per1* contributes to the basal; aldosterone-dependant transcription of *Scnn1*. *Scnn1* encodes the rate-limiting subunit of the epithelium sodium channel. Expression of these genes is also reduced in null mice (Gumz *et al,* 2010). In this way circadian function seem to be synergistic for kidney function.

The aim of this chapter was to define protocols for the synchronisation of HEK 293 cellular clocks in order to study circadian gene expression across a timecourse; eliciting a more detailed picture of clock function within this tissue. Furthermore, it extends this study into cell cycle regulation to determine whether the clock has any influence over this process in the cell-line.

4.2 MATERIALS AND METHODS

4.2.1 HEK CELLS AND CULTURE CONDITIONS

In this chapter all experiments were carried out on the Human Embryonic Kidney 293 cell-line (HEK 293). The HEK 293 cell-line was isolated in 1976 from human embryonic kidney cells grown in tissue culture, harvested from a healthy human embryo. The cells were then transformed using sheared adenovirus 5 DNA (Graham *et al*, 1977). This transformation resulted in the insertion of ~4.5kbs of the left arm of the viral genome in the human chromosome 19 of the cells (Louis *et al*, 1997). The specific cell-type of the cell-line is unknown, the embryonic kidney consisting of cells from endothelial, epithelial and fibroblastic lineages.

HEK 293 cells were cultured in Dulbecco's Modified Eagle Medium (DMEM) (Invitrogen at Life Technologies Ltd.) with 10% foetal calf serum (FCS, Biochrom AG), penicillin (100U/ml) and streptomycin (100µg/ml) (Invitrogen at Life Technologies Ltd.). Cells were cultured at 37°C, with 5% CO_2.

These cells were purchased from American Type Culture Collection (ATCC™, USA).

4.2.2 Synchronisation protocols

Dexamethasone Synchronisation: Dexamethasone is a synthetic member of the glucocorticoid class of steroid drugs as mentioned in section 4.1.2

Cells were cultured in standard culture medium to a confluency of ~90% in 6-well plates. To synchronise, culture medium was removed and cells were washed with 1ml PBS. 2.5ml of standard culture medium supplemented with 100nM dexamethasone (Sigma-Aldrich Company Ltd.) was then added to each well. Cells were incubated for 2 hours at 37°C, 5% CO_2. The dexamethasone culture medium was the removed and the cells washed with 1ml standard culture medium. 2.5ml of standard culture medium was then pipetted into the wells and the cells harvested as appropriate for the experiment.

The 100nM dexamethasone/medium solution was made from a stock of 10mM dexamethasone in ethanol. As a control a matching 0.001% ethanol/medium solution was used. This protocol was based on that documented in Balsolobre *et al*, 1998. The protocol was optimised for the 293 cell-line as described below.

Forskolin Shock: Forskolin is a labdane dierpene that is produced by the Indian Coleus plant (*Coleus forskholii)*. It stimulates cells to increase their levels of cyclic AMP (c AMP) and resensitises cells by activating the enzyme adenylyl cyclase. c-AMP is an important signal carrier coordinating cellular responses to extracellular stimuli such as hormone signals (Insel & Ostom, 2003)

To shock the cells with Forskolin, cells were cultured to ~90% confluency on 6-well plates. The culture medium was removed and cells washed with 1ml PBS. 2.5 ml standard culture medium with 10µM forskolin (Sigma-Aldrich Company Ltd.) was then

added. Cells were cultured for 2 hours at 37°C, 5% CO_2. After the shock cells were washed with 1ml standard culture medium and then 2.5ml standard culture medium was placed into each well. Cells were harvested as required for the experiment. This procedure is based on the protocol for the synchronisation of the circadian clock with Rat-1 fibroblasts, as discussed in Izumo *et al*, 2006). The 10µM forskolin/medium solution was produced from a stock on 100mM stock of forskolin in ethanol, and an equivalent ethanol/medium control was used.

Horse Serum shock: This protocol is based on that used to synchronise the clock within Rat-1 fibroblasts as mentioned above (Izumo *et al*, 2006). HEK 293 cells were cultured until ~ 90% confluent. The culture medium was then removed and the cells washed with 1ml PBS. Cells were then pulsed with 2.5ml DMEM with 50% Horse Serum (Biochrom AG) and incubated for 2 hours at 37°C, 5% CO_2. Following this the horse serum solution was removed, the cells washed with 1ml standard culture medium and 2.5mls standard culture medium placed back into the well. Cells were then harvested as appropriate for the experiment.

Water soluble dexamethasone: A water soluble compound comprising of a dexamethasone – cyclodextrin complex, was used in initial studies to determine the contribution of ethanol pulsing to preliminary results. Cells were pulsed using the same protocol and concentrations of dexamethasone as used above.

Optimisation of the dexamethasone shock protocol

Firstly expression of glucocorticoid receptors (GR) was determined. Specific GR quantitative PCR primers were designed as shown in table 2.2. Figure 4.1 shows the quantitative PCR results, displayed as cycle threshold (CT) ± SEM, n=3 for glucocorticoid receptor mRNA and reference gene TATA-Box binding protein.

Unsynchronised HEK 293 cells were harvest at 3 random time-points over the course of 24 hours. The CT level clearly shows formation of a specific product which has the appropriate melting temperature. This PCR product was then run on an agarose gel showing the correct band size of 150bp. The product was also sequenced and was confirmed to be the according section of glucocorticoid receptor mRNA. It has previously been descried that HEK 293 cells are able to express glucocorticoid receptors at low levels, which are able to response to dexamethasone pulsing (Ziera *et al*, 2009). The CT values reflect a present but low level of GR expression.

Figure 4.1 Confirming glucocorticoid receptor expression within HEK 293 cells.

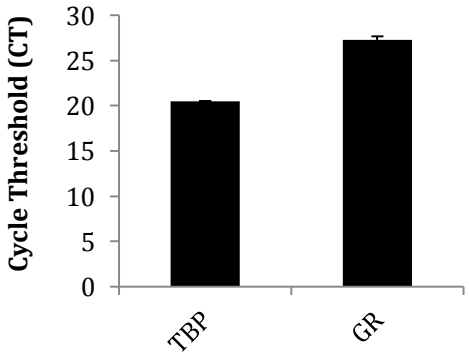

Figure 4.1. Unsynchronised HEK 293 cells were harvested at 3 random time-points during the course of 24 hours. Quantitative PCR results showing cycle threshold ± SEM, n = 3, for glucocorticoid receptor mRNA in comparison to reference gene TATA-Box binding protein (TBP).

To optimise the dexamethasone synchronisation process to this cell-line a series of experiments were carried out. Results of this process can be seen in figure 4.2. Firstly a dose-response curve testing concentrations of dexamethasone ranging from 25nM to 500nM were tested on HEK 293 cells. Fold induction of *Per1* over 24 hours was then used as a target response. Figure A shows the results of this experiment. Fold induction is shown ± SEM, n = 3. It was seen that the fold induction increases significantly in comparison to control in proportion to the dose

given, from 50nM up to 100nM, producing maximum fold induction of 5 fold. Concentrations above this dosage did not elicit significantly different or larger fold increases as assessed by one-way ANOVA. Cells treated with 500nM dexamethasone became unhealthy after a day in culture, consequently no data was collected.

Following this, the concentration or density of cells required for synchronisation was examined. Cells were plated at different concentrations resulting in 20%, 50%, 75%, 90% and confluent cell cultures upon dexamethasone shocking. Confluent cultures became non-viable over the period of a time-course. No significant increase in comparison to ethanol control is seen at 25 or 50% confluency; 75% and 90% confluency results in statically significant fold increases of 3.4 and 5.5 respectively.

In conclusion, the optimum dexamethasone shock protocol involves a 2 hour 100nM pulse when cells are ~90% confluent.

A

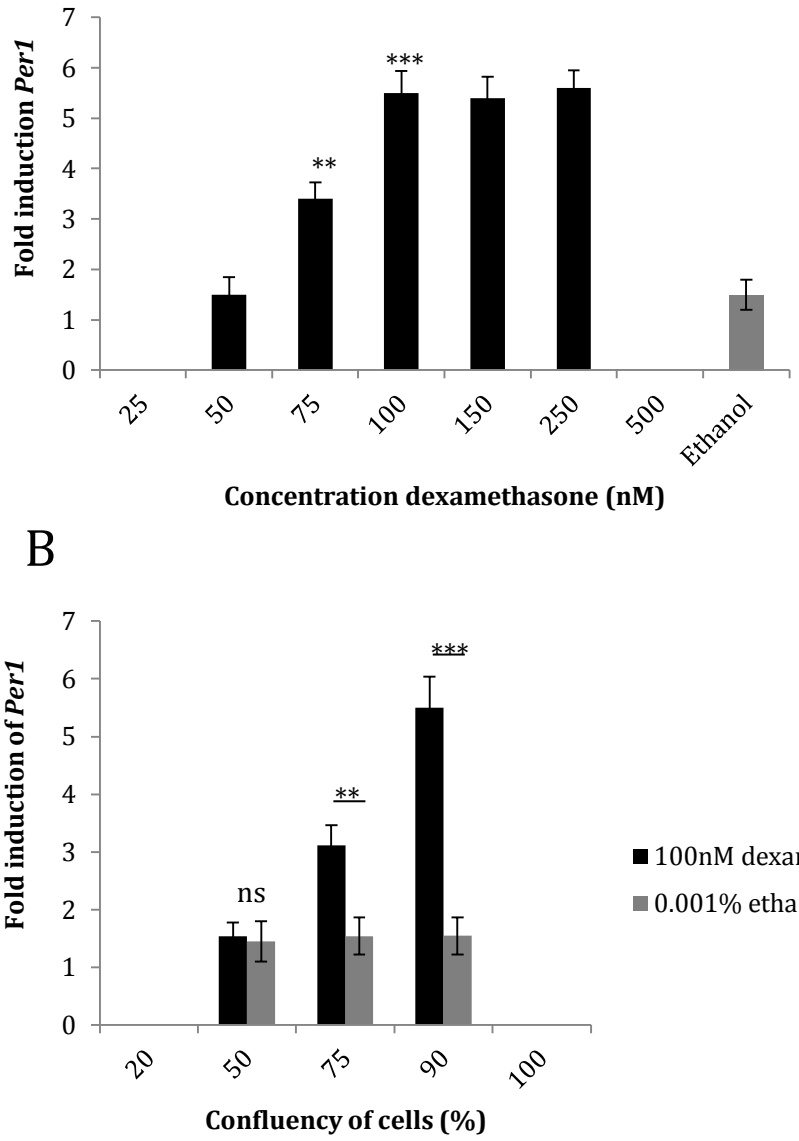

Figure 4.2. A) HEK 293 cells were cultured to ~90% confluency and treated with a 2 hour dexamethasone pulse, concentrations ranging from 25nM – 500nM or a 0.001% ethanol control. Cells were harvested at 26, 32, 38 and 44 hours post treatment and then pooled. B) HEK 293 cells cultured to a range of confluency, 25% to 100%, and treated with a 2 hour pulse of 100nM dexamethasone or 0.001% ethanol control. Cells were harvested 26, 32, 38 and 44 hour after treatment and then pooled. The graphs show the fold induction of *Per1* gene expression ± SEM, n = 3 for each concentration or confluency tested; expression in comparison to the reference gene TATA-Box binding protein. Analysis shown is results of Student T-test comparing dexamethasone shock to ethanol control, NS= P-value > 0.05, ** = p-value < 0.01, *** = p-value < 0.001

4.2.3 Disrupting the clock

In a previous study, performed on zebrafish, lighting regimes have been used to determine whether the rhythms observed are driven by the circadian clock. Due to the lack of direct light sensitivity within human cell culture, a more molecular approach must be taken.

For preliminary work the zebrafish *CLOCK1a DN* construct was used, as mentioned in section 3.2.7. Alignment of the zebrafish and human CLOCK protein sequences can be seen in Section 8.2. It is clear that the structure of these proteins is highly conserved and the b-HLH and two PAS domains marked, grey and red respectively, are highly similar. Any amino acid changes observed should not affect the activity of these domains. As we can see both contain a Q-rich activation zone, which has been removed within the CLOCK1a DN construct. As is it described in section 4.3.6 this construct appears fully functional within human cell lines.

In addition to this construct being used, and to allow later validation of these results, a human Bmal1-DN was constructed. The human Bmal protein has a very similar structure to that of CLOCK; a b-HLH domain followed by two PAS domains, before the Q rich activation region. Firstly a 1300bp section of the DNA coding for the 5' prime region of *Bmal1* was isolated by PCR using the following primers.

5' EcorV TGGATCTGGGATATCAGAACTGTG

3' BstB1 TGTGAGCCCTCGAAAGGTTGGG

Conditions were optimised to 95°C for 1 minutes, 30 cycles of 95°C for 30 seconds, 68°C for 3 minutes, followed by 68°C for 3 minutes.

The fragment was subsequently cloned into pGEMTeasy for sequencing and further cloning. The fragment was then digested and subcloned into the pcDNA3.1+ His/Myc vector (Promega).

4.2.4 Statistical analysis of qPCR time course data.

Time-course qPCR data was analysed statistically using the following algorithm. All statistical tests were performed using GraphPad Prism® (GraphPad UK).

Firstly a Two-way ANOVA was carried out on each test group (dexamethasone and ethanol control) separately to assess variation over time in these expression patterns. A post hoc T-test was then performed to determine at which time points there were significantly different levels of expression between the two test groups and if these repeated every 24 hours – this was deemed "rhythmic". The amplitude of any rhythm and the difference between the peaks and troughs of expression were assessed numerically, and a T-Test used to estimate the significance of these differences. Finally, an approximation of period was made of any rhythmic samples (rhythmic samples defined as those who has statistically significant variation in expression over time, which shown oscillatory characteristics), however due to low resolution data period could only be estimated to be between 20 and 32 hours (Balsalobre *et al*, 1998). Statistical p-values shown on figures for treatment groups

represent the significant difference between it and the control. The p-value for the control is also shown to confirm non-significance.

Owing to the nature of the data, mathematical analysis of the wave forms and proof of oscillation was difficult. This will be reviewed later within the discussion (Section 4.4).

4.3 RESULTS

4.3.1 Expression of clock genes by HEK 293 CELLS

As this cell-line had never been used for functional circadian studies before, expression of core clock genes was first determined using quantitative RT-PCR (qPCR). Figure 4.3 shows the qPCR results for clock components *Per1, Per2, Reverb-α, NPas2, Bmal* and *Clock*. HEK 293 cells were cultured until ~90% confluent then harvested for RNA extraction over 4 time points, 6 hours apart across 24 hours (starting at 10am) to determine any unsynchronised temporal variation in expression and minimise error. Figure 4.3 shows the relative expression of clock components *Per1, Per2, Reverb-α, NPas2, Bmal* and *Clock*., ± SEM, n=6 accompanied by average CT values ± SD for each gene. Specificity of products of these qPCR reactions was confirmed by gel electrophoresis and sequencing.

It can be clearly seen that all six of these core clock components are expressed by HEK 293 cells; there is no clear variation over time in unsynchronised populations as determined from the low standard deviation of CT for each gene across time.

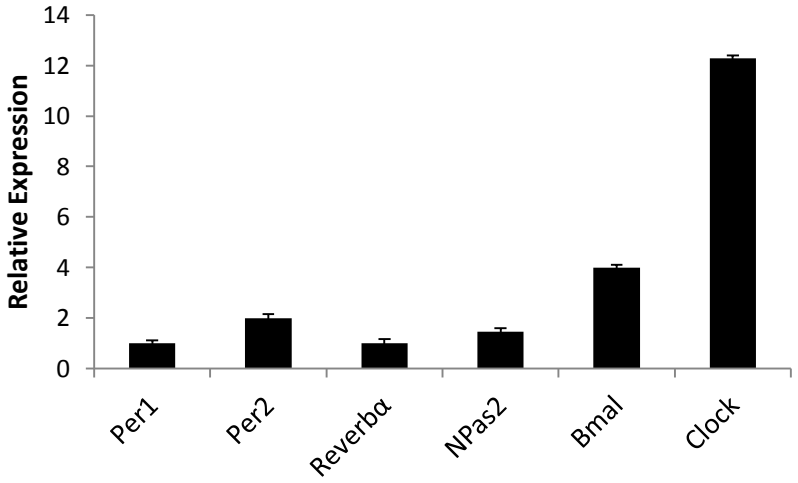

Gene	Avergae CT	Standard Deviation
Per1	25.4	0.25
Per2	24.87	0.4
Reverb-α	25.4	0.41
NPas2	24.86	0.36
Bmal	23.4	0.25
Clock	21.79	0.28

Figure 4.3 Quantitative PCR analysis showing the relative expression of *Per1, Per2, Reverb-α, NPas2, Bmal* and *Clock*., ± SEM, n=6, accompanied by average CT values ± SD for each gene. Samples were taken from unsynchronised HEK 293 cells. Data shown is relative expression ± SEM, compared to reference gene TATA-Box binding protein (TBP), n = 3.

4.3.2 Synchronisation of cellular clocks within culture

Considering that timecourse studies are rare within human cell-lines it was imperative to establish a correct synchronisation protocol. This method in turn must not directly affect the cell cycle, confounding any results that may appear in resulting studies.

Figure 4.4 shows the results of a trial of commonly used synchronisation agents, and their effects on expression levels of *Per1* over a 24 hour period. HEK 293 Cells were treated on the third day of culture (~90% confluency) with a 2 hour pulse of 100nM dexamethasone, 100nM water-soluble dexamethasone, 10nM forskolin, or 50% serum shock, along with control treatments of 0.001% ethanol, 0.001% water and media change. Cells were then harvested at 26, 32, 38 and 44 hours after drug treatment. Relative expression of *Per1*, as determined by quantitative PCR ± SEM, n=3. Variation in expression between time-point for each treatment group was determined by two-way ANOVA, variation between treatment and control groups was then determined by post-test T-test. (* = p-value <0.05, ** = p-value < 0.01 *** = p-value).

As documented in fibroblasts, serum shocking (Balsalobre *et al*, 1998) elicits strong oscillations within *Per1* expression. In Figure A a 3 fold peak/trough difference in *Per1* expression peaking at 38 hours post-treatment is observed. This is compared to a constant expression level in the control (no significant variation observed). Such expression patterns match in phase to those exhibited by rat-1 fibroblasts and hepatoma cells (Balsalobre *et al*, 1998).

The *Per1* expression pattern in Figure B, where cells have been pulsed with 100nM dexamethasone also displays a similarly phased oscillation. This, however, is much

more robust displaying a 5 fold peak-trough difference. The ethanol control within this experiment does shows more variation over time than the media change control, however this is not surprising. Ethanol pulsing has been shown to even elicit circadian rhythms from cultured rat-1 fibroblasts (Balsalobre, 2000). Here the variation is not significant.

Lest this ethanol stimulation might contribute to the expression pattern seen within ethanol soluble stimulants, a dexamethasone – cyclodextrin water soluble functional analog was tested in parallel. This expression pattern of *Per1* is similar in phase yet greatly diminished with a 2 fold peak-trough difference. As figure B shows that ethanol contribution is non-significant this diminished response is most likely due to the nature of the chemical compound resulting in a change in dose-response.

Lastly the cAMP stimulant Forskolin was tested due to its apparent effect on rat-1 fibroblasts. Although being shown to elicit Per1 expression patterns with a similar phase to the other agents in this paper, we see a markedly different pattern. *Per1* expression remains constant with exception of a 2 fold increase at 44 hours post treatment. As a control *p21* expression levels were measured concurrently with *Per1*. Forskolin elicited a large response in *p21* expression, disproportionate and out of phase for that expected of a circadian output (data not shown). It is likely that an antagonist of the cAMP pathways would have direct effects on the cell cycle and its regulation. This is seen to be the case. It was therefore excluded due to its potential to generate false positive results.

It is interesting to note and the average basal expression levels for *Per1* across the 24 hour time course is higher in the synchronised cells than within the unsynchronised populations. This will be discussed further in section 4.4.

From these results dexamethasone was seen as the synchronisation agent of choice. Further optimisation of the protocol was carried out as described in section 4.2.2.

A

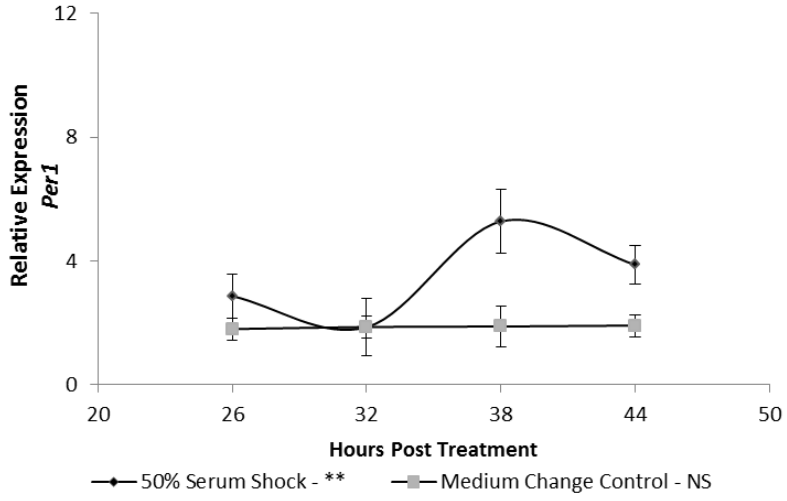

B

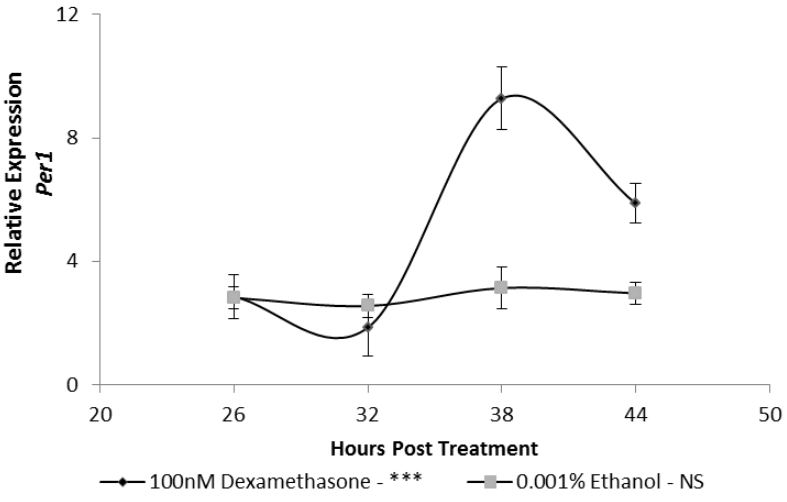

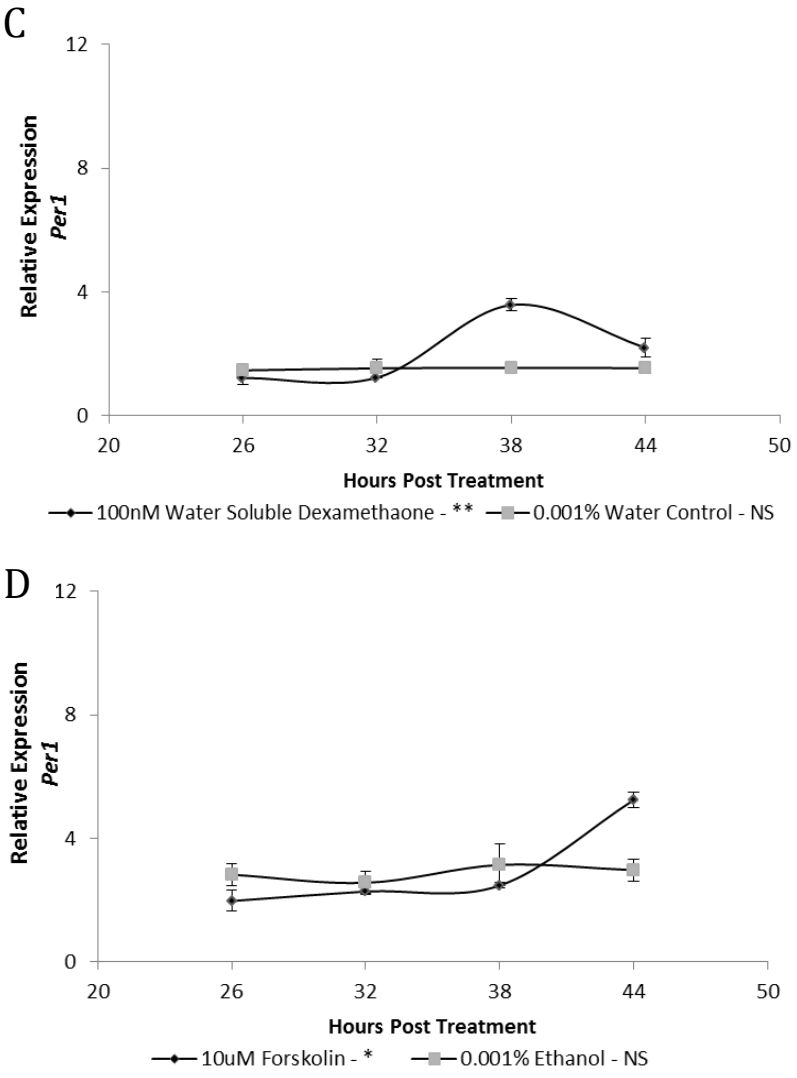

Figure 4.4. HEK 293 cells were cultured until 90% confluent. They were then pulsed for 2 hours with 50% horse serum or media change control, 100nM dexamethasone or 0.001% ethanol control, 100nM water soluble dexamethasone or 0.001% water control, 10nM forskolin or 0.001% ethanol control. (A-D respectively). Samples were then harvested 26, 32, 38 and 44 hours after treatment. The figure shows relative expression of *Per1,* ± SEM, for each time point compared to reference gene TATA-Box binding protein (TBP), n = 3. Variation in Per1 expression over time was analysed using a two way ANOVA (NS = No significance, * P-value = < 0.05, ** = p-value < 0.01, *** = p-value < 0.001.)

4.3.3 Expression of circadian clock genes in synchronised populations

The only previous timecourse assessments of synchronisation of peripheral circadian clock in culture were carried out on Rat-1 Fibroblasts. These were synchronised using serum shock and dexamethasone methods with clock function being measured by RNase protection assays of *Per1* and *Reverbα* (Balsalobre *et al,* 1998. Balsalobre *et al,* 2000). In addition bioluminescent constructs have been used as reporters of clock gene expression (Insel & Ostom, 2003), however these are limited by the omission of examining endogenous gene expression.

To complete a comparable experiment to Balsalobre's, within HEK 293 cultures, cells were grown to ~90% confluency. The cellular clocks were then synchronised with a 2 hour pulse of 100nM dexamethasone and a 0.001% ethanol control. Samples were harvested from the withdrawal of the pulse, every 6 hours for 3 days. Clock genes expression patterns were determined via quantitative PCR and are displayed in figure 4.5

Figure A shows expression of *Per1* over 3 days post synchronisation. A clear rhythm can be seen in expression peaking at 20 hours, 38-44 hours and 68 hours post treatment, an approximate τ of ~24 hours. The rhythm has 4.5 fold peak/trough amplitude. The phase of expression matched closely with that seen in the Balsalobre experiment, in which peaks were noted at 20 hours, 44 hours and 63 hours post synchronisation. It is interesting to note that the amplitude of this rhythm appears to increase over the three days. The control population show no significant variation over time, as assessed by ANOVA. However there is mild increase in basal levels of *Per1* expression over the timecourse.

Figure B shows the expression pattern of the *Per1* homolog *Per2*. A clear and significant oscillation is observed over the 3 days, which appears to be 6 hours out of phase with that seen for *Per1*; peaks in oscillation are observed at 20 hours, 44 hours and 68 hours in this analysis. A 4 hours phase different has been observed between *Per1* and *Per2* in fibroblasts, but due to the resolution of this experiment an exact phase difference cannot be established. The *Per2* rhythm has peak/trough amplitude of 3.5 fold. Such a variation is not observed within the control group.

Included with these expression patterns is that of *Rev-erbα.* Although *Reverbα* is involved in the secondary loop of the clock mechanism, its expression is under similar regulation by BMAL:CLOCK as the *Per* genes. In a fully functioning clock it should therefore display a similar rhythmic pattern. It can be seen this is true within HEK 293 cells. *Reverbα* expression displays oscillations peaking in phase with those of the *Per* genes; the amplitude of these rhythms being smaller with a 2 fold peak/trough difference. Whereas expression within the unsynchronised population remains constant.

Expression patterns of genes involved in the contrary section of the clock are then displayed below (Figure D, E and F). *Bmal1*, *Clock* can be seen to display robust antiphase oscillations when compared to those of *Per1*, *Per2* and *Reverbα* (amplitudes of 6 fold and 3 fold respectively). Peaks in expression occur at 8 hours, 32-38 hours and 56 hours post treatment. *Clock* expression patterns have been described as being highly tissue specific in mammals (Lowery, 2004). However, studies have shown it to be rhythmic within the kidney, a fact reflected in this data. *NPas2*, a mammalian *Clock* homolog, on the contrary, shows no demonstrable oscillation in comparison to the control. *NPas2*, has been described as robustly

rhythmic within blood cultures (Kusanagi *et al*, 2008). These results suggest that *NPas2*, like *Clock*, displays tissue specific expression patterns.

Amplitude and dampening of these patterns cannot be directly compared with previous studies as they employed RNAase protection or surrogate measures of gene expression by bioluminescent reporter. However, what is interesting is the maintained phase induced by dexamethasone synchronisation regardless of cell-type.

A Per1

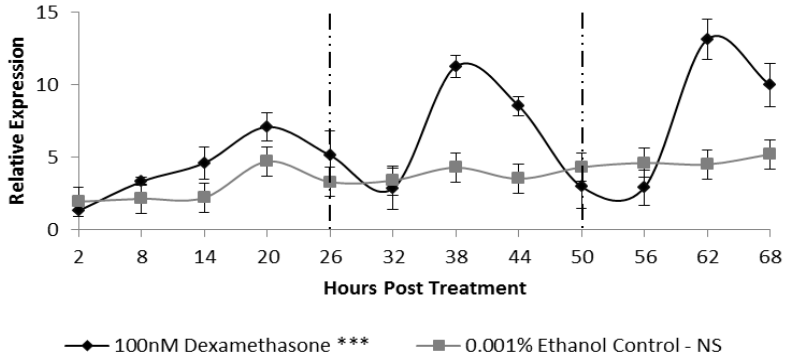

B Per2

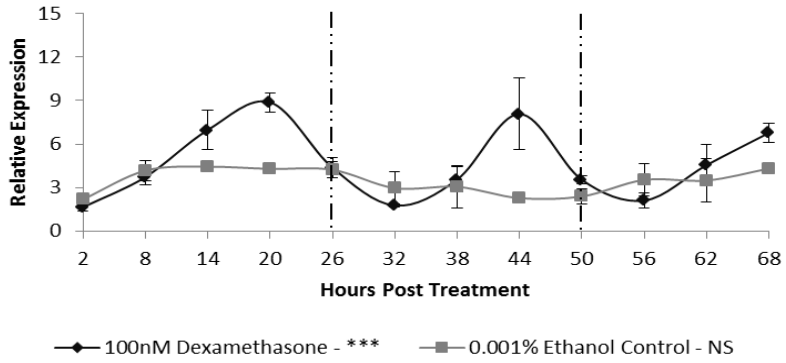

C Reverb-α

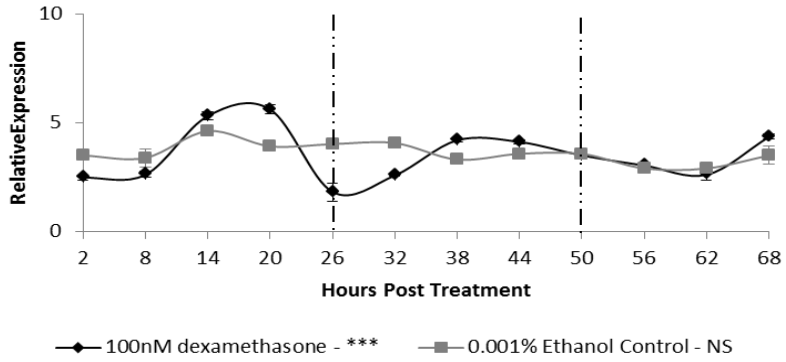

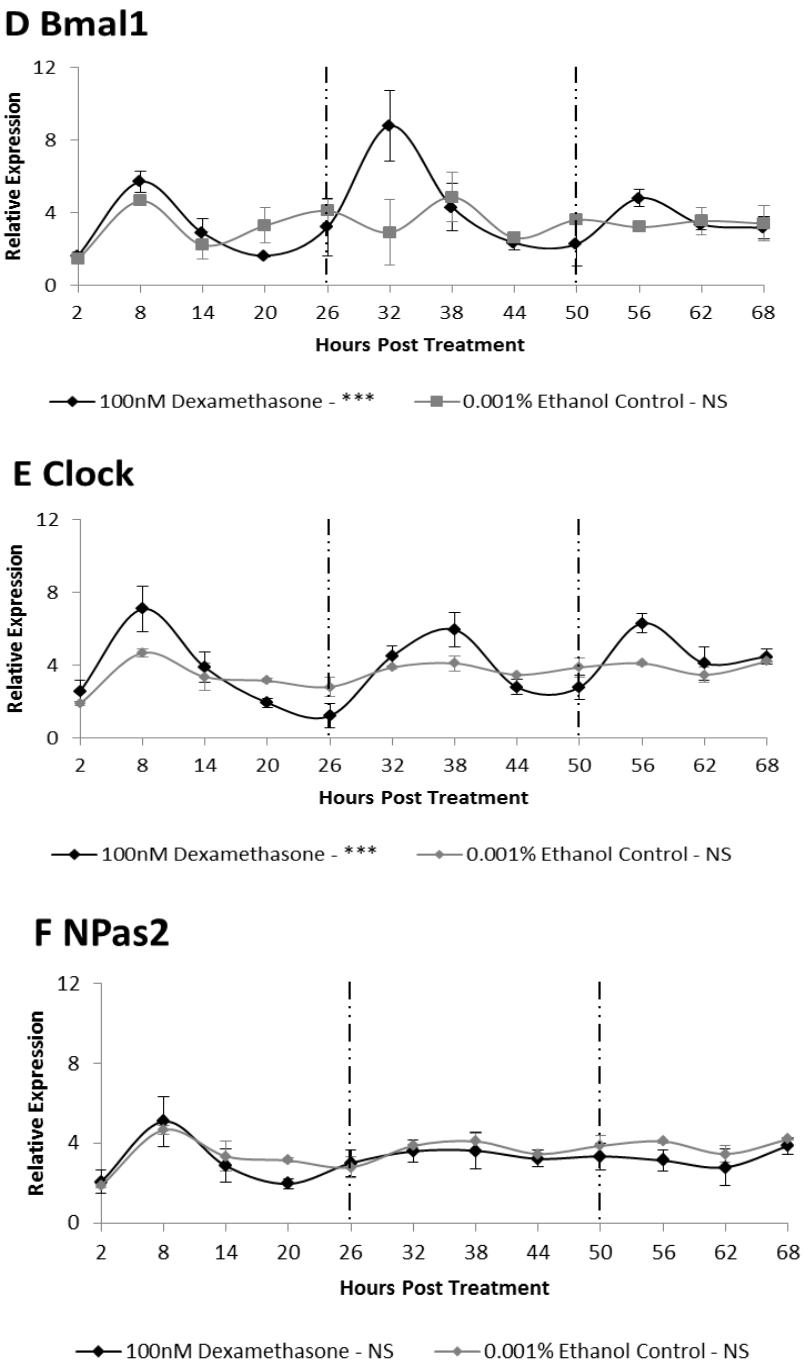

Figure 4.5. HEK 293 cells were pulsed for 2 hours with 100nM dexamethasone or 0.001% ethanol control and harvested every 6 hour following treatment over 3 days. Figures A-F show quantitative PCR results for clock genes *Per1, Per2, Reverbα, Bmal, Clock and Npas2* from these samples. Relative expression is shown ± SEM, compared to reference gene TATA-Box binding protein (TBP), n = 3. To assess variation in expression over the time-course a two-way ANOVA was used. Average peak/trough fold difference (amplitude) as assessed with a post-hoc T-test. (* P-value = < 0.05, ** = p-value < 0.01, *** = p-value < 0.001.)

4.2.4 Proteins within the synchronised clock

It is established that dexamethasone pulsing can produce coordinated rhythms in clock gene expression in culture. However, it is an assumption that synchronised gene expression patterns are automatically translated into functional protein rhythms and a coordinated and functional clock population. To further explore this hypothesis, western blot analysis was used to look that the levels of BMAL1 protein in synchronised and unsynchronised groups of HEK 293 cells. HEK 293 cells were grown to ~90% confluency and pulsed for 2 hours with 100nM dexamethasone or a 0.001% ethanol control. Cells were then harvested at 26, 32, 28 and 44 hours after treatment. BMAL1 protein expression was analysed with western blot using an anti-BMAL1 antibody (BMAL1 H-170, Santa Cruz Biotechnology, USA) as described in section 2.4. Figure 4.6 show a representative result from this experiment. Protein expression was quantified using Image J® Gel analysis software as described in section 2.4.4.

Levels of Bmal1 protein appear to vary over the 24hours in the synchronised population when compared the control. Levels of Bmal1 are seen to peak at 38 hours post treatment. mRNA levels for *Bmal1* are seen to peak at 32 hour post treatment. Such a delay in translation is not unusual, especially in a system where post translation modification plays such a role in protein function. (described in section 4.4). It can be seen that a small variation is seen in protein level in the ethanol control. It has already been stated that ethanol has a very mild induction effect on clock genes (Izumo *et al,* 2005), and this would account for any changes seen. However, the significance of this variation was not established due to

difficulties with over exposure of the α-tubulin loading control. This made accurate quantification impossible.

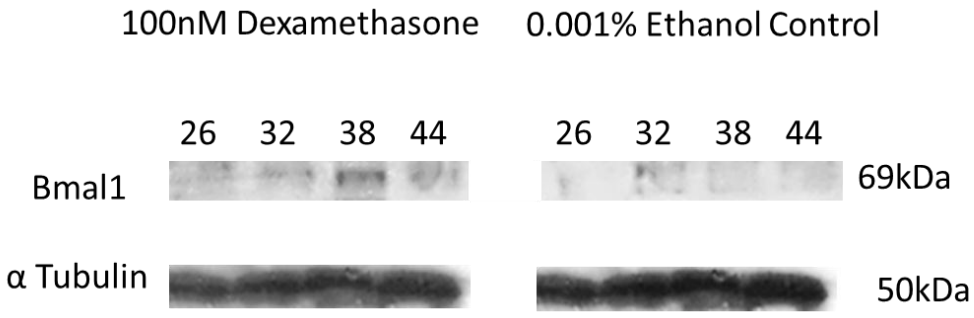

Figure 4.6. Western blot analyses of Bmal1 protein levels in synchronised and unsynchronised HEK 293 cells. HEK 293 cells were pulsed at ~90% with 100nM dexamethasone and 0.001% ethanol control for 2 hours. Harvesting took place 26, 32, 38 and 44 hours after treatment. Western blot carried out using 1:2000 dilution primary anti-Bmal1 antibody, followed by 1:1000 secondary anti-rabbit horse radish peroxidase (HRP). Antibodies to α-tubulin were used as a control. 1:1000 dilution of rat anti-α- tubulin, 1:1000 anti-rat (HRP). Quantification was not undertaken due to lack of accurate loading control.

4.2.5 Disruption of the circadian clock by the CLOCK1a DN construct.

To confirm that HEK 293 cells contained a functional clock and to validate the results above the clock mechanism was disrupted using the *CLOCK1a DN* construct mentioned earlier within section 3.2.7. Cells were transfection by Lipofectamine 2000 and selected using neomycin. Figure 4.7A confirms the presence and function of this vector within the cells. A control population was transfected with pCLNCX vector. Immunocytochemistry confirms the expression of the Flag-Tag protein by the *CLOCK1a DN* vector, confirming transcription of the insert. Figure 4.7B shows a Western blot using antibodies designed against the Flag-tag protein (section 3.2.7), which again confirms its presence within the transfected population and its absence within the control cell-line.

HEK 293 *CLOCK1a DN* and empty vector cells were then synchronised using the same dexamethasone protocol as mentioned above. Figure 3.7C shows the results of a qPCR assaying the expression pattern of *Per1* over 24 hours, within these cell-lines. *Per1* relative expression is displayed ± SEM, compared to reference gene TATA-Box binding protein (TBP), n = 3, for the second day post-synchronisation. It can be clearly seen that the expression of *Per1* varies over the 24 hours within the control cell-line (as confirmed by one way ANOVA p-value < 0.001). A 4-fold amplitude is displayed with a similar phase to that of the *Per1* expression shown in figure 4.4A. This confirms that the pCLNCX vector is having no effect on clock function or gene expression. No such expression pattern is seen within the HEK 293 *CLOCK1a DN* cell-line. *Per1* is consistently expression at a lower level than that endogenously seen (as confirmed by one-way ANOVA). This is consistent with the effects this vector is seen to have on Per1 expression within the PAC2 cell-line (section 3.3.6) and what is known

about how this construct obstructs clock function (section 3.2.7). This experiment confirms that the *CLOCK1a DN* is being expressed and is functionally active within these cell-lines. HEK 293 *CLOCK1a DN* do not contain a functional clock.

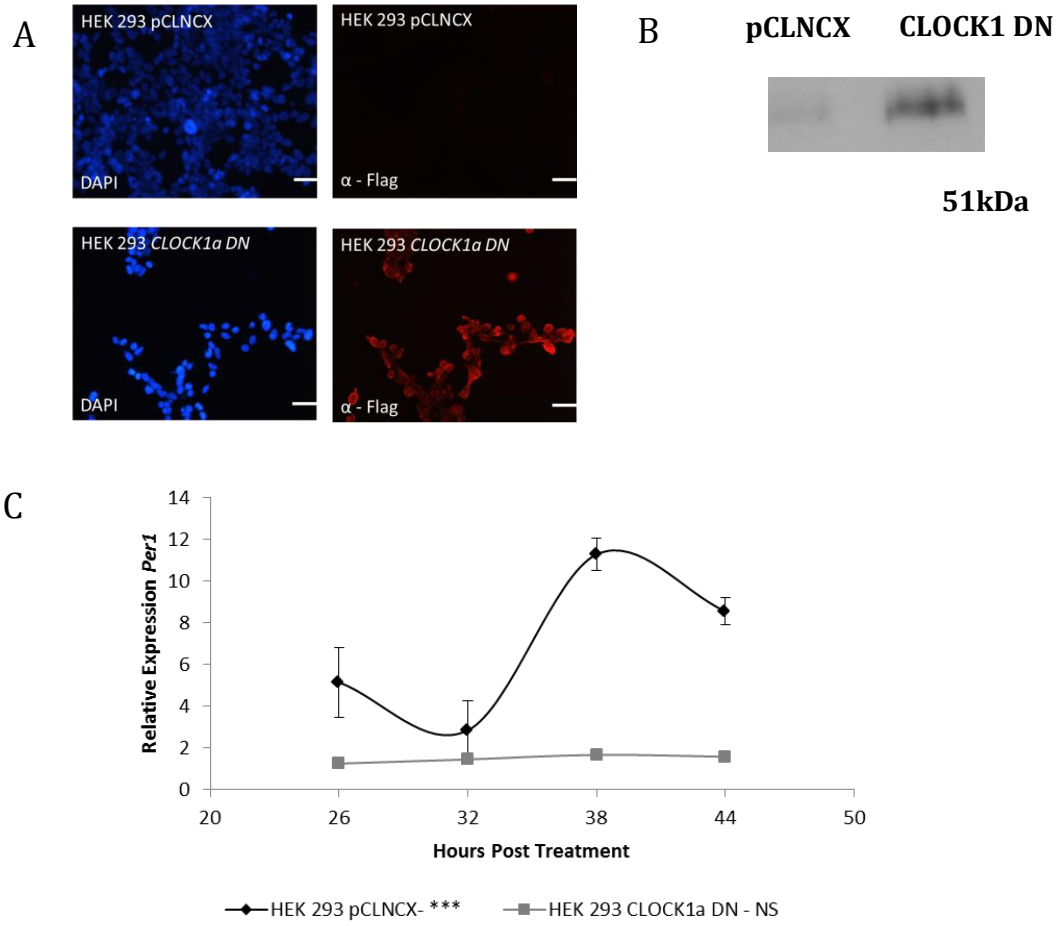

Figure 4.7.HEK 293 cells were transfected with the *CLOCK1a DN* construct or the *pCLNCX* vector. Figure A shows an 10X representative image of immunocytochemistry staining with α – Flag Tag antibody on HEK 293 *pCLNCX* and HEK 293 *CLOCK1a DN* cells. DAPI staining is also shown as a nucleic marker (Scale bar = 50μm). Figure B. shows a representative image of a western blot looking for the presence of the Flag Tag protein in HEK 293 *pCLNCX* and HEK 293 *CLOCK1a DN* cells compared to an α-tubulin control. Figure C shows qPCR data from HEK 293 *pCLNCX* and HEK 293 *CLOCK1a DN* cells which have been synchronised with a 2 hour pulse of 100nM dexamethasone. The figure displays the relative expression of *Per1*± SEM, compared to reference gene TATA-Box binding protein (TBP), n = 3, for the second day post synchronisation. One-way ANOVA analysis was used to look for temporal variance in *Per1* expression for each cell type. (NS – not statistically significant, *** = p-value < 0.001)

4.2.6 Synchronisation of the cellular clocks does not affect cell growth within the population.

The clock has been implicated in regulating the cell cycle. The rate at which the cell cycle progresses in turn would affect overall proliferation rates within the population. 5 day growth assays were carried out on HEK 293 cells. HEK 293 cells were plated at a concentration of 150,000 cells/ml and growth for 5 days. On the 3rd day of the experiment cells were treated with 100nM dexamethasone and 0.001% ethanol controls as described in the synchronisation protocol above (demonstrated by arrow). Figure 4.8 show the results of this assay. Concentration of HEK 293 cells per day are shown in cells/ml ± SEM for each treatment group. n=6. Growth was analysed using a one-way ANOVA with post-hoc T-test. HEK 293 cells demonstrate an exponential growth rate over the 5 days, with a doubling time estimated to ~32 hours. Neither synchronisation nor ethanol control has a significant effect on growth rates of the population, ANOVA revealed no significant variation p-value > 0.05.

4.2.7 Disruption of the circadian clock by CLOCK1a DN significantly decreases growth within HEK 293 cells

The growth rates of HEK 293 *CLOCK1a DN* and HEK 293 *pCLNCX* cells were assessed via growth assay. Both cell types were plated at a concentration of 150,000 cells/ml and grown for 5 days in standard culture. Figure 4.9 show the results of this assay. Concentration of HEK 293 *CLOCK1a DN*, HEK 293 *pCLNCX* and HEK 293 Wild-Type (WT) cells are shown per day as cells/ml ± SEM, n=6. Growth was analysed using a one-way ANOVA with post-hoc t-test, (* P-value = < 0.05, ** = p-value < 0.01)

Growth rates of HEK 293 empty vector cells match those of the WT and those seen in Figure 4.8 of untransfected cells; showing exponential growth with a doubling time of ~ 32 hours. HEK 293 *CLOCK1a DN* cells display a significantly decreased rate of growth over the four days after plating, as assessed by post hoc t-test. This suggests that the clock is required for optimal growth.

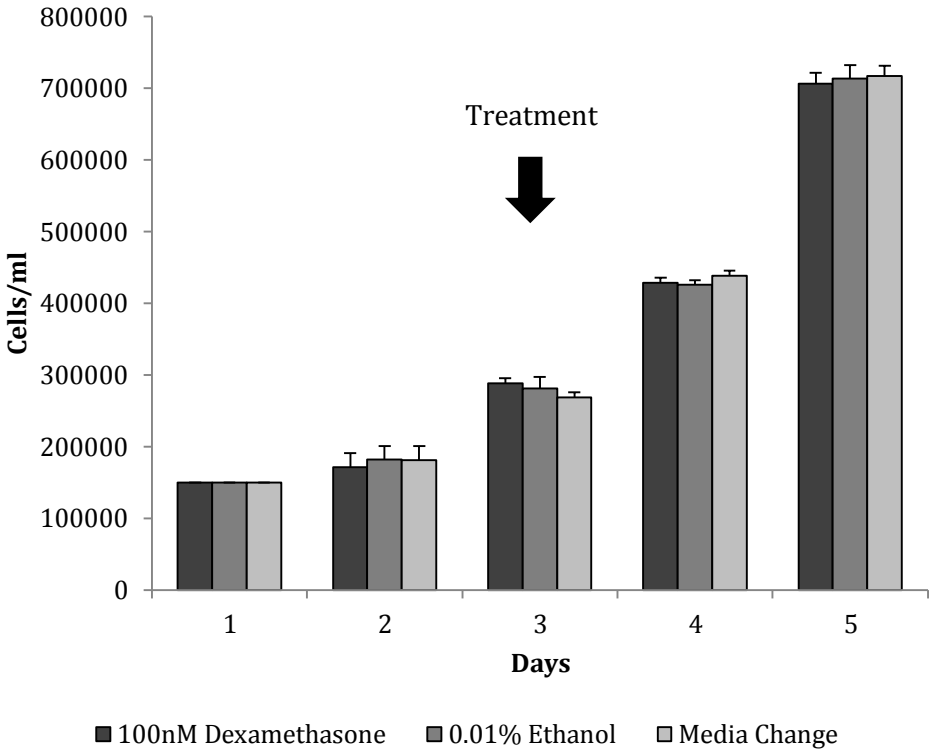

Figure 4.8. HEK 293 cells were plated at 150,000 cells/ml. The samples were cultured over 5 days, on the 3rd day of which samples were treated with a 2 hour pulse of 100nM dexamethasone, 0.001% or media change. The concentrations of cells were established for each treatment group for each of the 5 days. Figure shows growth as cells/ml ± SEM, n = 6. Variance between treatment groups was assessed by one-way ANOVA. No significant variation is observed. Arrow indicates treatment time.

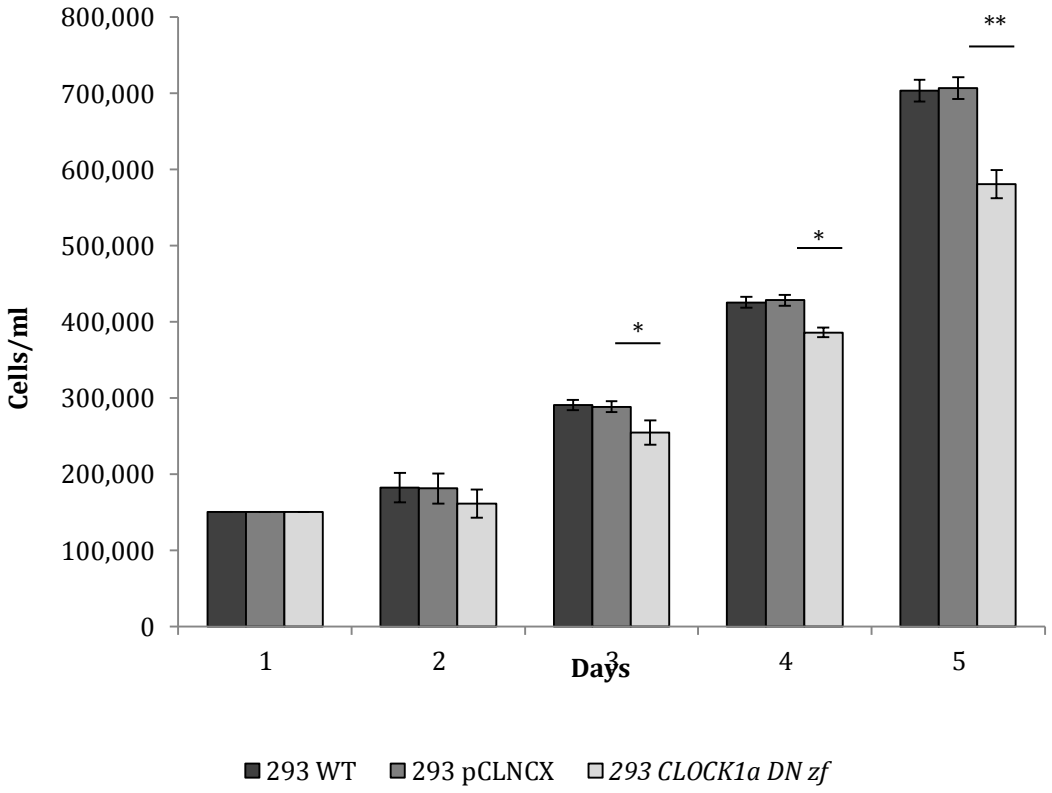

Figure 4.9. HEK wild-type (WT), HEK 293 *pCLNCX* and HEK 293 *CLOCK1a DN* cells were plated at a concentration of 150,000 cells/ml. They were cultured over 5 days and on each day concentration was assessed by growth assay. Figure 4.9 shows the concentration of cell (cells/ml) ± SEM, n = 6 for each day of culture. Variations in growth between the cell types were determined by one-way ANOVA and post-hoc T-test. No significant difference in growth was found between WT and *pCLNCX* (p-value > 0.05). Significant differences were found between HEK 293 *pCLNCX* and HEK 293 *CLOCK1a DN* cells as shown (* P-value = < 0.05, ** = p-value < 0.01).

4.2.8 Expression of Cell Cycle regulators

Disruption of the clock has a profound effect on the growth rate of HEK 293 cells. To elucidate whether this inhibition in growth could come from a disruption in clock regulation of the cell cycle, expression patterns for a number of cell cycle regulators were determined via quantitative PCR analysis.

As in previous experiments HEK 293 cells were grown to ~90% confluency and the synchronised with a 2 hour 100nM dexamethasone pulse and 0.001% ethanol control. Following this pulse, cells were harvested every 6 hours in parallel with an ethanol based control over a three day period. Figure 4.10 shows the results of these experiments. Within the first panel Figures A, B and C show the expression patterns for genes involved in the regulation of S-phase: *p21*, an S-phase inhibitor, *Cyclin E1*, part for the G1/S checkpoint cyclin/kinase complex and *pCNA* a processivity factor for DNA polymerase.

The expression pattern of *p21* is most striking. Following dexamethasone synchronisation the mRNA expression oscillates over the three days, with a 8-fold amplitude, peaking at 14-20, 38-44 and 62 hours post treatment. Both variance over time and average peak/trough values were found to be significant with p-values < 0.001 and <0.001 respectively. No significant variation in expression over time was seen in the ethanol control (p-value > 0.05). These oscillations have an average period of ~ 24 hours suggesting circadian regulation.

The mRNA expression pattern of p*21*'s target, *Cyclin E1*, also displays a significant oscillation in dexamethasone synchronised populations. The rhythm has a 2.5 fold amplitude, peaking at 26 and 50 hours post treatment. This is an anti-phase with

p21, as would be expected from the antithesis of function. The robustness of this rhythm is smaller than that seen of *p21*.

pCNA is a DNA polymerase facilitator, as a result one would expect its expression to display a similar pattern to that of *Cyclin E1*. The mRNA for *pCNA*, can be seen to vary across the 3 days, with a pattern suggesting of an oscillation, peaking at 8, 38 and 62 hours post synchronisation. This is a more similar pattern to *p21*, the S-phase inhibitor. However this oscillatory pattern is not significantly different from the expression pattern elicited by ethanol pulsing (p-value > 0.05). Expression of *pCNA* seems to be highly variable across all conditions.

The second panel of figures shows, genes involved in mitosis and apoptosis. Firstly, Figures D and E show the mitotic genes, *Wee1* and *Cyclin B1*. *Wee1*, as mentioned earlier is a mitotic inhibitor, shown within mouse regenerating liver to oscillate with a circadian phenotype post hepatectomy. However, it is not seen to oscillate in the zebrafish cell-line experiments (section 3.3.8). Here, in HEK 293 cells, synchronisation of the circadian clock has a significant effect on the *Wee1* expression. *Wee1* is seen to oscillate over time, with an amplitude of 3-fold, peaking at 32 and 62 hours post synchronisation. The expression pattern within the control cells displays no significant variation. What is interesting is that the period of this oscillation is ~30 hours, longer than that expected from the expression pattern of other cell cycle genes, shown above, and that of a circadian regulated gene, in general. This period is closer to that of HEK 293 cells natural cell cycle length. Could this rhythm be a by-product of the endogenous cell cycle timing rather than a circadian product? To further address this question we can look at Figure E, which shows the expression pattern of *Cyclin B1*. *Cyclin B1*, is not seen to

show any significant variation in expression in either the synchronised of unsynchronised populations. This is the opposite of what was noted within the zebrafish PAC-2 cell-line.

cMyc, has been implicated as a target of the *Per2* genes, and in this way facilitating their function as tumour suppressors (Lee *et al,* 2003). Within in this experiment HEK 293 cells however, there is a significant variation seen between the expressions of *cMyc*, between synchronised an unsynchronised cells, however, there is no ostensible rhythmic expression.

A p21

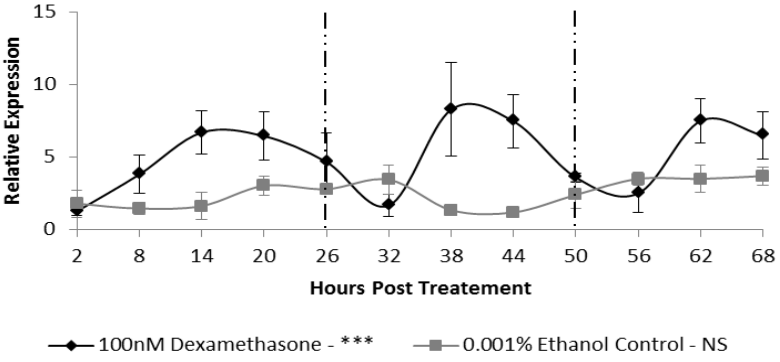

B Cyclin E1

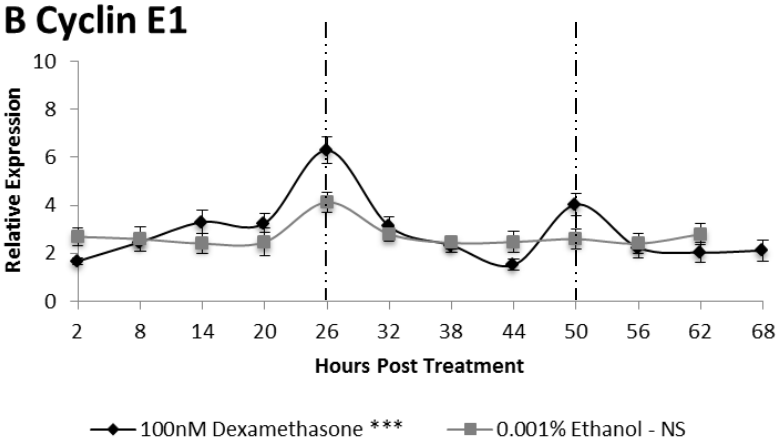

C pCNA

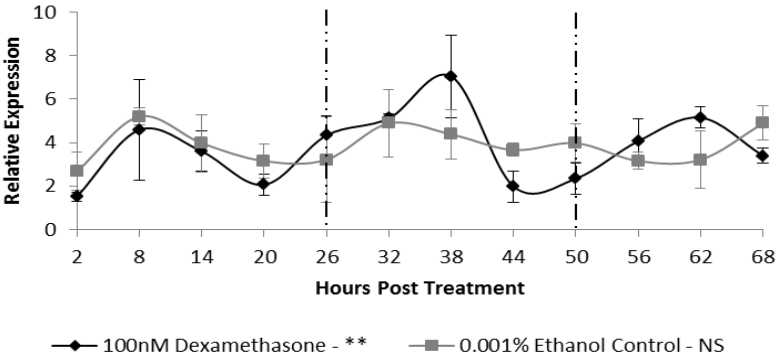

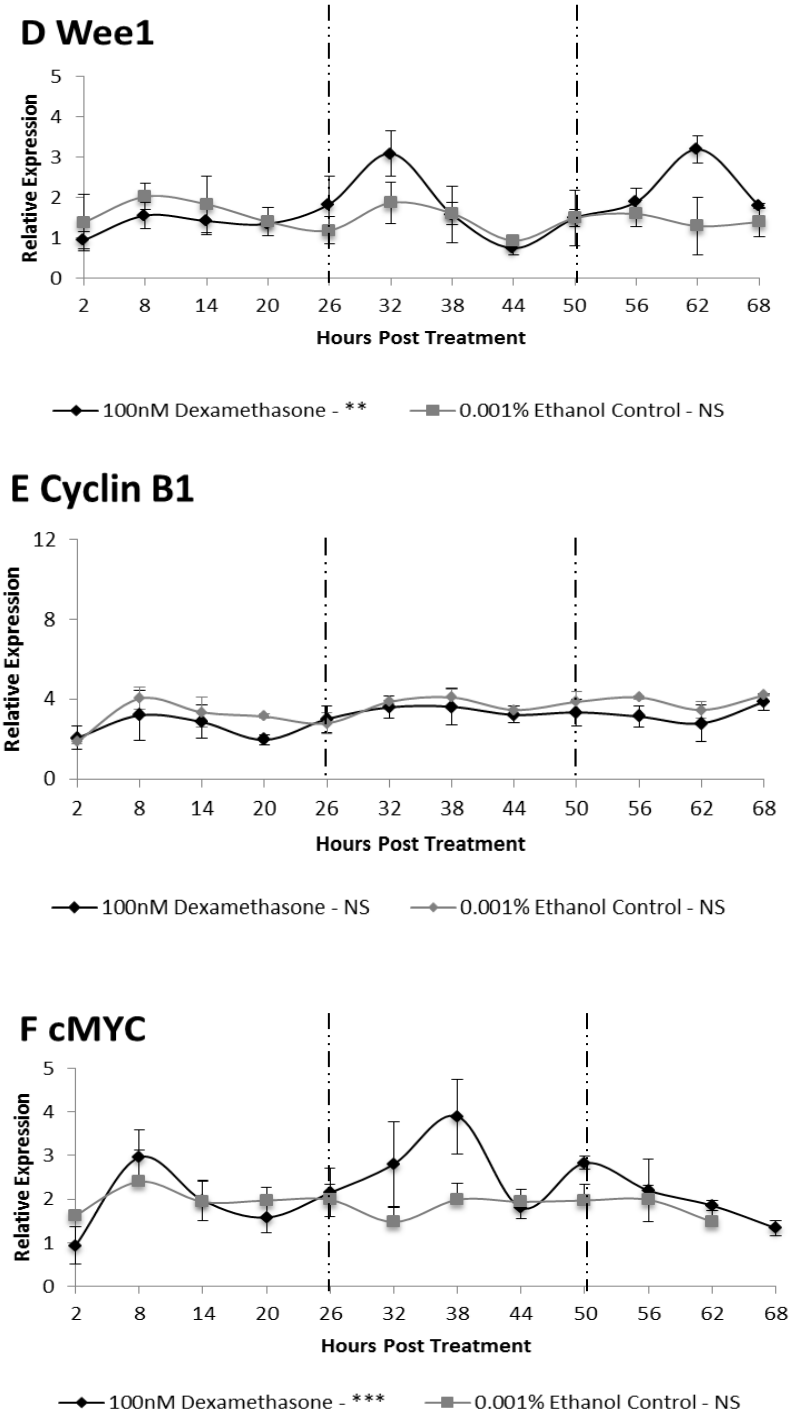

Figure 4.10. HEK 293 cells were treated with a 2 hour pulse of 100nM dexamethasone or 0.001% ethanol control and harvested every 6 hours for 3 days. This figure shows results of qPCR expression analysis for genes *p21, Cyclin E1, pCNA, Wee1, Cyclin B1* and *cMyc* (A-F) respectively. Relative expression is shown ± SEM, compared to reference gene TATA-Box binding protein (*TBP*), n = 3. To assess variation a two-way ANOVA was used. Average peak/trough fold difference (amplitude) as assessed with a post-hoc T-test. (NS = not significant, p-value > 0.05, * = P-value < 0.05, ** = p-value < 0.01, *** = p-value < 0.001.)

4.2.9 Expression of cell cycle regulators within HEK 293 CLOCK1a DN cell-lines.

It is clear from the results above that synchronisation of the clock does have some effect on the expression patterns of a number of core clock genes, *p21, Cyclin E1, Wee1* and subjectively though not significantly *cMyc*. An interesting observation is that 3 of these genes are members of groups previously mentioned to be regulated by circadian glucocorticoid signalling. In this way the cell cycle may be coordinated by the clock in these cells, however not through direct action of the cellular clock itself. In order to dissect these pathways, HEK 293 cells transfected with the *pCLNCX* and the *CLOCK1a DN* construct were used. These cells were subject to dexamethasone synchronisation as described earlier, and harvested at 26, 32, 38 and 44 hours post treatment. Figure 4.11 show the results of qPCR assays on these cells. In Figure A, the sample cDNAs were pooled to allow assessment of *CLOCK1a DN* effect on total expression of cell cycle genes *p21, Cyclin E1, pCNA, Wee1, Cyclin B1* and *cMyc.* Relative expression is shown ± SEM, compared to reference gene TATA-Box binding protein (*TBP*), n = 3. A student T-test was used to assess difference in expression levels. As can be seen disrupting the clock has no effect on the total expression level of any of these genes (T-test p-value > 0.05).

Figure B shows the relative expression of *p21, Cyclin E1, Wee1* and *cMyc* during the second day post treatment in *pCLNCX* and *CLOCK1a DN* cell-lines. Relative expression for each gene is shown ± SEM, compared to reference gene TATA-Box binding protein (*TBP*), n = 3, for each time point. Two-way ANOVA was used to assess variation. The expression level between cell-lines per time-point were then

assessed using post-hoc T-Test. Post hoc T-Tests was also used to assess the significance of any peak/trough differences.

It can be seen that in *CLOCK1a DN* cells variation over time in these genes, with the exception of *cMYC*, persists, despite clock dysfunction. These oscillations all appear in phase with those of the empty vector (*pCLNCX*) cell-lines. However amplitude is mildly reduced, as shown by lower average peak/trough values and significance.

Persistence of these variations, even if mildly attenuated, leads to the conclusion that these rhythms observed are mainly produced by glucocorticoid stimulation as described in section 4.1.3. Disruption of the clock within these cells has a small effect on cell growth and as seen here has a small effect on induction of cell gene rhythms. This may be due to simple redundancy of cellular clock based cell cycle regulation; this may result from an uncoupling of the cell cycle and the cellular clock in such immortalised cell-lines. Thirdly, it must not be forgotten that in *vivo* production and coordination of rhythms is driven by a multifactorial system, the lack of which in vitro may result in incomplete coordination of downstream pathways. These will all be discussed late in section 4.4.

A

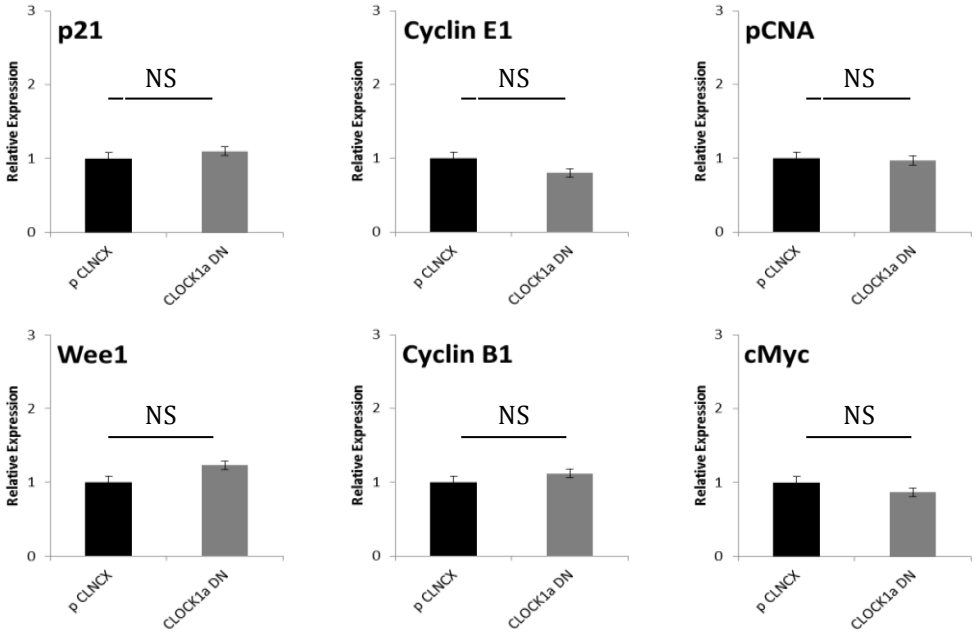
p21
NS
Relative Expression
p CLNCX
CLOCK1a DN
Cyclin E1
NS
pCNA
NS
Wee1
NS
Cyclin B1
NS
cMyc
NS

B

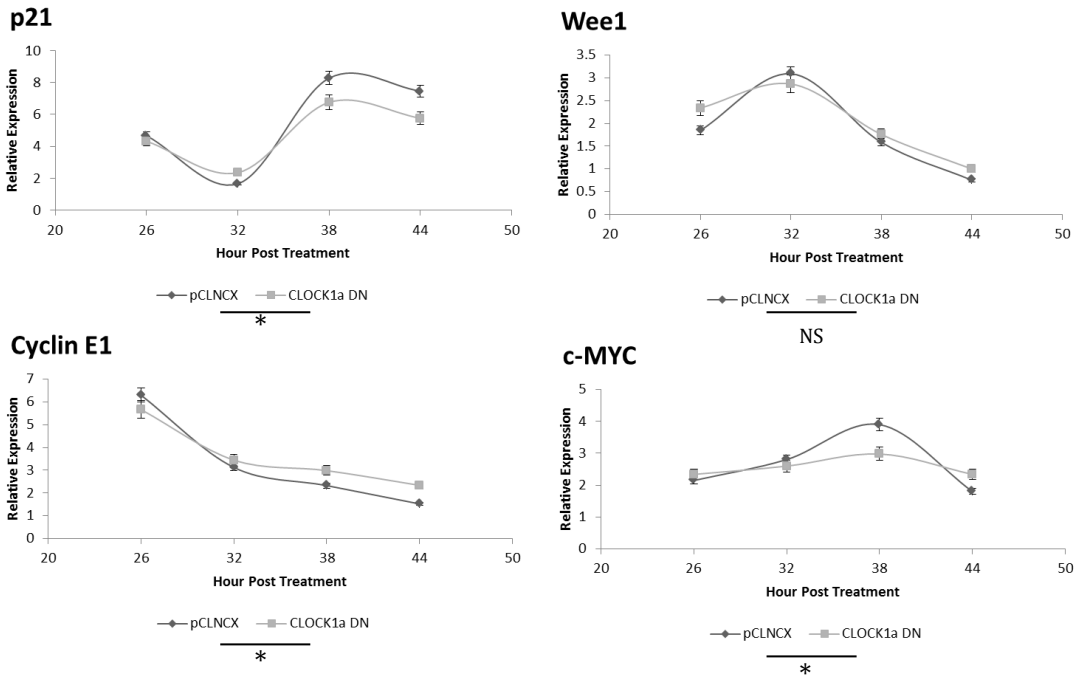

Figure 4.11 HEK 293 cells were transfected with pCLNCX and CLOCKK1a DN constructs. They were subsequently synchronised using a 2 hour 100nM dexamethasone pulse, and 0.001% ethanol control. Cells were harvested at 26, 32, 38 and 44 hour post treatment. Figure A shows the relative expression of cell cycle genes *p21, Cyclin E1, pCNA, Wee1, Cyclin B1* and *cMyc* (I-VI respectively) in pooled samples of each cell-line. Data analysed by student's T-test (NS = p-value > 0.05) Figure B shows the relative expression of *p21, Cyclin E1, Wee1* and *cMyc* over the second day post treatment for each cell-type. All relative expressions are shown ± SEM, compared to reference gene TATA-Box binding protein (TBP), n = 3. To assess variation in expression over the time-course a two-way ANOVA was used. Average peak/trough fold difference (amplitude) as assessed with a post-hoc T-test. (NS = not significant, p-value > 0.05, * = P-value < 0.05)

4.2.10 Cell cycle analysis

Finally, the functional implication that synchronising the cellular clock may have on cell cycle progression was analysed using cell cycle analysis. As a control to look at synchronisation of these cells by known cell cycle synchronisers, HEK 293 cells were synchronised using Thymidine and serum starvation block, released and harvested every 6 hours, over the following 3 days (data not shown). Upon release, 78% and 60% of cells had accumulated in S-phase and G1 as expected, giving an comparative figure for synchronisation efficiency. Cells progressed out of the block within 12 hours of release and were seen to have progressed through the cell cycle within 38-44 hours after release. Due to the low resolution of the data cell cycle length can only be estimated, therefore, to between 24 and 32 hours. However, this agrees with the cell growth data.

HEK 293 cells were cultured to ~90% confluency and pulsed for 2 hour with a media change control, 0.001% ethanol control and 100nM dexamethasone respectively. Cells were harvested every 6 hours after removal of treatment for 3 consecutive days. Cells were processed and stained using the DNA marker Propidium Iodide (as described in section 2.1.3).

Figure 4.12 shows the results of this experiment. The percentage of cells within the sample population is shown ± SEM, n = 6, for each time-point and treatment group. Variation over the time-course was assessed by one-way ANOVA. Figure A, shows cells progressing through S-phase, Figure B, those in passing through G2 and undergoing mitosis (the two states are indistinguishable by the methods of analysis). There was not significant variation in expression over time or between any treatment group, as assessed using the methods above. Subjectively the media

and ethanol control samples display no variation from one another, however when assessing the dexamethasone treated samples, there appears to be more variation, and that any trough in G2/M phase (20 and 44 hours post treatment) correlate with highest expression levels of p21. These genes expression patterns appear in antiphase with each other, as may be expected for opposing phases of the cell cycle. This data suggests that synchronisation of the clock, has no significant effect on the progression of the cell cycle, nor produces oscillation in this progression. However, one must consider the limitations of the data and statistical analysis, as will be discussed later in section 4.4. This lack of clock function, which has been descried in vivo (Yoem *et al,* 2010) also point to consideration for the three arguments made in section 4.2.9. Could this be a redundancy of clock function within this tissue? An uncoupling of the clock and cell cycle due to immortalisation? Or is the subjective differences observed attenuated responses, representing control that is produced by the culmination of synchronisation factors not considered in this study?

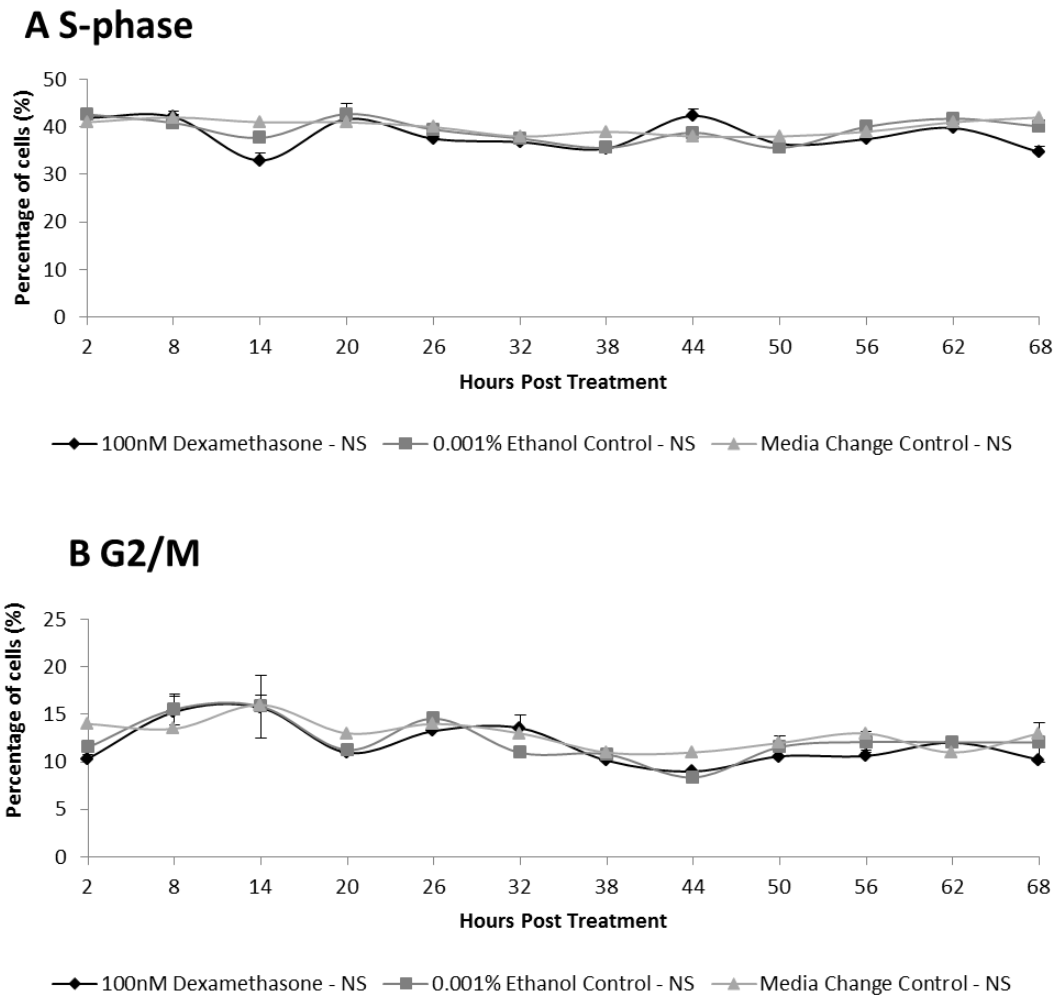

Figure 4.11 HEK 293 cells pulsed for 2 hours by a media change, 0.001% ethanol control or 100nM dexamethasone control. Cells were harvested every 6 hours after treatment over 3 consecutive days. Cell cycle progression was then analysed using propidium iodide and FACs analysis of cell cycle stage. Figures A & B show the percentage of cells in S-phase and G2/M within the population +/- SEM for each time-point and each treatment groups. Variation was assessed by two-way ANOVA (NS = P-VALUE > 0.05).

4.4 Discussion

This is the first time that circadian gene expression and function has been demonstrated in HEK 293 cells. Quantitative PCR and sequencing analysis has shown that these cells express the gene components regarded as crucial to the circadian clock mechanism. This study has also shown that rhythmic transcription of these genes can be generated by a number of stimuli, previously shown to produce rhythmic outputs within mammalian cell-lines (Izumo *et al,* 2005).

The rhythms observed are maintained over the three days examined and demonstrate a number of characteristics that allow them to be thought of as circadian in origin. Primarily, it has been demonstrated that only transcripts that are circadian in regulation *in vivo*, have been found to cycle post serum and dexamethasone shock *in vitro* (Balsolobre *et al*, 1998. Balsolobre *et al*, 2000). The oscillation produced display a period (τ) of ~24hrs, within the range of periodicity expected of human clocks (Brown *et al*, 2005). Secondly, the relative phases of these oscillations not only coordinate with each other in a manner expected of this auto regulatory feedback network, but also correspond with phases demonstrated in human primary blood cell and fibroblastic studies, but also the preceding rodent studies (Kusangi *et al*, 2004. Fukuya *et al*, 2007. Teboul *et al*, 2005. Brown *et al*, 2005).

There remain a number of interesting observations arising from this data. Firstly, the average levels of gene expression within unsynchronised population are lower than the average gene expression levels within synchronised cells. Synchronisation methods demonstrated in this chapter are based on the hypothesis that within a

population of cells, each cell contains a fully functioning clock; this clock runs autonomously, out of phase with their neighbours (Nagoshi et al, 2004). Stimulation with certain agents produces putative transcriptional changes, as discussed below, which cause the phases of the independent oscillators to align. Similarly after stimulation, if the phase is not maintained by a regular *zeitgeber*, as demonstrated by temperature pulsing (Brown *et al*, 2005) these clocks will start to free-run, lose synchrony and return to a population of independently running clocks. This theory doesn't indicate that synchronisation affects clock function within the cell, so average levels of gene expression would be constant regardless of synchronisation state.

Rhythms demonstrated in this study fit this model with the exception of *Per1* and *Bmal1* expression, which appears to gain robustness over the second day of the time-course. However, upon closer examination of this expression profile it can be seen that instead of amplitude of rhythm increasing, the basal levels (measured as the trough of the oscillation) are steadily increasing over time. Again synchronisation treatment with ethanol seems to be affecting the level of clock gene expression. This could represent the fact that these treatments tonically activate the expression of these genes, leading to a raised baseline. Or of course it could also reflect a change in cell number over time within the cultures. This may also be a temporal artefact. Rhythms stimulated by dexamethasone shocking and reported by bioluminescent reporter, oscillate for 5-6 days. It may be that these rhythms will start to dampen later after dexamethasone shock.

It was demonstrated early within this chapter that cell confluency affects the fold induction of circadian genes. If fold induction can be thought of as a function of

synchronicity or robustness of rhythm, could cell-cell communication be playing a role in maintaining co-ordination?

It has been demonstrated that the clock regulates a number of cell-cell communication and adhesion molecules, such as cadherins, adherins and connexions (Yamato M *et al*, 2010). Could reciprocal regulation or coupling between these systems be responsible for this increased robustness? Work carried out by Dr Peter Cormie within the Whitmore Lab has shown that within zebrafish cell-lines connexin regulated cell-cell communication is governed by the circadian clock, however knocking down connexin function using a connexin DN construct, has no effect on clock function (data unpublished). In this case no reciprocal regulation, however this does not exclude the possibility communication by other molecules is having an impact on peripheral clock synchronisation and function.

How do these agents produce phase synchronisation? It is interesting that phase induction of *Per1, Per2 and Reverb-α* is identical to the phase response seen in Rat-1 fibroblasts post serum and dexamethasone shocking. It is interesting that in the first of these papers *Per1* and *Per2* are described as immediate early genes and that synchronisation is dependent upon this characteristic (Balsalobre *et al*, 1998). *Per1, Per2 and Reverb-α* behave in a similar was to immediate early gene c-fos, which undergoes a rapid and transient increase in transcription rate following a given stimulus. As this then decays it manages to auto repress transcriptional activity and initiates subsequent transcription and initiating coordinated oscillation (Balsalobre *et al*, 1998). Initial expression increase (within the first hour) was not measured within these experiments. However, the expression profiles produced, could easily result from such a reaction.

One striking difference between the rhythms shown here and in previous rodent studies, when compared to zebrafish clock gene expression is the amplitude of the mammalian oscillation is extremely small. This dissimilarity can easily be explained by the differing nature of entrainment in the two models. With the zebrafish, a decentralised system, the tissue clock is directly entrained by environmental *zeitgebers*, the resulting rhythms are therefore highly robust. In mammals however, peripheral clock are at the "lowest rung of the circadian hierarchy" and respond to a variety of coordinating agents, generated largely in response to the SCN. The strength of signal is likely, therefore, to decrease as more pathways distance the external zeitgeber from the end-point clock. The decreased rhythm seen in clock target genes, compared to clock gene oscillations themselves, have a similar aetiology. Fish are simply a more robust circadian model than mammals.

Disrupting the clock is shown to result in slower growth rates, suggesting that a functional cellular clock is required for optimum growth; however synchronisation of these tissue clocks does not convey any advantage and is not necessary for optimal proliferation. This reduction in growth was also seen in the zebrafish cell-lines, and seemingly contradicts the light-at-night hypothesis. This theory suggests that irregular/unnatural *zeitgeber* activity results in deregulated circadian control of the cell cycle. The culmination of increased cell proliferation rate and decreased DNA checking, repair and mutation driven apoptosis, would lead to increased rates of cancer. There is no evidence to support this theory in this model, or the zebrafish or previous studies (Miller *et al.*, 2007. Antoch *et al.*, 2008)

It is also quite likely that clock genes, many of which are transcriptional regulators, have an effect on gene expression other than causing these genes to oscillate. In other words, the tonic activation of genes is likely to be critical, and disrupting this level of gene regulation could lead to slower growth even if this proves is not rhythmically regulated.

Interestingly this study shows that dexamethasone pulsing results in rhythmic gene expression within *p21, Cyclin E1* and *Wee1*. It has previously been mentioned that S-phase regulated genes have been shown to be sensitive to glucocorticoid induction (Mattern *et al*, 2007. Chebotaev *et al*, 2007). Here, *Wee1*, the mitotic regulator shows similar characteristics. This suggests that homeral clock outputs form part of a multi-targeted approach when coordinating the cell cycle. Another interesting observation from these experiments is that in *CLOCK1A DN* cell-line, glucocorticoids are able to mask rhythmic gene expression driven by the intracellular clock. In order to demonstrate function of the intracellular clock, a glucocorticoid antagonist such as mifepristone (RU-486), would have to be employed to reveal the underlying control. Evidence of current intracellular regulation is derived indirectly from the literature and promoter analysis of cell cycle genes.

As mentioned in the previous chapter, circadian rhythms in cell cycle gene expression is driven by clock genes binding to a number of conserved motifs within the promoter regions of the genes. These have been identified as predominately E-Box, D-Box and RORE's (Yan *et al*, 2008). As preliminary work for this study the promoter regions of circadian targets have been analysed for these motifs to evaluate the likelihood of them being clock targets. Promoter regions for

the genes *p21, Cyclin E1* and *Wee1* from both mouse and human were aligned and conservation of regulatory motifs assessed.

The promoter sequences for all three genes are highly conserved between mice and humans. The *Wee1* promoter region contains three canonical E-Boxes as well as D-box sequences. In a similar way the promoter region of *p21* has the capability to be highly clock regulated containing E-boxes, D-boxes and a RORE like region. It is interesting that *Cyclin E1* contains no E-boxes. This analysis allows leads to the conclusion there is not physical lack of binding motifs that would prevent intracellular circadian regulation. Of course, it equally does not prove that it does occur.

In a recent study, Yoem *et al*, 2010, it was shown that rhythmic *Cyclin B1* expression within Rat-1 fibroblasts was in fact independent of the cellular clock, and not temperature compensated. This has led to the hypothesis that the cell clock and the cell cycle may be uncoupled during the immortalisation process. In this way, immortalised cell-lines would behave more like the cancer cells. This is an interesting theory to bear in mind when considering the data in this study.

From this data one could draw the hypothesis that circadian coordination of the cell cycle is performed through a number of pathways both intra and extracellular. Intracellular clock function is crucial to cell viability and health, as reflected by the poor cell growth seen in *CLOCK1A DN* cell-lines. However, humoral circadian signals are responsible for the coordination of the intracellular clock as well as rhythmic cell cycle genes expression. The internal clock of the cell may have a role to play in gating cell cycle progression; however, this is masked by humoural regulation, and may be uncoupled within immortalised cell-lines.

A number of follow on experiments could be carried out to validate this hypothesis. Firstly, in order to explore the role of clock disruption on peripheral clock function and its down-stream targets, the human *Bmal DN* construct must be employed to support these results.

Secondly, one of the major difficulties when assessing endogenous gene expression within mammalian cell-lines is statistical analysis rhythms to confirm they are of circadian in origin. The experimental designs above, allow for endogenous gene expression to be monitored over a time-course. However due to the manual sampling required, the final data has only medium to low temporal resolution. This then proves difficult to statistically analyse using available software. They are programs which enable sine-wave fitting and Fast-Fourier analysis so that rhythmicity and period can be quantified. The data in this study is unsuitable or such programs. One way of producing such data is the use of reporter expression systems that allow high throughput and high resolution data, without manual handling. This includes the use of bioluminescent reporter constructs mentioned in Chapter 3. Through correspondence, two mammalian reporter vectors have been donated to the Whitmore lab: human *Per1_Luciferase* and human *Bmal1_lucierase* (Motzkus *et al*, 2002. Yoshikawa *et al,* 2008). Transfection and assaying such constructs will allow mathematical quantification of the rhythms observed in this study.

In conclusion, this study has shown

- That HEK 293 cells possess peripheral clocks
- That these may be synchronised using glucocorticoid pulsing.
- In addition it also shows that the *CLOCK1a DN* construct is able to disrupt peripheral clock function within this cell-line.
- Clock disruption results in decreased proliferation, displaying that clock function is crucial to optimal cell proliferation.
- Synchronisation of these clocks in culture, does not affect growth rates.
- There are rhythms in cell cycle regulators, but these do not seem to be abolished in clock mutant cells. These factors seem to be driven by humoural circadian messengers rather than the cellular clock itself.
- It is proposed that the mammalian circadian system utilises multiple levels of coordination in controlling the timing of the cell cycle, as illustrated in Figure 4.12. The interaction between the intracellular clock and the cell cycle cannot be assessed fully rom this data, however it suggests that this system may have been disrupted in immortalised cell-lines.

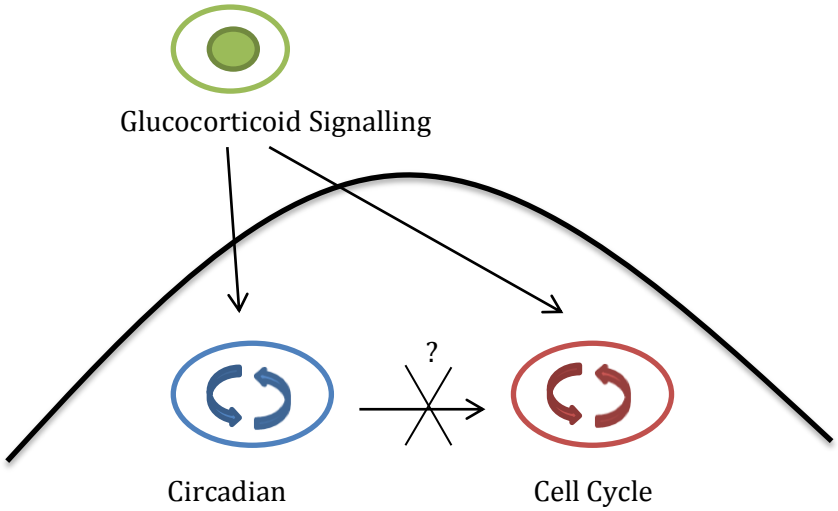

Figure 4.13. Schematic of the putative, integrated pathways linking the circadian clock and cell cycle within mammals. ? indicating possible disconnection of pathway in immortalised cell-lines.

CHAPTER 5

CLOCK FUNCTION WITHIN BENIGN AND MALIGNANT BREAST EPITHELIAL CELL-LINES.

5.1 INTRODUCTION

5.1.1 Breast Cancer Overview

Breast cancer is the most common form of cancer within women, contributing to 16% of all cancer diagnoses in 2008. During this year, 47,693 women were diagnosed, along with 341 men (1 in 100 people to develop breast cancer are male; prognosis is often worse due to delayed diagnosis) (Office of National Statistics, UK, 2010). Breast cancer is a malignant neoplasm involving the tissue of the breast. 85% of breast cancers are adenocarcinomas, those arising from the glandular tissue of the breast. Out of these 70% arise from the epithelial tissue within the ducts of the breast, the rest from lobar cells (Kumar & Clark, 2005). It is for this reason ductal epithelial cell-lines have been chosen for this study.

5.1.2 The Light at Night Theory

Breast cancer is endemic in developed countries. However, incidence varies 5-fold between non-developed and developed regions (Parkin *et al*, 2001). Curiously, incidence of breast cancer increased as countries become more industrialised, until the reach the same level as more developed areas (Stevens, 2005). The "Light at Night" hypothesis states that as countries industrialised the use of artificially lighting and shift work patterns emerge. This results in a disruption in entrainment of the circadian clock, which in turn will lead to asynchrony of downstream targets (Steven, 2006). The most prominent of these targets is the cell cycle, if the cell cycle becomes unregulated, malignancy will ensue (Stevens, 2005)

Epidemiological evidence supports this theory. A number of cohort studies, enlisting women who have undertaken prolonged periods of shiftwork have shown an increased incidence of breast cancer within this population compared to the control groups (Tynes *et al*, 1996. Hansen, 2001. Davis *et al*, 2001. Schernhammer *et al*, 2001). Standardised incidence ratios varied from 1.36 to 1.9, all with significant confidence intervals, suggesting a significant interaction. Approaching the hypothesis in a different way, the incidence of breast cancer is lower in blind women (with complete retinal dysfunction, who therefore free-run from a circadian perspective) than compared to the general population. (Hahn *et al*, 1991. Feyschting *et al*, 1998. Verkasalo *et al,* 1999). However, not all these studies show consistent results (Travis *et al*, 2004) and some criticism has arisen of their experimental design, especially the classification of "prolonged" shift work. Data can also be confounded as a result of question ambiguity (Stevens, 2005). The epidemiological studies however are not without support from genetic and molecular investigations.

5.1.3 Molecular evidence for clock contribution to breast malignancy

Rodent models have provided a solid basis of biological support to the epidemiological evidence. Increase incidence of breast neoplasms have been shown in mice in which the melatonin output rhythm is disturbed, either by pinealectomy or disrupting the light regime (Aubert *et al*, 1980. Mhatre *et al*, 1984). Furthermore, when human breast cancer xenografts, from MCF7 cell-line cultures (a ductal adenocarcinoma cell-line model), are implanted into nude rats constant and irregular lighting regimes result in a dramatic increase in xenograft

growth. This was the first time nocturnal illumination was shown to affect human derived tissue growth (Blask *et al*, 2003)

In order to define the exact mechanism for this reaction, clock genes and their function have been studied within rodent mammary tissue. Clock genes are fully expressed and developmentally regulated within these tissues (Metz *et al*, 2006). Interesting, *Per1* and *Per2* genes, in particular, act as tumour suppressors within mammary tissue (Fu *et al*, 2002. Gery *et al*, 2006). For example ectopic expression of *Per2* leads to decreased growth of cell cultures, whereas gene deletions leads to increase incidence of malignant lymphomas in test animal (Fu *et al*, 2002. Gery *et al*, 2005).

Although the underlying cause of this tumour suppression is unknown, clock genes have been shown to regulate a number of cell cycle regulators as mentioned previously in Section 1. CLOCK:BMAL heterodimers directly regulate the expression levels of *Wee1* (Matsuo *et al*, 2003), *c-Myc* and *Cyclin D* (Fu *et al*, 2002. Sahar & Sassone-Corsi, 2007) in rodents, While *Dec1* and *Dec2* have also been shown to regulate the *p53* dependant and independent apoptotic pathways within the human breast cancer cell-line, MCF7 (Wu *et al*, 2011). Results concentrating on *Cyclin D1* are particularly interesting as overexpression of this gene induces mammary tumorgenosis (Sahar & Sassone-Corsi, 2007). Increased expression of this gene is also a poor prognostic marker for human mammary carcinoma (Sahar & Sassone-Corsi, 2007). *Cyclin D1* also interacts with the *BRCA1* suppressor gene (Wang *et al*, 2005). *BRCA1* mutation is associated with familial breast carcinoma; it would be interesting to consider if deregulation of this gene could contribute to spontaneous carcinogenesis.

Temporal gene expression of a number of cell cycle regulators is also controlled by the intrinsic HAT activity of clock component CLOCK (Doi *et al*, 2004, Sahar & Sassone-Corsi, 2007). This adds an addition level of control.

5.1.4 Clinical evidence in support of circadian regulation of the cell cycle.

A recent clinical study looking at the expression levels of clock genes within biopsied tissue taken from human breast carcinomas, shows deregulated expression of all three human *Per* homologs. In fact, some form of *Per* down regulation was found in > 95% of the cancerous samples in comparison to near-by non-cancerous control tissue (Chen *et al*, 2005). Interestingly this deregulation was not the result of a gene mutation but of hyper-methylation of the *Per* promoter sequence (Chen *et al*, 2005) suggesting that clock gene disruption might have an additional epigenetic cause. Interestingly, decreased expression of *Per1* and *Per2* has also been described recently within familial cancers. In this study in many *BRCA1* related cancers *Per1* was expressed at a lower level that in non-heredity carcinomas (Winter *et al*, 2007).

In addition, a number of genetic polymorphisms have been described within *Per*, *Clock* and *Cry* genes, which occur in much higher frequency in individuals with breast carcinoma than the healthy population (Dai *et al,* 2011)

In summary, there is a growing body of evidence linking breast malignancy to circadian disruption. This study sets out to determine clock function within human cell-line models of breast epithelium and elicit whether there is any downstream regulation of the cell cycle.

5.2 MATERIALS AND METHODS.

5.2.1 Cell-lines and cell culture.

Michigan Cancer Foundation 10A (MCF10A): This cell-line was produced from a cultured tissue biopsy of human breast epithelium. The biopsy was taken from a 39 year old female, during tests for suspected fibro-cystic disease, and immortalised through long term culture in serum free medium with low Ca++ concentration. MCF10A were cultivated from the adherent population within this culture (Soule *et al,* 1990).

The MCF10A cell-line is regarded as a model for benign breast epithelium, as they have a diploid karyotype and are dependent on exogenous growth factors for proliferation. Microscopically these cells appear phenotypically similar to breast epithelial cells. More specifically, under electron microscopy cells appear more indicative of luminal ductal epithelium as opposed to myoepithlium. They also express breast epithelium specific antigens, MFA breast and MC-5. They are non-tumorigenic in immunosuppressed mice and do not form colonies in semisolid medium (two distinct markers of tumorigenic activity). When plated on a mixture of collagen and laminin they form 3D structures similar to that of ducal acini (Debnath *et al*, 2003).

Cells were cultured in Dulbecco's Modified Eagle Medium/F12 (Invitrogen at Life Technologies Ltd.), with 5% donor horse Serum (Biochrom AG), penicillin (100U/ml), streptomycin (100µg/ml) (Invitrogen at Life Technologies Ltd.), human epithelium growth factor (EGF) 20ng/ml, Insulin 10µg/ml, hydrocortisone 10ug/ml (All additives by Sigma-Aldrich Company Ltd.). Cells were cultured at 37°C, with 5% CO_2.

Cells were purchased from American Type Culture Collection (ATCC™).

Michigan Cancer Foundation 7 (MCF7) cell-line: The MCF7 cell-line was isolated in 1973, from a 69 year old female patient with known breast adenocarcinoma. The cells were cultured from the sample of pleural effusion, and found to be from the primary tumour, an invasive ductal adenocarcinoma (Soule et al, 1973). It was cultured without any further transformation.

It is regarded as a model for ductal adenocarcinoma. Although displaying phenotypic epithelial characteristics, cells are no longer reliant on exogenous growth factors due to the changes subsequent to the expression of oncogene *Tx-4*. The cells have, however, maintained the ability to process estradiol via cytoplasmic oestrogen receptors and are also sensitive to progesterone (Ross *et al*, 2001). They are tumorigenic is nude mice, however only in conjunction with oestrogen stimulation (Clarke *et al*, 1990).

Cells were maintained in DMEM with 10% FCS, penicillin (100U/ml) and streptomycin (100µg/ml). They were incubated at 37°C, with 5% CO_2.

MCF-7 cells were purchased from American Type Culture Collection (ATCC™).

MDA-MB-231 cell-line: This cell-line was isolated in 1973 from a 51 year old female with known metastatic breast adenocarcinoma. Cells were cultured from a pleural effusion, and no further immortalisation was performed (Cailleau *et al*, 1974)

Although these cells are morphologically epithelial-like, they appear phenotypically as spindle shaped cells. *In vitro* they display a highly invasive phenotype and are able to grow on agarose plates (a common indicator of

transformation and tumourigenicity. They are able to cause mammary fat pad tumours within nude mice. Interestingly this cell-line has lost the ability inherent to differentiated breast epithelium of being able to process oestrogens. It is also resistant to progesterones and melatonin (Cailleau *et al*, 1978).

What is especially of interest with this cell-line is that it is a *p53* mutant cancer line (Oliver *et al*, 2002) in contrast to MCF7s which have a competent *p53* (Lu *et al*, 2001). As mentioned in Section 1. *p53* plays a crucial role in activating DNA repair, delaying progress at the G1/S checkpoint and initiating apoptosis. Mutation in its coding gene *TP53* therefore leads to uncontrolled cellular regulation. Approximately 50% of all human cancers regardless of tissue type contain some form of *p53* mutation (Hainaut & Hollstein, 2000). Following a missense mutation within codon 280 with this cell-line, the AGA sequence is switched to AAA. The result is an arginine to lysine change – this modification leaves the *p53* unable to function appropriately (Hinds *et al,* 1990).

Cells were maintained in DMEM with 10% FCS, penicillin (100U/ml) and streptomycin (100µg/ml). They were incubated at 37°C, with 5% CO_2.

MDA-MB-231 cells were purchased from American Type Culture Collection (ATCC™).

For comparison experiments: All cell-lines were maintained in Dulbecco's Modified Eagle Medium/F12 (Invitrogen at Life Technologies Ltd.), with 5% donor horse Serum (Biochrom AG), penicillin (100U/ml), streptomycin (100µg/ml) (Invitrogen at Life Technologies Ltd.), human epithelium growth factor (EGF) 20ng/ml, Insulin 10µg/ml, hydrocortisone 10ug/ml (All additives by Sigma-

Aldrich Company Ltd). Preliminary work revealed that culture of MDA-MB-231 and MCF7 cell-lines within this medium showed no morphological or growth changes, and that basal expression rates for all genes investigated were unchanged.

5.2.2. Synchronisation of the circadian clock

Cells were cultured in standard culture medium to a confluency of ~90% in 6-well plates. To synchronise culture medium was removed and cells were washed with 1ml PBS. 2.5ml of standard culture medium plus 100nM dexamethasone (Sigma-Aldrich Company Ltd) was then added each well. Cells were incubated for 2 hours at 37°C, 5% CO_2. The dexamethasone culture medium was the removed and the cells washed with 1ml standard culture medium. 2.5ml standard culture medium was then plated into the wells and the cells harvested as appropriate for the experiment.

The 100nM dexamethasone/medium solution was made from a stock of 10mM dexamethasone in ethanol. As a control a matching 0.001% ethanol/medium solution was used. This protocol was based on that documented in Balsolobre *et al*, 1998.

5.2.3 Construction of per1 expression vector.

In light of the clock gene expression data described within this chapter for the MCF7 cell-line, a *Per1* expression vector has been constructed to allow further investigation. Firstly, the full length *Per1* coding region was isolated by PCR from MCF10A cDNA using the following primer:

5’ EcorV GGCCTCTCTGCGATATCTGTTCTGTTCT

3’ Xba1 GGACATAGGAGAAGAAGATCTCTCATGGAC

The following PCR design was used with the Advantage II Polymerase enzyme system (Clontech Laboratories Inc, USA): 95°C for 1 minutes, 30 cycles of 95°C for 30 seconds, 64°C for 3 minutes, followed by 64°C for 3 minutes, and 4°C ∞. This 3Kb fragment was then subcloned into pGEMTeasy (Promega Ltd, UK) to be sequenced and prepared for ligation into pcDNA3.1+ His/Myc (Promega Ltd, UK).

5.3 RESULTS

5.3.1 Differential expression level of core clock genes within benign and malignant breast epithelium.

As mentioned above, a number of clock genes function as putative tumour suppressors, especially *Per1* and *Per2* within rodent mammary tissue (Fu *et al*, 2002). Expression levels of clock genes were assessed, in order to determine whether similar differences in clock gene expression were present in the human malignancies.

HEK 293, MCF10A, MCF7 and MDA-MB-231 cells were grown to ~90% confluency within the same culture conditions. Samples of these cell lines were then harvested over a 24 hour period to assess for temporal variations in expression. Relative expression levels of core clock genes *Per1, Per2, Bmal1* and *Clock* were subsequently determined by quantitative PCR. Figure 5.1 shows the results of this experiment. The average relative expression over 24 hours is shown ± SEM for each gene relative to the reference gene TATA-Box binding protein, n = 6. Differential gene expression between cell-type was analysed by Student T-test (non-significant, NS, = p-value > 0.05, * = p-value < 0.05, ** = p-value < 0.01, *** = p-value < 0.001). Analysis of the standard deviation of the cycle times for each gene, showed that there was no significant temporal variation in genes expression over time (data not shown).

Figure A shows the data for HEK 293 compared to the benign breast epithelium control line, MCF10A. It can be seen that there is significant differences in expression levels of *Per1, Per2* and *Bmal* between these cell-lines, what is most striking however is the difference in the ratio of clock gene expression between

lines. Within HEK 293 cells, all clock genes are expressed to a somewhat similar level. There is no significant difference in expression levels of *Per1, Per2* and *Bmal*, with an average relative expression of 30 ± 3.5 (SEM). *Clock* expression is the exception with a relative expression 59 ± 5.3 (SEM). Within MCF10A a very different distribution of expression is seen. *Per1, Clock* and *Bmal* levels show no significant difference in expression (average relative expression 105± 15.1(SEM)), while there is a dramatic lowered expression of *Per2* (1.7 ± 0.7(SEM)). This is likely to reflect the differential expression of clock genes and clock function found between tissues within the mammalian system (Ko & Takahashi, 2006).

Figure B compared clock gene expression between benign and malignant breast epithelium. It can be seen that all clock genes assayed are expressed at lower levels in the malignant line with the exception of *Per2,* which is expressed equally between the two. *Clock* and *Bmal* expression is decreased 3 and 2 fold respectively. However, *Per1* expression is 15 times lower in the malignant line than the benign. This decrease is similar to the deregulation of *Per1* expression studied recently by immunocytochemistry within breast cancer biopsies (Chen *et al*, 2005).

Finally the expression patterns of clock genes between the benign, MCF10A, and the p53 mutant, MDA-MD-231, is displayed in Figure C. Again there is no significant difference between the expression levels of *Per2.* Interestingly, there is a different clock gene ratio pattern shown by the MDA-MB-231 than any of the cell types described so far. It appears that clock genes expression is very cell-type specific.

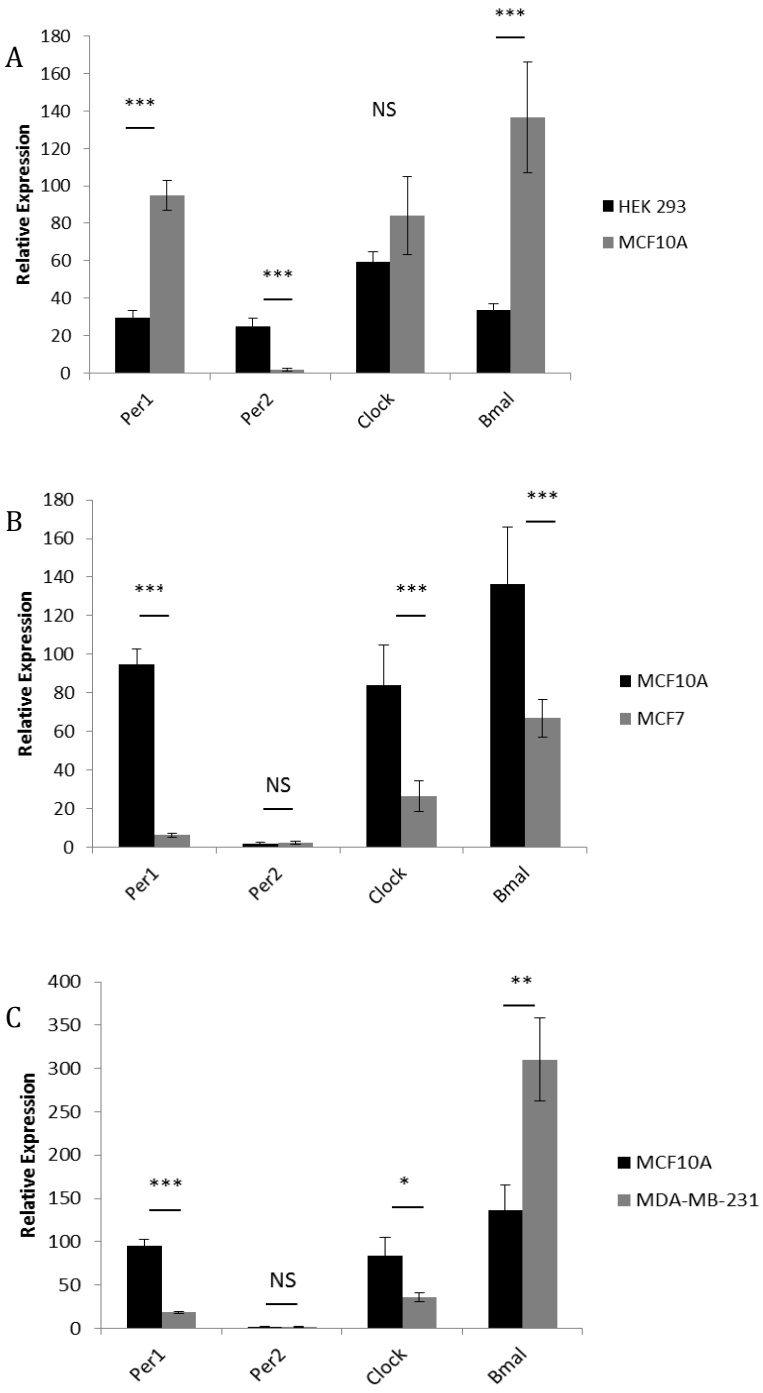

Figure 5.1. HEK 293, MCF10A, MCF7 and MDA-MB-231 cells were grown to ~90% confluency and harvested at four intervals over 24 hours. The graph shows relative expression of clock genes *Per1, Per2, Clock* and *Bmal* determined by quantitative PCR, standardised to reference gene TBP, n =6. T-test was used to analyse expression levels between cell-types. (not significant, NS = p-value> 0.05, * = p-value < 0.05, ** = p-value < 0.01, *** = p-value < 0.001)

5.3.2 Synchronisation of peripheral clocks within benign breast epithelium

It has been established that the MCF10A cell-line express core clock components crucial for intracellular clock function. The circadian pacemaker was synchronised in order to gain better understanding its function within this tissue. MCF10A cells were grown to ~90% confluency and then treated for 2 hours with a pulse of 100nM dexamethasone in standard culture medium or a 0.001% ethanol control. After the pulse, cells were harvested every 6 hours over the following 3 days. Figure 5.2 shows the results from this experiment. Relative expression of clock components *Bmal, Clock, Per1* and *Per2* are shown ± SEM for each time point and for both treated and control samples. All expression data is relative to reference gene TATA-Box binding protein (TBP), n=3. Variation in time and treatment group assessed by two-way ANOVA (not significant, NS = p-value >0.05, ** = p-value < 0.01, *** = p-value < 0.001)

Figure A shows the relative expression of *Bmal* over time. A significant rhythm can be seen to be elicited by dexamethasone synchronisation within these samples. A robust oscillation with amplitude of 5 fold can be seen, peaking at 26-32 and 56-62 hours post treatment and starting to dampen on the third day. No significant variation in expression is elicited by the ethanol control.

A less robust, but similarly phased response is seen in Figure B, showing the expression pattern of *Clock* over time. Significant peaks are seen at 26 and 56 hours post treatment, which are not elicited by the ethanol control. This result suggests that breast ductal epithelium is a tissue in which *Clock* expression is rhythmic (Ko & Takahashi, 2006).

Antiphase responses, as would be expected from a function clock system are seen within the expression patterns of *Per1* and *Per2*, Figure C and D. Both oscillate robustly, peaking in an anticipatory manner 6 hours before *Clock* and *Bmal* (20 and 50 hours post treatment) with amplitudes of 5 and 8 fold respectively. These traces also suggest a sharp induction of the *Per* genes during synchronisation, due to the increase expression at 2 hour post treatment. *Per* genes have been shown to behave in a similar was to *c-fos,* as an immediate response gene, upon dexamethasone administration within Rat-1 fibroblasts (Balsalobre *et al*, 1998). This induction prompts synchronisation of neighbouring clocks. This result suggests a similar mechanism is present in these breast derived cells.

A Bmal

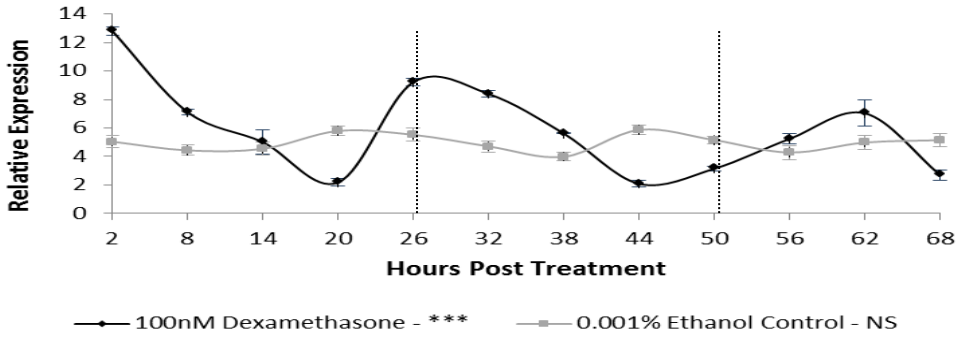

B Clock

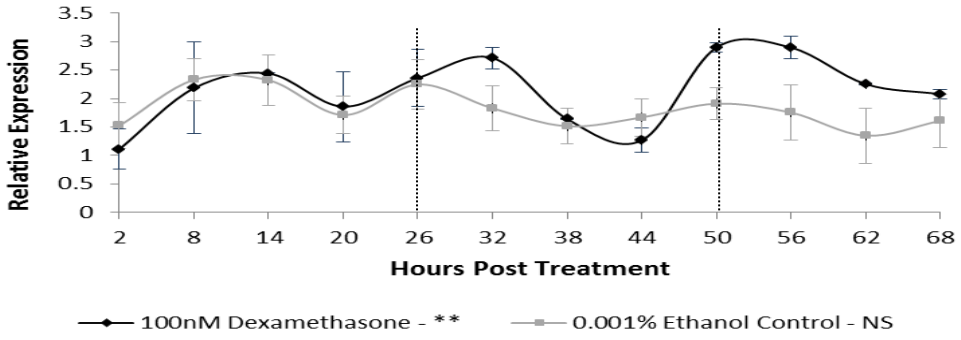

C Per1

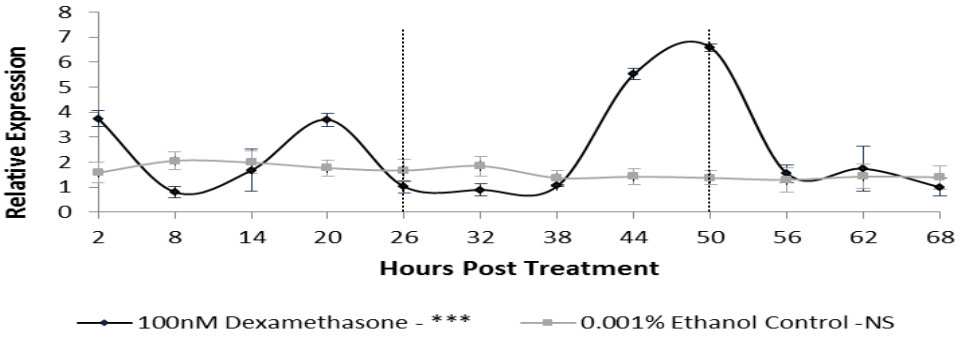

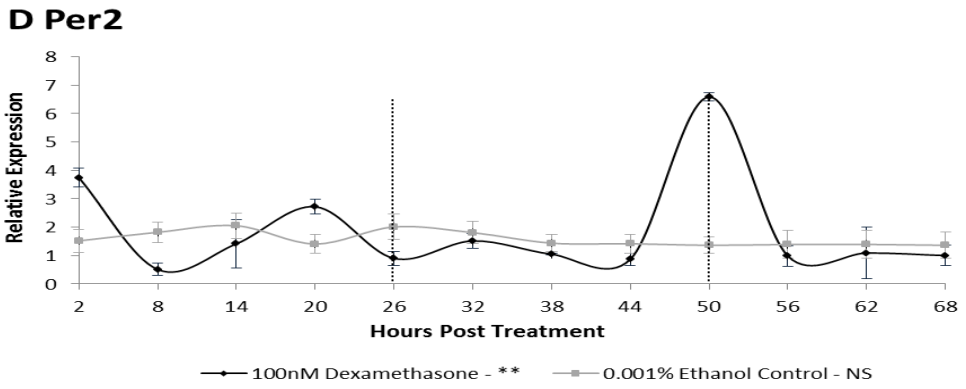

Figure 5.2 MCF10A cells were synchronised on third day of culture using a 2 hour pulse of 100nM dexamethasone or 0.001% ethanol control. Cells were then harvested at 2, 8, 14, 20, 26, 32, 38, 44, 50, 56, 62, 68 hours after treatment. Figure 5.2 shows the results of quantitative PCR assays carried on these samples. Relative expression ± SEM is shown for circadian genes *Per1* (A), *Per2* (B), *Bmal* (C) and *Clock* (D) for each time point and treatment group in comparison to reference gene TATA-Box binding protein (*TBP*). Variation in time and treatment group assessed by two-way ANOVA (not significant, NS = p-value >0.05, ** = p-value < 0.01, *** = p-value < 0.001)

5.3.3 Peripheral clock function within malignant breast epithelium

Striking differences were seen in the expression levels and relationships of clock genes between benign and malignant breast epithelium, as illustrated in Figure 5.1. The most prominent disparity was the 15 fold difference in *Per1* expression, which was markedly reduced in the malignant cell model. In order to assess if these difference led to alternations in clock function, the cellular clock was synchronised.

MCF7 cells were grown to ~90% confluency and treated with a 2 hour pulse of 100nM dexamethasone or 0.001% ethanol control. Cells were then harvested every 6 hours over the following 3 days. Relative expression of clock genes over this time was assessed by quantitative RT-PCR. Figure 5.3 shows the results of this experiment. Relative expression of all genes is shown ± SEM, for each time-point and treatment. All expression levels are standardised to the reference gene TATA-Box binding protein (*TBP*), and n=3.

Figure A shows the expression pattern of *Bmal1* within the malignant cell-line, which appears strikingly similar to that of the benign MCF10A cell-line. A robust rhythm is observed with amplitude of 10 fold, peaking with a similar phase at 26 and 56 hours post treatment. No significant variation is gene expression is elicited from the ethanol control. *Clock*, Figure B, on the other hand, has a different expression profile. No significant variation in gene expression is seen over the three days in either the dexamethasone or ethanol treatment samples. *Clock* gene expression appears arrhythmic.

A weak (p-value of variation < 0.05) anti-phasic oscillation is seen in *Per1* expression over time, peaking at 32-38 and 62 hours post treatment (Figure C),

whereas no significant variation in gene expression over time is seen within the *Per2* expression profile (Figure D). This set of data, suggests MCF7 cells contain an extremely altered clock compared to the MCF10 benign cell line

A direct comparison of clock gene expression between MCF10A and MCF7 cell-lines is shown in Figure 5.4. Here a direct comparison of profiles is shown, which takes into account the differing base-line levels of gene expression between the two cell-lines.

Figure A highlights the different phase angel between the *Bmal* oscillations of the two cell-types. *Bmal* within the MCF7 cell-line displays as 6 hour phase advance compared to the MCF10A cell-line. Clock is non-rhythmic within the MCF7 cell-line compared to the MCF10a, Figure B, as for *Per2* shown in figure D. Once the difference in gene expression is taken into consideration it can be seen that in comparison to the robust oscillations of *Per1* in the benign model, *Per1* is non-rhythmic is the malignant cell-line Figure C. In this way once again clock function is MCF7's is significantly altered.

With clock genes *Clock, Per1* and *Per2* showing little oscillation, Figure 5.4 begs the question of how the *Bmal* expression profile maintains its rhythmicity. The answer is found within the secondary loop of the circadian clock – that of *RORα* and *Reverb-α* – a section of the clock that has long been considered not crucial to clock function.

Figure 5.5 shows the relative expression as determined by qPCR for *Reverb-α* within synchronised MCF7s, over 3 days. This gene is shown to weakly oscillate, with an amplitude of 3 fold, in antiphase with Bmal, peaking at 38 and 62 hours

post treatment as would be expected for this secondary target of the CLOCK:BMAL heterodimer.

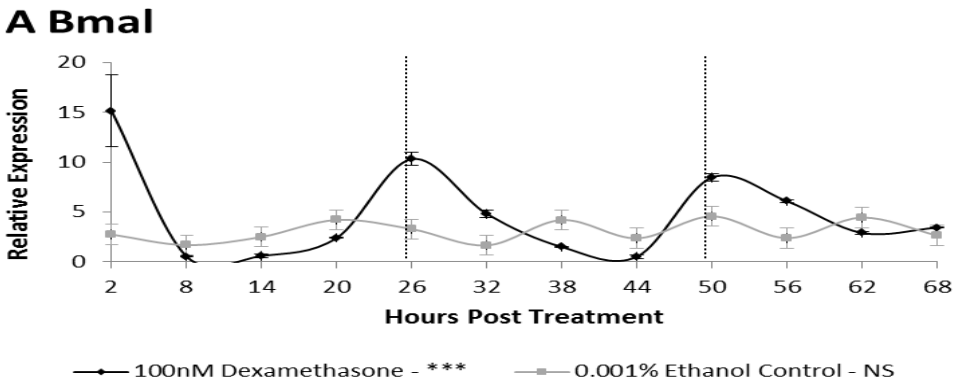

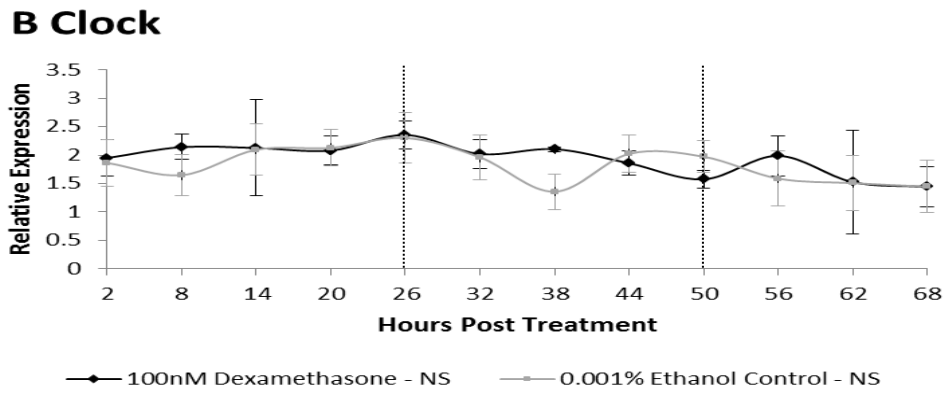

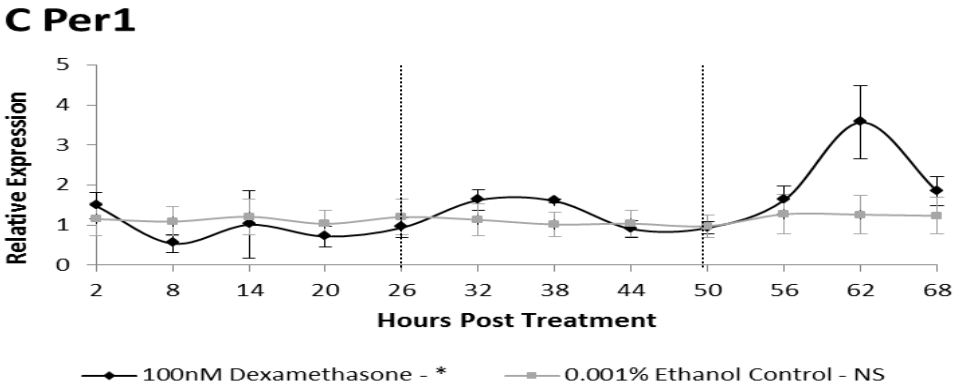

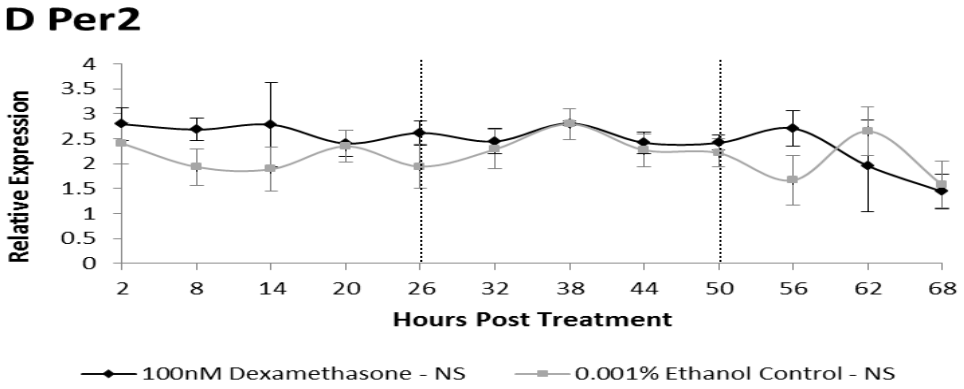

Figure 5.3. MCF7 cells were synchronised on third day of culture using a 2 hour pulse of 100nM dexamethasone or 0.001% ethanol control. Cells were then harvested at 2, 8, 14, 20, 26, 32, 38, 44, 50, 56, 62, 68 hours after treatment. Figure 5.3 shows the results of quantitative PCR assays carried on these samples. Relative expression ± SEM is shown for circadian genes *Per1* (A), *Per2* (B), *Bmal* (C) and *Clock* (D) for each time point and treatment group in comparison to reference gene TATA-Box binding protein (*TBP*). Variation in time and treatment group assessed by two-way ANOVA (not significant, NS = p-value >0.05, ** = p-value < 0.01, *** = p-value < 0.001)

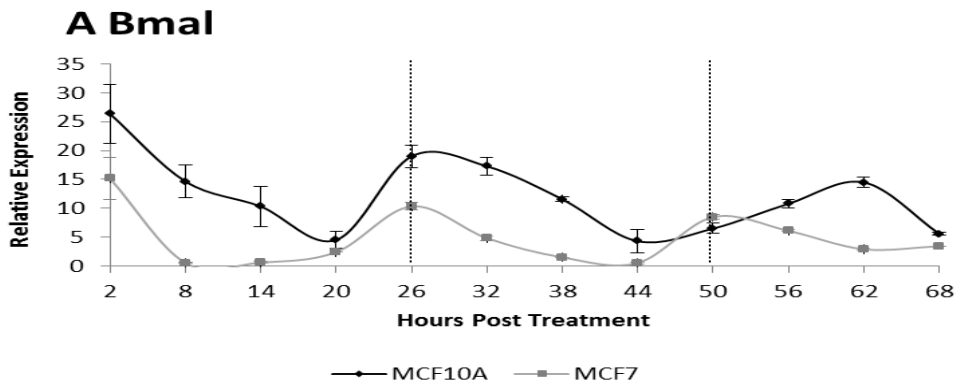
A Bmal
Relative Expression
35
30
25
20
15
10
5
0
2
8
14
20
26
32
38
44
50
56
62
68
Hours Post Treatment
MCF10A
MCF7

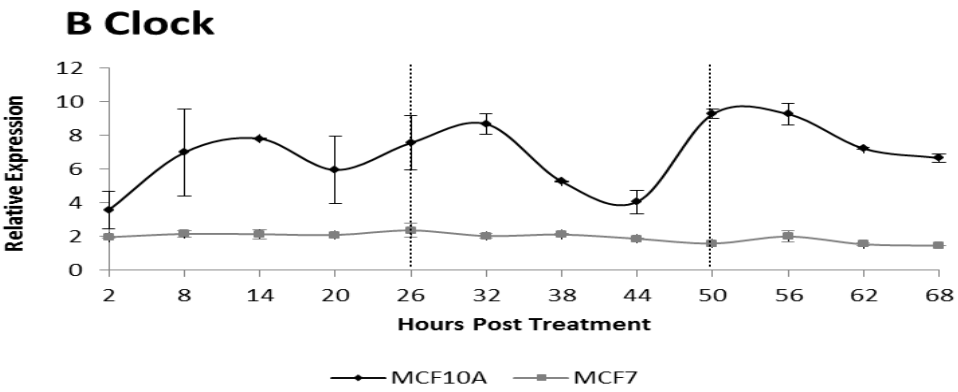
B Clock
Relative Expression
12
10
8
6
4
2
0
2
8
14
20
26
32
38
44
50
56
62
68
Hours Post Treatment
MCF10A
MCF7

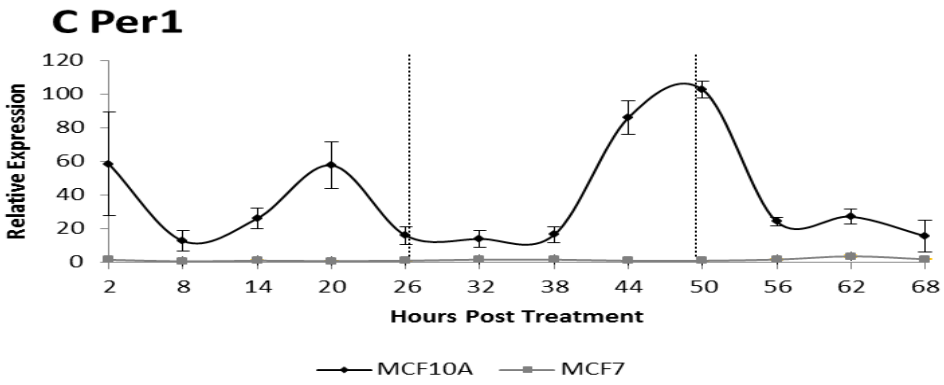
C Per1
Relative Expression
120
100
80
60
40
20
0
2
8
14
20
26
32
38
44
50
56
62
68
Hours Post Treatment
MCF10A
MCF7

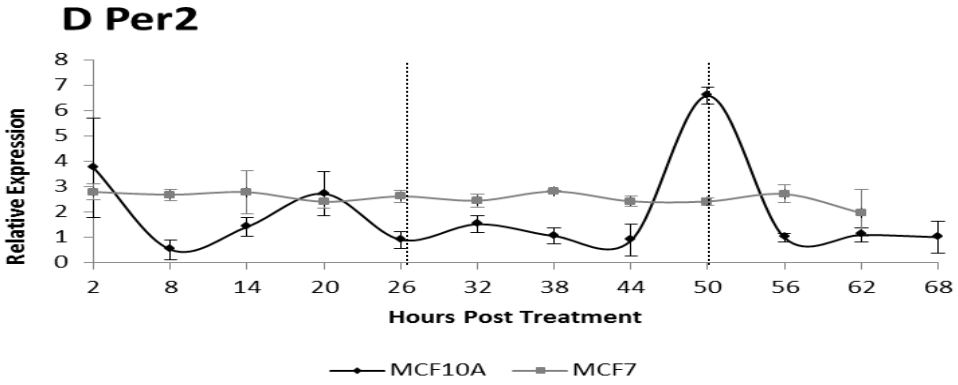

Figure 5.4. MCF7 cells were synchronised on third day of culture using a 2 hour pulse of 100nM dexamethasone or 0.001% ethanol control. Cells were then harvested at 2, 8, 14, 20, 26, 32, 38, 44, 50, 56, 62, 68 hours after treatment. Figure 5.4 shows the results of quantitative PCR assays carried on these samples. Relative expression ± SEM is shown for circadian genes *Per1* (A), *Per2* (B), *Bmal* (C) and *Clock* (D) for each time point and treatment group in comparison to reference gene TATA-Box binding protein (*TBP*).

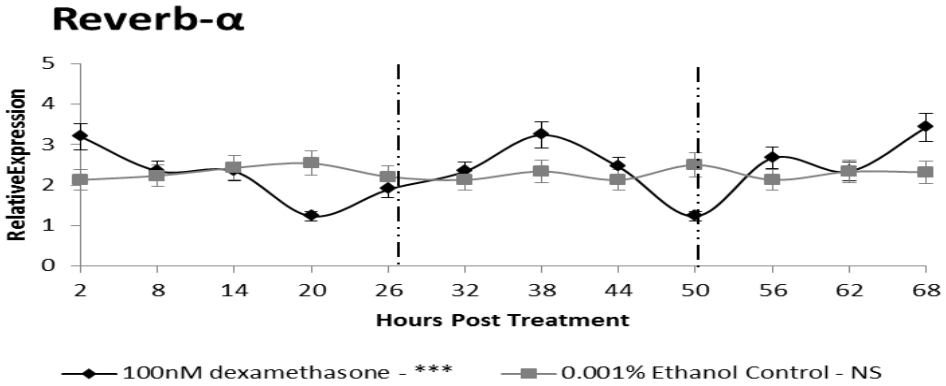

Figure 5.5. MCF7 cells were synchronised on third day of culture using a 2 hour pulse of 100nM dexamethasone or 0.001% ethanol control. Cells were then harvested at 2, 8, 14, 20, 26, 32, 38, 44, 50, 56, 62, 68 hours after treatment. Figure 5.5 shows the results of quantitative PCR assays carried on these samples. Relative expression ± SEM is shown for circadian gene *Reverb-α* for each time point and treatment group in comparison to reference gene TATA-Box binding protein (*TBP*).

5.3.4 Clock influence on cell proliferation within benign and malignant breast epithelium.

Having established that there is in alteration in clock function between the benign, MCF10A and malignant, MCF7, cell-lines. Cell cycle progression and control was assayed to look for associated changes in this putative clock output. Firstly growth rates within these cell types were assessed. Figure 5.6 shows a growth assay of MCF7 and MCF10A unsynchronised cells over 5 days. Both cell-types were plated at 150,000 cells per ml and each day of subsequent growth concentration of cell was measured. The graph shows the concentration of cell (cell/ml ± SEM) for each day of the assay. n=6. It can be clearly seen that MCF7 cells, in which clock function is altered, grow at a significantly faster rate than MCF10A. In previous experiments in which the clock has been disrupted by mutation, grow rates have decreased. The contrary is seen in this disrupted system. Though obviously it must be stressed that this observation is correlative, and not definitively causal.

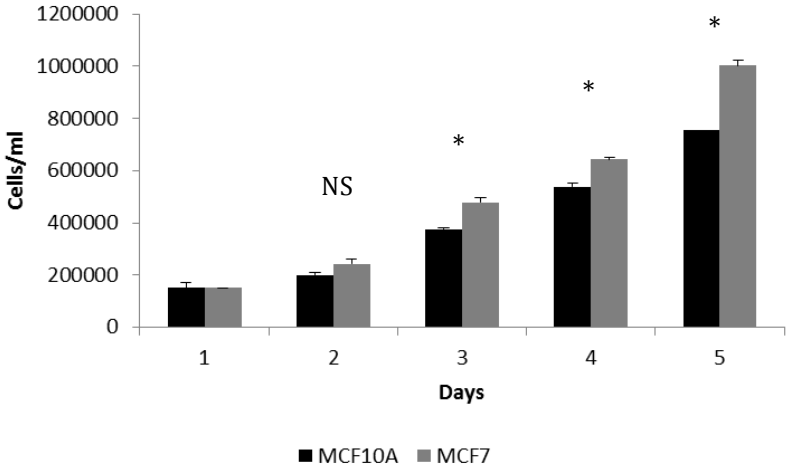

Figure 5.6. MCF10A and MCF7 cell-lines were plated at a concentration of 150,000 cells/ml and cultured over 5 days. On each day concentration of each cell-type was calculated. The graphs for concentration of cells as cells/ml ± SEM, n=3. Differences in concentration of cells between cells types was analysed for each day separately using a T-test (no significant difference, ns = p-value > 0.05, * = p-value < 0.05)

In order to investigate whether synchronisation of cellular clocks influence cell proliferation within these cell lines, growth assays of synchronised population were performed. MCF10 and MCF7 cell-lines were plated at 150,000 cell/ml and cultured for 5 days. On the third day of culture, samples of each cell-line were treated with 0.001% ethanol, 100nM dexamethasone of a 50% horse serum shock (Balsalobre *et al*, 1998). The results of this trial are shown in Figure 5.7. Concentration of cells for each cell type is shown ± SEM on each day of culture and or each treatment group. Figure A shows the results from the MCF10A culture, while Figure B shows the results from the MCF7 cell-line. Variation in growth between treatment and control groups was assessed by two-way ANOVA. It can be seen that synchronisation with either 100nM dexamethasone or 50% horse serum, has no significant effect on growth rates in either cell-types (p-value > 0.05 for each treatment group per time point).

To assess whether clock function had an effect on cell proliferation MCF10A and MCF7 cells were transiently transfected using Lipofectamine 2000 with the *zfCLOCK1A DN* construct and an empty vector control. Expression of the construct was assessed by immunocytochemistry, using an antibody against the Flag-Tag of the *CLOCK1A DN* construct. Cell proliferation was again measured by growth assay. Figure 5.8 shows the results of this experiment. Concentration of cells is shown as cells/ml ±SEM for each day and cell-type, n=3, differences in growth rates between cell types was assessed for each day using a T-test (not significant difference, ns = p-value > 0.05, *= p-value < 0.05). Figure A shows the growth assay of MCF10A *CLOCK1a DN* and *pCLNCX* cells. It can be seen that the clock disrupted cell line has a consistently slower rate of growth in comparison to the control. Figure B show the

growth assay of the MCF7 *CLOCK1a DN* and *pCLNCX* cell-lines. No significant difference is seen in growth rate between these to two cell-types.

These results are consistent with those seen for HEK 293 cells cultures. Synchronisation of a clock population has no effect on cell growth. But the presence of a functional clock is critical for optimal cell growth.

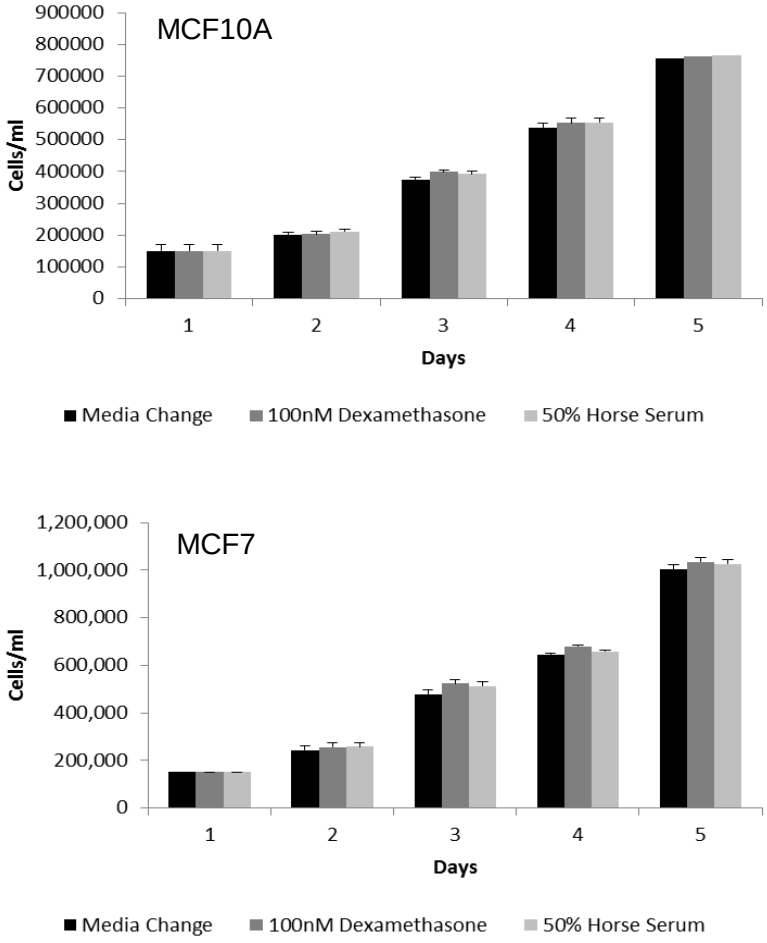

Figure 5.7. MCF10A and MCF7 cell-lines were plated at 150,000 cells/ml and cultured over 5 days. On the third day of culture samples were treated with a 2 hour 100nM dexamethasone shock or a 0.001% ethanol control. On each day concentration of each cell-type was calculated. The graphs for concentration of cells as cells/ml± SEM, n=3. Differences in concentration of cells between cells types was analysed for each day separately using a T-test (not significant difference, ns = p-value > 0.05).

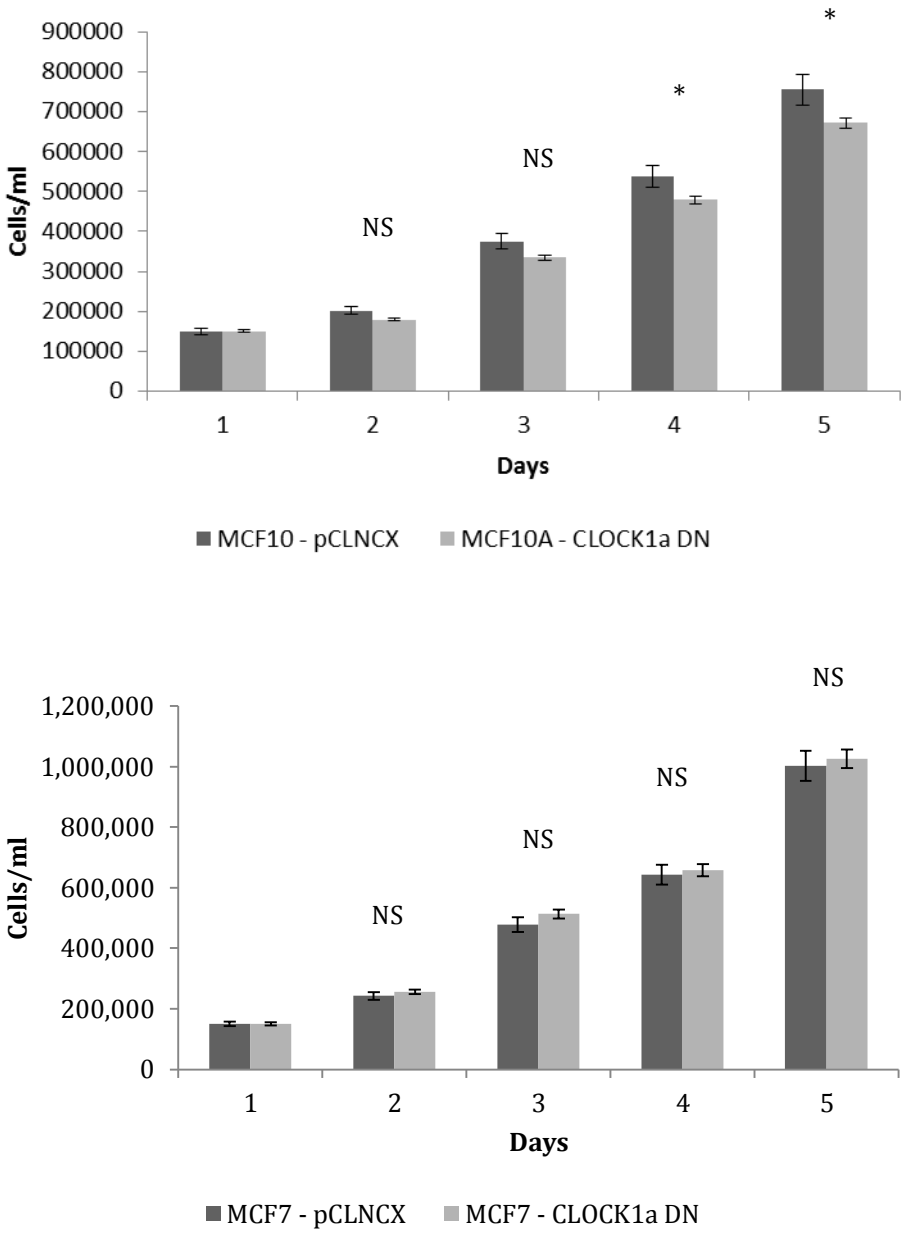

Figure 5.8. MCF10A and MCF7 were transiently transfected with *zfCLOCK1a DN* and *PCLNCX* Empty vector constructs. Samples of cell-line were plated at a concentration of 150,000 cells/ml and cultured over 5 days. On each day concentration of each cell-type was calculated. The graphs show concentration of cells as cells/ml± SEM, n=3. Differences in concentration of cells between cells types was analysed for each day separately using a T-test (not significant difference, ns = p-value > 0.05, * = p-value < 0.05)

5.3.5 Differential cell cycle regulation between benign and malignant breast epithelium

It has been shown that not only does the clock function differently between the benign and malignant cell-lines, but that cell growth also differs. Clock disruption has been shown to affect the growth of benign cells; however has no significant effect on malignant tissue. In order to understand these results, expression of cell cycle regulators was assessed within the cell-lines. MCF10A and MCF7 cells were grown to ~ 90% confluency and harvested, unsynchronised, at four time points over 24 hours. Expression levels of *p21, Wee1, p53* and *cMyc* were then compared using quantitative PCR analysis. Results are shown in Figure 5.9. Relative expression is shown for each gene ± SEM, all results standardised to the reference gene TATA-Box binding protein, n = 6. Differences in expression level were determined by T-test (* = p-value < 0.05, *** = p-value < 0.001, **** = p-value < 0.0001).

Within the normal regulation pathways of the cell cycle the potent cyclin-dependant kinase inhibitor *p21* is induced by p53, via a DNA damage response pathway (He *et al*, 2005), which it is repressed by the pro-proliferative agent, c-Myc, via AP4 induction (Jung *et al*, 2008). Wee1, the negative regulator of G2/M progression is regulated by separate pathways. The MCF10A expressions shown by Figure 5.9, reflects these pathways. It can be seen that *p53* expression is higher in MCF10A when compared to MCF7, subsequently *p21* expression is higher in the benign line in comparison to the malignant. *C-Myc* is the opposite, and expressed at a lower level in the benign line as would be expected. *Wee1*, a regulator of mitosis is low in the malignant line, as expected from highly proliferative line.

Interestingly, Figure B shows the relative expressions of *Per1* between the benign and malignant cell-lines as previously shown as part of Figure 5.1. MCF10A cells expressing 15 times the amount of *Per1* when compare to MCF7. The *Per* genes have been described as potent tumoursuppressors. We can see that in a situation where *Per1* is decreased the cell cycle regulators are showing expectant alterations, cell cycle gating genes and additional tumoursuppressors are down regulated while the pro-proliferative gene is up regulated. However, no exact causation is demonstrated by the data. A *Per1* rescue experiment, where MCF7 cells were transfected with an expression vector coding for *Per1* could prove a direct interaction. This construct has been completed as described in section 5.2.3 and is ready for transfection into host MCF7 cells.

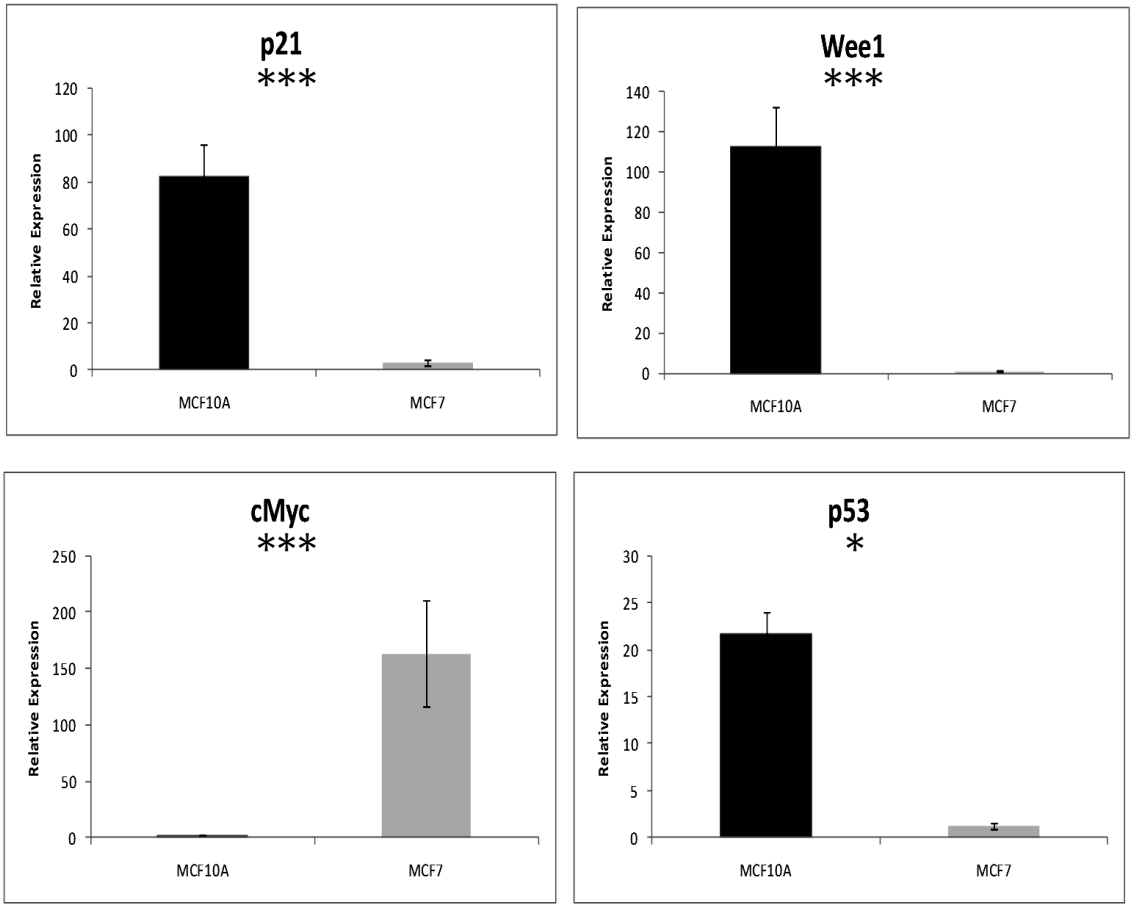

Figure 5.8. MCF10A and MCF7 cultures were grown until ~90% confluency and then harvest at four time-points over the course of 24 hours. Figure A shows expression levels of cell cycle regulators *p21, Wee1, c-Myc* and *p53* were then determined by quantitative PCR. Figure B the expression levels of clock gene *Per1.* The graphs show relative expression ± SEM, each standardised to the reference gene TATA-Box binding protein, n=6. Differences in expression level were analysed using a standard T-test. * = p-value < 0.05, ** = p-value < 0.01, *** = p-value < 0.001

5.3.5 Clock synchronisation has no effect on the regulation of cell cycle gene expression

Disruption of the clock within MCF10A cells has been shown to cause a decrease in growth rate, while MCF7 cells remain unaffected by the mutation. In order to determine the mechanism by with the clock controls the cell cycle, expression patterns of cell cycle regulators were assayed over a day period. MCF10A and MCF7 cells were grown to ~90% confluency and treated with a 2 hour pulse of 100nM dexamethasone or a 0.001% ethanol control. Samples were then harvest every 6 hour over a 3 day time course. Figure 5.9 displays the results of this experiment. Relative expression of cell cycle regulations was determined by quantitative PCR and is shown ± SEM, standardised to reference gene TATA-box binding protein (TBP), N=3. Figure A and B reflect the data from cell types MCF10A and MCF7 respectively.

The expression of *Wee1, p21, p53* and *c-Myc* can be seen in Figure 5.9. There is no circadian expression profile seen for any of the genes studied. What's more is that there is no significant difference between the dexamethasone and ethanol treated cell-lines. The glucocorticoid signally induction of circadian-like expression outputs does, therefore, not occur in these cells as seen in HEK 293 cells.

Figure A

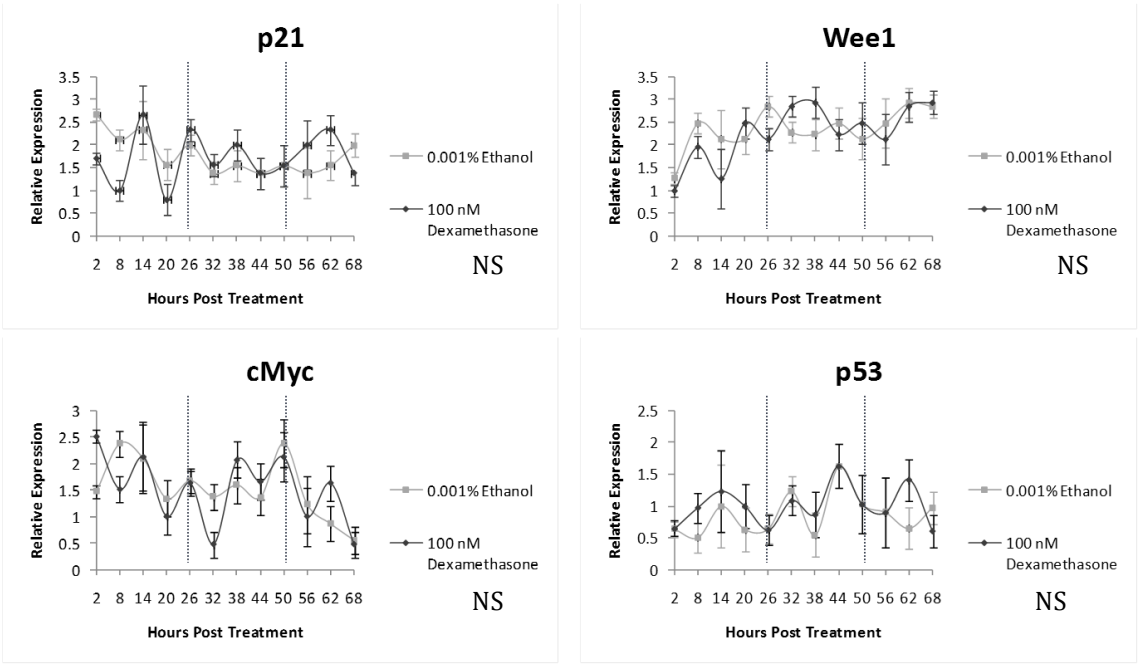
p21
Relative Expression
Hours Post Treatment
0.001% Ethanol
100 nM Dexamethasone
NS
Wee1
Relative Expression
Hours Post Treatment
0.001% Ethanol
100 nM Dexamethasone
NS
cMyc
Relative Expression
Hours Post Treatment
0.001% Ethanol
100 nM Dexamethasone
NS
p53
Relative Expression
Hours Post Treatment
0.001% Ethanol
100 nM Dexamethasone
NS

Figure B

Figure 5.9. MCF10A and MCF7 cells were grown to ~90% confluency and then synchronised with a 2 hour pulse of 100nM dexamethasone or a 0.001% ethanol pulse. Samples were harvested every 6 hours after treatment over 3 days. Expression patterns of *p21, p52 Wee1* and *c-Myc* are shown in the Figure A and B (MCF10A and MC7 cell-lines respectively. Relative expression determined by quantitative PCR is shown ± SEM, standardised to the reference genes TATA-Box binding protein, n = 3. Variation in expression over time was determined NS e-way ANOVA as shown (not significant, NS, p-value > 0.05).

5.3.6 Clock synchronisation has no effect on cell cycle progression.

In order to examine for any functional regulation of the cell cycle by the clock, cell cycle analysis was performed over a time-course for synchronised cell cultures. MCF10A and MCF7 cells were grown to ~ 90% confluency before being pulsed for 2 hours with 100nM dexamethasone or 0.001% ethanol control. Cells were then harvested every 6 hours, from the removal of treatment for a following 3 days. Cells were stained with propidium iodide and cell cycle analysis was performed by FACS array. The results of this experiment are shown below in Figure 5.10. Percentage of cells in each stage is shown ± SEM, n=3.

Figure 5.10A shows the results of the MCF10A samples tested. It can be seen that there is no clear circadian rhythm, defined as an oscillation with an ~24 hour period, reflected in the data. In fact there is no difference between the variation seen in percentage of cells over three days between the dexamethasone treated population and that which received the ethanol control. From this we can conclude that there is no demonstrable circadian gated timing of the cell cycle within MCF10A cells. One must however consider that these are an immortalised cell-line. Once again the possibility of uncoupling between the two cycling mechanisms may be a possible cause of this negative data.

Figure 10B shows the results of the MCF7 samples. As above there is no significant difference detected for any cell cycle stage between the dexamethasone test and ethanol control populations. This result is consistent with the hypothesis that the clock is highly altered within this cell-line and therefore may not function properly, nor interacts with its downstream targets. Interestingly, the patterns displayed are very similar to the circadian competent MCF10A cell-lines. This may again support

the hypothesis, that this lack of regulation is actually an artefact produced by immortalised cell-lines.

Figure 5.10. MCF10A and MCF7 cells were cultured to ~ 90% confluency and pulsed or 2 hours with 100nM dexamethasone or a 0.001% ethanol control. Cells were then harvested every 6 hours for 3 days for cell cycle analysis. Cells were fixed and stained with propidium iodide, before being subjected to FACS analysis. Percentage of cell in each phase can be seen ± SEM, n=6. Figure A-B show the results of MCF10A and MCF7 respectively. To judge variance a two way ANOVA was performed (not significant, NS = p-value >0.05).

5.4.7 Cell Cycle disruption has no effect on clock function

Circadian disruption has long been implicated in the regulation of the cell cycle (Matsuo *et al*, 2003). However, little is known regarding the impact of the cell-cycle on the clock, do these two systems form there on feedback loop. MDA-MB-231 cells are a cell-line of breast epithelial origin which carries one of the most common mutations found in heredity breast malignancy, the *p53* mutation, associated with Li-Fraumeni syndrome (Hill *et al*, 2009). This cell-line contains an altered cell cycle due to do this mutation, making it an idea model to assess cell cycle function on the clock. MDA-MB-231 cells were plated at ~90% confluency and pulsed for 2 hours with 100nm dexamethasone or 0.001% ethanol control. Samples of cells were then harvested at 26, 32, 38 and 44 hours after treatment. Quantitative PCR was then used to determine the expression patterns of clock genes *Bmal, Clock, Per1* and *Per2* over this second day. Figure 5.11 show relative expression of these genes, ± SEM, standardised to reference gene TATA-Binding protein, n=3. One way ANOVA was used to assess variation in expression over time (* = p-value < 0.005, ** = p-value < 0.001, *** = p-value < 0.001).

It can be seen that robust variation in expression can be seen in all clock genes of the 24 hours measured. The expression pattern of *Bmal, Clock, Per1* and *Per2,* Figure A-D, are similar to that seen in benign MCF10A cell lines, displaying the same phase upon entrainment and relationships to one another. Each gene appears to respond to synchronisation and behave in an expected way. The amplitude of these rhythms is slightly smaller 15.-2 fold. This is likely to be natural variation in clock function between the cell-types.

These results are consistent with the idea that he cell cycle is unable to feedback and regulate the clock itself. Similar results have been shown within the zebrafish model, where the use of cell cycle inhibitors such as hydroxyurea (data not shown), has had little impact of the reporter traces of clock genes. It would appear therefore this is a conserved one-way pathway. The only evidence where this might not be the case is following DNA damage events, where the act of applying a DNA damaging agent does appear to influence clock timing (Oklejewicz *et al,* 2008).

Figure 5.11. MDA-MB-231 cells were cultured to ~90% confluency and harvested at 26, 32, 38 and 44 hours post treatment. Relative expression of clock genes *Bmal, Clock, Per1* and *Per2*, determined by quantitative PCR are shown ± SEM, standardised to the reference genes TATA-Box binding protein (*TBP*), n = 3. Variation in expression over time was determined by one-way ANOVA as shown (not significant, NS, p-value > 0.05, ** p-value < 0.001).

5.4 DISCUSSION

The advent of industrialisation and subsequent globalisation of markets, has led to the development of the 24 hour society. This has led to a rising incidence of certain forms of illness, related to circadian disruption such as cardiovascular disease, cancer and mental illness. The most prominent of these however, is the increase in cancer formation, brought to the fore by recent epidemiological studies linking shift work in nurses to increased risks of breast cancer development.

Based on the body of evidence that suggests the circadian clock can coordinate the cell cycle. There is the "Light-At-Night" hypothesis. This hypothesis puts forward that disruption of regular light/dark patterns leads to circadian disruption (Stevens, 2006) and disruption to the 24 hour cycle of hormone release, in particular melatonin (Stevens, 2005, which is discussed separately in Chapter 6). These hormonal signals are thought to synchronise the cells with the SCN and external environment. If this does not occur, or occurs on a disrupted basis, downstream pathways of the circadian clock will also be affected. This would include the cell cycle. As a consequence the incidence of malignancy would rise.

This chapter set out to study clock function with benign and malignant human breast epithelial cells. Firstly to determine whether there was clock malfunction, that had a secondary impact on the cell cycle, and secondly whether these cell-lines were a valid model for study of the circadian clock in vitro.

The study shows for the first time that MCF10A and MCF7 and MDA-MB-231 cells express core clock components. Comparison of general expression levels reveals that expression of such genes is very tissue specific, as the profile of HEK 293 cells

varies a great deal from the breast epithelial lines. It can also be seen that slight variations in the ratio of gene expression occur between breast epithelial lines. This is likely to reflect changes in the clock subsequent to the specific cell-types modifications, and from the differing mutations present. Most importantly this is the first time, the commonly used malignant cell-line MCF7 has been directly compared to a benign cell-line, MCF10A. A marked decrease in the expression of putative tumour suppressor *Per1* is seen in MCF7 cell-line.

Upon synchronisation MCF10A, shown a robust oscillatory pattern in the clock genes studied, which occur at the appropriate phases with one another suggesting a fully functional clock. Within MCF7, on the other hand, *Bmal* can be seen to oscillate with a similar phase relationship to MCF10A. However, the *Per1* genes are grossly altered; neither showing any significant oscillation. The rhythmic output of *Clock* is also lost. *Clock* is known to display differential expression profiles, a rhythm being dependant on tissue type. It is therefore not unlikely or unexpected that these malignant cells, have a slightly modified tissue type, precipitating the loss in *Clock* rhythm. However, the most striking result is the arrhythmicity and low expression of *Per1* and *Per2*, a significant component of the negative feedback loop of the clock. These data represent a natural extension of what is known about *Per* function within breast cancer tissues and cells. Expression levels have been described as deregulated/down-regulated in a number of studies. However, this is the first study to show *per1* arrhythmicity, and a dramatically altered expression profile. A major question arising from this data however, is with all this alteration, how is the *Bmal* rhythm still present? *Per3*, was assessed within this cell-line (data not shown) and seen to contribute no rhythmic “second arm” component to the

clock mechanism. Interestingly, a member of the inhibitory arm of the secondary feedback loop *Reverb-α*, maintains its rhythm. This could be a source of rhythmic *Bmal* expression. It also suggests that the major point of alteration is at the level of *Per* gene regulation, and that the clock otherwise retains the ability to function. It may not be clock function itself that is required, merely one component of that clock.

As seen with the HEK 293 cell line, synchronisation of peripheral clocks has no direct impact on cell growth rate. However, disrupting the clock through use of the *CLOCK1a DN* construct leads to slowed growth in MCF10A cell-lines. No such reaction is seen within MCF7 cell-lines. This might suggest that cell cycle has become disconnected from the cock in this cell-line and no longer required its control. On the other hand, it must be remembered that this clock within the cell-line is already highly disrupted, is likely not to be functional, and so disrupting it further is unlikely to have an effect. This cell-line therefore acts like a clock mutant/disrupted model without the *CLOCK1a DN* construct. This growth rates we measure may be the slowed growth rates of an already circadian "incompetent" cell line. This may, however, be unlikely as cell growth occurs at a much higher rate in this cell-line. This leaves a number of questions open as to the role of the clock in cell proliferation.

Cell cycle gene regulators are disrupted in MCF7s. Interestingly this pattern follows that that would be predicted if *Per1* did function as a tumour suppressor. Down regulation of *Per1* would lead to down regulation of *p21, Wee1, p53* and up regulation of *c-Myc*, as demonstrated here. However, no causal relationship can be shown from these results and the disrupted expression patterns in both systems

may be caused by an upstream mutation. A construct expressing the human *Per1* gene, therefore, was created, as described above. This will be transfected into the MCF7 cell-line as a future experiment, to determine whether expression of this plasmid restores cell cycle expression profiles to within expected ranges of a benign cell-line. Such an experiment might also slow the growth of this cell-line.

This study shows that the cellular clock and glucocorticoid pulsing do not elicit rhythmic expression of cell cycle regulators and appear to have no control over cell cycle progression. It must be kept in mind that both these cell-lines are immortalised. Immortalization, as mentioned in Chapter 4, is thought to possibly disconnect the cellular clock from its *in vivo* downstream target, the cell cycle. HEK 293 cells, demonstrated that though this uncoupling may have taken place on a cellular level, the cycle can still react to humoural circadian messengers. This data therefore shows that glucocorticoids are not the primary humoural messengers for this tissue type. Interestingly, the immortalization theory would support the data shown. Up until now the two cell-lines have displayed different responses to the treatments given. However in this study their reactions to synchronisation are the same.

Disconnecting the two systems, clock and cell cycle, is also a mechanism put forward to occur in cancer development. Therefore, if this immortalization related uncoupling is present, both cell types are acting as malignant lines with regards to temporal organization of the cell cycle.

This study also begs the question, if glucocorticoid signalling is not the humoural messenger for this cell-type what other circadian hormones or other factors could be playing this role? Melatonin has long been associated with breast epithelium

and the control of its growth, making it the perfect candidate (Blask *et al,* 2005). This idea will be explored further in the next chapter.

There has been much discussion over the years as to whether the cell cycle is able to feedback onto the clock mechanism itself. This study demonstrates that cell cycle mutation does not have an automatic impact on the circadian clock. Although, as is known with mammalian clock, each clock has a very tissue specific phenotype, and this may only be true for breast epithelium cell-lines studied. A future goal of this research would be to expand the number and breadth of cell lines studied, comparing further benign and malignant cell types, if possible from selected patients.

One of the primary aims of this Chapter was to evaluate the use of these cell-lines for circadian study. It must be highlighted that these cell-lines are isolated each from one different person. In themselves they are therefore only an n=1 for each cancer type studied. From what is known regarding interpersonal circadian variation this limits the degree to which the cell-types can be directly compared with one-another and how representative of a specific cancer type they can be regarded as being (Brown *et al,* 2005). However, the cell lines we have chosen to examine a classical models within breast cancer research; MCF7 and MDA-MB-231 being the model for 40% of all published studies on breast cancer cell-lines (Lacroix *et al,* 2004). It is therefore useful to employ them in this study, as it allows direct comparison to a large body of literature already available.

Ideally, the cell-lines would be grown from biopsies taken from the same person, to eliminate interpersonal variation. Primary tissue samples would also negate the

immortalization hypothesis from confounding any results. However, passage number for primary cell-types is low, and there is also a hypothesis which predicts that the injury inflicted by biopsy will have a direct effect on the physiology of the same including the clock, so a period in culture is required for the cell-type to recover (J. Vaidya, 2010). As discussed in Section 1. *In vivo*, biological study is difficult and demanding, especially in patients with cancer. Use of these cell-lines can be therefore seen as a useful tool to study clock function, or dysfunction within this cell-type. However an alternative method of downstream pathway regulation must be established.

In conclusion this chapter shows that:

- MCF10A, MCF7 and MDA-MB-231 possess peripheral clocks.
- Direct comparison between benign MCF10A and malignant MCF7 cells reveals a marked down regulation of the clock gene, *Per1.*
- MCF10A cells can be synchronised using dexamethasone shocking, and display clock gene expression profiles consistent with a functional clock.
- MCF7 cells can be synchronised using a dexamethasone shock, but display a grossly altered and somewhat non rhythmic clock gene profile, suggesting a disruption in clock function.
- Cell proliferation within benign cells, MCF10A, is not affected by synchronisation; however, we show that a functional clock is required for optimal cell growth.

- Cell proliferation in malignant cells functions independently of the clock. It is not affected by synchronisation or clock disruption.
- Cell cycle regulator expression levels are altered between the benign and malignant lines to fit a highly proliferated and uncontrolled profile. This profile also fits the result that would be predicted following the down regulation of putative tumour suppressor *Per1*.
- These cell-lines are not sensitive to cell cycle regulator synchronisation by glucocorticoids and display not rhythm expression patterns within these genes.
- These cells do not display evidence of rhythmic cell cycle progression.
- The clock can remain intact within a cell cycle mutant cell-line, indicating there is no reciprocal feedback from this system.

CHAPTER 6

DOES MELATONIN PLAY A ROLE IN SYNCHRONISING PERIPHERAL CLOCKS?

6.1 INTRODUCTION

6.1.1 MELATONIN

Melatonin is an indolamine hormone synthesised primarily by the central nervous system. Pinealocytes, cells that make up the endocrine glandular tissue of the pineal gland, are the principle manufacturers of melatonin (Reiter, 1993). However, cells in the retina (Zawliska *et al*, 1991), Harderian gland (Djeridan *et al,* 2001), gastrointestinal tract (Bubenik *et al,* 2002) testes (Tijmes *et al*, 1996) human lymphocytes and skin cells (Carillo-Vico *et al*, 2004) express enzymes required for melatonin production and are known to produce the hormone at low concentrations. Melatonin synthesis is under circadian control. It is synthesised during the dark phase of the external light/dark cycle in all species known to express the hormone (Reiter, 1991).

6.1.2 Melatonin synthesis and degradation

Melatonin is produced from the tryptophan. The rate of melatonin synthesis is controlled by the enzyme, arylalkylamine N-acetyl transferase (AA-NAT). Levels of this enzyme vary between 7-150 fold higher in the night than the subjective day time (Reiter, 1994). Activity of this enzyme is controlled by the SCN. As mentioned in Chapter 1 light intensity is measured by melanopsin within the retinal ganglion cells. These cells then send the photic information along the Retinohypothalamic path directly to the SCN (Moore, 1972). The SCN neurons project through a variety of pathways as shown to coordinate AA-NAT activity. AA-NAT levels are regulated by post-translational mechanisms. For example the rapid degradation of AA-NAT

since following night-time light pulses is controlled by proteasomal proteolysis (Gastel *et al*, 1998).

Melatonin has a very short half-life, between 20 and 60 minutes. The major degradation pathway of melatonin involves 6-hydroxylation and subsequent compounded with sulphate. This allows it to be excreted (Yu et al, 2004). There are also a number of secondary degradation pathways involving metabolism by: CYP1A (Yaleswaram *et al,* 1999), CYP1A2 (Skene *et al*, 2001) AND CYPI1B1 (Ma *et al,* 2005). Interestingly, the two former enzymes are located in the liver, while the latter is an extra-hepatic enzyme. This demonstrates metabolic activity is occurring outside of the liver.

6.1.3 Melatonin receptors.

Melatonin in mammals mainly acts through one of the three melatonin receptors, MT1, MT2 and MT3. MT1 and MT2 being G-coupled 7-trans-membrane receptors (Dubocovich *et al*, 2003). These receptors are expressed differentially in difference tissues of the body. In connection to this study it has been shown that breast tissue only expressed MT1 (Ram *et al,* 2002).

6.1.4 Melatonin and the circadian system

It has been known for a long time that melatonin is able to coordinate many physiological circadian rhythms within humans. Melatonin can elicit phase shifts in core body temperature, endogenous melatonin synthesis and sleep patterns. Phase delays occur after morning administration, phase advances with subjective evening administration (Lewy *et al*, 1998). Using this knowledge melatonin can also be used as an adjuvant therapy after acute phase-shifts such as that which

occurs in jet lag (Dawson *et al*, 2007). In addition rhythmic melatonin pulsing has the ability to entrain free-running circadian rhythms, as demonstrated within human blind people (Sack *et al*, 1993).

Melatonin is thought to be a simple messenger for the circadian clock, synchronising cells with the outputs of the SCN (Reiter *et al,* 1991)

6.1.5 Melatonin and breast cancer.

In vivo, melatonin has been shown to prevent growth of spontaneous and chemically induced mammary tumours in rodents. *In vitro*, melatonin inhibits breast cancer proliferation and invasiveness (Blask *et al,* 2005). Within human cell-lines melatonin has been shown the affect the growth of oestrogen positive lines MCF7A, TZ7D and ZR-75-1, as well as oestrogen negative cell-lines MDA-MB-468 and MDA-MB-361. Decreased growth seem is precipitated by delayed progression through the cell cycle (Hill *et al,* 1988. Blask *et al,* 2002. Cos *et al*, 1991. Hill *et al,* 2009). These interactions exhibit a bell-shaped dose-response curve, peaking at physiological nocturnal melatonin levels, 1nM (Hill *et al,* 2009). The cell-line MDA-MB-231 however has been documented as melatonin resistant (Hill et al, 2009). Human and mouse breast xenografts also show decreased growth in the presence of melatonin in nude rats (Blask *et al*, 2005). The anti-proliferative activity of melatonin has also been described in other cell-types, more specifically prostate, ovary endometrium, liver and colon (Blask *et al*, 2002). Interestingly these are also the tissues which exhibit robust clock function and in which clock regulation cell cycle progression has been noted.

6.1.6 Conclusion and aims

In conclusion melatonin plays an important role, as a circadian messenger to peripheral clocks. However, the aim of this study is to determine whether this messenger is able to synchronise the peripheral clocks in culture. Melatonin has clear oncostatic effects in some breast malignances, this study also aims to dissect the signally pathways melatonin uses to exert this action.

6.2 METHODS

6.2.1 Cell culture with melatonin

All cell-types were cultured in the same standard MCF10A medium. Previous optimisation studies have shown no difference between growth of cell cycle gene expression in cell-lines when exposed to this medium (data not shown). On the second day of culture, cells were treated with 10nM or 1nM melatonin in culture medium solutions. They were counted 12 hour after treatment.

6.2.2 Acute melatonin pulsing protocols.

All cell-types were cultured in the same standard MCF10A medium. Medium was removed from the cells, a 1 ml PBS wash was performed and then either 10nM, 1nM or a 0.001% ethanol control was added to the cells. After 3 hours the medium was removed, another 1 ml wash performed and standard growth media replaced.

6.3 RESULTS

6.3.1 Expression of Melatonin and Oestrogen receptors within human cell-lines

Firstly, the relative expression of melatonin, oestrogen and glucocorticoid receptors was established. These receptors are all crucial to the action of melatonin, as referred to above. HEK 293, MCF10A, MF7 and MDA-MB-231 cells were cultured to ~90% confluency and then harvest at four separate time-points across a 24 hour period. They were left unsynchronised. Expression of receptors was then determined by quantitative RT-PCR, with primers specifically designed to each receptor type and iso-form. PCR products were subject to gel electrophoresis and sequencing to confirm the product.

Figure 6.1 shows the relative expression of each receptor ± SEM, standardised to reference gene TATA-Box binding protein, n = 6. Differences is receptors expression between cell-type were analysed by one-way ANOVA followed by post hoc T-test if required (NE = not expressed, NS = not significant, *** = p-value > 0.05)

It can be seen that the glucocortoid receptor gene (*GR*) are expressed in all fours cell types (Figure A). There is no significant difference between the expression of GRs between the breast epithelial cell-lines, MCF10A, MCF7, MDA-MB-231. HEK 293 cells have a 2 fold lower expression of *GR* is comparison. They shall therefore be excluded from this study, and this confirms that synchronisation reaction cannot be intercompared between these cell-lines as a result.

Melatonin receptor 1 (*MT1*) is expressed in all three epithelial cell-types (Figure B). There is no difference in the level of expression between MCF10A and MCF7, allowing direct comparison of melatonin reactions. MDA-MB-231 has a two-fold lower expression profile. However it is documented that MDA-MB-231 are melatonin resistant cells (Hill et al, 2009) and will therefore act as the negative control within this chapter. Melatonin receptor 2 (*MT2*) is not expressed within these tissues as supported by the literature (Ram *et al,* 2002).

Finally oestrogen receptor expression is displayed in Figure C. MCF10A express very low levels of both oestrogen receptors α and β, whereas MCF7 is clearly seen to over-express oestrogen receptor α, as previously described.

Expression of these receptors over a two day time course was also studied after cell stimulation with the relevant specific agonist. Cell samples were taken every 6 hours post treatment. There was no significant variation in the expression levels of the receptors over the two days. One way ANOVA giving p-value > 0.005, for each receptor type (data not shown). This confirms receptor expression is not under circadian or temporal variation, which would great confound any results in this chapter. Variance in expression between cell-types was assessed by post hoc T-test if required (NE = not expression, NS = not significant, *** p-value > 0.001).

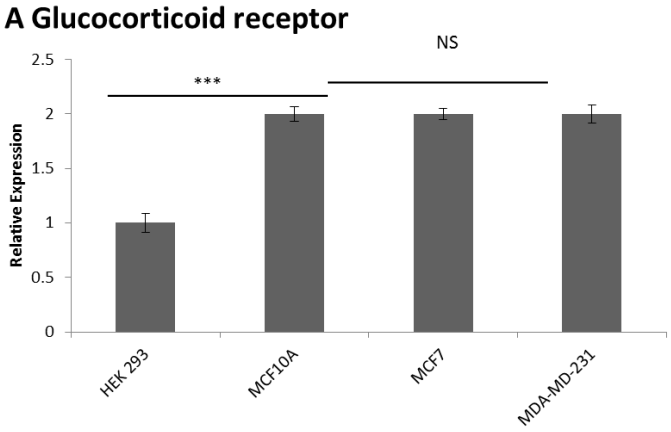
A Glucocorticoid receptor
NS
***
Relative Expression
2.5
2
1.5
1
0.5
0
HEK 293
MCF10A
MCF7
MDA-MD-231

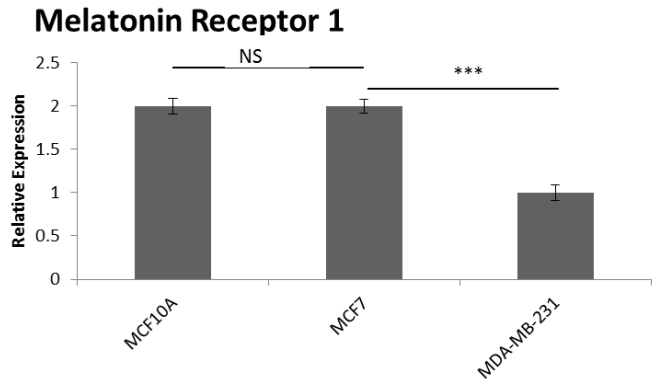
Melatonin Receptor 1
NS
***
Relative Expression
2.5
2
1.5
1
0.5
0
MCF10A
MCF7
MDA-MB-231

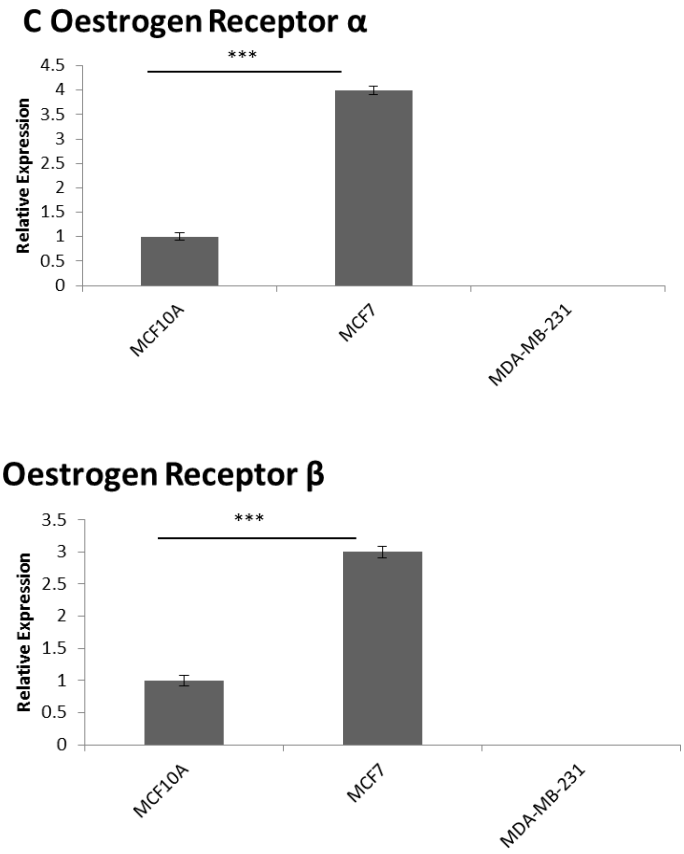

Figure 6.1. HEK 293, MCF10A, MCF7 and MDA-DA-231 cell-lines were grown to ~90% confluency and harvested every 6 hours over a 24 hours' time course. Relative expression of glucocorticoids receptors, melatonin receptors and oestrogen receptors were then determined by quantitative PCR as shown here for each cell-type ± SEM. All results standardised to reference gene, TATA-Box binding protein, n=6. One way ANOVA was used to determine variance in expression between cell-types followed by post hoc T-test if required (NE = not expression, NS = not significant, *** p-value > 0.001).

5.2.2 Effect of melatonin on growth rates of human cell-lines

The effect of melatonin of the growth rate of the MCF7 cell-line has been well documented, as illustrated in Section 6.1 (Hill *et al*, 1988). It is interesting pulsing of melatonin also has an effect on non-oestrogen receptor positive cell-lines (Blask *et al*, 2002).

MCF10A and MCF7 cells were plated at a density of 150,000 cells/ml, and cultured for 5 days. On the second day cultures were treated with either 10nM melatonin, 1nM melatonin or a 0.001% equivalent ethanol control. Growth of these cultures was then monitored every day by assessing concentration. The results can be seen in Figure 6.2. Concentration is shown as cells/ml ± SEM, n=3. Two-way ANOVA with post hoc T-test was used to assess for variance over time.

Figure A shows the effect of melatonin on the growth rate of MCF7 cultures. Both melatonin concentrations produce a significant decreased rate of proliferation over the 3 days after treatment. Treated cultures are just 80% of the density expected, as determined from the control, in keeping with previous studies (Hill *et al*, 1988).

Interestingly, melatonin has some small effect on the growth rate of MC10A cells. Growth is reduced by 4.2% by the third day of culture, by both melatonin concentrations in comparison to the control. There is no significant variation in between these concentrations.

As expected melatonin has no effect on the growth rates of MDA-MB-231, data not shown.

From this we can conclude that melatonin has the ability for affect the cell-line, directly, independently of the oestrogen signally system. However, the majority of its inhibitory action is directed through this secondary pathway.

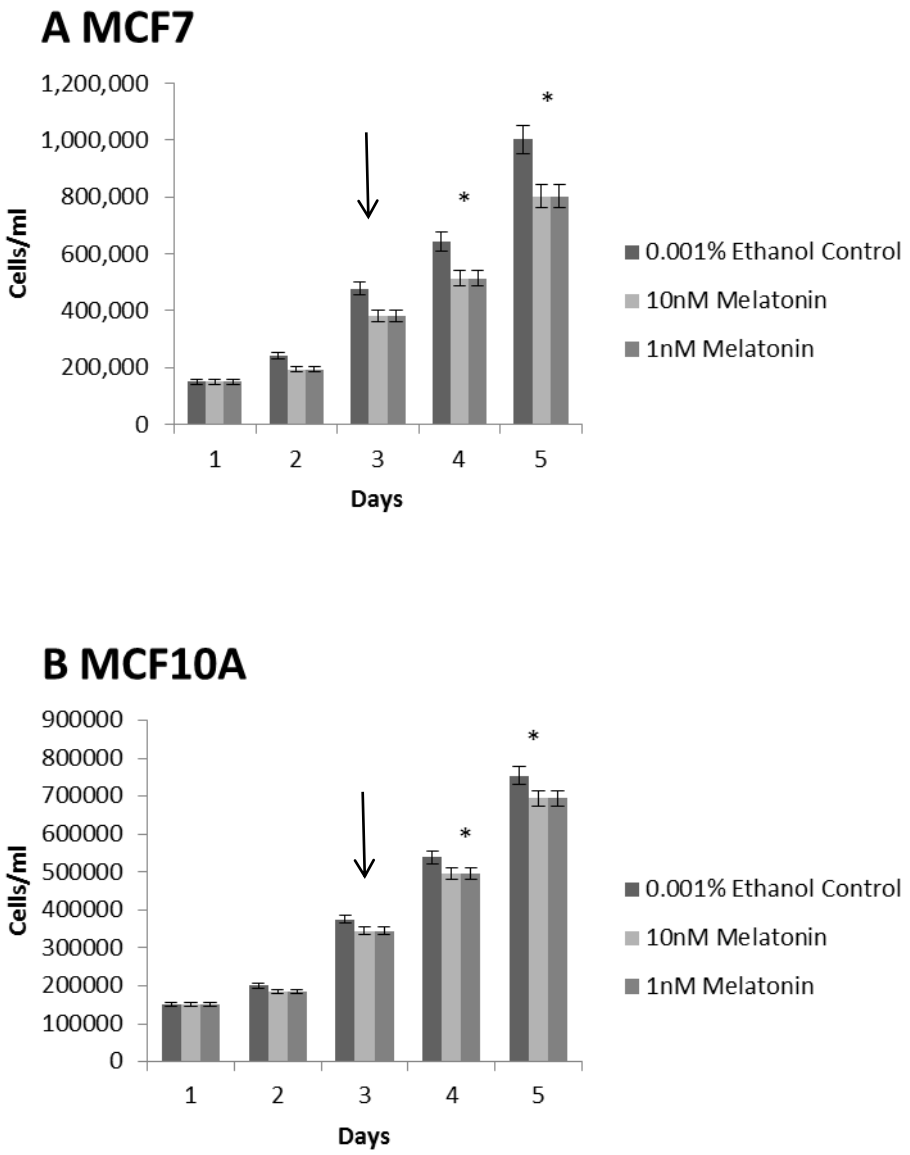

Figure 6.2. MCF7 (Figure A) and MCF10A (Figure B) were plated at 150,000 cells/ml and cultured over 5 days. On the second day of culture, as indicated by the arrow, samples were treated with 10nM or 1nM melatonin or an ethanol based 0,001% control. Cell concentration was then determined for each day post treatment, shown here ± SEM, n = 3. Two-way ANOVA with post hoc T-test was then used to assess variation in growth rates. (* = P-value< 0.05)

5.2.3 Effects of acute melatonin pulsing on clock gene expression.

There has been a hypothesis put forward that melatonin may be a hormonal synchroniser of peripheral clocks within mammals. It is thought that it may have oestrogen-exclusive control of cell growth. This control may be delivered by coordinating circadian control of the cell cycle, or by regulating the cell cycle directly.

MCF10A and MCF7 cells were cultured until ~ 90 % confluent and then pulsed for 3 hours with 10nM melatonin, 1nM melatonin or a 0.001% ethanol control. Samples of these cells were then harvested at 0, 3, 6 and 9 hours during and after treatment (0 being onset of treatment). Relative expression of circadian clock genes *Per1* and *Bmal1* were then analysis using quantitative PCR. The results are shown in Figure 6.3, relative expression for each gene is shown ± SEM, standardised to reference gene TATA-Box binding protein, n=6. Variation over the time course was analysed by two-way ANOVA followed by post hoc T-test if required.

Figure 6.3A, shows the results seen in the MCF10A cell-type. As described in Section 5, MCF10A appear two have a normal expression profile of clock genes, and an intact circadian clock. It can be seen that a 3 hour pulse of melatonin has mild acute effects on the expression of *Per1* and *Bmal* over the 9 hours observed. *Per1* is seen to be stimulated by the presence of melatonin, its expression rising to a peak at 3 hours post treatment, before returning to slightly below base-line at 6 hours and base-line at 9 hours. *Bmal* can be seen to have an antiphasic response, as predicted. It appears mildly supressed at 3 hours post treatment and shows a

recovery peak at 6 hours, before recovering to base-line at 9 hours. All these changes are significant in comparison to the control.

Figure 6.3B, however, shows the reaction of circadian incompetent MCF7 cells to melatonin. No significant effect is seen on the expression of *Per1* nor *Bmal* over the 9 hours, however there is some subjective changes in *Bmal*. This may again be related to the activity of the secondary loop of the clock, as will be discussed later. In conclusion however, melatonin elicits no effect on the clock gene expression within this cell-type.

As predicted melatonin had no significant effect on the expression of *Per1* and *Bmal* within MDA-MB-231 cells (p-value > 0.005).

These results indicate that melatonin is able to influence the expression of clock genes in the presence of a "normal" circadian clock. These results do however beg the question, can melatonin, therefore, act as a peripheral synchroniser?

To test this hypothesis, MCF10A cells were plated at ~90% confluency and pulsed for 3 hours with 10nM melatonin, 1nM melatonin or a 0.001% ethanol control. Cells were then harvested at 6, 12, 18, 24 and 30 hours after treatment. *Bmal* expression within these samples was then determined by quantitative PCR and is shown in Figure 6.4 ± SEM, standardised to reference genes TATA-Box binding protein, n=3.

As seen in Figure 6.3B, there is a mild increase in expression at 6 hours post treatment. However the expression profile of *Bmal* then returns to pre-treatment baseline (as indicated by cross on y-axis), and remains there for the whole of the time-course.

There is no evidence for entrained circadian oscillations at physiological levels of melatonin. However melatonin is a circadian hormone, and therefore will be endogenous pulsing tissues at a specific time-point each day. Lack of obvious entrainment by this hormone does not rule out melatonin acting as a daily modulator of clock function.

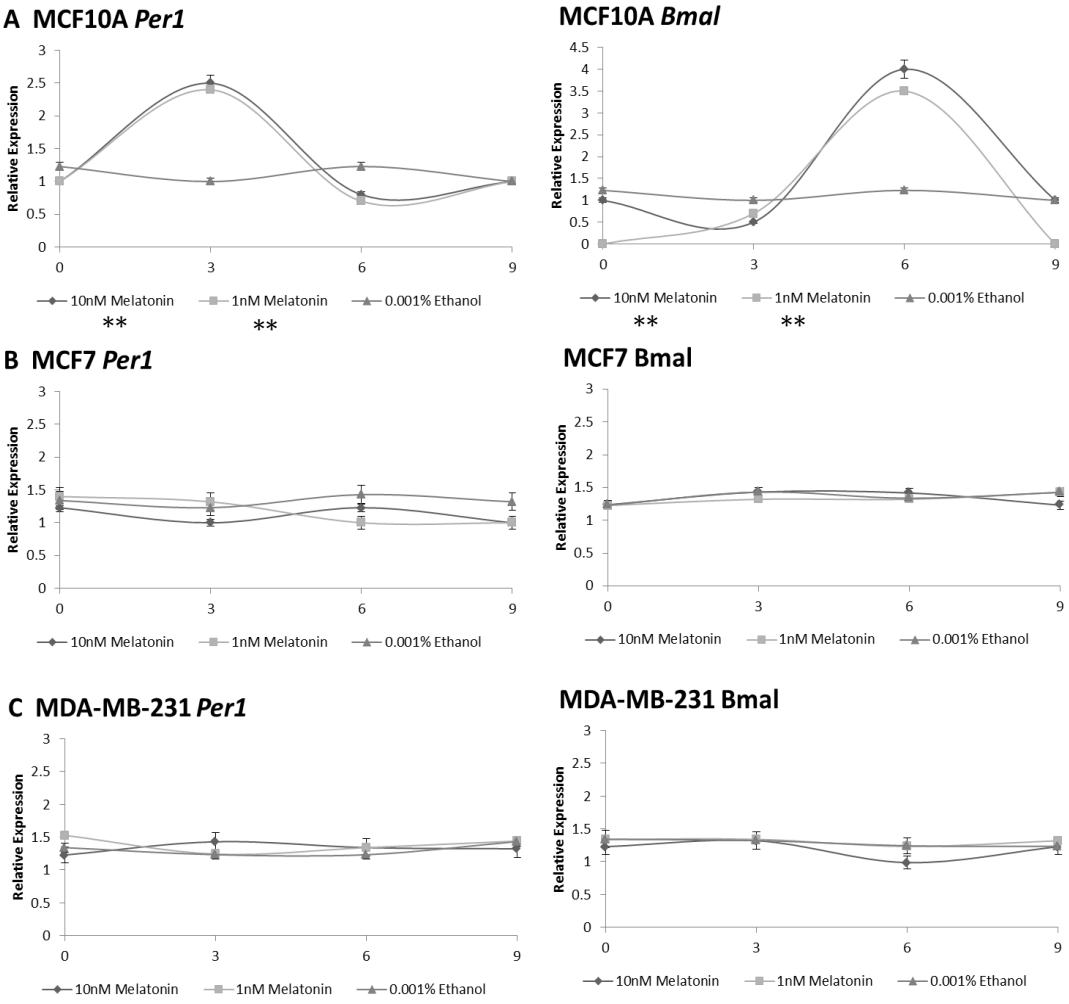

Figure 6.3. MCF10A and MCF7 cells were cultured until ~ 90 % confluent and then pulsed with 10nM melatonin, 1nM melatonin or a 0.001% ethanol control. Samples of these cells were then harvested 0, 3, 6 and 9 hours post treatment. Relative expression of circadian clock genes *Per1, Bmal1* was then analysis using quantitative PCR. The results are shown in Figure 6.3, relative expression for each gene is shown ± SEM, standardised to reference gene TATA-Box binding protein, n=6. Variation over the time course was analysed by tow-way ANOVA followed by post hoc T-test if required. (** = P-value < 0.01)

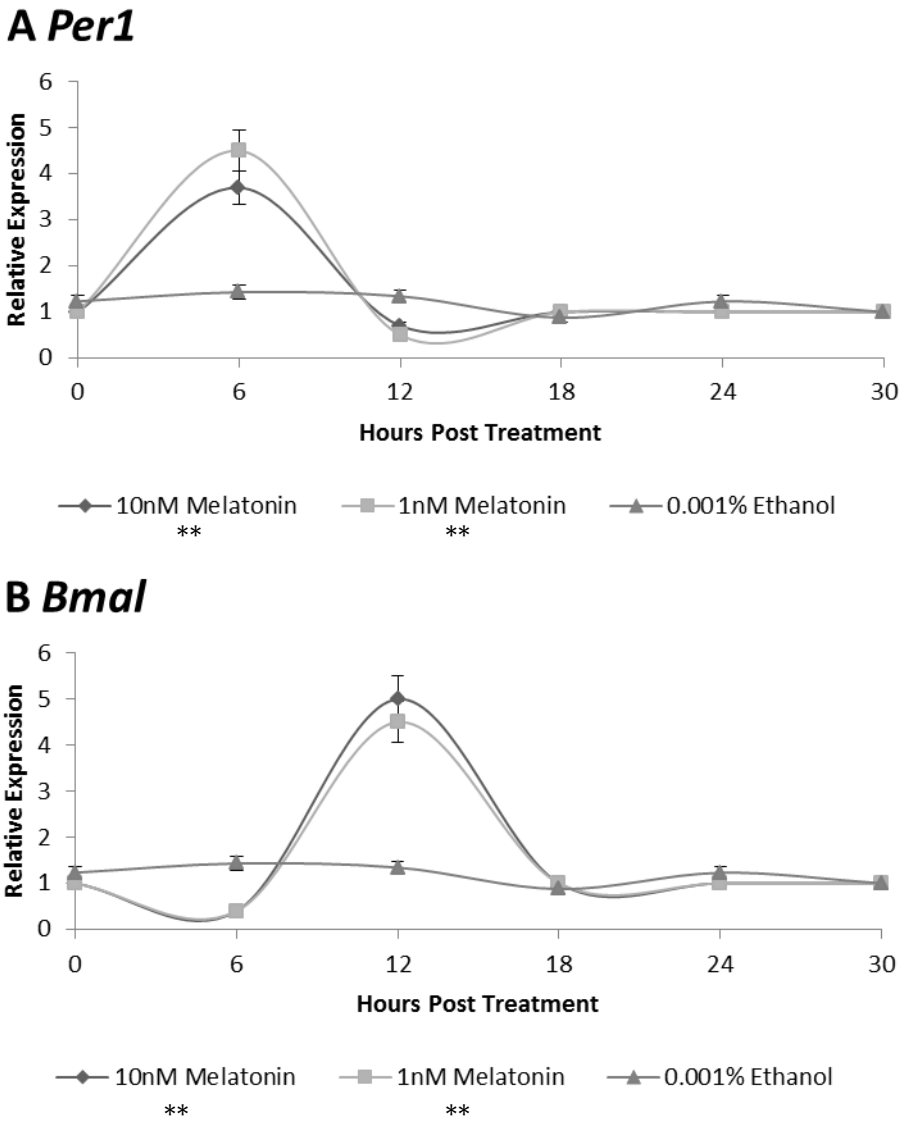

Figure 6.4. MCF10A cells were cultured to ~90% confluency and the pulsed for 3 hours with 10nM melatonin, 1nM melatonin or a 0.001% ethanol control. The expression of *Per1* and *Bmal1* was then determined at 6, 12, 18, 24 and 30 post treatment by quantitative PCR. It is shown here a relative expression ± SEM, standardised to reference gene TATA-Box binding protein, n=3. (** = P-value < 0.01).

5.2.4 Effects of acute melatonin pulsing on cell cycle gene expression

Melatonin has a significant effect on the growth of benign and malignant breast epithelial cells, however, it shows little ability to directly affect peripheral clocks within these tissues. Therefore cell cycle gene expression was studied to dissect the mechanism by which melatonin may be exerting this control.

MCF10A and MCF7 cells were cultured to ~90% confluency and then pulsed for 3 hours with 10nM melatonin, 1nM melatonin and 0.001% ethanol control. Samples were then harvested at 0, 3, 6 and 9 hours during and after treatment (0 hours being treatment onset). The expression of cell cycle genes *p21, Wee1, p53* and *c-Myc* was then determined for each time point by quantitative PCR. Results are shown in Figure 6.5 as relative expression standardised to TATA-Box binding protein, n=3.

Figure 6.5A shows the result for the benign cells, MCF10A. It can be seen that a mild increase in *p21* is induced by melatonin pulsing, as is *p53*, this induction persists across the 6 hours sampled. No significant variation in expression of *Wee1* or c-Myc is seen.

The pulsing of melatonin has a more profound effect on the malignant cell-line, MCF7. A 3.5 fold increase is seen in the expression of *p21*, which remains constantly higher for the 6 hours post treatment removal. Expression of tumour suppressor *p53* is also enhanced by the pulse of melatonin, and remains high for the time course of the experiment. *Wee1* and *c-Myc* remains unchanged and shows no significant variation.

This study confirms that melatonin has direct effect on cell cycle control. This control is increased in a malignant setting.

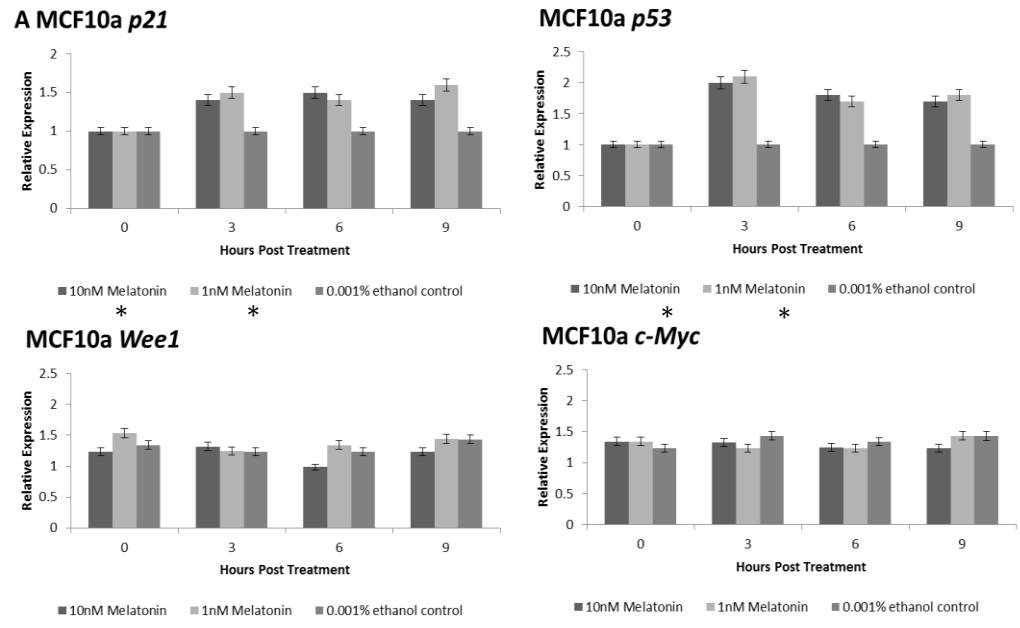

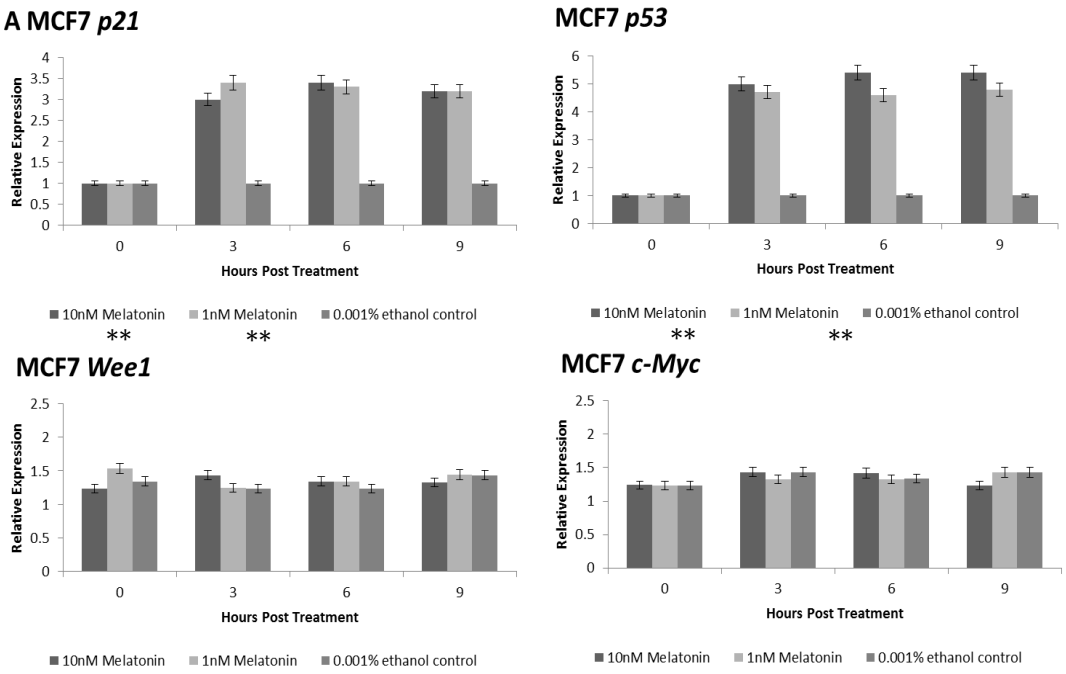

Figure 6.5. MCF10A and MCF7 cells were grown to ~90% confluency and pulsed for hours with 10nM melatonin, 1nM melatonin or 0.001% ethanol control. Samples were then harvested at 0, 3, 6 and 9 hours during and post treatment (0 being treatment onset). Relative expression of *p21, p53, Wee1* and *c-Myc* determined by quantitative PCR is shown ± SEM, standardised to reference TATA-box binding protein, n=3. (* = p-value < 0.01, ** = p-value < 0.001).

5.4 DISCUSSION

Use of melatonin as an adjuvant chemotherapeutic agent has been the subject of discussion for the past two decades (Reiter *et al,* 1991). There is growing evidence for its use, as studies reveal a significant impact on growth of tumours from a variety of tissues (Blask *et al*, 2005). Melatonin has been known to be highly active within breast tissue, especially that expressing oestrogen receptors (Hill *et al*, 1988). It has been shown that melatonin can behave as an agonist for the oestrogen signalling system. This system promotes the expression of cell cycle regulators *p21, p53* and *p27*, reducing cell proliferation rates (Kim & Yoo, 2010) Melatonin is therefore a potent oncostatic for oestrogen positive breast tumours (Hill *et al,* 1988). Interestingly, it has also been shown to affect the growth rate of oestrogen negative breast cancer cell-lines (Blask *et al,* 2002,).

This study confirms that melatonin has a significant effect on the growth rates of MCF7 cells. However, it also shows that melatonin exerts some effect on the growth of benign tissue. This tissue is also seen to have an incredibly low level of oestrogen receptor expression, and is noted to be oestrogen insensitive within the literature (Hill *et al,* 2009). This study therefore reveals that melatonin has an oestrogen independent mechanism of growth control.

As more study is performed on the mammalian peripheral clock, it is being noted that a number of humoural agents are employed by the master clock to coordinate, in part, the peripheral tissue oscillators. However, this study reveals that melatonin does not entrain or induce rhythmic outputs with peripheral clock gene expression. Such synchronisation has been demonstrated previously by the use of glucocorticoids. A mild acute effect is shown within benign tissue; however this is

completely abolished within the malignant cell model. This difference in effect is most likely caused by the presence of abnormally functioning clock within the tissue, as shown in chapter 5. No long term effect of melatonin pulsing is seen.

This does rule out melatonin playing a role is coordination of peripheral clocks. Melatonin is a circadian hormone, and therefore will be endogenous pulsing tissues at a specific time-point each day (Reiter, 1991). Lack of obvious entrainment by this hormone does not rule out melatonin acting as a daily modulator of clock function. Owing to the acute induction of clock genes observed, melatonin regulation could be through of as a short term control pathway, allowing the clock to adapt itself day-to-day to slight changes in the external environment.

This study does, in addition, show that melatonin has a direct effect on the cell cycle. Pulsing of melatonin induced cell cycle regulators *p21* and *p53*, in both benign and malignant cell-lines. The effect is enhanced in the malignant setting. This study suggests that the melatonin signalling pathway and the oestrogen signally pathway induces the same genes. Therefore, there is a cumulative effect between the direct melatonin induction and induction through oestrogen signalling. Inhibition of the oestrogen signalling pathways by antagonists such as Tamoxifen would prove helpful in distinguishing between these two interactive pathways.

Interestingly literature has also shown that the *p21* and *p53* pathways cumulatively regulated the expression of *BRCA1*. *BRCA1* is a cell cycle regulator, a common mutation of which is associated with hereditary breast cancers in particular ethnic populations, resulting in a syndrome of breast and ovarian

neoplasm (Chen *et al*, 2011). Study of this gene within spontaneous neoplasm has therefore been limited. A recent study has found that the BRCA1 promoter contains three canonical E-Boxes, making it a plausible target for clock regulation (Chen *et al,* 2011). Studies looking an down-regulation of Per genes within breast biopsies have also shown an accompanying deregulation of this gene (Winter *et al*, 2007). It would be interesting to see whether BRCA1 plays a role in the development of non-hereditary cancers also. As it is a possible clock regulated gene and an additional regulator of clock regulated cell cycle genes, *p21* and *p53.* This will be discussed further in Chapter 7.

As with the experiments in Chapter 5, it must be kept in mind the limitations of using immortalised cell-lines, and comparison of cell-lines derived from different donors. These results would therefore need validation from primary tissues, and biopsies from single donors, which would eliminate any interpersonal circadian variation.

In conclusion this study shows:

- That melatonin inhibits the growth of both MCF10A and MCF7 cell-lines.
- That melatonin is able to induce acute changes in the expression level of clock genes, however is not able to synchronise peripheral clock populations or produce rhythmic oscillations.
- Melatonin regulated the expression of *p21* and *p53* within MCF10A and MCF7 cell-line.

- Melatonin has a larger effect on MCF7 cells compared to MCF10As, this is putatively caused by the over expression of oestrogen receptors in this cell-line, enhancing melatonin action through the oestrogen signalling pathway.

CHAPTER 7

General Discussion

7.1 General Discussion

The circadian clock is an adaptive mechanism that has evolved in response to the 24 hour variations in the external environment. It allows the host to anticipate such changes and exploit them to its best advantage. It is found ubiquitously across all light-sensitive organisms, as this environmental pressure has remained relatively unchanged for hundreds of thousands of years. As a result it has been incorporated into the governance of multiple biological, physiological and behavioural pathways.

The 2005 governmental paper "The 24/7 Society" set out to address the health issues resulting from the round the clock form of industrial activity found in within the UK. This activity has resulted from scientific advancement, increased global development and increased global commercial demand. The special health report documented the health detriments caused by disrupting circadian function within the individual. Increased risk of cardiovascular disease, sleep problems and psychological disorders featured heavily. However, the most fundamental issue to be addressed was the significant increase in relative risk of cancer development, and accelerated cancer progression within shift-workers and the circadian disrupted (Parliamentary Office of Science and Technology). This move has echoed similar bills and reports from across Europe, developed and developing countries. To the extent that Denmark is now issuing compensation to shift workers who had developed health problems as a result of irregular working hours (Wise, 2009).

Disruption of environmental light patterns has therefore been proposed to disrupt circadian function and as a result circadian output. One putative output is the cell cycle. This thesis has therefore set out to address whether the cell cycle is indeed

regulated by the clock within mammalian cells, and if as an extension circadian disruption leads to cell cycle malfunction.

By working is the zebrafish, one is able to take advantage of the decentralised circadian system it processes (Whitmore *et al*, 2000). This allows a cell-line model to be used to accurately represent circadian function within the animal (Tamai *et al*, 2007).

Within the zebrafish this thesis shows that mitosis is rhythmic, peaking during the late night/early morning. These rhythms are similar to the mitotic rhythms reported in regenerating mouse-liver post-hepatectomy; they fulfil all the criteria of a circadian regulated output and are abolished in clock disrupted cell-lines (Foster & Lucas, 1999). In order to elucidate the pathway through which the clock is exerting its control, quantitative PCR analysis of the expression patterns of mitotic regulators were studied. Interesting, the key target of the clock within mammals, the mitotic inhibitor *Wee1*, (Matsuo *et al,* 2003) is not rhythmic and displays no evidence for being under circadian control in the zebrafish. However, the genes *Cyclin B1* and *cdc2,* which code for Wee1's targets, display robust rhythmic expression patterns that are abolished in a clock mutant setting. Promoter analysis of these genes, revealed transcription factor binding motifs - E-boxes, D-Boxes and RREs - used by circadian components (Yan *et al,* 2008) to direct downstream rhythmic outputs. However, mutational analysis of these sites has reveals differential results and suggest that the regulation of this gene is either indirect or through combined and interdependent pathways.

This work has led to similar studies looking at the timing of S-phase within the zebrafish. In support of work published regarding zebrafish larvae (Dekens *et al,*

2008), these cell-lines have shown to display rhythmic DNA replication, which is also clock driven. The key candidate target within this pathway is the G1/S-phase checkpoint regulator, p21.

Chapter 4 addresses some of the key issues that arise when translating circadian study methods into human cell-line models; the mammalian circadian system remaining strictly hierarchical, requires chemical synchronisation (Stratmann & Schibler, 2006).

It was demonstrated that HEK 293 cells express core clock components in a pattern consistent with a population of functional cellular clocks, which can be synchronised by dexamethasone shocking. Clock function in this cell-line was disrupted using the *zfCLOCK1A DN* construct. The resulting mutant population displayed reduced growth rates, but the construct had little downstream effect on cell cycle gene expression. In fact, rhythmic cell cycle genes expression was primarily determined by dexamethasone pulsing, which was capable of masking the impact of any possible clock malfunction. This study showed that coordination of the cell cycle was regulated on a number of levels by the clock, both by intracellular interactions and circadian humoural messengers.

Due to the growing evidence that clock mutation leads to a higher incidence of breast cancer, the study within Chapter 5 set out to further elucidate this connection. Clock function was studied in benign breast ductal epithelium, the cell types most commonly affected in breast malignancy, and a form of ductal adenocarcinoma itself. It was demonstrated for the first time that the benign tissue contained a functional clock, which generated rhythmic outputs over a time-course, and was somewhat affected by the *zfCLOCK1a DN* construct. The malignant

cell-line on the other hand displayed a highly altered clock and independent cell growth. Cell cycle gene expression seemed unaffected by both glucocorticoid stimulation and clock function in these cell-types. The hypothesis that the transformation processes implemented to produce immortalised mammalian cell-lines may disconnect the cell cycle from its circadian regulation is therefore supported by this data (Yoem *et al*, 2010). Interestingly, immortalised cell-lines are documented as highly glucocorticoid responsive in vivo (Vaidya *et al*, 2010). On the other hand, this result may show that different tissues are under the control of different humoural messengers, especially as clock function has been demonstrated to be crucial for optimal cell-growth in benign tissues.

In the case of breast epithelium, this highly hormonally responsive tissue is known to be highly sensitive to melatonin (Blask *et al,* 2005B). Melatonin is also the primary hormone implicated by the Light-at-Night hypothesis for coordinating the peripheral cell cycle and tissue based circadian behaviours (Stevens, 2006), and is disrupted by prolonged shift-work (Stevens, 2006).

The studies in Chapter 6 set out to address this interaction and also the possibility that melatonin may have a similar role to the glucocorticoids, as a peripheral clock synchroniser. It is shown that melatonin has a significant effect on oestrogen positive malignant breast epithelial cells, and causes a much smaller growth reduction in benign tissue. This is possible coordinated by melatonin regulating expression of certain cell cycle regulators which is partly supported this data. However, although melatonin can induce short term expression changes in core clock genes, it is unable to produce clock gene rhythms and cellular synchronisation as seen with dexamethasone. One can conclude that melatonin

function is part of culmination of other factors which combine to regulate cell cycle progression, however is less involved in peripheral clock coordination.

There are a number of specific experiments resulting from these studies, that will allow confirmation of a number of theories put forward throughout the thesis. One of the most important would be the attempt to rescue a normal phenotype from malignant breast epithelium by exogenously expression *Per1*. This would confirm whether the cell cycle differences observed are truly *Per1* driven.

However, these studies also pose much bigger questions. The validity of *in vitro* and cell-culture studies for mammalian clock study being the most prominent. The peripheral clock *in vivo* is subject to a plethora of interconnected synchronising stimuli (Stratmann & Schibler, 2006). Although individual stimuli can be applied to cell-lines in the *in vitro* setting to stimulate the clock, as seen in this thesis, these experiments cannot be seen as representative of what goes on in the more complicated in vivo system. Validation has been drawn from the similarities in clock function described in rodent *in vivo* and human biopsy and haematological *in vitro* studies, which support the use of *in vitro* synchronisation. However the limitations of this technique must be considered. Although it allows for the study of peripheral clock function, it seems limited when extended to downstream targets of these clocks.

The gold standard in this setting would be a large scale clinical study of clock function within biopsied samples matched to donor controls. However, as discussed in Section 1, there are a number of complications in human studies, unique to circadian biology.

One of the main reasons the Light-At-Night hypothesis is still controversial is the lack of consistent supportive data. For example the epidemiological studies these precipitated these biological studies, vary widely in their sample size, analysis and structure and have a result come under criticism. A structured meta-analysis of the epidemiological studies would be required to produce a secure evidence base. This is of upmost importance due to the scope of impact these studies would have.

The possible regulation of the cell cycle by the circadian clock would be an important discovery for both cell biology and for clinical medicine (Levi & Schibler, 2007).

Starting on the broadest reaching perspective validating the link between circadian function and carcinogenesis is important for public health and disease prevention. As proposed by "The 24/7 Society" paper, health promotion and the engagement of individuals on both an industry and personal perspective is imperative (Parliamentary Office of Science and Technology). As with any risk factor that will predispose to certain illness, education and modification would be key to prevent clock disruption related cancers.

Individuals whose cancer maintains circadian competence have a much better prognosis that those which are circadian disrupted (Levi & Schibler, 2007). This phenomenon could be easily utilised as a prognostic marker for disease progression. In the same way maintaining circadian function during illness, appears to act as a disease modifier. Side effects, the psychological impact of disease and sleep disorders seem greatly reduced in circadian competent patients. As well as being associated with better prognosis (Levi & Schibler, 2007). This would have implications on the non-medical management of cancer patients. This

work can also be transferred into the therapeutic setting by using chronopharmacology as described in Section 1 (Kobayshi *et al*, 2002).

The two main hurdles chronobiologists must face is firstly the difficulty in managing personal based medical approaches. As each person's chronotype is slightly different, a person's treatment must be individual (Scully *et al,* 2011). Secondly, chronobiology has unfortunately gained a "poor reputation" within the medical profession; this is hindered more by lack of teaching and understanding of the subject (Kegan, 2004).

In conclusion the circadian regulation of the cell cycle is a complicated and multifaceted phenomenon in the mammal. Further work on this system holds a number of limitations. Yet at the same time dissecting these pathways would reveal a fascinating amount of possible clinical applications, and have a major effect on a number of medical specialties.

CHAPTER 8

APPENDIX

8.1 GROWTH ASSAY FOR CELL CULTURE.

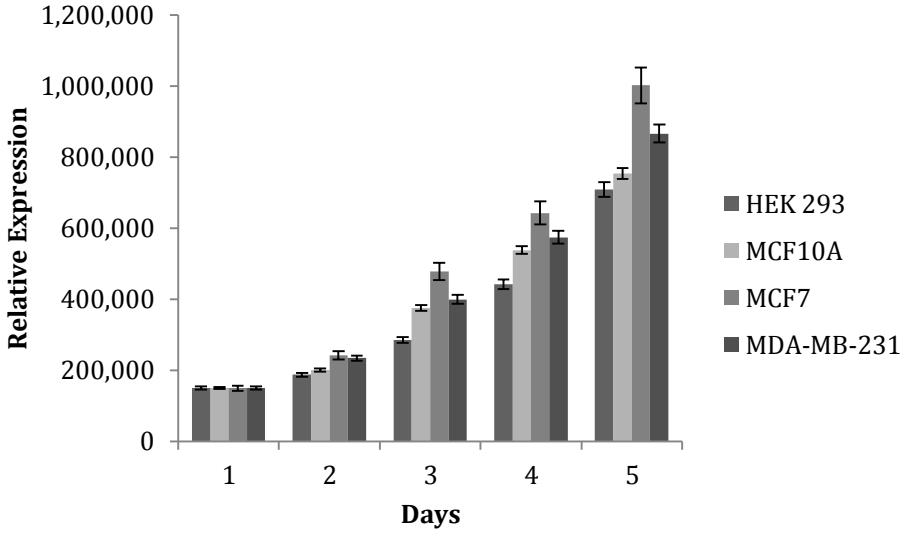

8.2 Alignment of Human and Zebrafish Clock Proteins.

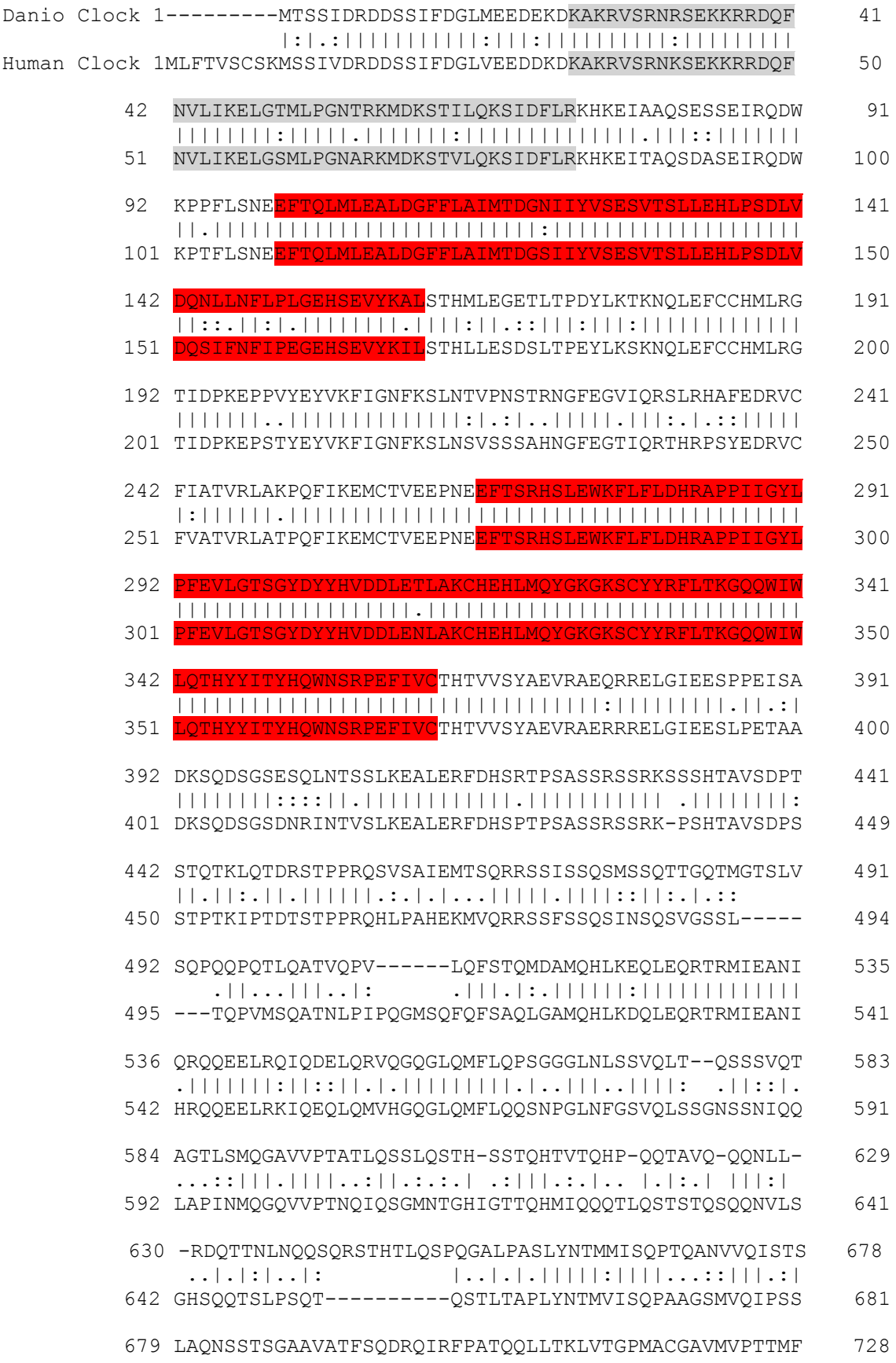

```
    :.|| ||..|||.||:||||||||...|||:|||||.|:|||||||||:||.
682 MPQN-STQSAAVTTFTQDRQIRFSQGQQLVTKLVTAPVACGAVMVPSTML    730


729 MGQVVTA---FAPQQGQPQTISIAQQPSAQTADQQTHTQAQTQAAATAQQ    775
    |||||||   ||.||.|.||:|:.||...|::.:|..|..|.
731 MGQVVTAYPTFATQQQQSQTLSVTQQQQQQSSQEQQLTSVQQ--------    772

776 QGQNQAQLTQQQTQFLQAPRLLHSNQSTQLILQAAFPLQQQGTFTTATQQ    825
      .:||||||...||||..||||.|.||||||.||||| ||.||.
773 --PSQAQLTQPPQQFLQTSRLLHGNPSTQLILSAAFPL-QQSTFP-----    814

826 QQQLHQQQQQLQQQQQLQQQQQQQQQQLQQQHQQQQQQLQQQHQQQQQQL   875
                                |..|||.|       .||||||
815 ----------------------------QSHHQQHQ-------SQQQQQL   829

876 AAHRSDSMTERSNPPPQ    892
      :.||:||:.:.|...|
830 SRHRTDSLPDPSKVQP-    845
```

Basic Helix-Loop-Helix domain

Per – Arntl – Single minded domain

REFERENCES

Allada, R. White, NE. So, WV. Hall, JC. Rosbash, M. (1998) A mutant Drosophila homolog of mammalian Clock disrupts circadian rhythms and transcription of period and timeless. Cell. **93(5):**791-804.

Allebrandt, KV. Roenneberg, T. (2008) The search for circadian clock components in humans: new perspectives for association studies. *Brazilian Journal of Medical and. Biological Research*. **41:**716–721.

Alonso, G. (2000) Prolonged corticosterone treatment of adult rats inhibits the proliferation of oligodendrocyte progenitors present throughout white and graymatter regions of the brain. *Glia*. **31:**219–231.

Alvarez, JD. Sehgal, A. (2005) The thymus is similar to the testis in its pattern of circadian clock gene expression. *Journal of Biological Rhythms.* **20**:111-121.

Akashi, M. Nishida, E. (2000) Involvement of the MAP kinase cascade in resetting of the mammalian circadian clock. *Genes and Development.* **14**:645–49.

Akashi, M. Tsuchiya, Y. Yoshino, T. Nishida, E. (2002) Control of intracellular dynamics of mammalian period proteins by casein kinase I 1 (CKI1) and CKId in cultured cells. *Molecular Cell Biology.* **22**:1693–1703.

Akashi, M. and Takumi, T. (2005) The orphan nuclear receptor RORaregulates circadian transcription of the mammalian core-clock Bmal1. *Nature Structural Molecular Biology*. **12:**441–448.

Akhtar, RA. Reddy, AB. Maywood, ES. Clayton, JD. King, VM. Smith, AG. Gant, TW. Hasting, MH, Kyriacou, CP. (2002) Circadian cycling of the mouse liver transcriptome, as revealed by cDNA microarray, is driven by the suprachiasmatic nucleus. *Current Biology.* **12:**540-550.

Ancoli-Israel, S. (2003) The role of actigraphy in the study of sleep and circadian rhythms. *Sleep*. **26:**342–392.

Antoch, M.P. Gorbacheva, VY. Vykhovanets, O. Toshkov, IA. Kondratov, RV. (2008) Disruption of the circadian clock due to the Clock mutation has discrete effects on aging and carcinogenesis. *Cell Cycle.* **7:**1197-2004.

Aschoff, J. (1965) Circadian rhythms in man. *Science.* **148:**1427–1432

Asher, G. Gatfield, D. Stratmann, M. Reinke, H. Dibner, C. (2008) SIRT1 regulates circadian clock gene expression through PER2 deacetylation. *Cell.* **134**:317–28.

Aubert, C. Janiaud, P. Lecalvez, J. (1980) Effect of pinealectomy and melatonin on mammary tumour growth in Sprague-Dawley rats under different lighting conditions. *Journal of Neuronal Transmission*. **47:**121-30.

Balsalobre, A. Damiola, F. Schibler, U. (1998) A serum shock induces circadian gene expression in mammalian tissue culture cells. *Cell.* **93**:929–37.

Balsalobre, A. Marcacc, L. Schibler, U. (2000) Multiple signalling pathways elicit circadian gene expression in cultured Rat-1 fibroblasts. *Current Biology.* **10:**1291-1294.

Balsalobre, A. Brown, SA. Marcacci, L. Tronche, F. Kellendonk, C. Reichardt, HM. Schütz, G. Schibler, U. (2000) Resetting of circadian time in peripheral tissues by glucocorticoid signaling. *Science.* **289:**2344-2347.

Beaver, LM. Rush, BL. Gvakharia B. O. Giebultowicz J. M. (2003) Noncircadian regulation and function of clock genes period and timeless in oogenesis of *Drosophila Melanogaster.* Journal of Biological Rhythms. **18**:463-472.

Berson DM, Dunn FA, Takao M. (2002). Phototransduction by retinal ganglion cells that set the circadian clock. *Science.* **295**:1070–73.

Bjarnason, GA. Jordan, R. (2000) Circadian variation of cell proliferation and cell cycle protein expression in man: clinical implications. *Cell Cycle Research*. **4:**193–206.

Blais, A. Dynlacht, BD. (2007) E2F-associated chromatin modifiers and cell cycle control. Current Opinions in Cell Biology. **19:6**:658-662.

Blask, DE. Sauer, LA. Dauchy, RT. (2002) Melatonin as a chronobiotic/anticancer agent: cellular, biochemical, and molecular mechanisms of action and their implications for circadian-based cancer therapy. *Current Topics in Medicinal Chemistry.* **2:**113–32.

Blask, DE, Dauchy, RT, Sauer LA. (2003) Growth and fatty acid metabolism of human breast cancer (MCF7) xenografts in nude rate: impact of

constant light induced nocturnal melatonin suppression. *Breast Cancer Research Treatment.* **79:**13-320.

Blask, DE. Brainard, GC. Dauchy, RT. (2005A) Melatonin-depleted blood from premenopausal women exposed to light at night stimulates growth of human breast cancer xenografts in nude rats. *Cancer Research*. **65:**11174–84.

Blask, DE. Dauchy, RT, Sauer LA. (2005B) Putting cancer to sleep at night:the neuroendocrine/circadian melatonin signal. *Endocrine.* **27:**179–88

Bolige, A. Hagiwara, S. Zhang, Y. Goto, K. (2005) Circadian G2 arrest as related to circadian gating of cell population growth in Euglena. *Plant Cell Physiology.* **46:** 931-36.

Bolsover, SR. (2003) Cell Biology. Willy-Liss UK.

Bornstein, SR. (2008) Dissociation of ACTH and glucocorticoids. *Trends in Endocrinology and Metabolism.* **19 :**175–180.

Bos, NP. Mirmiran, M. (1990) Circadian rhythms in spontaneous neuronal discharges of the cultured suprachiasmatic nucleus. *Brain Research.* **511:**158–62.

Bostock, CJ. Prescott, DM. Kirkpatrick, JB. (1971) An evaluation of the double thymidine block for synchronizing mammalian cells at the G1-S border. *Experimental Cell Research*. **68:1:**163-168.

Brown, SA. Zumbrunn, G. Fleury-Olela, F. Preitner, N. Schibler, U. (2002) Rhythms of mammalian body temperature can sustain peripheral circadian clocks. *Current Biology.* **12:**1574–83.

Brown, SA. Fleury-Olela, F. Nagoshi, E. Hauser, C. Juge, C. (2005) The period length of fibroblast circadian gene expression varies widely among human individuals. *PLoS Biology.* **3**:e338.

Bubenik, G.A. (2002) Gastrointestinal melatonin: localization, function, and clinical relevance. Digestive Diseases and Sciences **47(10):** 2336-48.

Buijs, RM. (1999) Anatomical and functional demonstration of a multisynaptic suprachiasmatic nucleus adrenal (cortex) pathway. *European Journal of Neuroscience*. **11:**1535–1544.

Bunger, MK. Walisser, JA. Sullivan, R. Manley, PA. Moran, SM. Kalscheur, VL. Colman, RJ. Bradfield, CA. (2005) Progressive arthropathy in mice with a targeted disruption of the Mop3/Bmal-1 locus. *Genesis.* **41:**122–130.

Cahill, GM. Hurd, MW. Batchelor, MM. (1998) Circadian rhythmicity in the locomotor activity of larval zebrafish. Neuroreport. **26;9(15):**3445-9.

Cailleau, R. (1974) Breast tumour cell lines from pleural effusions. *Journal of the National Cancer Institute*. **52:**661-674.

Cailleua, R. (1978) Long term breast carcinoma cell lines of metastatic origin: preliminary characterization. *In Vitro*. **14:**911-915.

Cao, Q. Gery, S. Dashti, A. Yin, D. Zhou, Y. Gu, J. Koeffler, HP. (2009) A role for the clock gene per1 in prostate cancer. *Cancer Research*. **69:19:**7619-25.

Cardone, L. Hirayama, J. Giordano, F. Tamaru, T. Palvimo, JJ. Sassone-Corsi, P. (2005) Circadian clock control by SUMOylation of BMAL1. *Science*. **309:**1390–1394.

Carr, AJ. Whitmore, D. (2005) Imaging of single light-responsive clock cells reveals fluctuating free-running periods. Nature Cell Biology. **7(3):**319-21.

Carrillo-Vico, A., J.R. Calvo, P. Abreu, P.J. Lardone, S. Garcia-Maurino, R.J. Reiter, and J.M. Guerrero, Evidence of melatonin synthesis by human lymphocytes and its physiological significance: possible role as intracrine, autocrine, and/or paracrine substance. Faseb J, 2004. 18(3): p. 537-9.

Castel, M. Belenky, M. Cohen, S. Ottersen, OP. Storm-Mathisen, J. (1993) Glutamate-like immunoreactivity in retinal terminals of the mouse suprachiasmatic nucleus. *European Journal of Neuroscience.* **5:**368–81.

Ciarleglio, CM. Ryckman, KK. Servick, SV. Hida, A. Robbins, S. Wells,N. Hicks, J. Larson, SA. Wiedermann, JP. Carver, K. Hamilton, N. Kidd, KK. Kidd, JR. Smith, JR. Friedlaender, J. McMahon, DG. Williams, SM. Summar, ML. Johnson, CH. (2008) Genetic differences in human circadian clock genes among worldwide populations. *Journal of Biological Rhythms*. **23:**330–340.

Chebotaev, D. Yemelyanov, A. Budunova, I. (2007) The mechanisms of tumour suppressor effect of glucocorticoid receptor in skin. *Molecular Carcinogenesis.* **46:**732–740.

Chen, ST. Choo, KB. Hou, MF. Yeh, KT. Kuo, SJ. Chang, JG. (2005)Deregulated expression of the PER1, PER2 andPER3 genes in breast cancers. *Arcinogenesis.* **26 (7):**1241-1246.

Chen, Y. Xu, J. Borowicz, S. Collins, C. Huo, D. Olopade, OI. (2011) c-Myc activates BRCA1 gene expression through distal promoter elements in breast cancer cells. BMC Cancer. **11:**246.

Chrousos, GP. Harris, AG. (1998) Hypothalamic-pituitary-adrenal axis suppression and inhaled corticosteroid therapy. 1. General principles. *Neuroimmunomodulation.* **5:**227-287.

Chu, LW. Zhu, Y. Yu, K. Zheng, T. Yu, H. Zhang, Sesterhenn, Y. I. Chokkalingam, A.P. Danforth, K.N. Shen, M.C. Stanczyk, F.Z. Gao, Y.T. Hsing, A.W. (2008) Variants in circadian genes and prostate cancer risk: a population-based study in China. *Prostate Cancer Prostatic Disease*. **11:**342–348.

Clarke, R. Dickson, RB. Brunner, N. (1990) The process of malignant progression in human breast cancer. Annals of Oncology. **1**:401-407.

Conlon, M. Lightfoot, N. Kreiger, N. (2007) Rotating shift work and risk of prostate cancer. *Epidemiology.* **18:**182–18.

Cos, S. Blask, DE. Lemus-Wilson, A. (1991) Effects of melatonin on the cell cycle kinetics and "oestrogen-rescue" of MCF-7 human breast cancer cells in culture. *Journal of Pineal Research.* **10:**36–42.

Czeisler, C. A. (1999) Stability, precision, and near-24-hour period of the human circadian pacemaker. *Science*. **284**:2177–2181.

Dai, H. Zhang, L. Cao, M. Song, F. Zheng, H. Zhu, X. Wei, Q. Zhang, W. Chen, K. (2011) The role of polymorphisms in circadian pathway genes in breast tumorgenosis. *Breast* Cancer Research Treatments. **127:**531-40.

Damiola, F. Le Minh, N. Preitner, N. Kornmann, B. Fleury-Olela, F. Schibler, U.(2000). Restricted feeding uncouples circadian oscillators in peripheral tissues from the central pacemaker in the suprachiasmaticnucleus. *Genes and Development.* **14:**2950–61.

Dauchy, RT. Dauchy, EM. Sauer, LA. Blask, DE. Davidson, LK. Krause, JA. Lynch, DT. (2004) Differential inhibition of fatty acid transport in tissue-isolated steroid receptor negative human breast cancer xenografts perfused in situ with isomers of conjugated linoleic acid. *Cancer Letters.* **8:209** 7-15.

Davis, S. Mirick, DK. Steven, RG. (2001) Night shift work, light at night, and risk of breast cancer. *Journal of National Cancer Institute*. **93:**1557-1562.

Dawson, D. Encel, N.(1993) Melatonin and sleep in humans. Journal of Pineal Research. 15:1-12

Debnath, J. Muthuswamy, S.K. Brugge, JS. (2003) Morphogenesis and oncogenesis of MCF-10A mammary epithelial acini grown in three-dimensional basement membrane cultures. *Methods*. **30:**256-68.

DeBruyne, JP. Noton, E. Lambert, CM, Maywood, ES. Weaver, DR. Reppert, SM. (2006) A clock shock: mouse CLOCK is not required for circadian oscillator function. *Neuron*. **50:**465–477.

Dekens, MP. Santoriello, C. Vallone, D. Grassi, G. Whitmore, D. Foulkes, NS. (2003) Light regulates the cell cycle in zebrafish. *Current Biology.* **13:**2051-2057.

Dekens, MP. Whitmore, D. (2008) Autonomous onset of the circadian clock in the zebrafish embryo. EMBO Jounral. **27:**2757-65.

de Mairan, J. (1729) Observation botanique. *Histoire de l'Academie Royale des Sciences.* 35–36

Dibner, C. Sage, D. Unser, M. Bauer, C. d'Eysmond, T. (2009) Circadian gene expression is resilient to large fluctuations in overall transcription rates. *EMBO Journal.* **28:**123–34.

Dickmeis, T. (2009) Glucocorticoids and the circadian clock. J*ournal of Endocrinology.* **200:**3-22.

Djeridane, Y. Touitou, Y. (2001) Melatonin synthesis in the rat harderian gland: age- and time-related effects. Experimental Eye Research. **72(4):** 487-92.

Doi, M. Hirayama, J. Sssone-Corsi, P. (2006) Circadian regulator CLOCK is a histone aceytltransferase enzyme. *Cell.* **125:**497-508.

Dubocovich, ML. Rivera-Bermudez, MA. Gerdin, MJ. Masana M.I. (2003) Molecular pharmacology, regulation and function of mammalian melatonin receptors. *Front Bioscience*. **8:** d1093-108.

Duffield, GE. Best, JD. Meurers, BH. Bittner, A. Loros, JJ. Dunlap, JC. (2002) Circadian programs of transcriptional activation, signalling, and protein turnover revealed by microarray analysis of mammalian cells. *Current Biology.* **12:**551-557.

Dunlap, JC. Loros, JJ. Liu, Y. Crosthwaite, SK. (1999) Eukaryotic circadian systems: cycles in common. Genes to Cells. **4(1):**1-10.

Ebisawa, T. Numazawa, K., Shimada, H. Izutsu, H. Sasaki, T. Kato, N. Tokunaga, K. Mori, A. Honma, K. Honma, S. Shibata, S. (2010) Self-sustained circadian rhythm in cultured human mononuclear cells isolated from peripheral blood. *Neuroscience Research.* **66:**223-227.

Engeland,WC. Arnhold,MM.(2005)Neural circuitry inthe regulation of adrenal corticostero ne rhythmicity. **Endocrine. 28:**325-32

Essen, LO. Klar, T. (2006) Light-driven DNA repair by photolyases. Cell and Molecular Life Sciences. **63(11):**1266-77.

Feyschting, M. Osterlund, B. Ahlbom A. (1998) A reduced cancer incidence amount the blind. *Epidemiology.* **9:**490-494.

Filipski, E. King, VM. Li, X. Granda, TG. Mormont, MC. Liu, X. Claustrat, B. Hastings, MH. Levi, F. (2002) Host circadian clock as a control point in tumour progression. *Journal of the National Cancer Institute.* **94:** 690–697.

Filipski, E. Delaunay, F. King, VM. Wu, MW. Claustrat, B. Grechez-Cassiau, A. Guettier, C. Hastings, MH. Francis, L. (2004) Effects of chronic jet lag on tumour progression in mice. *Cancer Research.* **64:**7879–7885.

Filipski, E. Innominato, PF. Wu, M. Li, XM. Iacobelli, S. Xian, LJ. Levi, F. (2005) Effects of light and food schedules on liver and tumour molecular clocks in mice. *Journal of the National Cancer Institute.* **97:**507–517.

Foligne, B. (2001) Changes in cell proliferation and differentiation of adult rat small intestine epithelium after adrenalectomy: kinetic, biochemical, and morphological studies. *Digestive and Dispositional Science.* **46:**1236–1246

Foster, RG. Lucas, RJ. (1999) Clocks, criteria and critical genes. *Nature America*. **22:** 217-219.

Fu, L. Pelicano, H. Liu, J. Huang, P. Lee, C. (2002) The circadian gene Period2 plays an important role in tumour suppression and DNA damage response in vivo. *Cell.* **111:41**-50.

Fukuya, H. Emoto, N. Nonaka, H. Yagita, K. Okamura, H. Yokoyama, M. (2007) Circadian expression of clock genes in human peripheral leukocytes. *Biochemical and Biophysical Research Communications.* **354**:924-928.

Gastel, J.A. Roseboom, P.H. Rinaldi, P.A. Weller, J.L. Klein D.C.. (1998) Melatonin production: proteasomal proteolysis in serotonin N-acetyltransferase regulation. *Science.* **279(5355):** 1358-60.

Gauger, MA.Sancar, A. (2005) Cryptochrome, circadian cycle, cell cycle checkpoints, and cancer. *Cancer Research.* **65:**6828–6834.

Gekakis, N. Staknis, D. Nguyen, H.B. Davis, FC. Wilsbacher, LD. King, DP. Takahashi, JS. Weitz, CJ. (1998) Role of the CLOCK protein in the mammalian circadian mechanism. *Science.* **280**:1564–1569.

Gery, S. Gombart, AF. Yi, WS. Koeffler, C. Hofmann, WK. Kos, M. (2005) Transcription profiling of C/REP targets identifies Per2 as a gene implicated in myeloid leukaemia. *Blood.* **106:**2827-36.

Gery, S. Komatsu, N. Baldjyan, L. Yu, A. Koo, D. Koeffler, HP. (2006) The circadian gene Per1 plays an important role in cell growth and DNA damage control in human cancer cells. *Molecular Cell***. 22:**375-82.

Gery, S. Komatsu, N. Kawamata, N. Miller, CW. Desmond, J. Virk, RK. Marchevsky, A. Mckenna, R. Taguchi, H. Koeffler, HP. (2007) Epigenetic silencing of the candidate tumour suppressor gene Per1 in non-small cell lung cancer. *Clinical Cancer Research.* **13:5** 1399-404.

Gery, S. Virk, R. Chumakov, K. Yu, A. Koeffler, HP. (2007) The clock gene Per2 links the circadian system to the oestrogen receptor. Oncogene. **26:**7916–7920

Gery, S. Koeffler, HP. (2009) Per2 is a C/EBP target gene implicated in myeloid leukaemia. Integrative Cancer Therapeutics. **8:**317–320.

González, A. Martínez-Campa, C. Mediavilla, MD. Alonso-Gonzales, C. Sánchez-Mateos, S. Hill, SM. Sanchez-Barceló, EJ. Cos, S. *(*2007) Effects of MT1 melatonin receptor over expression on the aromatase-suppressive effect of melatonin in MCF-7 human breast cancer cells. *Oncology Reports.* **17:4** 947-53.

Goodspeed, MC. Lee, CC. *(*2007) Tumour Suppression and Circadian Function. *Journal of Biological Rhythms.* **22:**291.

Gooley, JJ. Lu, J. Chou, TC. Scammell, TE. Saper, CB. (2001). Melanopsin in cells of origin of the Retinohypothalamic tract. *Nature Neuroscience.* **4:**1165.

Goto, K. Johnson, CH. (1995) Is the cell division cycle gated by the circadian clock? The case of *Chlamydomonas reinhardii*. *Journal of Cell Biology.* **129:4** 1061-1069.

Gould, SJ. Subramani, S. (1988) Firefly luciferase as a tool in molecular and cell biology. Analytical Biochemistry. **175 (1):** 5–13.

Gréchez-Cassiau, A. Rayet, B. Guillaumond, F. Teboul, M. Delaunay, F. (2008) The circadian clock component BMAL1 is a critical regulator of

p21WAF1/CIP1 expression and hepatocyte proliferation. *Journal of Biological Chemistry.* **283:8** 4535-42.

Green, DJ. Gillette, R. (1982). Circadian rhythm of firing rate recorded from single cells in the rat Suprachiasmatic brain slice. *Brain Research.* **245:**198–200.

Groos, G. Hendriks, J. (1982). Circadian rhythms in electrical discharge of rat suprachiasmatic neurones recorded in vitro. *Neuroscience Letters.* **34:**283–88

Guillaumond, F. Dardente, H. Giguere, V. Cermakian, N. (2005) Differential control of Bmal1 circadian transcription by REV-ERB and ROR nuclear receptors. *Journal of Cell Biology.* **20:**391–403.

Gumz, ML. Cheng, K. Lynch, IJ. Stow, LR. Greenlee, MM. Cain, BD. Wingo, CS. (2001) Regulation of ENaC expression by the circadianclock protein period 1 in mpkCCDc14 cells. *Biochim Biophys Acta*.**1799:** 622– 629

Guo, H. Brewer, JM. Lehman, MN. Bittman, EL. (2006). Suprachiasmatic regulation of circadian rhythms of gene expression in hamster peripheral organs: effects of transplanting the pacemaker. *Journal of Neuroscience.* **26:**6406–6412.

Hahn, RA. (1991) Profound bilateral blindness and incidence of breast cancer. *Epidemiology*. **2:**208-210.

Hainaut, P. Hollstein, M. (2000) p53 and human cancer: the first ten thousand mutations. *Advances in Cancer Ressearch*. **77:** 81–137.

Halberg, F. Zander, HA. Houglum, MW. Muhlemann, HR. (1954) Daily variations in tissue mitoses, blood eosinophils and rectal temperatures of rats. *American Journal of Physiology.* **177:3** 361-6.

Hannibal, J. Ding, JM. Chen, D. Fahrenkrug, J. Larsen, PJ. (1997). Pituitary adenylate cyclase-activating peptide (PACAP) in the retinohypothalamic tract: a potential daytime regulator of the biological clock. *Journal of Neuroscience.* **17**:2637–44.

Hansen, J. (2001) Increased breast cancer risk among women who predominately work at night. *Epidemiology*.**12:**74-77.

Hara, R. (2001) Restricted feeding entrains liver clock without participation of the suprachiasmatic nucleus. *Genes and Cells*. **6:**269–278.

Hardin, P. E. (2004). Transcription regulation within the circadian clock: the E-box and beyond. *Journal of Biological Rhythms.* **19:**348-360.

Hastings, MH. Field, MD. Maywood, ES. Weaver, DR. Reppert, SM. (1999). Differential regulation of mPER1 and mTIM proteins in the mouse suprachiasmatic nuclei: new insights into a core clock mechanism. *Journal of Neuroscience.* **19:**RC11.

Hattar, S. Liao, HW. Takao, M. Berson, DM. Yau, KW. (2002) Melanopsin-containing retinal ganglion cells: architecture, projections, and intrinsic photosensitivity. *Science.* **295**:1065–70.

Hawkins, GA. Meyers, DA. Bleecker, ER. Pack, AI. (2008) Identification of coding polymorphisms in human circadian rhythm genes PER1, PER2,

PER3, CLOCK, ARNTL, CRY1, CRY2 and TIMELESS in a multi-ethnic screening panel. *DNA Sequencing.* **19:**44–49.

He G, Siddik ZH, Huang Z, Wang R, Koomen J, Kobayashi R, Khokhar AR, Kuang J. (2005) Induction of p21 by p53 following DNA damage inhibits both Cdk4 and Cdk2 activities. *Oncogene.* **24:**2929-2943.

Helfrich-Förster, C. Yoshii, T. Wülbeck, C. Grieshaber, E. Rieger, D. Bachleitner, W. Cusamano, P. Rouyer, F. (2007) The lateral and dorsal neurons of Drosophila melanogaster: new insights about their morphology and function. *Cold Spring Harbor Symposium Quantitative Biology*. **72**:517-25.

Hendzel, MJ. Wei, Y. Mancini, MA. Van Hooser, A. Ranalli, T. Brinkley, BR. Bazett-Jones, DP. Allis, CD. (1997) Mitosis-specific phosphorylation of histone H3 initiates primarily within pericentromeric heterochromatin during G2 and spreads in an ordered fashion coincident with mitotic chromosome condensation. Chromosoma. **106(6):**348-60.

Hill, SM. Blask, DE. (1998) Effects of the pineal hormone melatonin onthe proliferation and morphological characteristics of human breast cancer cells (MCF-7) in culture. *Cancer Research*. **48:**6121–6.

Hill, SM. Frasch, T. Xiang, S. Yuan, L. Duplessis, T. Mao, L. (2009) Molecular mechanisms of melatonin anticancer effects. *Integrative Cancer Therapeutics.* **8:**337-46.

Hinds, PW. Finlay, CA. Quartin, RS. Baker, SJ. Fearon, ER. Vogelstein, B. (1990). Mutant p53 DNA clones from human colon carcinomas

cooperate with ras in transforming primary rat cells: a comparison of the "hot spot" mutant phenotypes. *Cell Growth Differences.* **1:** 571–580.

Hirayama, J. Kaneko, M. Cardone, L. Cahill, G. Sassone-Corsi, P. (2005) Analysis of circadian rhythms in zebrafish. Methods in Enzymology. **393**:186-204.

Hirota, T. Fukada, Y. (2004). Resetting mechanism of central and peripheral circadian clocks in mammals. *Zoological Science.* **21:**359–68.

Hoffman, AE. Zheng, T. Ba, Y. Zhu, Y. (2008) The circadian gene NPAS2, a putative tumour suppressor, is involved in DNA damage response. *Molecular Cancer Research.* **6:**1461–1468.

Hoffman, AE. Zheng, T. Stevens, RG. Ba, Y. Zhang, Y. Leaderer, D. Yi, C. Holford, TR. Zhu, Y. (2009) Clock-cancer connection in non-Hodgkin's lymphoma: a genetic association study and pathway analysis of the circadian gene cryptochrome 2. *Cancer Reseach.* **69:**3605–3613.

Horne, J. A. & Ostberg, O. (1976) A self-assessment questionnaire to determine morningness–eveningness in human circadian rhythms. *International Journal of Chronobiology.* **4:** 97–110.

Hughes, ME. DiTacchio, L. Hayes, KR. Vollmers, C. Pulivarthy, S. (2009). Harmonics of circadian gene transcription in mammals. *PLoS Genetics.* **5:**e1000442.

Ikehata, H. Ono, T. (2011) The mechanisms of UV mutagenesis. Journal of Radiation Research (Tokyo). **52(2):**115-25.

Innominato, PF. Focan, C. Gorlia, T. Moreau, T. Garufi, C. Waterhouse, J. Giacchetti, S. Coudert, S. Iacobelli, S. Genet, D. Tampellini, M. Chollet, P. Lentz, MP. Mormont, MC. Levi, F. Bjarnason, GA. (2009) Circadian rhythm in rest and activity: a biological correlate of quality of life and a predictor of survival in patients with metastatic colorectal cancer. *Cancer Research.* **69:**4700–4707.

Insel, P. Ostem, R. (2003) Forskolin as a Tool for Examining Adenylyl Cyclase Expression, Regulation, and G Protein Signaling. *Cellular and Molecular Neurobiology.* **23:**305-314.

Joels, M. Karst, H. DeRijk, R. de Kloet, ER. (2008) The coming out of the brain mineralocorticoid receptor. *Trends in Neuroscience.* **31:**107

Kang, T.H. Reardon, JT. Kemp, M. Sancar, A. (2009) Circadian oscillation of nucleotide excision repair in mammalian brain. *Proceedings of the National Academy of Science USA*. **106:**2864–2867.

Kang, TH. Lindsey-Boltz, LA. Reardon, JT. Sancar, A. (2010) Circadian control of XPA and excision repair of cisplatin-DNA damage by cryptochrome and HERC2 ubiquitin ligase. *Proceedings of the National Academy of Science USA.* **107:**4890–4895.

Kassel, O. Herrlich, P. (2007) Crosstalk between the glucocorticoid receptor and other transcription factors: molecular aspects*. Molecular and Cellular Endocrinology.* **275:**13-29

Kaushnik, R. Nawathean, P. Busza, A. Murad, A. Emery, P. Rosbash, M. (2007) PER-TIM interactions with the photoreceptor cryptochrome mediate circadian temperature responses in *Drosophila*. *PLoS Biology.* **5:**e146.

Kazimi, N. Cahill, GM. (1999) Development of a circadian melatonin rhythm in embryonic zebrafish. Brain Research Developmental Brain Research. **117(1):**47-52.

Kim, CH. Yoo, YM. (2010) Melatonin Induces Apoptotic Cell Death via p53 in LNCaP Cells. *Korean Journal of Physiology and Pharmacology.* **14(6):**365-369.

Ko, C. Takahasi, JS. (2006) Molecular components of the mammalian circadian clock. *Human Molecular Genetics.* **15:2** R271-R277.

Kobayashi, M. Wood, PA. Hrushesky, WJ. (2002) Circadian chemotherapy for gynaecological and genitourinary cancers. *Chronobiology International.* **19:** 237–251.

Kondratov, RV. Kondratova, AA. Gorbacheva, VY. Vykhovanets, OV. Antoch, MP. (2006) Early aging and age-related pathologies in mice deficient in BMAL1, the core component of the circadian clock. *Genes and Development*. **20:**1868–1873.

Kondratova, AA. Lee, C. Nikitin, AY. (2008) Disruption of the circadian clock due to the Clock mutation has discrete effects on aging and carcinogenesis. *Cell Cycle*. **7:** 1197–1204.

Kondo, T & Ishiura, M. (2000) The circadian clock of cyanobacteria. *Bioessays*, **22:** 10-15.

Konopka, RJ. Pittendrigh, C. Orr, D. (1989) Reciprocal behaviour associated with altered homeostasis and photosensitivity of *Drosophila* clock mutants. *Journal of Neurogenetics.* **6:**1–10.

Konturek, SJ. Konturek, JW. Pawlik, T. Brzozowski, T. (2004) Brain-gut axis and its role in the control of food intake. *Journal of Physiological Pharmacology.* **55:**137–54.

Krishan, A. (1975) Rapid flow cytofluorometric analysis of mammalian cell cycle by propidium iodide staining. *The Journal of Cell Biology.* **66:**188-193.

Kubo, T. Ozasa, K. Mikami, K. Wakai, K. Fujino, Y. Watanabe, Y. Miki, T. Nakao, M.. Hayashi, K. Suzuki, K. Mori, M. Washio, M. Sakauchi, F. Ito, Y. Yoshimura, T. Tamakoshi, A. (2006) Prospective cohort study of the risk of prostate cancer among rotating-shift workers: findings from the Japan collaborative cohort study. *American Journal of Epidemiology.* **164:**549–555.

Kume, K. Zylka, MJ. Sriram, S. Shearman, LP. Weaver, DR. Jin, X. Maywood, ES. Hastings, MH. Reppert, SM. (1999) mCRY1 and mCRY2 are essential components of the negative limb of the circadian clock feedback loop. *Cell*. **98:**193–205.

Kusanagi, H. Hida, A. Satoh, K. Echizenya, M. Shimizu, T. Pendergast, JS. Yamazaki, S. Mishima, K. (2008) Expression profiles of 10 circadian clock genes in human peripheral blood mononuclear cells. *Neuroscience Research*. **61:**136-42.

Lacroix, M. Leclercq, G. (2004). Relevance of breast cancer cell lines as models for breast tumours: an update. Breast Research and Treatment. **83 (3):** 249–289.

Langner, R. Rensing, L. (1972) Circadian rhythm of oxygen consumption in rat liver suspension culture: changes of pattern. *Z. Naturforsch. Teil B.* **27:**1117–18.

Lee, S. Donehower, LA. Herron, AJ. Moore, DD. Fu, L. (2010) Disrupting circadian homeostasis of sympathetic signalling promotes tumour development in mice. *Proceedings of the National Academy of Science USA.* **107:21** 9665-70.

Lehman MN, Silver R, Gladstone WR, Kahn RM, Gibson M, Bittman EL. (1987) Circadian rhythmicity restored by neural transplant. Immunocytochemical characterization of the graft and its integration with the host brain. *Journal of Neuroscience.* **7:**1626–38.

Le Minh, N. (2001) Glucocorticoid hormones inhibit food-induced phase-shifting of peripheral circadian oscillators. *EMBO Journal*. **20**:7128–7136.

Lewy, AJ. Bauer, VK. Ahmen, D. Thomas, KH. Culter, NL. Singer, CM. Moffit, MT. Sack, RL. (1998) The human Phase Response Curve (PRC) to Melatonin is about 12 hour out of phase with the PRC to light. *Chronobiology International.* **15:**71-83.

Lin, S. Gaiano, N. Culp, P. Burns, JC. Friedmann, T. Yee, JK. Hopkins, N. (1994) Integration and germ-line transmission of a pseudotyped retroviral vector in zebrafish. Science. **265(5172):**666-9.

Liu, Y. (2003) Molecular Mechanisms of Entrainment in the Neurospora Circadian Clock. *Journal of Biological rhythms*. 18: 195-205

Lowrey, PL. Shimomura, K. Antoch, MP. Yamazaki, S. Zemenides, PD. Ralph, MR. Menaker, M. Takahashi, JS. (2000) Positional synthetic cloning and functional characterization of the mammalian circadian mutation tau. *Science.* **288:**483–492.

Lowrey, P.L. and Takahashi, J.S. (2004) Mammalian circadian biology: elucidating genome-wide levels of temporal organization. *Annual Reviews of Genomics Human Genetics.* **5:**407–441

Lu, X. Errington, J. Curtin, NJ. Lunec, J. Newell, DR. (2001). The impact of p53 status on cellular sensitivity to anti-folate drugs. *Clinical Cancer Research*. **7:** 2114–2123.

Ma, X. Idle, JR. Krausz, KW. Gonzalez, FJ. (2005) Metabolism of melatonin by human cytochromes p450. *Drug Metabolism and Diposition*. **33(4):**489-94.

Mahtre, MC. Shah, PN. Junje, HS. (1984) Effect of carrying photoperiods on mammary morphology, DNA synthesis and hormonal profile in female rats. *Journal of National Cancer Institute*. **72:**1411-6.

Manchester, RC. (1933) The diurnal rhythm in water and mineral exchange. Journal of *Clinical Investigations.* **12:** 995–1008.

Matsuo, T. Yamaguchi, S. Mitsua, S. Emi, A. Schimodo, F. Okamura, H. (2003) Control mechanisms of the circadian clock for timing of cell division in vivo. *Science*. **203:**255-59.

Mattern, J. Buchler, MW. Herr, I. (2007) Cell cycle arrest by glucocorticoids mayprotect normal tissue and solid tumors from cancer therapy. *Cancer Biology and Therapeutics*. **6 :**1345–1354.

Megdal, S. Kroenke, C. Laden, F. Pukkala, E. Schernhammer, ES. (2005) Night work and breast cancer risk: a systematic review and meta-analysis. *European Journal of Cancer.* **41:**2023–2032.

Meier, AH. (1976) Daily variation in concentration of plasma corticosteroid in hypophysectomized rats. *Endocrinology*. **98:**1475–1479.

Menaker M, Moreira LF, Tosini G. (1997) Evolution of circadian organization invertebrates. *Brazilian Journal of Medical Biology Research*. **30:** 305–313.

Metz, RP. QU, X. Laffin, B. Earnest, D. Porter, WW. (2006) Circadian clock and cell cycle gene expression in mouse mammary epithelial cells and in the developing mouse mammary gland. *Developmental Dynamics*. **235:**263-7.

Miles, A. Philbrick, D. (1987) Melatonin: perspectives in laboratory medicine and clinical research. *Critical Reviews of Clinical Laboratory Sciences.* **25:3** 231-53.

Miller, BH. McDearmon, EL. Panda, S. Hayes, KR. Zhang, J. Andrews, JL. Antoch, MP. Walker, JR. Esser, KA. Hogenesch, JB. Takahashi, JS. (2010) Circadian and CLOCK-controlled regulation of the mouse transcriptome and cell proliferation. **5:6** 10995.

Moore, R.Y. Lenn, N.J. (1972) A retinohypothalamic projection in the rat. *Journal of Comparative Neurology*. **146(1):** 1-14.

Moore, RY. Eichler, VB. (1972) Loss of a circadian adrenalcorticosterone rhythm following suprachiasmatic lesions in the rat. *Brain Research.* **42**:201-206.

Mori, T. Binder, B Johnson, CH. (1996) Circadian gating of cell division in cyanobacteria growing with average doubling times of less than 24 hours. Proceedings of the National Academy of Science USA. **93(19):**10183-8.

Mori, T. Johnson, CH. (2001) Independence of circadian timing from cell division in cyanobacteria. *Journal of Bacteriology*. **183:8** 2439-2444.

Mormont, MC. Waterhouse, J. Bleuzen, P. Giacchetti, S. Jami, A. Bogdan, A. J. Lellouch, J. Misset, J. Y. Touitou, Y. F. Levi, F. (2000) Marked 24-h rest/activity rhythms are associated with better quality of life, better response, and longer survival in patients with metastatic

colorectal cancer and good performance status. *Clinical Cancer Research.* **6:**3038–3045

Motzkus,D. Albrecht,U.Maronde,E.(2002)The human PER1 gene is inducible by interleukin -6. *Journal of Molecular Neuroscience.* **18:**105-109.

Nader, N. Chrousos, GP. Kino, T. (2009) Circadian rhythm transcription factor CLOCK regulates the transcriptional activity of the glucocorticoid receptor by acetylating its hinge region lysine cluster: potential physiological implications. *FASEB J.* 23:1572–1583.

Nagoshi, E. Saini, C. Bauer, C. Laroche, T. Naef, F. Schibler, U. (2004) Circadian gene expression in individual fibroblasts: cell-autonomous and self-sustained oscillators pass time to daughter cells. *Cell.* **119:**693–705.

Nakahata. Y. Kaluzova, M. Grimaldi, B.. Sahar, S. Hirayama, J. (2008) The NAD+-dependent deacetylaseSIRT1 modulates CLOCK-mediated chromatin remodeling and circadian control. *Cell.* **134:**329–40.

Nakamura, TJ. Sellix. MT. Menaker. M, Block, GD. (2008) Estrogen directly modulates circadian rhythms of PER2 expression in the uterus. *American Journal of Physiology, Endocrinology and Metabolism.* **295:5** E1025-31.

Nakamura, TJ. Sellix, MT. Kudo, T. Nakao, N. Yoshimura, T. Ebihara, S. Colwell, CS. Block GD. (2010) Influence of the oestrous cycle on clock gene

expression in reproductive tissues: effects of fluctuating ovarian steroid hormone levels. *Steroids.* **75:3** 203-12.

Nigg, EA. (1995). "Cyclin-dependent protein kinases: key regulators of the eukaryotic cell cycle". *Bioessays.* **17**: 471–80.

Norris, D. O. 1997. Vertebrate Endocrinology. 3rd ed. Academic Press. San Diego, CA.

Noshiro, M. Furukawa, M. Honma, S. Kawamoto, T. Hamada, T. Honma, K. Kato, Y. (2005) Tissue-specific disruption of rhythmic expression of Dec1 and Dec2 in clock mutant mice. *Journal of Biological Rhythms.* **20:** 404 – 418,

Nunez, R. (2001) DNA measurement and cell cycle analysis by flow cytometry. Current Issues Molecular Biology. **3(3):**67-70.

Oda, A. Katayose, Y. Yabuuchi, S. Yamamoto, K. Mizuma, M. Shirasou, S. Onogawa, T. Ohtsuka, H. Yoshida, H. Hayashi, H. Rikiyama, T. Kim, H. Choe, Y. Kim, K. Son, H. Motoi, F. Egawa, S. Unno, M. (2009) Clock gene mouse period2 overexpression inhibits growth of human pancreatic cancer cells and has synergistic effect with cisplatin. *Anticancer Research.* **29:**1201-1209.

Office for National Statistics. (2010) Cancer Statistics registrations: Registrations of cancer diagnosed in 2008. Series MB1 no.39.

Olivier, M. Eeles, R. Hollstein, M. Khan, MA. Harris, CC. Hainaut, P. (2002) The IARC TP53 database: new online mutation analysis and recommendations to users. *Human Mutations*. **19:** 607–614.

O'Neill, JS. Reddy, AB. (2011) Circadian clocks in human red blood cells. *Nature.* **469:**498-503

Oshima, T. Takenoshita, S. Akaike, M. Kunisaki, C. Fujii, S. Nozaki, A. Numata, K. Shiozawa, M. Rino, Y. Tanaka, K. Masuda, M. Imada, T. (2011) Expression of circadian genes correlates with liver metastasis and outcomes in colorectal cancer. Oncology Reports. 25:1439-1446.

Oster, H. Damerow, S. Kiessling, S. Jakubcakova, V. Abraham, D. (2006) The circadian rhythm of glucocorticoids is regulated by a gating mechanism residing in the adrenal cortical clock. *Cell Metabolism.* **4:**163–73.

Ozturk, N. Lee, H. Gaddameedhi, S. Sancar, A. (2009) Loss of cryptochrome reduces cancer risk in p53 mutant mice. *Proceedings of the National Academy of Science USA.* **106:**2841–2846.

Panda, S. Antoch, MP. Miller, BH. Su, AI. Schook, AB. Straume. M, Schultz, PG. Kay, SA. Takahashi, JS. Hogenesch, JB. (2002) Coordinated transcription of key pathways in the mouse by the circadian clock. *Cell.* **109:**307-320.

Pando, MP. Pinchak, AB. Cermakian, N. Sassone-Corsi, P. (2001) A cell-based system that recapitulates the dynamic light-dependent regulation of the

vertebrate clock. Proceedings of the National Academy of Science U S A. **98(18):**10178-83.

Pardini, L. Kaeffer, B. Trubuil, A. Bourreille, A. Galmiche, JP. (2005) Human intestinal circadian clock: expression of clock genes in colonocytes lining the crypt. 22:951.961.

Parkin, DM. Bray, FI. Devesa, SS. (2001) Cancer Burden in the year 2000: the global picture. *European Journal of Cancer.* **37:**S4-S66.

Pittendrigh, CS. (1954). On temperature independence in the clock system controlling emergence time in *Drosophila*. *Proceedings of the National Academy of Science US* **40:**1018–29.

Pittendrigh, CS. (1960) Circadian rhythms and the circadian organisation of living systems. *Cold spring Harbour Symposium on Quantitative Biology.* **25:**159-184

Pons, M. Cambar, J. Waterhouse, JM. (1996) Renal hemodynamic mechanisms of blood pressure rhythms. *Annals of the New York Academy of Science.* **783:** 95–112.

Provencio, I. Jiang, G. De Grip, WJ. Hayes, WP. Rollag, MD. (1998) Melanopsin: an opsin in melanophores, brain, and eye. *Proceedings of the National Academy of Science USA*. **95:**340–45

Provencio, I. Rodriguez, IR. Jiang, G. Hayes, WP. Moreira, EF. Rollag, MD. (2000) A novel human opsinin the inner retina. *Journal of Neuroscience.* **20:**600–5.

Ralph, MR. Foster, RG. Davis, FC. Menekar, M. (1990) Transplanted suprachiasmatic nucleus determines circadian period. *Science*. **247**:975-978.

Ram, PT.Dai, J. Yuan, L. Dong, C. Kiefer, TL. Lai, L. Hill, SM.(2002) Involvement of the mt1 melatonin receptor in human breast cancer. *Cancer Letters.* 2002. **179(2):**141-50.

Reddy, AB. (2007) Glucocorticoid signaling synchronizes the liver circadian transcriptome. *Hepatology.* **45:**1478–1488.

Reiter, RJ. (1980) The pineal and its hormones in the control of reproduction in mammals. *Endocrinology ReviewS.* **1:2** 109-31.

Reiter, RJ. (1991) Melatonin: the chemical expression of darkness. *Molecular Cellular Endocrinology.* **79(1-3):** C153-8.

Reiter, R.J. (1993) The melatonin rhythm: both a clock and a calendar. *Experientia.* **49(8):**654-64.

Reiter, RJ. (1994) Melatonin suppression by static and extremely low frequency electromagnetic fields: relationship to the reported increased incidence of cancer. *Reviews in Environmental Health*. **10(3-4):**171-86

Ross, DT. Perou, CM. (2001) A comparison of gene expression signatures from breast tumours and breast tissue derived cell lines. Diseases Markers. **17**: 99–109.

Rudic, RD. McNamara, P. Curtis, AM. Boston, RC. Panda, S. Hogenesch, JB. Fitzgerald, G.A. (2004) BMAL1 and CLOCK, two essential components of the circadian clock, are involved in glucose homeostasis. *PLoS Biology*. **2:**e377.

Sack, RL. Brandes, RW. Kendall AR. Lewy, AJ. (2000) Entrainment of free-running circadian rhythms by melatonin in blind people. *New England Journal of Medicine.* **343:**1070-1077.

Sack, R. L. (2007) Circadian rhythm sleep disorders: part I, basic principles, shift work and jet lag disorders. An American Academy of Sleep Medicine review.*Sleep*. **30:**1460–1483

Sahar, S. Sassone-Corsi, P. (2007) Circadian Clock and Breast Cancer: A molecular Link. *Cell Cycle*. **6:**1329-1331.

Sancar, A. Lindsey-Boltz, LA. Unsal-Kacmaz, K. Linn, S. (2004) Molecular mechanisms of mammalian DNA repair and the DNA damage checkpoints. *Annual Reviews in Biochemistry.* **73:**39–8.

Sato, TK. Panda, S. Miraglia, MJ. Reyes, TM. Rudic, RD. McNamara, P. Naik, KA. FitzGerald, GA. Kay, SA. Hogenesch, JB. (2004) A functional genomics strategy reveals Rora as a component of the mammalian circadian clock. *Neuron*. **43:**527–537.

Sato, TK. Yamada, RG. Ukai, H. Baggs, JE. Miraglia, LJ. Kobayashi, TJ. Welsh, DK. Kay, SA. Ueda, HR. Hogenesch, JB. (2006) Feedback repression is required for mammalian circadian clock function. *Nature Genetics.* **38:**312–319.

Sato, F. Nagata, C. Liu, Y. Suzuki, T. Kondo, J. Morohashi, S. Imaizumi, T. Kato, Y. Kijima, H. (2009) PERIOD1 is an anti-apoptotic factor in human pancreatic and hepatic cancer cells. *Journal of Biochemistry.* **146:**833-838.

Schernhammer, E.S. Laden, F. Speizer,FE, Willett, WC. Hunter, DJ. Kawachi, I. Colditz, GA. (2001) Rotating night shifts and risk of breast cancer in women participating in the nurses' health study. *Journal of the National Cancer Institute*. **93:**1563–1568.

Schernhammer, E.S. Laden, F. Speizer, FE, Willett, WC. Hunter, DJ. Kawachi, I. Colditz, GA. (2003) Night-shift work and risk of colorectal cancer in the nurses' health study. *Journal of the National Cancer Institute*. **95:**825–828.

Schibler, U. (2003) Circadian rhythms: Liver regeneration clock on. *Science.* **302:**234-235.

Schibler, U. Naef, F. (2005) Cellular oscillations: rhythmic gene expression and metabolism. *Current Opinions in Cell Biology.* **17:2** 223-229.

Schwartz, WJ. Gainer, H. (1977) Suprachiasmatic nucleus: use of 14C-labeled deoxyglucose uptake as a functional marker. *Science.* **197:**1089–91.

Scully, CG. Abdoulaye, K. Wie-Min, L. Meyer, J. Innominato, PF. Chon, KH. Gorbach, AM. Levi, F. (2011) Skin surface temperature rhythms as potential circadian biomarkers for personalized chronotherapeutics in cancer patients. Interface Focus. **6:**48-60.

Segall, L.A. (2006) Glucocorticoid rhythms control the rhythm of expression of the clock protein, *Period2*, in oval nucleus of the bed nucleus of the stria terminalis and central nucleus of the amygdala in rats. *Neuroscience*. **140:**753–757.

Sehadova, H. Glaser, FT. Gentile, C. Simoni, A. Giesecke, A. Albert, JT. Stanewsky, R. (2009) Temperature Entrainment of *Drosophila's* Circadian Clock Involves the Gene *nocte* and Signalling from Peripheral Sensory Tissues to the Brain. *Neuron.* **64:**251-266.

Senghaas, N. Köster, RW. (2009) Culturing and transfecting zebrafish PAC2 fibroblast cells. Cold Spring Harbor Protocols. **9(6):**5235.

Semo, M. Peirson, S. Lupi, D. Lucas RJ. Foster RG. (2003) Melanopsin retinal ganglion cells and the maintence of circadian and pupillary response to light in ages rodless/coneless (rd/rd cl) mice. *European journal of Neuroscience*. **17:** 1793-1801.

Sephton, S.E. Sapolsky, R.M.. Kraemer, H.C Spiegel, D. (2000) Diurnal cortisol rhythm as a predictor of breast cancer survival. *Journal of the National Cancer Institute*. **92**:994–1000.

Shackelford, RE. Kaufmann, WK. Paules, RS. (1999) Cell cycle control, checkpoint mechanisms, and genotoxic stress. *Environmental Hleath Perspectives*. **107:**Supp 1:5-24

Shearman, LP. Sriram, S. Weaver, DR. Maywood, ES. Chaves, I. Zheng, B. Kume, K. Lee, CC. van der Horst, GT. Hastings, M. (2000) Interacting molecular loops in the mammalian circadian clock. *Science.* **288**:1013–1019.

Shimba, S. Ishii, N. Ohta, Y. Ohno, T. Watabe, Y. Hayashi, M.Wada, T. Aoyagi, T. Tezuka, M. (2005) Brain and muscle Arnt-likeprotein-1 (BMAL1), a component of the molecular clock, regulates adipogenosis. *Proceedings of the National Academy of Science, USA*. **102(34):**12071-6.

Shin. JS. Hong, SW. Lee, SL. Kim, TH. Park, IC. An, SK. Lee, WK. Lim, JS. Kim, KI. Yang, Y. Lee, SS. Jin, DH. Lee, MS. (2008) Serum starvation induces G1 arrest through suppression of Skp2-CDK2 and CDK4 in SK-OV-3 cells. *International Journal of Oncology*. **32(2):**435-9.

Skene, DJ. Papagiannidou, E. Hashemi, E. Snelling, J. Lewis, D.F. Fernandez, M. Ioannides, C. (2001) Contribution of CYP1A2 in the hepatic metabolism of melatonin: studies with isolated microsomal preparations and liver slices. *Journal of Pineal Research.* **31(4):** 333-42.

Smaaland, R. (2002) Rhythms in human bone marrow and blood cells. *Chronobiology International.* **19:**101–127.

Son, GH. (2008) Adrenal peripheral clock controls the autonomous circadian rhythm of glucocorticoid by causing rhythmic steroid production.

Proceedings of the National Academy of Science. U.S.A. **105:**20970–20975

Soule, HD. Vazquez, J. Long, A. Albert, S. Brennan, M. (1973) A human cell line from a pleural effusion derived from a breast carcinoma. Journal of the National Cancer Institute. **51 (5):** 1409–1416.

Soule, H.D. (1990) Isolation and characterization of a spontaneously immortalized human breast epithelial cell line, MCF-10. *Cancer Research.* **50(18):**6075-86.

Stephan, FK. Zucker, I. (1972) Circadian rhythms in drinking behaviour and locomotor activity of rats are eliminated by hypothalamic lesions. *Proceedings of the National Academy of Science, USA.* **69**:1583-1586.

Stevens, RG. (2005) Circadian disruption and breast cancer: From melatonin to clock genes. *Epidemiology.* **16:**254-8.

Stevens RG. (2006) Artificial lighting in the industrialized world: Circadian disruption and breast cancer. *Cancer Causes Control*. **17:**501-7.

Stokkan, KA. Yamazaki, S. Tei, H. Sakaki, Y. Menaker, M. (2001) Entrainment of the circadian clock in the liver by feeding. *Science.* **291:**490–93.

Stow, LR. Gumz, ML. (2011) The circadian clock in the kidney. *Journal of the American Society of Nephrology.* **22:**598-604.

Stratmann, M. Schibler, U. (2006) Properties, entrainment, and physiological functions of mammalian peripheral oscillators. *Journal of Biological Rhythms.* **21:6** 494-506.

Sujino, M. Masumoto, KH. Yamaguchi, S. van der Horst, GT. Okamura, H. Inouye, ST. (2003). Suprachiasmatic nucleus grafts restore circadian behavioural rhythms of genetically arrhythmic mice. *Current Biology.* **13**:664–68.

Sun, ZS. Albrecht, U. Zhuchenko, O. Bailey, J. Eichele, G, Lee, CC. (1997) RIGUI, a putative mammalian ortholog of the *Drosophila* period gene. *Cell.* **90:**1003–11.

Sweeney, BM. (1987) Rhythmic Phenomena in Plants. (Academic Press, San Diego).

Takahashi, J.S. Hong, H.K. Ko, C.H. McDearmon, E.L. (2008) The genetics of mammalian circadian order and disorder: implications for physiology and disease. *Nature Reviews Genetics*. **9:**764–775.

Takeuchi, T. Hinohara, T. Kurosawa, G.Uchida, K. (2007) A temperature-compensated model for circadian rhythms that can be entrained by temperature cycles. *Journal of Theoretical Biology.* **246:**195–204.

Takizawa, CG. Morgan, DO. (2000) Control of mitosis by changes in the subcellular location of cyclin-B1-Cdk1 and Cdc25C. *Current Opinions Cell Biology.* **12(6):**658-65. Review.

Tamai, TK. Carr, AJ. Whitmore, D. (2005) Zebrafish circadian clocks: cells that see light. Biochemical Society Transactions. **33(Pt 5):**962-6.

Tamai, TK. Young, LC. Whitmore, D. (2007) Light signalling to the zebrafish circadian clock by Cryptochrome 1a. Proceedings of the National Academy of Science U S A. **104(37):**14712-7.

Teboul, M. Barrat-Petit, MA. Li, XM. Claustrat, B. Formento, JL. Delaunay, F. Lévi, F. Milano, G.(2005) Atypical patterns of circadian clock gene expression in human per ipheral blood mononuclear cells. *Journal of Molecular Medicine*. **83:**693-699.

Tijmes, M. Pedraza, R. Valladares, L. (1996) Melatonin in the rat testis: evidence for local synthesis. *Steroids*. **61(2):** p. 65-8.

Toh, KL. Jones, CR. He, Y. Eide, J. Hinz, WA. Virshup, DM. Ptacek, LJ. Fu, YH. (2001) An *hPer2* phosphorylation site mutation in familial advanced sleep phase syndrome. *Science.* **291:**1040–1043.

Travis, RC. Allen, DS. Rentimen, IS. (2004) Melatonin and Breast cancer: a prospective. *Cancer epidemiology biomark*ers. **96:**475-482.

Tynes, T. Hannevik, M. Andersen, A. (1996) Incidence of breast cancer in Norwegian female radio and telegraph operator. *Cancer Causes Control* . **7:**197-204

Vaidya, JS. Baldassarre, G. Thorat, MA. Massarut, S. (2010) Role of glucocorticoids in breast cancer. *Current Pharmaceutical Design* .**16:**3593-3600.

Vallone, D. Gondi, SB. Whitmore, D. (2004) E-box function in a period gene repressed by light. *Proceedings of the National Academy of Science USA.* **101(12):** 4106–4111.

Verkasalo, PK. Pukkala, E. Steven, RG. (1999) Inverse association between breast cancer incidence and degree of visual impairment in Finland. *British Journal of Cancer*. **80:**1459-1460.

Viswanathan, A.N. Hankinson, S.E. Schernhammer, E.S. (2007) Night shift work and the risk of endometrial cancer. Cancer Res. **67:**10618–10622.

von Schantz, M. (2008) Phenotypic effects of genetic variability in human clock genes on circadian and sleep parameters. *Journal of Genetics.* **87:**513–519.

Vujovic, N. Davidson, AJ. Menaker, M. (2008) Sympathetic input modulates, but does not determine, phase of peripheral circadian oscillators. *American Journal of Physiology. Regulatory, Integrative and Comparative Physiology.* **295:**R355–60.

Wang, C. Fan, S. Li, Z. Fu, M. Rao, M. Ma, Y. Lisanti, MP. Albanese, C. Kartzenellenbogen, BS. Kushner, PJ. Weber, Rosen, EM. Pestell, RG. (2005) Cyclin D1 antagonises BRCA1 repression of oestrogen receptor alpha activity. *Cancer Research*. **65:**6557-67.

Watson, JV. Chamber, SH. Smith, PG. (1987) A pragmatic approach to the analysis of DNA histograms with a definable G1 peak. *Cytometery*. **8:**1 8.

Welsh, DK. Logothetis, DE. Meister, M. Reppert, SM. (1995). Individual neurons dissociated from rat suprachiasmatic nucleus express independently phased circadian firing rhythms. *Neuron.* **14:**697–706.

Welsh, DK. Yoo, SH. Liu, AC. Takahashi, JS. Kay, SA. (2004). Bioluminescence imaging of individual fibroblasts reveals persistent, independently phased circadian rhythms of clock gene expression. *Current Biology.* **14:**2289–95.

Westerfield, M. (2007) The Zebrafish Book, 5th Edition; A guide for the laboratory use of zebrafish (Danio rerio), Eugene, University of Oregon Press. USA.

de Wet, JR. Wood, KV. Helsinki, DR. DeLuca, M. (1985) Cloning of firefly luciferase cDNA and the expression of active luciferase in Escherichia Coli. *Proceedings of the National Academy of Science.* **82:**7870-7873.

Whitmore, D. Foulkes, NS. Strähle, U. Sassone-Corsi, P. (1998) Zebrafish Clock rhythmic expression reveals independent peripheral circadian oscillators. *Nature Neuroscience*. **1(8):**701-7.

Whitmore, D. Foulkes, NS. Sassone-Corsi, P. (2000) Light acts directly on organs and cells in culture to set the vertebrate circadian clock. Nature. **404(6773):**87-91.

Whitmore, D. Cermakian, N. Crosio, C. Foulkes, NS. Pando, MP. Travnickova, Z. Sassone-Corsi P. (2000) A clockwork Orange. *Biological Chemistry*. **381(9-10):**793-800.

Winter, SL. Bosnoyan-Collins, L. Pinnaduwage, D. Andrulis, IL.(2007) Expression of the circadian clock genes Per1 and Per2 in sporadic and familial breast tumors. Neoplasia. **9(10):**797-800.

Wise, J. (2009) Danish night shift workers with breast cancer awarded compensation *British Medical Journal* **.338:**b1152.

Wu, Y. Sato, F. Bhawal, UK. Kawamato, T. Fujimoto, K. Noshiro, M. Morohashi, S. Kato, Y. Kijima, H. (2011) Basic Helixloop leix transcription factors DEC1 and DEC2 regulate paclitaxel-induced apoptotic pathway of MCF7 human breast cancer cells. *International Journal of molecular medicine*. **27:**492-495

Yagita K, Tamanini F, van der Horst GT, Okamura H. 2001. Molecular mechanisms of the biological clock in cultured fibroblasts. *Science* 292:278–81

Yamato, M. Ito, T. Iwatani, H. Yamato, M. Imai, E. Rakugi, H. (2010) E-cadherin and claudin-4 expression has circadian rhythm in adult ratkidney. *Journal of Nephrology.* **23:** 102–110.

Yan, J. Wang, H. Liu, Y. Shao, C. (2008) Analysis of gene regulatory networks in the mammalian circadian rhythm. *PLos Computational Biology.* **4(10):**e1000193.

Yang, MY. Yang, WC. Lin, PM. Hsu, JF., Hsiao, HH. Liu, YC. Tsai, HJ. Chang, CS. Lin, SF. (2011) Altered expression of circadian clock genes in human chronic myeloid leukemia. Journal of Biological Rhythms. 26:136-148.

Yamamoto, T. Nakahata, Y. Soma, H. Akashi,M. Mamine, T. Takumi, T. (2004). Transcriptional oscillation of canonical clock genes in mouse peripheral tissues. *BMC Molecular Biology.* **5:**18.

Yamazaki, S. Numano, R. Abe, M. Hida, A. Takahashi, R. (2000). Resetting central and peripheral circadian oscillators in transgenic rats. *Science* **288:**682–85.

Yamazaki, S. Yoshikawa, T. Biscoe, EW. Numano, R. Gallaspy, LM. (2009) Ontogeny of circadian organization in the rat. *Journal of Rhythms.* **24:**55–63.

Yeleswaram, K. N. Vachharajani, N. Santone, K. (1999) Involvement of cytochrome P-450 isozymes in melatonin metabolism and clinical implications. *Journal of Pineal Research.* **26(3):** 190-1.

Yeom, M. Pendergast, JS. Ohmiya, Y. Yamazaki, S. (2010) Circadian-independent cell mitosis in immortalized fibroblasts. *Proceedings of the National Academy of Science USA*. **107:21** 9665-70.

Yoo, SH. Yamazaki, S. Lowrey, PL. Shimomura, K. Ko, CH. (2004). PERIOD2::LUCIFERASE real time reporting of circadian dynamics reveals persistent circadian oscillations in mouse peripheral tissues. *Proceedings of the National Academy of Science USA*. **101:**5339–46.

Young, MW. Kay, SA. (2001) Time zones: A comparative genetics of circadian clock *Nature Reviews Genetics.* **2:**704.

Yoshikawa, A. Shimada, H. Numazawa, K. Sasaki, T. Ikeda, M. Kawashima, M. Kato, N. Tokunaga, K. Ebisawa, T. (2008) Establishment of human cell-lines showing circadian rhthyms of biolouminescence. *Neuroscience Letters*. **446:**40-44.

Yu, AM. Idle, JR. Byrd, KW. Krausz, LW. Kupfer, A. Gonzalez, FJ. (2003)Regeneration of serotonin from 5-methoxytryptamine by polymorphic human CYP2D6. *Pharmacogenetics,* **13(3):** 173-81.

Zawilska, J. J.Z. Nowak, J.Z. (1991) Regulation of melatonin biosynthesis in vertebrate retina: involvement of dopamine in the suppressive effects of light. *Folia Histochemical Cytobiology*. **29(1):** p. 3-13.

Ziv, L. Levkovitz, S. Toyama, R. Falcon, J. Gothilf, Y. (2005) Functional development of the zebrafish pineal gland: light-induced expression of period2 is required for onset of the circadian clock. Journal of Neuroendocrinology. **17(5):**314-20.

Zhu, Y. Leaderer, D. Guss, C. Brown, HN Zhang, Y. Boyle, P. Stevens, R.G. Hoffman, A. Qin, Q. Han, X. Zheng, T. (2007) Ala394Thr polymorphism in the clock geneNPAS2: a circadian modifier for the risk of non-Hodgkin's lymphoma. *International Journal of Cancer.* **42**:432–435.

Zhu, Z. Stevens, RG. Hoffman, AE. Fitzgerald, LM. Kwon, EM. Ostrander, EA. Davis, S. Zheng, T. Stanford JL. (2009) Testing the circadian gene hypothesis in prostate cancer: a population-based case–control study. *Cancer Research*. **69:**9315-9322.

Zhu, Z. Brown, H.N. Zhang, Y. Stevens, RG Zheng, T. (2005) Period3 structural variation: a circadian biomarker associated with breast cancer in young women. *Cancer Epidemiology Biomarkers.* **14:** 268–270.

Zhu, Z. Stevens, RG. Leaderer, D. Hoffman, AE. Holford, T. Zhang, Y. Brown, H.N. Zheng, T. (2008) Non-synonymous polymorphisms in the circadian gene NPAS2 and breast cancer risk. *Breast Cancer Research Treatments.* **107:**421–425.

Zuber, AM. Centeno, G. Pradervand, S. Nikolaeva, S. Maquelin, L. Cardinaux, L. Bonny, O.Firsov, D. (2009) Molecular clock is involved in predictive circadian adjustment of renal function. *Proceedings of the National Academy of Science USA***, 106:** 16523–16528.